

Open Research Online

The Open University's repository of research publications and other research outputs

Interactions of flavones and related compounds with nucleic acids.

Thesis

How to cite:

Ragazzon, Patricia Alejandra (2006). Interactions of flavones and related compounds with nucleic acids. PhD thesis The Open University.

For guidance on citations see [FAQs](#).

© 2006 Patricia Alejandra Ragazzon



<https://creativecommons.org/licenses/by-nc-nd/4.0/>

Version: Accepted Manuscript

Link(s) to article on publisher's website:

<http://dx.doi.org/doi:10.21954/ou.ro.0000fe4b>

Copyright and Moral Rights for the articles on this site are retained by the individual authors and/or other copyright owners. For more information on Open Research Online's data [policy](#) on reuse of materials please consult the policies page.

oro.open.ac.uk

Interactions of flavones and related compounds with nucleic acids

A thesis submitted for the degree of
Doctor of Philosophy to

The Open University

by

Patricia Alejandra Ragazzon

Postgraduate specialization in Molecular Biology (Fundación
Campomar, Universidad de Buenos Aires, Argentina)
Licenciature in Chemistry (Universidad del Salvador, Argentina)

June 2006

Department of Chemistry
Open University
Walton Hall
Milton Keynes MK7 6AA
UNITED KINGDOM

ProQuest Number: 13917227

All rights reserved

INFORMATION TO ALL USERS

The quality of this reproduction is dependent upon the quality of the copy submitted.

In the unlikely event that the author did not send a complete manuscript and there are missing pages, these will be noted. Also, if material had to be removed, a note will indicate the deletion.



ProQuest 13917227

Published by ProQuest LLC (2019). Copyright of the Dissertation is held by the Author.

All rights reserved.

This work is protected against unauthorized copying under Title 17, United States Code
Microform Edition © ProQuest LLC.

ProQuest LLC.
789 East Eisenhower Parkway
P.O. Box 1346
Ann Arbor, MI 48106 – 1346

Statement

The work embodied in this thesis was carried out by the author between October 2002 and November 2005 in the laboratories of the Department of Chemistry, Open University, Milton Keynes under the supervision of Dr Sotiris Missailidis and Dr Jim Iley and the cell work has been carried out in the Department of Structural Biology, University of Nottingham, Nottingham, under the supervision of Mr. Charles Matthews.

I declare that the work presented is the result of my own investigations.

The material within this thesis has not been submitted, nor is currently being submitted, for any other degree.

Parts of the work have been presented as listed below.

- “Flavonoids as DNA interacting agents”. Patricia Ragazzon, Jim Iley and Sotiris Missailidis. Presented at “The 2005 NCRI Cancer conference”, 2-5 October 2005; Birmingham, United Kingdom. (Poster presentation)
- “Development of novel DNA-binding chemotherapeutic agents based on flavonoid scaffolds of active ingredients isolated from Chinese herbal remedies”. Patricia Ragazzon, Jim Iley and Sotiris Missailidis. Presented at “Younger Physical Organic Chemists Residential meeting”, Castleton, 25-26 June 2005; United Kingdom. (Poster presentation)
- “Development of novel DNA-binding chemotherapeutic agents based on flavonoid scaffolds of active ingredients isolated from Chinese herbal remedies”. Patricia Ragazzon, Jim Iley and Sotiris Missailidis. Presented at “Structural

Biology of Cancer”, CNIO (Cancer National Institute of Research), 27-29 September 2004; Madrid, Spain. Book of abstracts, page 49. (Poster presentation)

- “Structure activity related studies between the flavonoid skeleton and DNA duplex, triplex and tetraplex structures”. Patricia Ragazzon, Jim Iley and Sotiris Missailidis. Presented at “Frontiers in Chemical Biology: the Chemical Biology of Cancer”, 8-10 September 2004; The School of Pharmacy, University of London, UK. Book of abstracts, page 21. (Poster presentation)
- “Molecular encounters between active ingredients and DNA”. Patricia Ragazzon, Jim Iley, Sotiris Missailidis. Presented on the Fourth European Workshop on Drug Design, May, 2003; Sienna, Italy. (Poster presentation)

Patricia A. Ragazzon

June 2006

Acknowledgements

I want to thank my supervisors Dr Jim Iley and Dr Sotiris Missailidis for assisting me during these 3 years of hard work and short vacations. I also want to thank them for giving me the opportunity to believe in my work, and more important in myself, and for teaching me how to think while doing research in science.

I want to thank Dr Jim Iley for teaching me how to synthesise compounds, to understand how to characterize them, and for being so nice while I was learning.

I want to thank Dr Sotiris Missailidis for helping me with the binding fitting data, and for helping me to go to so many conferences during this project and to be able to do whatever experiment I was having in mind.

I want to thank Prof Malcolm Stevens for allowing me to use the facilities in the University of Nottingham for my biological studies.

I want to thank Charlie Matthews, University of Nottingham, for helping me with the cell work and for being such a great friend. I hope I will assist to his wedding.

I want to thank the Open University for funding me and for giving me the chance to have a PhD in such a wonderful country as it is UK; and Prof David Shuker, Dr David Roberts and Dr James Bruce for helping and encouraging me.

I want to thank Pravin, Graham, Gordon, Colin and Allen for helping me to do this project, and without them I would not have managed to finish it. And to Glen for helping and teaching me mechanisms of reactions, providing me with reactants and assisting me every time I was in trouble. I still hope Glen will write a book called: "Shortcuts to Chemistry". I will be the first one buying it.

I want to thank Catia, Antonio, Julia, Michelle, Ourania, Raman, Sharon, Yoseph and Patrick for giving me advice while working, giving me company in my low moments and for being always there for me. I wish we will always be there for each other. And Julia will keep cooking sushi for me.

I want to thank my sister, Carolina for sending me sweets and advices; my mum, Stella Maris for encouraging me to study science and to calm me down in my stressful moments.

I want to thank my grandma, Tata for always believing in me and helping me to apply for this PhD.

I want to thank David Smith for being always with me, giving me support, companionship, advice and for helping me with everything.

I want to thank my friends in Buenos Aires, Marga, and Laura for giving me an ear when I needed it the most.

I dedicate this thesis to my grandma, who always believed in me; and to Kim & Titina
who I lost during these years.

Contents

Page

Abstract

1

Chapter 1: Introduction

3

1.1.a: Cancer

4

1.1.b: Cell cycle and apoptosis

7

1.1.c: Signalling pathways

9

1.1.d: Therapies

13

1.1.e: Herbal remedies as cancer therapy

14

1.2.1.a: Terpenoids

17

1.2.1.b: Artemisinin and artesunate

17

1.2.1.c: Cantharidin

22

1.2.2.a: Flavonoids and isoflavonoids

23

1.2.2.b: Baicalein and baicalin

26

1.2.2.c: Quercetin and rutin

29

1.2.2.d: Daidzein

35

1.2.2.e: Puerarin

37

1.3.a: The role of DNA

39

1.3.b: Types of DNA interactive agents

41

1.3.c.1: Duplex DNA structures

43

1.3.c.2: DNA triplex structures

46

1.3.c.3: Telomeres

48

1.3.d: DNA –metal interactions

52

1.4: Aims of this PhD

54

Chapter 2: Materials and methods

56

2.1.a:	Buffers	57
2.1.b:	Nucleic acids	57
2.1.c.1:	Chemicals	58
2.1.c.2:	Synthesis	59
2.1.d.1:	Isoflavone	59
2.1.d.2:	Thioflavone	60
2.1.d.3:	Azaflavone	61
2.1.d.4:	Flavone	61
2.1.d.5:	3',4'-Dichloroflavone	62
2.1.d.6:	2-Acetylphenyl-3,5-dinitrobenzoate	63
2.1.d.7:	3',5'-Dinitroflavone	64
2.1.d.8:	2,6-Dihydroxy-8-nitroacetophenone	65
2.1.d.9:	5-Hydroxy-8-nitroflavone	65
2.1.d.10:	5-Hydroxyflavone	66
2.1.d.11:	6-Hydroxyflavone	67
2.1.d.12:	7-Methoxyflavone	69
2.1.d.13:	5-Hydroxy-7-methoxyflavone	69
2.1.d.14:	5,7-Dimethoxychrysin	70
2.1.d.15:	5,7-Diacetoxychrysin	70
2.1.d.16:	7-Dimethylaminoethoxy-5-hydroxyflavone	71
2.1.d.17:	7-Dimethylaminopropoxy-5-hydroxyflavone	72
2.1.d.18:	7-Morpholinoethoxy-5-hydroxyflavone	73
2.1.e:	Tumour cell lines	73
2.2.a.1:	Methods	74
2.2.a.2:	Spectroscopical methods for the study of DNA-drug interactions	75
2.2.a.3:	Temperature denaturing studies	75
2.2.a.4:	UV titrations	77
2.2.a.5:	Data fitting and experimentation	78
2.2.a.6:	Fluorescence titrations	80
2.2.a.7:	Competition dialysis	83
2.2.b:	Determination of pKa	84

2.2.c.: Nucleic acid damage	84
2.2.d: Linear Taq polymerase stop PCR and footprinting assays	84
2.2.e: Topoisomerase I and II inhibition - DNA unwinding	90
2.2.f.1: Evaluation of compounds in tumour models	93
2.2.f.2: Flow cytometry	93
2.2.f.3: MTS cell proliferation assay	95
2.2.f.4: Comet assay	96
2.2.g: CYP1A1	98
2.2.h.: Hemin sesquiterpenes interactions	100
 <i>Chapter 3: Preliminary results</i>	 101
3.1: Screening of natural compounds	102
3.2: Drug – DNA interactions	102
3.2.a: Melting temperature	102
3.2.b.1: Association binding constants	107
3.2.b.2: Duplex binding	110
3.2.b.3: Competition dialysis	113
3.2.b.4: Triplex binding	116
3.2.b.5: G-quadruplex binding	117
3.2.b.6: DNA – drug – metal interactions	118
3.2.c: Nucleic acid damage assay	120
3.2.d: Linear Taq Polymerase stop PCR and footprinting assay	121
3.2.e: Topoisomerase I & II inhibition assay	123
3.2.f: Flow cytometry	127
3.2.g: MTS proliferation assay	128
3.2.h: Comet assay	130
3.2.i: Hemin sesquiterpenes interactions	131
3.2.j: CYP1A1 metabolites assay	135
3.2.k: Determination of pKa	140
3.3: Conclusions for the foundation compounds	144

<i>Chapter 4: Structure activity related studies</i>	147
4.1: Obtaining DNA intercalating agents	148
4.2: Organic synthesis	150
4.2.a: Flavone and its derivatives	154
4.3: Obtaining binding constants	164
4.3.a: Localization of the B ring and the relevance of the double carbon bond in the C ring	165
4.3.b: Three fused rings	166
4.3.c: Sulfur and nitrogen in the 3-ring system	167
4.3.d: The difference between flavones and flavonols	170
4.3.e: Modifications on A ring	171
4.3.f: Modification on B ring	177
4.3.g: DNA – drug metal interactions	178
4.4: Selectivity for different structures	180
4.4.a: Competition dialysis	180
4.5: Stabilisation of the double helix	191
4.5.a: Melting points	191
4.6: Biological evaluation	193
4.6.a: Cell viability results	193
4.7: Conclusions to chapter 4	195
 Chapter 5: Conclusions and further work	 197
 <i>References</i>	 202
 <i>Appendix</i>	 215

List of Tables

Table 1: Melting point	106
Table 2: Extinction coefficients	107
Table 3: Binding association constants duplex	112
Table 4: Binding association constants triplex	117
Table 5: Binding association constants quadruplex	118
Table 6: Titration of metal – drug – DNA interactions	120
Table 7: Flow cytometry	128
Table 8: MTS cell proliferation assay	129
Table 9: CYP1A1	136
Table 10: pKa values	141
Table 11: Binding constants	166
Table 12: Binding constants	167
Table 13: Binding constants	170
Table 14: Binding constants	176
Table 15: Binding constants	178
Table 16: Binding constants for DNA – drug – metal interactions	179
Table 17: Melting points	192
Table 18: Cell viability results	194

List of Figures

Figure 1: Development of cancer	6
Figure 2: Cell cycle stages	8
Figure 3: Central dogma	40
Figure 4: DNA interactive agents	43
Figure 5: DNA duplexes	45
Figure 6: Hydrogen bonding	45
Figure 7: Triplex base arrangements	47
Figure 8: Guanine quartets	51

Figure 9a: Intramolecular chain	51
Figure 9b: Intermolecular chain	51
Figure 9c: Intramolecular basket G	51
Figure 9d: Intermolecular basket G	51
Figure 10: Metal ions	53
Figure 11: DNA binding sites	80
Figure 12: Electronic states during fluorescence process	82
Figure 13: Dnase I footprinting	86
Figure 14: DNA binds to topoisomerase I	90
Figure 15: Topoisomerase II	91
Figure 16: Comet assay	97
Figure 17a: Melting point STDNA	103
Figure 17b: Representation of G-quadruplex	103
Figure 18: Melting point polydAdT-dAdT – artesunate	104
Figure 19: Melting point polydAdTdT – quercetin	105
Figure 20: Baicalein – STDNA	109
Figure 21: Baicalein – STDNA fitting	109
Figure 22: Quercetin – polydAdTdT	110
Figure 23a: Baicalein competition dialysis	114
Figure 23b: Baicalin competition dialysis	114
Figure 23c: Daidzein competition dialysis	115
Figure 23d: Puerarin competition dialysis	115
Figure 23e: Quercetin competition dialysis	115
Figure 23f: Rutin competition dialysis	116
Figure 24: Nucleic acid damage	121
Figure 25: Footprinting	122
Figure 26a: Topoisomerase II cleavage activity part 1	124
Figure 26b: Topoisomerase II cleavage activity part 2	125
Figure 26c: Topoisomerase II relaxation activity	126
Figure 27a: MCF7 comet assay	131
Figure 27b: MCF7 comet assay positive control	131
Figure 27c: MCF7 comet assay with baicalein	131

Figure 28a: Hemin titrated with DNA	133
Figure 28b: Hemin titrated with artesunate	133
Figure 28c: Hemin titrated with artesunate in presence of Fe^{2+}	134
Figure 28d: Hemin titrated with DNA in presence of artesunate	134
Figure 28e: Hemin titrated with DNA in presence of Fe^{2+} and artesunate	135
Figure 29: Titration of thioflavone	169
Figure 30: Titration of thioflavone, fitting	169
Figure 31a: Competition dialysis flavone	181
Figure 31b: Competition dialysis thioflavone	182
Figure 31c: Competition dialysis azaflavone	182
Figure 31d: Competition dialysis 3'4'-dichloroflavone	183
Figure 31e: Competition dialysis 3'5'-dinitroflavone	183
Figure 31f: Competition dialysis 5-hydroxy 8-nitroflavone	184
Figure 31g: Competition dialysis luteolin	184
Figure 31h: Competition dialysis 3'4'-dihydroxyflavone	185
Figure 31i: Competition dialysis chrysin	185
Figure 31j: Competition dialysis 5-hydroxy 7-methoxyflavone	186
Figure 31k: Competition dialysis 5,7-dimethoxychrysin	186
Figure 31l: Competition dialysis 5,7-diacetoxychrysin	187
Figure 31m: Competition dialysis 7-dimethylaminoethoxy 5-hydroxyflavone	187
Figure 31n: Competition dialysis 7-dimethylaminopropoxy 5-hydroxyflavone	188
Figure 31o: Competition dialysis 7-morpholinoethoxy 5-hydroxyflavone	188
Figure 31p: Competition dialysis 7-hydroxyflavone	189
Figure 31q: Competition dialysis 7-methoxyflavone	189
Figure 31r: Competition dialysis 5-hydroxyflavone	190
Figure 31s: Competition dialysis 6-hydroxyflavone	190
Figure 32: Melting point of 3'5'-dinitroflavone	191

List of Schemes

Scheme 1: Mode of action of quercetin	33
---------------------------------------	----

Scheme 2: CYP1A1 – baicalein	137
Scheme 3 CYP1A1 – baicalin	138
Scheme 4 CYP1A1 – daidzein	138
Scheme 5 CYP1A1 – puerarin	139
Scheme 6a: Atesunate pKa	141
Scheme 6b: Baicalein pKa	141
Scheme 6c: Baicalin pKa	142
Scheme 6d: Daidzein pKa	142
Scheme 6e: Puerarin pKa	142
Scheme 6f: Quercetin pKa	142
Scheme 6g: Rutin pKa	143
Scheme 7: Different chromone possibilities	151
Scheme 8: Isoflavone synthesis	152
Scheme 9: Flavothione synthesis	153
Scheme 10: Introduction of nitrogen in the A ring	153
Scheme 11: Synthesis of 3-azaflavone	154
Scheme 12: The Baker-Venkataram approach	155
Scheme 13: The pyridine approach	156
Scheme 14: Cushman's approach	157
Scheme 15: Ares' approach	158
Scheme 16: 3',5'-dinitroflavone synthesis	159
Scheme 17: 5-hydroxy-8-nitroflavone synthesis	160
Scheme 18: Methoxylation of A ring	162
Scheme 19: Acetylation	162
Scheme 20: Mitsunobu reactions	163
Scheme 21: Tertiary amine derivatives	164

List of Compounds

Comp 1: Artemisinin	18
Comp 2: Artesunic acid	18

Comp 3: Cantharidin	22
Comp 4: Baicalein	26
Comp 5: Baicalin	26
Comp 6: Quercetin	29
Comp 7: Rutin	30
Comp 8: Daidzein	36
Comp 9: Puerarin	38
Comp 10: Favone	165
Comp 11: Flavanone	165
Comp 12: Isoflavone	165
Comp 13: Xanthone	167
Comp 14: Thioflavone	168
Comp 15: Azaflavone	168
Comp 16: 3-Hydroxyflavone	170
Comp 17: Luteolin	171
Comp 18: 7-Hydroxyflavone	172
Comp 19: 6-Hydroxyflavone	172
Comp 20: 5-Hydroxyflavone	172
Comp 21: Chrysin	172
Comp 22: 5,7-Dimethoxychrysin	173
Comp 23: 5,7-Diacetoxychrysin	173
Comp 24: 7-Methoxyflavone	173
Comp 25: 5-Hydroxy-7-methoxyflavone	173
Comp 26: 5-Hydroxy-8-nitroflavone	174
Comp 27: 7-Dimethylaminoethoxy-5-hydroxyflavone	174
Comp 28: 7-Dimethylaminopropoxy 5-hydroxyflavone	174
Comp 29: 7-Morpholinoethoxy-5-hydroxyflavone	174
Comp 30: 3',5'-Dinitroflavone	177
Comp 31: 3',4'- Dihydroxyflavone	177
Comp 32: 3',4'-Dichloroflavone	177

List of Structures

Structure 1: Flavopiridol	16
Structure 2: Flavonoid primary skeleton	25
Structure 3: Flavonoid chromane skeleton	25

List of abbreviations

5-HT2c	human serotonin receptor
DMBA	7-12-dimethylbez[<i>a</i>]anthracene
EROD	7-ethoxyresorufin O-diethylase
ARNT	AhR nuclear translocator protein
ALT	alternative lengthening of telomeres
AhR	aromatic hydrocarbon receptor
Ah	aromatic hydrocarbons
BZD	benzo-diazepine
CoA	coenzyme A
CDKs	cyclin dependent kinases
dGMP	deoxyguanosine monophosphate
DIAD	diisopropyl azodicarboxylate
DMSO	dimethylsulfoxide
FGF-1 and -2	fibroblast growth-factor
hsp	heat shock protein
HCT	human colon tumour
IgE	immunoglobulin E
IgG	immunoglobulin G
IR	infra red
IL-2	interleukine 2
LPO	lipid peroxidation
LDL	low density lipoprotein
MDA	malondialdehyde
MAO	monoamine oxidase
hepes	N-(2-Hydroxyethyl)piperazine-N'-(2-ethanesulfonic acid)
BSTFA	N-methyl-N-(trimethylsilyl)-trifluoroacetamide
NMR	nuclear magnetic resonance
PMS	phenazine methosulfate

PBS	phosphate buffer saline
PAh	polycycle aromatic hydrocarbons
KOBu	potassium tert-butoxide
pp	protein phosphatase
p-TSA	p-toluenesulfonic acid
Py	Pyridine
ROS	reactive oxygen species
GSH	reduced glutathione
STDNA	salmon testes deoxyribonucleic acid
SCLC	small cell lung cancer cell
SOD	superoxide dismutase
THF	Tetrahydrofuran
TLC	thin layer chromatography
TF	Transferring
TEA	Triethylamine
TPP	Triphenylphosphine
TFO	triplex forming oligonucleotide
TAE	tris-acetate-EDTA
TBE	tris-boric-EDTA
TE	tris-EDTA
type II EBS	type II estrogen binding site
VEGF	vascular endothelial growth-factor
XRE	xenobiotic responsive elements

Abstract

This project focused on a group of active ingredients isolated from herbal medicines, most of them flavonoids, as a foundation for the development of new anticancer drugs. Interactions between these compounds and genomic DNA, synthetic polynucleotides, or higher order DNA isoforms (triple and quadruple helical forms) have been studied using a range of physicochemical and biological techniques. The studies demonstrated that flavonoids and isoflavonoids bind to the various nucleic acid forms with weak or moderate affinities and no significant specificity, apart from quercetin that demonstrated a differential binding for G-quadruplex structures.

Rational drug design has been subsequently employed to elucidate the mode of binding and novel compounds have been synthesized in order to provide precise structure-activity related studies and result in a second generation of chemotherapeutic anticancer agents with improved properties. Interaction with DNA is thought to involve the planar ring structures. The double bond of the O in C4 in a flavone scaffold gives planarity to the molecule, and this allows the molecule to intercalate between the bases in the different nucleic acid structures. The comparison between flavone, flavanone and isoflavonoid indicates that the position of the B ring and the double bond in the C ring are important for the interactions with DNA. Introduction of nitrogen in the ring did not improve the binding but tertiary amines improved binding 100 fold. Introduction of sulfur produced two binding constants. Position 7 in the A ring of the flavones is extremely relevant for the binding to the

nucleic acids, but substitutions in the B ring did not improve the binding. Methoxylation or acetoxylation in positions 5 and 7 decreased the affinity for DNA. Novel compounds were tested for their specificity against different DNA isoforms and their anticancer activity in various tumour cell lines.

1.1.a: Cancer

The adult human is composed of approximately 10^{15} cells, many of which are required to divide and differentiate in order to repopulate organs and tissues (Mauelera *et al.*, 1999). Control of cell growth is due to different pathways working in harmony, even though some of them are not well defined. Cells which have the capacity for division are called stem cells and this ability is found on germ cells and some specific organs that require turnover. Normal human somatic cells can divide 30–50 times; the event limiting this replication is the erosion of the ends of chromosomes, which are normally capped by a repetitive six base pair sequence (TTAGGG) named telomere (Kamenetskii *et al.*, 1995).

In germ and certain stem cells, the enzyme telomerase is in charge of maintaining a normal telomere length. This enzyme is not expressed in somatic cells; therefore, after 30–50 cycles of division, the cell enters quiescence. To keep cells continuously active, some pathways must be maintained. These pathways receive and process growth-stimulatory signals transmitted by other cells. Cell-to-cell signalling generally begins when one cell secretes growth-factors. After this event, the proteins move through the extra cellular matrix and bind to the specific receptor on the surface of the nearby cell.

When the growth-factor attaches to the receptor, the interaction conveys a proliferative signal to proteins in the cytoplasm. These downstream proteins emit stimulatory signals to a succession of other proteins. Transcription-factors respond by activating a group of genes that help the cell through its growth cycle.

Normal cells have certain characteristics namely, the ability to:

- reproduce an exact copy of themselves
- terminate reproduction at the appropriate time
- attach to neighbouring cells
- self destruct if they are damaged
- specialise or mature

Cancer is the result of the accumulation of cells that can move, survive and divide by passing the body's normal control mechanisms, and its incidence increases dramatically with age. One of the main characteristics of cancer is its complexity. Clinically, cancer appears as a diverse set of illnesses with inappropriate cell growth (Hanahan *et al.*, 2000). Certain mutations play critical roles in programming the malignant state; some mutations are inherited, while others are caused by exposure to radiation or to mutation-inducing chemicals. Mutations can also occur spontaneously as a result of mistakes during replication. When cells acquire mutations in specific genes that control proliferation, such as proto-oncogenes or tumor suppressor genes, these changes are copied with each new generation of cells (Aerssens *et al.*, 2001).

The key features of a malignant clone are:

- immortality – the cells do not mature and do not die
- independence – the clone does not rely on signals from other cells to survive or to divide

- mobility – ability to violate boundaries between anatomical compartments and to seed remote colonies (metastasis)
- subversion – malignant tumours inhibit components of the immune system, and may influence non-malignant cells to create a favourable milieu for the cancer cell
- instability – a characteristic of virtually all malignancies is that they spin off ever more genetically aberrant sub-clones
- angiogenesis induction – malignant tumours, and possibly some benign tumours have the capacity to induce the growth of new blood vessels to nourish the developing tumour (Boveri, 1914)

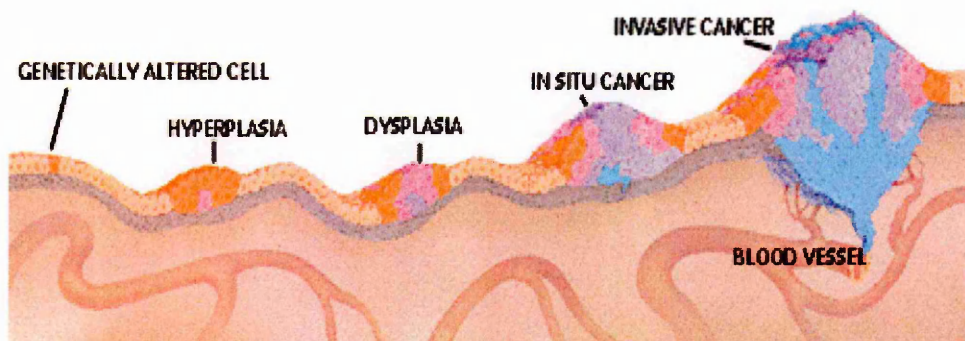


Figure 1: Development of cancer. A genetically altered cell gives rise to an accumulation of altered cells that can survive by passing the body’s control mechanism forming an *in situ* cancer that can form metastases in the individual’s body if these cells enter the blood vessels and disperse into other organs (Weinberg *et al.*: “When cancer arises”, *Scientific American*, 62-70, 1996).

1.1.b: Cell Cycle and Apoptosis

The cell cycle is a sequence of stages during which DNA is copied, the fidelity of that copying is checked, the cell repairs any errors (or undergoes apoptosis if they are irreparable), and the new DNA must be packaged into chromosomes and distributed within the cell such that each daughter cell will receive an appropriate complement. All this takes some hours in the normal cell, and in cancer cells the division time is frequently faster (up to 5 times).

The cell cycle is composed of 4 stages (Vourc'h *et al.*, 1993), see Figure 2:

- G1 (gap 1): the cell increases its size and prepares to copy its DNA by synthesis of proteins and molecules
- S (synthesis): the cell copies the DNA and enables itself to duplicate chromosomes
- G2 (gap 2): the cell prepares for mitosis by synthesis of proteins
- M (mitosis): the parent cell divides in half to produce two cells

The majority of cells, when not dividing or preparing to divide, are in G0 or rest phase. Entry into the cell cycle is controlled by a group of regulatory compounds (cyclins) – these in turn transmit their messages to proteins called cyclin dependent kinases (Knudson, 2001).

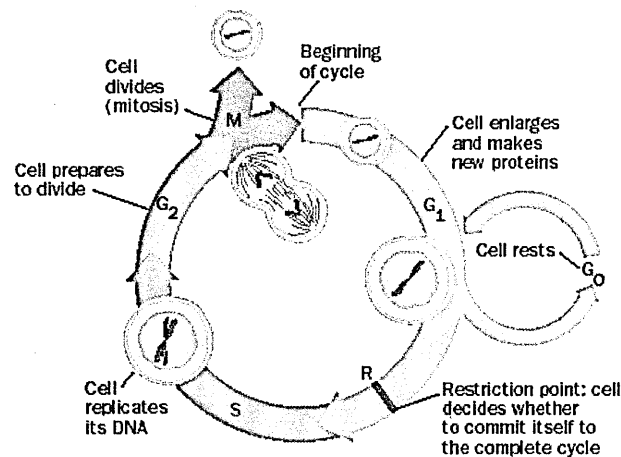


Figure 2: Cell cycle stages (Weinberg *et al.*: “When cancer arises”, *Scientific American*, 62-70, 1996).

The cell cycle programs this elaborate succession of events by using various molecules. The two essential components, cyclins and cyclin-dependent kinases, associate with one another and initiate each of the stages of the cell cycle.

The last stage in a cell’s life cycle is cell death. There are at least two distinct forms of cell death:

- necrosis: here a whole group of neighbouring cells die spilling out their contents which excites an inflammatory response
- apoptosis: here an individual cell packages its internal contents, breaks down its DNA and then displays markers on its surface promoting phagocytic cells to come and clear away the debris (Krontiris *et al.* , 1995)

There is no inflammatory response to apoptosis which is a vital physiological process. This is probably because apoptosis is the mechanism whereby the body eliminates cells that have acquired defects in their genome. This is a vital part of the

defences against cancer. There are several apoptosis-based anti-cancer agents currently under development. Although most cancer therapies depend to some extent on the induction of apoptotic pathways, these therapies are designed specifically to trigger apoptotic pathways. In the human genome there are approximately 3 billion base pairs which must be accurately replicated each time a cell divides. A proof-reading and error correction pathway ensures the accuracy of this process; this is so accurate that the 3 billion base pairs genome will only change by about 10-20 bases a year. A back-up system to ensure the integrity of the genome assesses any errors and ensures the success of the dividing cell in correcting these. If the cell fails this assessment, the apoptotic pathways are triggered and the cell self destructs. It is only if both the DNA repair and the apoptosis pathways are defective or suppressed that a cell can become malignant (Hahn *et al.*, 1999).

1.1.c: Signalling pathways

Genes are carried in the DNA molecules of the chromosomes. A gene specifies a sequence of amino acids that must be linked together to make a particular protein. The protein then carries out the work of the gene. When a gene is switched on, the cell responds by synthesizing the encoded protein. Mutations in a gene can disrupt this activity. Cells in a tumour descend from a common cell that at one point initiates inappropriate reproduction. Furthermore, the malignant transformation gives rise to the accumulation of mutations in specific classes of genes (Bertram *et al.*, 2001).

Four classes of genes play major roles in triggering cancer (Weinberg *et al.*, 1996):

- proto-oncogenes encourage growth whereas tumour suppressor genes inhibit it. When mutated, proto-oncogenes can become carcinogenic oncogenes that drive excessive replication. Some oncogenes force cells to overproduce growth factors, and others perturb the signal cascade
- oncogenes typically act in a dominant fashion and can contribute to malignant transformation. They frequently code for tyrosine kinases (internal messengers), which act as intermediaries between the signal received by growth factor receptors at the cell surface and the sites within the nucleus where genes are switched in response to those growth signals. Usually, the normal function of an oncogene falls within one of four gene families:
 - growth factors
 - cell surface receptors
 - transcription factors
 - signal transmission proteins

Growth factors are normally produced by one cell to regulate the behavior of another cell; if a cancer cell develops the ability to produce its own growth factors it becomes independent of external signals. Under normal circumstances there are three types of growth factor regulation:

- endocrine (is released into the circulation and regulates behavior of distant cells)
- paracrine (acts on a close neighbour of the secreting cell)

- autocrine (releases a growth factor which can bind to receptors on the same cell) (Bertram *et al.*, 2001)

When a cell, which should be regulated by endocrine or paracrine growth factors, acquires the capacity for autocrine growth factor secretion it may become capable of autonomous division. In some cases cancer cells will secrete paracrine growth factors so that they stimulate each other's growth.

- tumour suppressor genes contribute to cancer when they are inactivated by mutations. Tumour suppressor genes are negative regulators of cell division. They are necessary for the effective operation of DNA repair mechanisms. On proof reading of DNA, if anything above a minimal threshold of errors is met, pathways are initiated which put division on hold while DNA repair is attempted. If repair is unsuccessful, the cell initiates apoptosis and sacrifices itself to save the other cells. If tumour suppressor genes are absent or defective then arrest of the cell division process may fail to occur and the cell may generate a clone of faulty daughter cells. One of the most important tumour suppressor genes is called p53, which monitors stress (like anoxia, insufficiency of nucleotides for DNA synthesis, inappropriate inactivation of oncogenes and DNA lesions) and directs the cell towards an appropriate response (Levine *et al.*, 1997).
- DNA repair genes are the fourth class of genes important for tumour development. Genomic instability is a virtually invariant feature of cancer cells. If it is assumed that loss of stability of the genome is an early event in malignant transformation, then the subsequent rate of accumulation of

mutations will be much higher. As in other cases, the DNA repair genes are highly conserved across species, implying that they emerged very early in eukaryote evolution and are of great importance to the cell. There are various different pathways to DNA repair; which pathway is activated depending on the exact nature of the defect in the DNA molecule. In some forms of DNA damage the two strands will no longer fit together (DNA mismatch). The repair mechanism can identify the original strand because it carries methyl tags which identify it while the daughter strand does not acquire these tags for some minutes after copying occurs. During this time the repair machinery compares the two strands and attempts to correct any errors detected (Westwell *et al.*, 2001).

To ensure a satisfactory supply of nutrients necessary for continued growth, and to eliminate products of metabolism which would potentially be lethal, cells create a new network of vessels and capillaries. This process is called angiogenesis and occurs through the invasion of endothelial cells from existing vessels in response to multiple extra cellular signals such as vascular endothelial growth-factor and fibroblast growth-factor. This process is controlled and balanced by inhibitors of angiogenesis, such as thrombospondin (Gao *et al.*, 1995). Tumour cells enhance expression of pro-angiogenic factors as well as suppress negative regulators. Oncogenes and tumour suppressor genes are involved in both processes. Immortality is an escape from senescence and deregulation of cell cycle and proliferation programmes.

1.1.d: Therapies

There is a range of different therapies (Hurley, 2000) for treating cancer, summarised as follows:

- surgery: removal of a localised tumour.
- chemotherapy: treatment of cancer with anticancer drugs. It is often used to treat patients with cancer that has metastasized and can be used as an adjuvant after surgery.
- radiotherapy: exposure of the tumour cells to radiation from a radioactive substance / source.
- angiogenesis inhibitors: these prevent the construction of new blood vessels for the transport of oxygen and nutrients that rapidly dividing cancer cells require.
- immune and vaccine therapy: treatment to stimulate and restore the immune system to fight the cancer cell. It normally employs antibodies and vaccines.
- bone marrow and peripheral blood stem cell transplantation: stimulation using growth factors of growth of stem cells in a donor blood, which are isolated and transplanted into the bone marrow of the patient, to stimulate the growth of healthy new cells.
- gene therapy: technique for correcting defective genes responsible for disease development. A normal gene is inserted into an abnormal gene (from cancer cells). For delivering the gene, a carrier vector is used (usually a virus).

- laser and photodynamic therapy: investigational technique that employs a photosensitizer (e.g. haematoporphyrin), light sources (lasers), and oxygenation of tissues.

Chemotherapy is capable of combating the most widespread of metastases. By entering into the bloodstream, the chemical compounds are able to disperse throughout the body and attack cancer cells. Chemotherapy is not without its side effects, and one of the most problematic aspects of creating an anti-cancer agent is identifying a way to kill only cancerous cells. Therefore, a group of agents that work via different mechanisms has been developed. Unfortunately, most of the chemicals that have been found to be successful anti-cancer agents are extremely toxic and must be administered very carefully. The side effects incurred are numerous and include fatigue, hair loss, anemia, vomiting, diarrhea, nausea, and, more seriously for the patient, decreased resistance to infection, increased likelihood of hemorrhaging and a possible need of blood transfusions and kidney – liver – heart failure. Many of these effects are temporary and can be eased by the intake of palliative medicines, but sometimes many of the side effects debilitate the patient so much that they can no longer carry on with the treatment.

1.2.a: Herbal remedies as cancer therapy

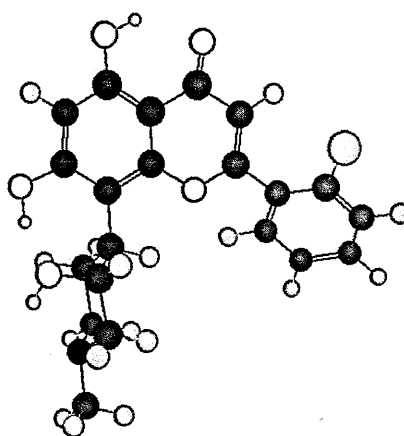
Worldwide, for many centuries different diseases have been treated with herbs or herbal extracts. These treatments are based on common and empiric knowledge. Over the course of the 20th century, medicinal knowledge became divided into

contemporary (or western) and alternative medicine. Contemporary medicine mainly refers to the use of synthetic and semi-synthetic drugs and vaccines; alternative medicine includes the use of herbal medicines. The action of such herbal remedies is due to one or more active ingredients with therapeutic properties. In the constant search for new medicines, these active ingredients have been put under scrutiny for their therapeutic effect or have formed the basis for the generation of novel compounds with improved therapeutic properties.

Plant therapy was the first medical system to be used to diagnose, treat, and prevent illnesses (Nestler, 2002). Over the centuries, plants have been used to treat countless conditions, such as obesity, diabetes, high cholesterol, male (Becker *et al.*, 2000) and female fertility disorders, Alzheimer's disease, digestive disorders, recurrent cystitis, allergies (Armstrong *et al.*, 1999), sinusitis, addictions, pain (Lee *et al.*, 2001), menopausal symptoms, osteoporosis, arthritis, infections, sleep disorders, stress, constipation, and more recently as chemo-preventative and antineoplastic agents (Wong *et al.*, 2001; Yuan *et al.*, 2000).

Plants are considered a vast source of anticancer agents (Craig *et al.*, 1999) and several studies have been conducted since the 1950s to test natural and synthetic substances for antiproliferative properties. The compounds extracted from plants belong to various classes of molecules, including flavonoids, phytoestrogens, polymers, carbohydrates, terpenes. Some of these molecules have proved to be powerful agents against various conditions and some of them have formed the basis for new therapeutic agents (Baguley *et al.*, 1981). Of the tested compounds, earlier discoveries include the vinca alkaloids from Madagascar periwinkle; etoposide

(Kimchi-Sarfaty *et al.*, 2002), teniposide (Zhou *et al.*, 2002), semi synthetic derivatives of epipodophylotoxin (Kosmas *et al.*, 2002) extracted from *Podophyllum*. More recently, taxanes and camptothecins (Engin *et al.*, 2002) attracted attention as new anticancer agents. Another group of agents is constituted by flavonoids. They are a large chemical class in the plant kingdom, with over 5,000 different flavonoids described. One flavonoid to receive a significant attention as a potential anti-cancer agent is flavopiridol (Aventis) (Structure 1). This semi-synthetic compound (it is an N-methylpiperinidyl, chlorophenyl flavone) is based on a compound extracted from *Rohitukine*, and is a potent cyclin-dependent kinase inhibitor capable of producing mitotic arrest in either G1 or G2 (Murthi *et al.*, 2000).



Structure 1: Flavopiridol (www.oup.com/.../ch18/ch18_fig70flavopiridol.jpg , 20/07/2006)

Various studies show flavonoids as a chemical class offering an important approach to cancer therapy, as they target and regulate a wide range of enzymatic pathways and signal transduction mechanisms in human cells. Flavonoids also appear to be relatively discriminating, acting predominantly on dysfunctional cells (Traganos *et al.*, 1992).

Finally, another class of compounds, isolated from plant extracts, that has found use in disease treatment is the terpenoids. Examples from this family are artemisinin and artesunate (refer to next section for a full description) which have been used in the treatment of malaria.

Furthermore, terpenoids have been shown to increase tumour latency, decrease tumor multiplicity, elicit a significant reduction in total cholesterol concentration and act as a strong antioxidant. Tumour cells synthesize and accumulate cholesterol faster than normal cells; therefore the use of terpenoids in cancer therapy would affect tumour growth without producing any change in blood lipid concentrations (Zheng *et al.*, 1992).

Due to their potential as anticancer agents, in this project we have selected for preliminary studies two main families of natural extracts:

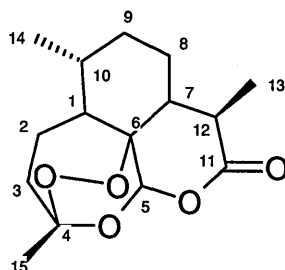
- terpenoids: from this group we studied artemisinin, artesunate and cantharidin
- flavonoids: baicalein, baicalin, daidzein, puerarin, quercetin and rutin

1.2.1.a: Terpenoids

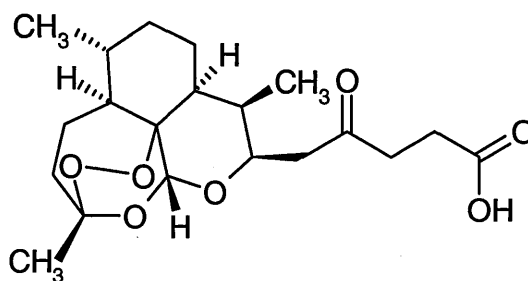
1.2.1.b: Artemisinin and artesunate

Artesunate or artesunic acid is the most widely available and widely used of the artemisinin derivatives. These drugs have become an essential component of the treatment of multidrug resistant *Falciparum malaria*. Artesunate (Compound 2) is a

semi synthetic derivative of artemisinin (Compound 1). For structure see compounds 1 and 2.



Compound 1: Artemisinin



Compound 2: Artesunic acid (artesanate)

These compounds belong to a molecular group named sesquiterpene endoperoxides. Artemisinin and its derivatives are difficult to identify by standard spectrophotometric methods, because they have no distinct UV/Visible spectra or fluorescent properties (Batty *et al.*, 1996; Green *et al.*, 2000). Artemisinin and artesunate (usually as Na-artesunate) have a range of applications in health science, even though the mode of action of the compounds is not yet defined. They can be used in the recovery of the immune system after a disease (Singh, 2001), because

they have been found to increase the production of IL-2 (interleukin 2) from mouse splenocytes stimulated with ConA after bone marrow transplantation.

As an antimalarial drug, artesunate coordinates to ferriprotoporphyrin monomers in erythrocytes blocking the formation of hemozoin, thus allowing a significant concentration of heme-antimalarial complex to remain in solution, from where it makes a plasmo-diotoxic effect by catalysing the formation of reactive oxygen species (Campanale *et al.*, 2003). The nature of the iron atom environment in the drug complexes is of prime importance since the iron is the redox centre of the molecule and thus the catalytic point at which oxygen activation will occur. Artesunate and artemisinin seem to produce reactive oxygen species like hydroxyl radicals. This activity could be responsible for the formation of DNA strand-breaks. A study involving depletion of glutathione would indicate the formation of free radicals and subsequent DNA strand breaks as a mechanism of action. The glutathione redox cycle is a detoxification pathway for the elimination of DNA damage and the alkylation of proteins (Ho *et al.*, 1992). The redox cycle catalyses the reduction of H_2O_2 and other hydroperoxides (Ho *et al.*, 1992).

In vertebrates, an iron transport system involves a specific interaction between the serum iron binding protein transferrin and a cell surface transferrin receptor. This interaction results in the facilitated transport of iron across cell membranes. Due to their high rates of division, most cancer cells express a higher cell surface concentration of transferrin receptors than normal cells and have high rates of iron intake. Therefore, cancer cells would be more susceptible to the cytotoxic effect of

artemisinin and its derivatives under conditions of high iron availability (Batty *et al.*, 1996; Efferth *et al.*, 2000).

An experiment using dihydroartemisinin (with an OH group in carbon 10) on a normal breast cell line and on a human breast tumour cell line with epithelial cell morphologies, using holotransferrin as supplier of iron, revealed a synergistic activity between the artemisinin derivative and iron (Reizenstein *et al.*, 1999). In other experiments involving holotransferrin combined with artemisinin and using human lymphoblastoid cell lines, the drug proved to be less effective as measured by cell death. Considering this result, an *in vivo* experiment was designed to determine the selective cytotoxic effect of oral administration of artemisinin and ferrous sulfate on the growth of implanted fibrosarcoma in rats. The experiment showed that the combination of artemisinin and ferrous sulfate acts together to slow down cancer growth. However, neurotoxicity has been reported with certain analogues of artemisinin (Moore *et al.*, 1995).

Different mechanisms could be used to explain the results obtained from different cell lines. A study performed on ovarian carcinoma cell lines showed no cytotoxicity with artemisinin derivatives containing carbonyl and carboxypropyl groups (probably because of a negative charge). However, deoxoartemisinin (with a methylene group in the C10 position) showed an antitumour effect in the same cell line, indicating that lipophilicity might be closely related to their cytotoxic activity. This explanation, however, can not be extended to all cases. In human epidermoid carcinoma, it seems that carbonyl oxygen of artemisinin acts as a hydrogen bond donor and thus artemisinin is able to form hydrogen bonding with tumour target proteins to improve

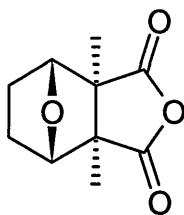
cytotoxicity (Lee *et al.*, 2000). Experiments using leukaemic cells show that artesunate induces apoptosis. The appearance of an additional A_0 phase at lower concentrations is characteristic of cells treated with the drug, even though antineoplastic activity has not been proven (Efferth *et al.*, 1996). This correlates with the fact that artesunate is active in leukaemia and colon cancer cells *in vitro*, as well as in renal, melanomas and central nervous system tumors. Compared with a regime composed of cyclophosphamide, methotrexate and vincristine, artesunate is more active for breast cancer treatment (Efferth *et al.*, 2001).

The necessity of iron for enhancing the antitumour activity of artesunate and artemisinin, allowed the study of different targets, like transferrin receptors for the iron-carrying protein (TF). This enhancing of activity occurs in only a few types of human cells like basal epidermal keratinocytes, pancreatic islet cells, and liver parenchyma. The receptor is more abundant in tumor cells that are rapidly proliferating, in particular drug-resistant cells. Since the ligand-bound TF receptor is internalised, tumor cells exposed to TF may have increased cellular Fe^{2+} concentrations. As Fe^{2+} is necessary for activation of artesunate cytotoxicity, this suggests a hypothetical strategy for the use of the compound in drug-resistant cells: preload the cells with TF and then expose them to artesunate. A study testing this hypothesis in drug-sensitive and drug-resistant (that have double concentration of TF receptors) SCLC cells, showed that artesunate induced the gradual formation of DNA fragments in the cells (pro-apoptotic) which was confirmed by terminal deoxynucleotidyl transferase-mediated dUTP nick-end labeled (TUNEL, method indicating apoptosis) staining (Sadava *et al.*, 2002). The same principle was used in a

holotransferrin treatment on breast cancer cells (Adams *et al.*, 1996) and in implanted fibrosarcomas in rats (Beekman *et al.*, 1997). The results obtained indicate that an uptake of ferrous sulfate or ferrous citrate makes cells more susceptible to the cytotoxic effect of artemisinin and artemisinin-like compounds, but nephrotoxicity was found as a side effect in some of the rats.

1.2.1.c: Cantharidin

Cantharidin (Compound 3) has been isolated from the dried body of the Chinese blister beetle *Mylabris phalerata Pallas*. Cantharidin showed the effect of producing congestion in the urethral mucosa, and because of this effect has been used in the treatment of impotence and as an aphrodisiac. Recent studies showed cantharidin to have antitumour activity, increasing the number of leucocytes and being a potent and selective protein phosphatase inhibitor (Wang *et al.* , 2000).



Compound 3: Cantharidin

Cantharidin showed toxic side effects like nephrotoxicity and severe toxicity to mucous membrane. Amongst the properties that cantharidin possesses, the most important is its ability to act as a protein phosphatase inhibitor (protein phosphatases are enzymes that remove phosphate groups in proteins). The result of this activity is the regulation of many different cellular processes (glycogen metabolism, calcium

transport, muscle contraction, gene expression, protein synthesis, intracellular transport, photo-transduction, cell cycle progression and apoptosis). In compounds possessing the anhydride bridge of cantharidin (or a derivative like norcantharidin), a single carboxylic acid group and a basic residue gives rise to a new class of compounds with the ability to inhibit PP1 and PP2A (McCluskey, 2001).

1.2.2.a: Flavonoids and isoflavonoids

The most powerful antioxidants are to be found amongst the flavonoids and 18 flavonoids are now known for having 20 times the potency of vitamin C and 50 times the potency of vitamin E. They are essential for processing vitamin C and are needed to maintain capillary walls as well as protect against infection (Tucker, 2003). It is possible that the inhibition of oxidation of low density lipoprotein supports their antioxidant and antibacterial properties. They also inhibit inflammation by decreasing the release of inflammatory mediators and stabilizing cell membranes. Many flavonoids possess antifungal properties, especially the nonpolar polymethylated flavones and the prenylated isoflavone. In mammalian biology, flavonoids have been implicated in immunity, inflammation and carcinogenicity. *In vitro*, they inhibit the activity of a number of enzymes including histidine decarboxylase, alleviating histamine-induced gastric acid secretions; hyaluronidase, responsible for the breakage of glucosaminidic bonds involved in tumour cell invasiveness and hypersensitivity phenomena; protein kinase C (serine / threonine phosphorylation) involved in a wide range of cellular activities including tumour promotion, mitogenesis, inflammation and T lymphocyte functions; and lipoxygenase which metabolises arachidonic acid released from membrane phospholipids to vasoactive leukotrienes that are involved in

signal transduction and cell division processes related to immune systems and activated by hormones, neurotransmitters and growth.

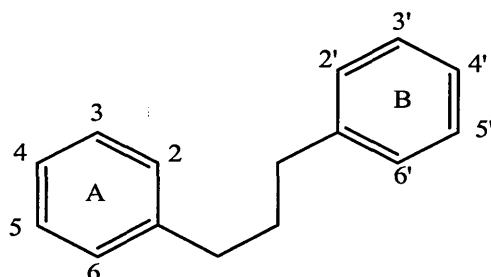
In general they inhibit carcinogenesis by acting as blocking agents via:

- inhibiting metabolic P450 mediated activation of the carcinogen to its reactive intermediates
- inducing the enzyme involved in detoxification of the carcinogen, and / or
- binding to reactive forms of the carcinogen.

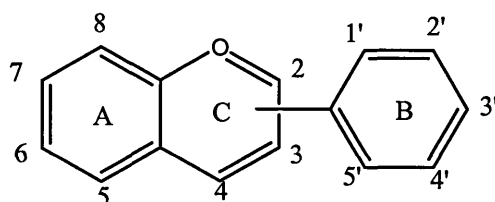
They are known to inhibit several biochemical events associated with the transformation of non-malignant fibroblasts to sarcoma cells (Ibrahim, 2002). Many flavonoids exhibit high radical scavenging activity indicating that a diet rich in these flavonoids would reduce cancer promoting actions of these radicals and possibly other diseases and conditions caused by oxygen related radicals (Sawa *et al.*, 1999).

Flavonoids and isoflavonoids, found in higher plants constitute a large class of compounds containing a number of phenolic hydroxy groups attached to ring structures. Many of them form the flower pigments in most angiosperm families but they can be found in all parts of the plant. Flavonoids are multifunctional and can act as reducing agents, hydrogen donating antioxidants and singlet oxygen quenchers (Rice-Evans *et al.*, 1996). Amongst the medicinal properties, they are reported to have free radical scavenging activity and anticarcinogenic effects, to be anti-inflammatory, antiviral and antiallergic agents, and to inhibit several steps in the cell cascade (Ho *et al.*, 1992). The primary structure posses 15 carbon atoms and involves two benzene rings joined by a linear three carbon chain see Structure 2. The

formation of the C ring (Structure 3) gives rise to a family of compounds, amongst which we can find isoflavonoids, flavones, flavonols, flavanones, anthocyanines, etc.



Structure 2: Flavonoid primary skeleton, can be represented as a $C_6 - C_3 - C_6$ system



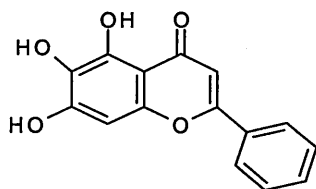
Structure 3: The flavonoid chromane skeleton. The B ring can be positioned at C2 as well as C3 giving rise to two families of compounds (flavonoids and isoflavonoids respectively)

All flavonoids derive their carbon skeletons from two basic compounds, malonyl-CoA (synthesized from acetyl-CoA and carbon dioxide) and coenzyme A ester of a hydrocinnamic acid. Both of these precursors are derived from carbohydrates. The aromatic ring B and its adjacent 3-carbon side chain are derived from L-phenylalanine via the shikimate pathway, whereas ring A is formed by the head-to-tail condensation of three acetate units via the polyketide pathway that is proposed for

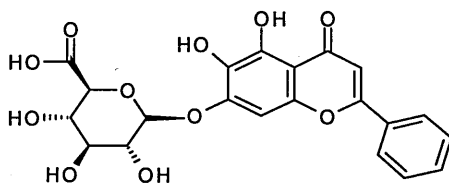
the biosynthesis of phloroglucinol and resorcinol derivatives (Charron *et al.*, 2000), leading to the formation of a C15 chalcone intermediate (Martens & Forkmann, 1998).

1.2.2.b: Baicalein and baicalin

Flavonoids are phenolic compounds isolated from plants, and several have been documented to be effective in preventing cancer. Baicalein (Compound 4) and its derivative baicalin (Compound 5), two flavones extracted from the root of *Scutellaria baicalensis*, are widely used as health supplements and herbal medicines in Asia. One of the supplements is the well known PC-SPES (PC is for prostate cancer and SPES is for hope), which is a potent eight - herb formulation sold directly to consumers that has promising efficacy in the treatment of prostate cancer (Marks, *et al.* 2002).



Compound 4: Baicalein



Compound 5: Baicalin

The preventive cancer activity of these flavones may be due to an interaction with drug metabolizing enzymes. This interaction has been under study on PAH (polycyclic aromatic hydrocarbons that are capable of forming carcinogen-DNA adducts), Ah receptors (located in cytosolic compartments) and the AhR nuclear translocators. The complex can initiate transcription of genes that contain cis-active lipophilic xenobiotic responsive elements in their promoter region. The cytochrome P450 family of enzymes (monooxygenases that generally act to protect cells) are the downstream responsive genes of AhR transactivation. The enzymes CYP1A1 and CYP1B1 are expressed in normal and cancer tissue and transform procarcinogens to carcinogens. Their inhibition is beneficial in the prevention of PAH-DNA adducts. Baicalein has shown effects on CYP 1A1 and CYP1B1 and shown an antiproliferative effect on prostate cancer, hepatoma cells and vascular smooth muscle cells. These effects have been measured by EROD (7-ethoxyresorufin O-ethylase) assay in breast cancer cells, using 7-12-dimethylbenz[*a*]anthracene (DMBA) as DNA damage inducing agent. The result obtained in this experiment allowed the conclusion that baicalein is a competitive inhibitor of EROD and decreases the expression of CYP1A1 & CYP1B1 through the interruption of AhR transactivation (Chan *et al.*, 2002).

Interaction with DNA has been supposed on a basis of an almost planar structure, which was determined by crystallography (Rossi *et al.*, 2001). The compound exists in an almost planar conformation with a C-2-C-1' bond distance of 1.476 Å. The position of the three hydroxyl groups maximizes intramolecular hydrogen bonding, and each of the hydroxyl hydrogen atoms is a donor in a three-center hydrogen bond.

The carbonyl oxygen, O-4, is an acceptor in an intramolecular hydrogen bond (with OH-5) and is also an acceptor in an intermolecular hydrogen bond with OH-6. The planarity of the flavone framework is dependent on structural and/or electronic forces that stabilize the negative charge on the exocyclic oxygen atom, O-4.

Baicalein and baicalin were found to have different activities, showing different modes of action. Both compounds exhibit inhibition of DNA polymerase. The glycosylation of hydroxyl groups on the flavones resulted in compounds that behaved gradually as weaker inhibitors as the number of substituents increased (Spampinato *et al.*, 1994).

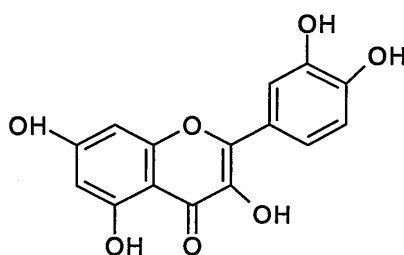
The antitumour activity of baicalin has been studied on different prostate cancer cell lines. The experiments were performed using growth inhibition assay, fluorescent staining of nuclei, cytotoxicity assay and TUNEL labeling, analysis of DNA fragmentation and Western blot analysis. As a result, baicalin was demonstrated to be cytotoxic to the majority of the studied prostate cancer cell lines. The inhibition effect was found in concentrations $> 200 \mu\text{M}$. The presence of baicalin in the nucleus was confirmed by the staining of apoptotic cells. It was found that baicalin given orally is not toxic, but intramuscular injection can cause fever and muscle aches (Chan *et al.*, 2000; Hiipaka *et al.*, 2002) and it shows activity against human hepatoma cells (Motoo *et al.*, 1994).

Structural studies in breast cancer cell lines showed that hydroxyl groups at positions in carbons 3' and 4' decreased antitumour activity. Apparently, there must be an optimal pattern of hydroxylation that is necessary for a flavonoid to have estrogenic activity. The flavones with hydroxyl substituents at carbon atoms 4' and 7' were

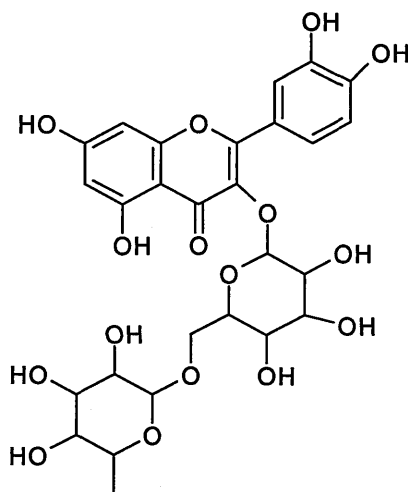
invariably estrogenic and an additional group at carbon 5' increased estrogenic activity. Despite of having more than 4 hydroxyl groups, a methoxylated substituent would abolish the estrogenic activity (So *et al.*, 1997). The antiproliferative effect may not be due to the effect of the binding to the estrogenic receptor, according to results observed in other types of breast cancer cells that do not express the estrogen receptor. In these, the flavones inhibited protein kinase C activity in intact cells (So *et al.*, 1996; Ferriola *et al.*, 1989).

1.2.2.c: Quercetin and rutin

Quercetin and rutin (Compounds 6 and 7 respectively) are present in *Artemisia scoparia* (Janbaz *et al.*, 2002). They are found to be potent as chemopreventative agents (Gerhause *et al.*, 2003) and are used in a wide range of conditions. They are sold as supplements and drugs. Between them, quercetin is the most known and different studies have been performed to test their activities.



Compound 6: Quercetin



Compound 7: Rutin

Quercetin is an inhibitor of HIV-1 protease (Xu, 2000) and of the Vpr gene product (the Vpr gene encodes a protein which induces arrest of cells in the G2 phase of the cell cycle). Quercetin also presents a mechanism of action in haem catabolism (Khong *et al.*, 1990; Kopach *et al.*, 1980). As a flavonoid, quercetin has been tested for activity as an antiallergic and anti-inflammatory agent. Studies showed that quercetin inhibits IgE (immunoglobulin E) mediated release from mast cells, IgG mediated histamine and SRS-A (slow reaction substance of anaphylaxis) from chopped lung fragments, as well as effective inhibition of AE5 – lipoxygenase (Welton *et al.*, 1986). Furthermore, rutin also possess hepatoprotective activity (La Casa *et al.*, 2000).

Anticancer activity has been under study in different *in vitro* and *in vivo* assays. Experiments showed that quercetin inhibits the growth of several cancer cell lines and the antiproliferative activity of the molecule is mediated by a type II estrogen binding site.

An investigation of the effect of quercetin and cisplatin, alone and in combination, on ovarian cancer cells showed a synergistic antiproliferative activity (Scambia *et al.*, 1990).

The same result was found on human promyelocytic leukemia cells as well as in murine leukemia cells (Cipak *et al.*, 2003). Probably one of the modes of action of quercetin for its antitumour activity is the influence on mitosis (Gawron, 1995), as well as inhibition of mutated p53 (Avila, 1994).

This last result was observed on breast cancer cells where an accumulation of cells at the G₂ – M phase was observed. The cytotoxic effect of quercetin would be via an intracellular metabolic activation of the compound to *o*-quinone (Segura-Aguilar *et al.*, 1999).

Quercetin appears to be cell-type specific, displaying a decrease in heat-induced synthesis of hsp27 (heat shock protein) and hsp70 in hepato carcinoma cells.

The drug displayed inhibition of HSF (heat shock factor) (1 and 2), DNA-binding activity and HSF expression (Hansen *et al.*, 1997).

Derivatives of quercetin have been under investigation on human myelogenous leukemia cells and adriamycin-resistant human myelogenous leukemia cells. As a result, a rank order of anticancer promoting activity of flavonoid derivatives has been established as: pentaallyl ethers > pentamethyl ethers > pentaethyl ethers > pentapropyl ethers > pentabutyl ethers (Ohtani *et al.*, 2002).

Considering the flavonol structure, quercetin could induce apoptosis by the release of cytochrome c to the cytosol, by procaspase-9 processing, and through a caspase-3-dependent mechanism (Lin M *et al.*, 1999).

The activity of quercetin on breast cancer cells has been extensively investigated. Inhibition of protein, DNA and RNA synthesis has been observed, as well as an increase in the amount of intracellular reduced glutathione content. Alteration on the cell morphology of the cells after a 24 h exposure to 25 μ M of quercetin has been observed.

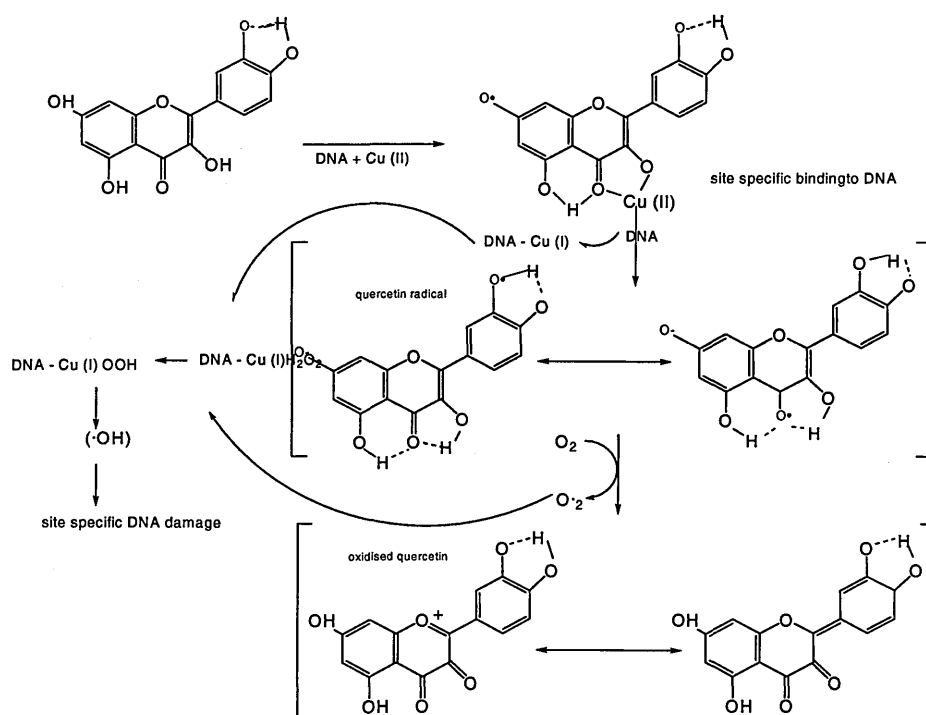
Quercetin seems to inhibit the activity of DT-diaphorase, NADPH cytochrome *c* reductase and glutathione reductase (Rodgers *et al.*, 1998). Quercetin appears also to inhibit the transcription with RNA polymerase II. This was observed in the transcription of α -amanitin-sensitive and resistant transcription in permeable cells (Rodgers *et al.*, 1998).

Dietary iron may contribute to colon cancer risk by production of reactive oxygen species. To prove this premise, effects of Fe-NTA were measured with H₂O₂ in a Fenton reaction with quercetin (in concentrations of 25–100 μ M) in breast adenocarcinoma. Inhibition of damage by quercetin reflects the potential of antioxidant compounds to influence this risk factor (Nose *et al.*, 1984; Latunde-Dada *et al.*, 2002).

Quercetin is known to inhibit heat shock protein synthesis of cancer cells and has being compared with the mixture of flavonoids named Sunphenon on effects on human cholangio-cellular carcinoma cell lines. Quercetin showed an inhibitory effect on tolerance to heat shock treatment. This effect may be due to a marked suppression

of hsp72 and a delay in the reorganization of filamentous actin (F-actin) during the recovery period after the heat shock. As hsp90 could preserve F-actin structure during stress, quercetin might affect the interaction between hsp90 and F-actin without influencing hsp90 expression (Kudo *et al.*, 1999).

Quercetin has been investigated as a potential chemopreventative agent against certain carcinogens. Acting alone, quercetin showed no interaction with DNA, but in the presence of Cu (II) quercetin induced DNA damage. The most effective doses of quercetin are 20 μM , 50 μM and 100 μM . A possible mechanism is shown in Scheme 1(Yamashita *et al.*, 1999).



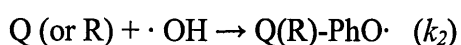
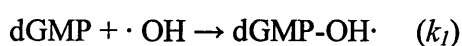
Scheme 1: The mode of action of quercetin (Yamashita, 1999)

Flow linear dichroism spectra showed evidence that quercetin can intercalate DNA. The interaction is probably due to van der Waals interactions between the most

hydrophobic segment of the flavonol (benzopyran-4-one) and the intercalation site (Zhu *et al.*, 2002), also 3' and 4' adjacent hydroxyl groups play an important role in the process of intercalation. This allows the chromophore to penetrate the DNA helix and to arrange its planar structure more or less parallel to the adjacent planes of the nitrogenous bases. However, the affinity is very low compared with that of a typical intercalating agent (Yamashita *et al.*, 1999).

Repair effects of rutin and quercetin on purine deoxynucleotide radical cations were proposed as a chemopreventative activity of the flavonols. A pulse radiolysis technique was used for testing this premise on oxidizing deoxyguanosine monophosphate (dGMP). DNA damage can be caused by ionizing radiation, UV light, chemical agents and / or reactive oxygen species formed in the normal metabolism. The primary and transient forms of DNA damage are DNA base radicals, including radical cations and anions, which are the major products of ionizing radiation or oxidizing intermediates of chemical carcinogens. These radicals may be responsible for inducing strand breaks and form stable base lesions. Quercetin and rutin act as potent antioxidants, reacting with the reactive oxygen species (with high rate constants) and producing a stable phenoxyl radical. These properties are also essential for the fast repair of purine deoxynucleotide radical cations (Solimani *et al.*, 1996; Wang *et al.*, 2001).

The mechanism of action (Zhao *et al.*, 2002; Evgeny *et al.*, 2003) could be explained by:



where the reaction probability (P) is:

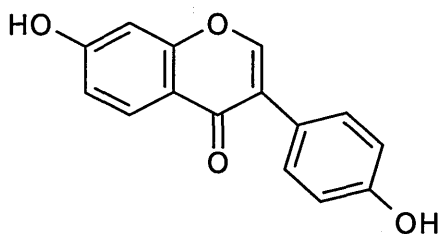
$$P = k_1[\text{dGMP}] / (k_1[\text{dGMP}] + k_2[\text{Q}]) = 0.966$$

This calculated result means that 96.6% of $\bullet\text{OH}$ produced react with dGMP to form dGMP-OH \bullet . The P of dGMP reacting with $\bullet\text{OH}$ in repair system containing 0.1mM rutin was calculated to be 97.4%. Therefore, it may be assumed that in the present repair system $\bullet\text{OH}$ reacts with dGMP predominantly to generate dGMP-OH \bullet . Addition of $\bullet\text{OH}$ to dGMP produced two types of $\bullet\text{OH}$ adducts with respect to their redox properties, oxidizing $\bullet\text{OH}$ adduct (50%) and reducing $\bullet\text{OH}$ adduct (50%). The oxidizing dGMP-OH \bullet is formed mainly by the addition of $\bullet\text{OH}$ to C4 (dGMP-4-OH \bullet) of the purine ring. With unpaired spin density located on O atom, dGMP-4-OH \bullet is oxidizing, and hence can react with quercetin and rutin. High stability of the complexes Q-PhO \bullet and R-PhO \bullet would prevent phenoxy radicals reacting with other biomolecules.

1.2.2.d: Daidzein

Daidzein (Compound 8) belongs to a variety of organic molecules named isoflavonoids.

Isoflavonoids are divided into seven categories: isoflavone, isoflavane, isoflavanone, coumestane, pterocarpane, rotenoid, coumarone and chromone.



Compound 8: Daidzein.

The majority of isoflavonoids are present in soybeans. Daidzein, amongst them, is present in the form of glycoside; esterified with malonic acid (Watanabe *et al.*, 2002). Isoflavonoids are thought to be the biologically active components in soy. They play a role in the prevention of coronary heart disease and breast and prostate cancer. Mechanisms to explain how isoflavonoids mediate beneficial effects have not yet been clearly established.

Another characteristic of isoflavonoids is their structural similarity with estrogens. They are, thus, named phytoestrogens (plant substances similar to 17-beta-estradiol with estrogenic effects (Lei *et al.*, 2002).

The antitumour activity of daidzein has been tested in order to elucidate a mechanism of action. It has been found that daidzein is active against human colon tumour cells. A study based on cell cycle progression and differentiation of murine and human cells, showed that daidzein increased the cell number at S phase and decreased the cell number at G1 phase.

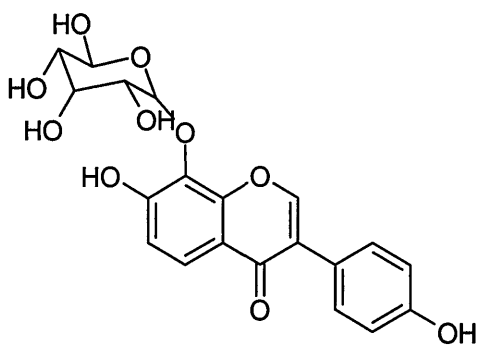
Daidzein can inhibit certain malignant phenotype of melanomas via different mechanisms, and could be a potential candidate for melanoma cancer therapy (Wang G *et al.*, 2002). Some epidemiological studies suggest a protective effect on the development of colon cancer in humans, even though this hypothesis could not be

proven in *ApcMin* mice model (Sorensen, 1998). Some dietary studies demonstrated that certain phytoestrogens are capable of reductase induction on the ratio of NADPH:quinone (NADPH is reduced β -nicotinamide adenine dinucleotide phosphate) in colon cells by promoting NADPH:quinone reductase mRNA expression. This suggests a novel mechanism by which dietary phytoestrogens may be implicated in colorectal cancer chemoprevention (Wang W *et al.*, 1998).

Other targets have also been related to the activity of daidzein. Daidzein presents the ability to induce osteoclasts directly or indirectly from their progenitors and might be a tool for the study of osteoclast differentiation (Tobe *et al.*, 1997).

1.2.2.e: Puerarin

Puerarin is the major active ingredient isolated from *Radix puerariae* (Compound 9). In China, it has long been used to treat patients with coronary atherosclerosis, because it has the effect of dilating coronary arteries. Puerarin decreases the myocardial oxygen consumption by a receptor blocking effect (Youwen *et al.*, 1999) and improves the microcirculation both in animal and in patients. Puerarin also acts by blocking the L-type calcium channels in ventricular myocytes, thus improving microcirculation.



Compound 9: Puerarin

Reactive oxygen species play an important role in the genesis and development of many diseases, such as ageing, hypertension, inflammation, shock and atherosclerosis. ROS turn LDL into oxidized LDL by oxidative modification. A new way to prevent atherosclerosis is the scavenging of free radicals and preventing LDL oxidation. To test the puerarin activity, studies were performed using a riboflavin system to generate superoxide anions, Fenton reactions to generate hydroxyl radical, hydrogen peroxide to induce strand breaks on DNA and UV radiation and Cu(II) sulfate to cause the oxidative modification of LDL. The scavenging activity on ROS, the inhibitory effects on oxidative erythrocyte hemolysis, and the inhibitory action of puerarin on the oxidative modification of LDL were studied. The results showed that puerarin is active on reactive oxygen species and inhibits the oxidative effect on modifications of LDL; it also decreases the content of malondialdehyde and enhances the activity of superoxide dismutase. Puerarin could also inhibit the oxidative erythrocyte hemolysis and decrease the production of LPO induced by hydrogen peroxide (Guerra *et al.*, 2000).

It seems that puerarin acts as an enzymatic inhibitor of oxygen radical production, mediated by the peroxidase/H₂O₂/luminol/enhancer radical reactions, rather than a

true antioxidant. A protective effect of puerarin against myocardial reperfusion injury has been shown, as well as ischemic retinopathy, since oxygen free radicals are the major culprits in these physiopathological processes (Overstreet *et al.*, 1996).

The isoflavonoid puerarin has been traditionally used to combat alcohol problems. A study using rats chronically exposed to alcohol and withdrawn, showed an anxiety-like behavior generated by a BZD agonist or a human serotonin receptor agonist in a social interaction test. Puerarin increased and induced significantly the level of social interactions in the alcohol-withdrawn rats by modifying the GABAergic (γ -aminobutyrate receptor) and serotonergic systems that underlie alcohol withdrawal symptoms (Lin R *et al.*, 1996).

1.3.a: The role of DNA

The definition of cancer chemotherapy is the use of cytotoxic drugs either to effect a cure or to prolong the life of cancer patients, on their own or as an adjuvant to surgery or radiation.

The desired effects of an antineoplastic drug are the disruption of the cell cycle in any phase and the interference with the ability of malignant cells to synthesise proteins, enzymes or cell-support chemicals.

The targets of cancer therapies are the molecules that participate in cell reactions leading a cell to a carcinogenic state or molecules vital to the survival of the cancer

cell. The three most common targets for interrupting a disease process are: enzymes, receptors, nucleic acids.

The genetic information stored in the DNA double helix is replicated with a high degree of fidelity, transcribed into messenger RNA, maintained by DNA repair, rearranged by recombination processes, and translated into amino acid sequences of proteins (this is called the “central dogma” of molecular biology (Figure 3)) (Alberts, 1994).

We can consider that attacking the DNA will produce an effect by interrupting the transcription of an undesirable protein and / or the replication of the DNA in the dividing cancerous cell.

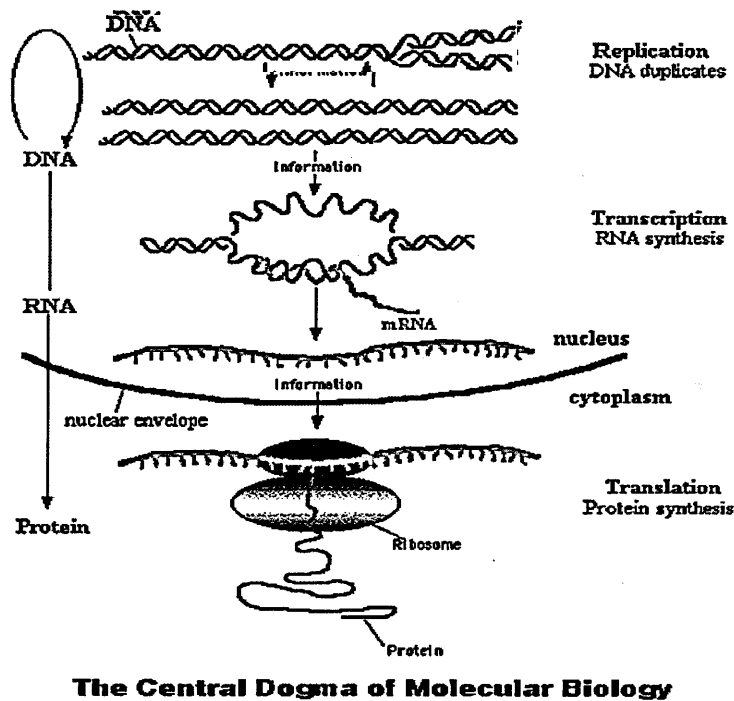


Figure 3: The “central dogma” of molecular biology
(<http://www.accessexcellence.org>, 20/07/2006)

The process starts with the replication of DNA and the transcription of the coded information by a transcription process involving synthesis of RNA. The information, as messenger-RNA and transcription-RNA crosses the nuclear membrane where is translated in the ribosomes into proteins.

Cancer cells divide rapidly and an anticancer agent's task is to prevent the cell from dividing. Each division requires the replication of the cell's DNA (S phase of the cell cycle) and the transcription and translation of genes needed for growth; therefore any drug that can attack DNA is a potential inhibitor of cancer cell growth.

1.3.b: Types of DNA interactive agents

The interaction between the DNA and a drug can be addressed according to the properties that the drug shows towards DNA. Drugs bind to DNA in the following ways:

- intercalation: a drug slips between the base pairs thereby unwinding the DNA
- covalent binding: the drug binds covalently to N2, N7, O6, etc groups. The preference for guanines can be attributed to the participation of the 2-amino group in nucleophilic substitution and addition reactions
- groove binding: the drug binds no-covalently to specific regions of the major and/or minor grooves of the DNA, such binding occurs via:
 - hydrogen bonding between the drug and the hydrogen bond acceptors / donors of the base in the major and minor groove

- close van der Waals contacts
- electrostatic attraction between drug and DNA

These ways of binding to DNA are used to describe and divide the drugs into the following different categories (Figure 4):

- alkylators: the oldest class and most widely used anticancer agents. Almost all of these molecules are direct acting or latent prodrug forms of nitrogen mustards. The prodrug forms require enzymatic activation or chemical breakdown to the active species. Alkylators like quinacrine, bind covalently to electron-rich nucleophilic moieties (Stockmana *et al.*, 2002). The most frequent site of DNA alkylation is the N-7 position of guanine; however, adducts are also formed at the O-6 and N-1 positions of guanine; N-7, N-3, and N-1 positions of adenine; the N-3 position of cytosine; and the O-4 position of thymidine (Ren *et al.*, 1999).
- intercalators: the intercalation process involves the insertion of an agent, usually a compound containing a planar, aromatic ring between the base pairs of the duplex nucleic acid, together with localization of substituents on the ring system in opposite grooves of the helix (Ren *et al.*, 1999). In the binding process, therefore, one of the side chains needs to pass through the duplex. It has been found that intercalation is a necessary, though insufficient, property for high *in vivo* and *in vitro* anticancer activity.

- crosslinking agents: these drugs are bi-functional and are able to covalently bind to DNA and link either the 2 strands of DNA covalently together or link two parts of the same DNA chain in an intramolecular way. The chemical groups capable of this are present in nitrogen mustards, nitrosoureas, hydrazines and platinum compounds.
- code reading agents: These have the ability to bind sequentially and selectively certain segments of DNA.
- double stranded breaking agents: they are usually known as a specific category of antibiotics.

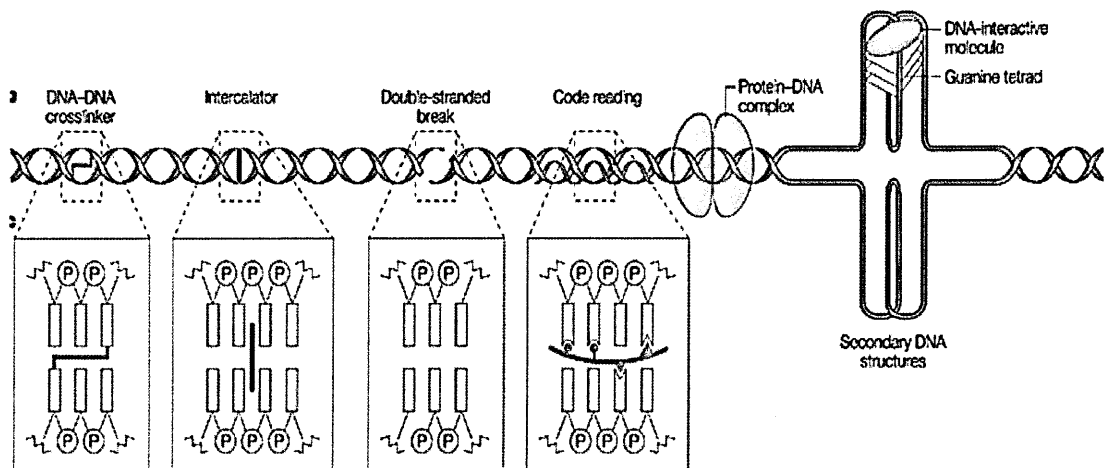


Figure 4: DNA interactive agents (Hurley, 2000). This figure clearly shows the mode of binding of a crosslinker agent, and intercalator, a double stranded break, a code reading agent and a quadruplex interactive agent.

1.3.c.1: Duplex DNA structures

Cancers mostly originate from alterations in the DNA, leading to the expression of unwanted enzymes and proteins. Targeting the DNA is one possible way to stop the cancer cells from reproducing themselves. Some types of DNA anticancer agents (cisplatin, doxorubicin) are non-selective agents, targeting the whole genome, while others are sequence selective agents permitting the interference with an undesired gene (amide linked imidazole / pyrrole oligomers) (Hurley, 2000).

Different types of DNA structures can be found in cells. In the most common duplex DNA form (Figure 5, B-DNA), the ribose – phosphate backbone is on the outside, due to the mutual repulsion of the negative charges of the phosphates; therefore the bases face inwards and pack together. The bases are associated by complimentary hydrogen bonding: A:T and G:C. The bonding C:G is stronger than A:T due to the formation of 3 hydrogen bonds instead of two as in A:T (Baguley, 1981). The two chains are held together (Figure 6) by hydrogen bonds between these complementary bases. The planes of the bases are perpendicular to the fibre axis and they are joined in pairs. One of the pair must be a purine and the other a pyrimidine for bonding to occur. If it is assumed that the bases only occur in the structure in the most plausible tautomeric forms (that is, with the keto rather than the enol configurations) it is found that only specific pairs of bases can bond together. These pairs are: adenine (purine) with thymine (pyrimidine), and guanine (purine) with cytosine (pyrimidine) (Sun *et al.*, 2003). At lower water contents the bases tilt so that the structure could become more compact leading to an unusual form of DNA (Figure 5, A-DNA). Another

unusual form of DNA is the so-called Z-DNA that appears under high salt concentrations, low pH and the DNA contains a large amount of G-C sequence.

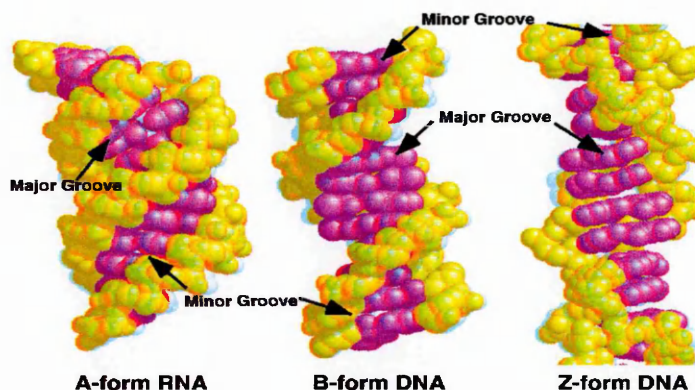


Figure 5: DNA duplexes (www.tulane.edu) in 3 possible conformations. Form A appears under dehydration, form B is the most common, and Z appears under high salt concentrations.

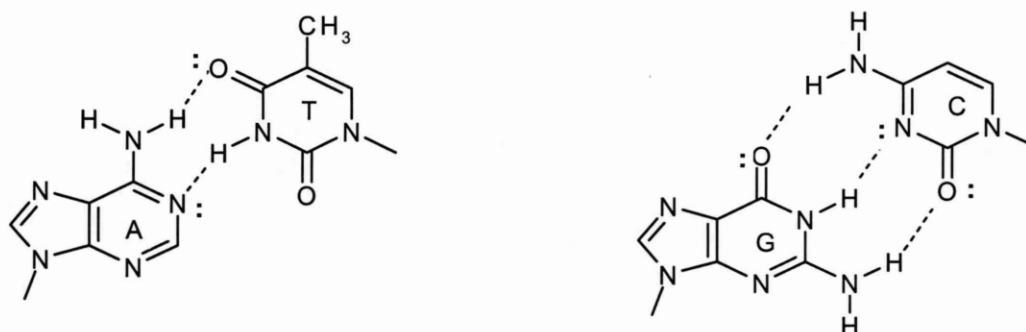


Figure 6: Hydrogen bonding (www.chembio.uoguelph.ca) between adenine - thymine and guanine – cytosine.

B-DNA is the most stable helical form adopted by random sequence DNA in physiological conditions (see Figure 5) and is the one mostly targeted by DNA interactive agents.

A-DNA is a conformation that appears under dehydrating conditions. This conformation is also stable for RNA because it avoids the steric interference of 2'-O and phosphate as well as for DNA-RNA hybrids.

Z-DNA is formed at high salt concentrations by sequences rich in GC and have alternating purine – pyrimidine pairs (GCGCATGCGC). Its relevance is still controversial (Mergny *et al.*, 1992).

1.3.c.2: DNA triple structures

Intermolecular triplex DNA only forms under certain conditions and thus its normal appearance in cells is still a matter of research. However, the formation of this unusual structure is explored as part of the antigene therapy, where triplex forming oligonucleotides have been shown to inhibit transcription of a promoter region, indicating that they could be used as selective gene repressors in cells (Spitzner *et al.*, 1995). Some drugs (NB-506) are known to stabilize these structures allowing a better repression of the genes (Ren *et al.*, 2000). The inter-molecular DNA triplex is formed when pyrimidine or purine bases occupy the major groove of the DNA double helix, forming additional Hoogsteen pairs with purines of the Watson-Crick base pairs (Figure 7). Intermolecular triplexes, formed by the addition of a sequence specific third strand to the major groove of duplex DNA, are shown to have potential as site-directed mutagens, repressors of transcription and inhibitors of replication. Antigene therapy is based on the use of triplex forming oligonucleotides to control gene transcription and replication (Jenkins, 2000).

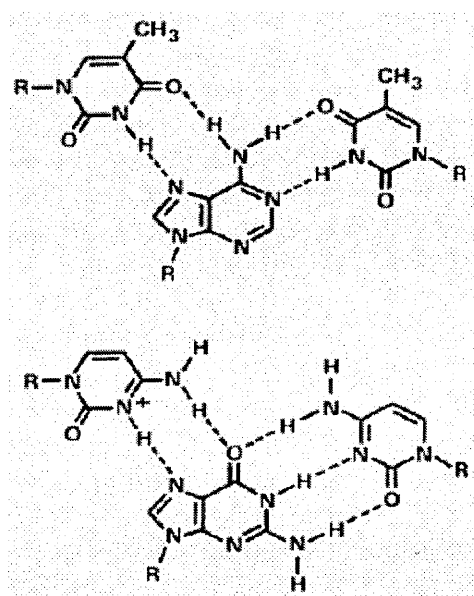


Figure 7 - Triplex base arrangements. The first arrangement is an example of TA.T triplet, the second is an example of CG.C⁺ triplet (which is protonated). The Watson – Crick hydrogen bonds are the ones between the two bases on the right (in both examples), and the Hoogsteen hydrogen bonds are located on the left. Reverse Hoogsteen bonds (antiparallel fashion) can be found when the third strand consists of purine bases (www.imbg.ku.dk)

The triplet AT:T is more stable than CG:C, the latter requiring a non-ground-state protonated form of C. There are two types of triplex motifs: parallel motif (YRY) and antiparallel motif (RRY). The parallel motif is characterised by a homopyrimidine (dT, dC) third strand that binds parallel to the homopurine strand (dA, dG) of the duplex (central strand of the triplex). This motif has two types of triplets: a T:AT triplet which is formed when a thymine in the third strand Hoogsteen base pairs with an adenine in the duplex; and a C⁺:GC triplet which is formed when a protonated cytosine in the third strand Hoogsten base pairs with a guanine in the duplex (favoured by low pH) (Lipsett, 1964). The antiparallel motif is characterised by a homopurine third strand that binds antiparallel to the homopurine strand of the

duplex. This motif has three canonical triplets: a G:GC triplet which is formed when a guanine in the third strand reverse Hoogsteen base pairs with a guanine in the duplex; an A:AT triplet which is formed when an adenine in the third strand reverse Hoogsteen base pairs with an adenine in the duplex; and a T:AT triplet which is formed when a thymine in the third strand reverse Hoogsteen base pairs with an adenine in the duplex. The canonical triplets are not isosteric (Rajagopal *et al.*, 1989).

1.3.c.3: Telomeres

The vast majority of cancers occurring in human adults are carcinomas of epithelial origin. These tumours present highly rearranged karyotypes with a high frequency of non – reciprocal translocations. These events are closely linked to cancer development by the generation of fused genes, modification of gene copy number or de-regulation of the expression of various oncogenes (O'Hagan *et al.*, 2002). Epithelial tumours derived from normal cell lineages undergo continual proliferation throughout life, even though they present low telomerase activity leading to progressive telomere shortening in these cells (Maser *et al.*, 2002). The frequency of chromosomal fusion events seems to be proportional to the frequency of rapid telomere length changes. Some chromosomes with less than 200 base pairs telomere sequence show a rapid and heterogenous increase in chromosomal instability (Murnane *et al.*, 1994).

Telomeres are complex structures comprised of higher order chromatin loop and specific binding proteins at each chromosome end. Telomeres can contain repetitive

sequences such as G₄T₄G₄, generated by telomerase, which are species dependent. Their function is to extend the genomic sequence so that the loss of nucleotides from the 3' end is harmless.

Telomere length may be maintained in cancer cells by:

- the ribonucleoprotein telomerase (a specialised reverse transcriptase) (Lingner *et al.*, 1997) or
- an alternative lengthening of telomeres (ALT) mechanism. The significance of this mechanism in carcinogenesis remains unclear (Stewart, 2002), 10% of human tumours present no detectable telomerase activity and some of them display an ALT positive mechanism, meaning that ALT + cells could induce tumours *in vivo* without excluding the possibility that some telomerase negative tumours might not have any telomere lengthening mechanism

Cytogenetic studies suggest that telomere maintenance via an ALT mechanism or telomerase activity is not equivalent in tumorigenesis efficiency (Scheel *et al.*, 2001). Inherited abnormalities of telomere maintenance may contribute to cancer and ageing (Reddel *et al.*, 2003).

In normal human cells, the telomeres contain up to 15 kilobases of tandem repeats of the hexanucleotide, TTAGGG, and this amount decreases by an average of 50-150 base pairs per cycle, this event limits the number of times a cell can divide and acts as a tumour suppressor mechanism (Desmaze *et al.*, 2003). The great majority of cancers escape from the limitations on proliferation, imposed by normal telomere shortening, via activation of a telomere length maintenance mechanism. In most

cancers, telomere length is maintained by telomerase, but some are telomerase-negative and they maintain the length of their telomeres by ALT. The telomeric DNA sequence is recognised by specific binding proteins, and they form a putative cap structure that protects the chromosome end from degradation or from attempted DNA repair. The telomere of normal and telomerase positive cells form a loop structure in which the chromosome end is effectively hidden. Uncapping results in the recognition of the telomere by the cell as a DNA break, and the probability of uncapping increases as the telomere shortens (Blackburn, 2000). Repression of telomere maintenance in ALT cell lines results in cell death or senescence, this suggests that inhibitors to telomere length maintenance mechanism may be a useful form of cancer treatment (Perrem *et al.*, 1999).

Telomere sequences are composed by four strands that associate through guanine quartets, (Figure 8); this structure is called a tetraplex or quadruplex. A central role for the whole structure is played by the single stranded 3'G – rich overhang of around 150 – 200 bases in length, which can form characteristic G-quadruplex secondary structures under physiologic ionic conditions.

DNA quadruplex and G quartets are four stranded structures, (Figure 9). They are found naturally as terminating sequences at the ends of eukaryotic chromosomes or telomeres (Wang J, 1991).

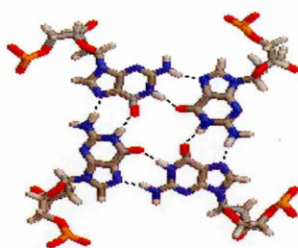
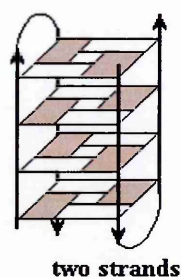
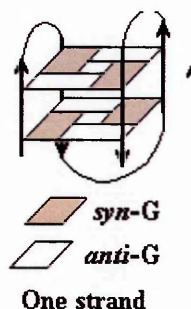


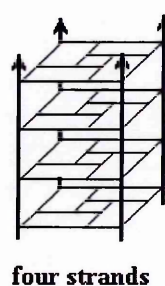
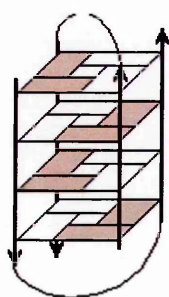
Figure 8: Guanine quartets (www.il.mahidol.ac.th/.../quadruplex3.gif, 20/07/2006)

Quadruplex strands may be arranged parallel or antiparallel; when they are antiparallel the guanines are in *syn* conformation on one strand and in *anti* on the other; see Figures 9 (Cheng, 1999).



a) Intramolecular G–quadruplex

b) Intermolecular antiparallel G–quadruplex



c) Intramolecular basket G–quadruplex

d) Intermolecular basket G – quadruplex

Figure 9: Quadruplex models in 4 possible forms (www.femto.snu.ac.kr/research/SMFRET/SMFRET5.gif, 10/02/2006)

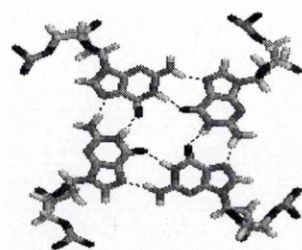
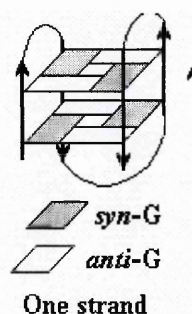
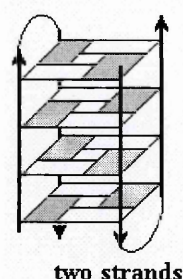


Figure 8: Guanine quartets (www.il.mahidol.ac.th/.../quadruplex3.gif, 20/07/2006)

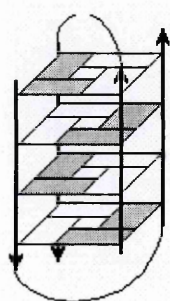
Quadruplex strands may be arranged parallel or antiparallel; when they are antiparallel the guanines are in *syn* conformation on one strand and in *anti* on the other; see Figures 9 (Cheng, 1999).



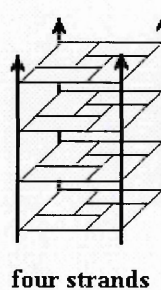
a) Intramolecular G–quadruplex



b) Intermolecular antiparallel G–quadruplex



c) Intramolecular basket G–quadruplex



d) Intermolecular basket G – quadruplex

Figure 9: Quadruplex models in 4 possible forms (www.femto.snu.ac.kr/research/SMFRET/SMFRET5.gif, 10/02/2006)

The intermolecular antiparallel G – quadruplex model and the intramolecular basket G – quadruplex model are potentially involved as anaphase bridges, telomeric and promoter regions. It has been hypothesised that these structures might be important for telomere function (Sen, 1988); the 3' overhang structure could hinder the telomere from elongating and inhibit the activity of the enzyme. Compounds like 3,6-bis-amidoacridines (Schultes *et al.*, 2004) stabilise G-quadruplex structures and stabilisation of these structures is an attractive target for telomerase (or ALT in some cancers) inhibition leading to a new strategy in the search of anticancer agents.

1.3.d.e: DNA – metal interactions

Trace and ultratrace metal concentrations play a definitive role in many biological processes and without their intervention many reactions would not proceed. Metals have a natural aptitude for interacting with DNA because of their affinity for basic nitrogen and oxygen donors. Cellular regulation also depends on metals, in the form of metallonucleases, to catalyse and repair DNA strand breaks. Lewis acidic metal ions like Cu^{2+} , Zn^{2+} , Fe^{3+} are supposed to cleave the phosphodiester bonds as they would lower the pK_a of coordinated water forming an active hydroxide nucleophile (Boerner *et al.*, 2005).

A positively charged metal ion can interact in different ways with the negatively charged residues of DNA phosphates and the electron donor atoms of the bases, such

as N and O. The predominant mode of metal binding takes place at the N7 and O⁶ of guanine, the N7 and N1 of adenine, and the N3 of pyrimidines.

Alkali metal ions prefer to interact with AT rich region of the minor groove. Transition metal ions usually bind directly to the bases and indirectly to the phosphate groups. Most of them react with the N7 atom of purine or N3 of pyrimidine thereby disturbing the double helix. The binding of transition metal ions particularly at G–C sites of DNA leads to damage through radical generation from oxidation by H₂O₂. Figure 10 shows different possibilities of metal – DNA binding.

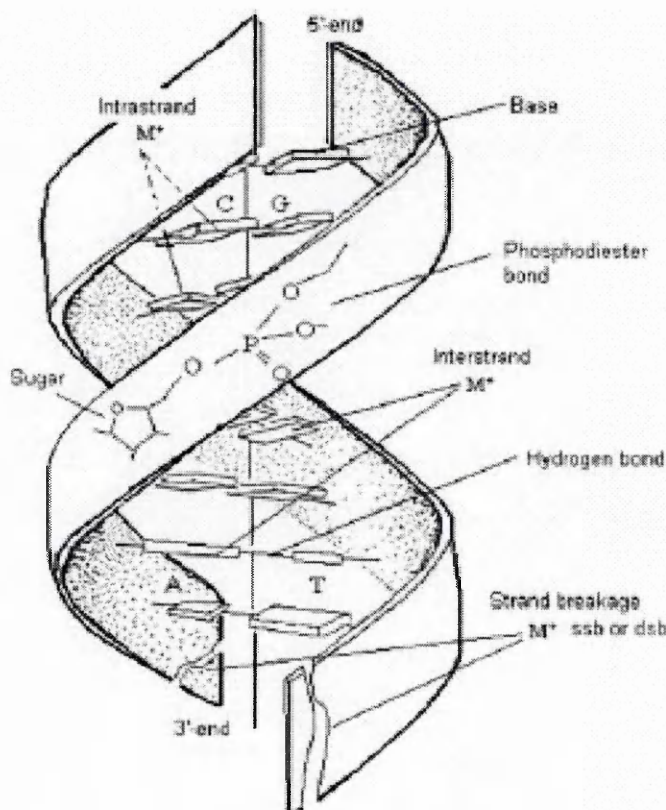


Figure 10: Metal ions can bind to one or two sites of the same strand (intrastrand) or of the opposite strand (interstrand), or through intercalation in a complex form between the bases. The binding of metal ions can lead to single strand break (ssb) or to double strand breaks (dsb) (Anastasopoulou, 2003).

1.4: Aims of this PhD

The development of drugs that are highly selective and produce minimal toxicity to host tissue remains one of the most difficult challenges in cancer therapeutics. Since the majority of malignancies are treated with drugs in combination, one approach to solve this problem is to develop new therapeutic agents that will potentiate the effectiveness of current clinical treatments.

Drug discovery begins with the extraction of molecules from natural products, combinatorial libraries or by computer aided drug design; biophysical and biological tests are performed in order to identify a lead compound. Progressive modifications are performed in the selected scaffold with the aim of improving binding and anticancer activity; this is an iterative step, where tests give indications for synthesising a next generation of compounds, which are tested again. This leads to candidate compounds, to be tested in hospital facilities at clinical trials.

The intentions of this project are:

- to understand the mode of binding of selected compounds of natural origin with proven anticancer activity to a selected target
- to generate structure-activity studies that will provide a better insight into their mode of binding
- to synthesise compounds with improved affinity, selectivity and anticancer activity

To do this we have used a range of different biophysical and biological techniques to study drug – DNA interactions. We subsequently used the results from these studies

to propose additional structures to investigate and organic synthesis in order to obtain the desired molecules. We divided this project in 3 main steps:

- analysis of natural products for activity against a chosen target (Chapters 3);
from here we selected a scaffold appropriate to use as a foundation for a first generation of modified compounds
- organic synthesis in order to modify the scaffold (chapters 2 and 4)
- structure-activity related studies and biological evaluation of the first generation of compounds with DNA (chapter 4).

Chapter 2: Materials and methods

2.1.a: Buffers

Buffer A: Na_2HPO_4 2 mM, NaH_2PO_4 8 mM with 1mM EDTA (Ethylenediaminetetraacetic acid), pH 7.4.

Buffer B: Na_2HPO_4 20 mM, NaH_2PO_4 80 mM, NaCl 300mM, EDTA 0.1mM.

Buffer C: cacodylate 50 mM, MgCl_2 50mM, EDTA 0.1mM, pH 6.5.

Buffer D: Na_2HPO_4 6 mM, NaH_2PO_4 2 mM, NaCl 185mM, EDTA 0.1mM, pH 7.4.

Buffer PBS: NaCl 150 mM, Na_2HPO_4 8.1 mM, NaH_2PO_4 1.9 mM,

Buffer TE 1X: Tris HCl 1 mM, EDTA 0.1 mM

Buffer TBE 1X: Tris borate 89 mM, EDTA 2 mM

Buffer TAE 1X: Tris acetate 0.8 mM, 0.02 mM EDTA

Buffer E: hepes (N-(2-Hydroxyethyl)piperazine-N'-(2-ethanesulfonic acid))10 mM

2.1.b:- Nucleic acids

STDNA (highly polymerized sodium salt; 58.8% A–T and 41.2% G–C (Arrowsmith, 1999)), was purchased from SIGMA Aldrich (United Kingdom) and used in filtered buffer solutions. The molar concentration was determined spectrophotometrically, using an extinction coefficient: $\epsilon_{260} = 13200 \text{ M}^{-1}\text{cm}^{-1}$ for STDNA (Arrowsmith, 1999) and expressed in base pairs. Poly(dAdT)₂, poly(dGdC)₂, polydAdT, polydGdC, polydT polynucleotides were purchased from Sigma Aldrich (United Kingdom) and dissolved in water to generate stock solutions. The molar concentrations were determined spectrophotometrically, using the following extinction coefficients: $\epsilon_{260} = 13100 \text{ M}^{-1}\text{cm}^{-1}$, $16800 \text{ M}^{-1}\text{cm}^{-1}$, $12000 \text{ M}^{-1}\text{cm}^{-1}$, $14800 \text{ M}^{-1}\text{cm}^{-1}$ (in the case of polydGdC we used maximum wavelength 253 nm, ϵ_{253}) and $\epsilon_{260} = 8500 \text{ M}^{-1}\text{cm}^{-1}$ respectively and expressed in base pairs (Arrowsmith, 1999). Triplex DNA polydAdTdT was prepared using a ratio of 1:1 poly(dAdT):poly(dT). The molar

concentration was determined spectrophotometrically, using the following extinction coefficient: $\epsilon_{260}=17200 \text{ M}^{-1}\text{cm}^{-1}$ (Arrowsmith, 1999) and expressed in base triplets. Triplex purine ($\text{G}_3\text{A}_4\text{G}_3:\text{C}_3\text{T}_4\text{C}_3:\text{G}_3\text{A}_4\text{G}_3$) was prepared using a ratio of 2:1 ($\text{G}_3\text{A}_4\text{G}_3:\text{C}_3\text{T}_4\text{C}_3$). The molar concentrations were determined spectrophotometrically, using the following extinction coefficient: $\epsilon_{255}=11500$ for $\text{G}_3\text{A}_4\text{G}_3$ and $\epsilon_{271}=8300 \text{ M}^{-1}\text{cm}^{-1}$ for $\text{C}_3\text{T}_4\text{C}_3$ (Arrowsmith, 1999). For the quadruplex DNA, the human telomeric sequence ($\text{AG}_3\text{T}_2\text{AG}_3\text{T}_2\text{AG}_3\text{T}_2\text{AG}_3$), was used. The molar concentration was determined spectrophotometrically, using the following extinction coefficient: $\epsilon_{260}=73000 \text{ M}^{-1}\text{cm}^{-1}$ and expressed in base quadruplex (Arrowsmith, 1999). Oligonucleotides were purchased from MWG (United Kingdom) and SIGMA Genomics (United States of America).

2.1.c.1: Chemicals

All compounds used in binding studies were dissolved in DMSO in stock concentration solutions of 10 mM. Artemisinin, baicalein, baicalin, chrysin, flavanone, flavone, hemin, holotransferrin, luteolin, puerarin, quercetin, rutin and 7-hydroxyflavone were purchased from Sigma – Aldrich (United Kingdom). Artesunate was donated by Dr Thomas Efferth (Germany). 3',4'-Dihydroxyflavone was purchased from Lancaster Chemicals (United Kingdom). Daidzein was purchased from Acros Chemicals (United Kingdom). 8,13-Diethyl-6-methylquino[4,3,2-*k*]acridinium iodide (in the future referred to as acridine derivative) was provided by Prof. Malcolm Stevens (University of Nottingham), $\epsilon_{506 \text{ nm}} = 11635 \text{ M}^{-1} \text{ cm}^{-1}$ (Missailidis, 2002). FeCl_2 , FeCl_3 , MgCl_2 , ZnCl_2 , CuO and MnCl_2 were dissolved in DMSO to form stock concentration solutions of 10 mM.

2.1.c.2: Synthesis

Instruments:

Mass Spectrometry: ESMS VG Quattro from Fisons with a Waters 7.1.7 autosampler, solvent 10:90 water:methanol.

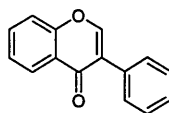
^1H NMR and ^{13}C NMR: 300 MHz Jeol instrument, chemical shifts and coupling constants are given in ppm and J in Hz, solvent used deuterated chloroform (CDCl_3).

IR (infrared): Perkin Elmer: 1710 Infrared Fourier Transform Spectrometer, all the samples were measured in methanol as solvent.

Melting point: Electrothermal Digital Melting Point apparatus, all measures were uncorrected.

Elemental Analysis: Medac Ltd.

2.1.d.1 - Isoflavone (3-Phenyl-4*H*-chromen-4-one)

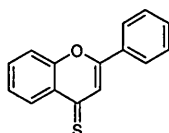


Compound 12

We followed the protocol of Singh (Singh *et al.*, 1990): TTA (thallium (III) acetate) (1.2 equiv.) was added to a solution of flavanone (0.672g, 3 mmol) in acetonitrile (20 ml) in the presence of p-toluenesulfonic acid (p-TSA, 0.4 equiv.). The reaction mixture was refluxed at 95°C for 24 h and cooled to room temperature; CH_2Cl_2 (50 ml) was added and the solution kept at 0°C for 15 min; the reaction was followed by TLC. The solid obtained was filtered to remove thallium salts and washed with CH_2Cl_2 (2 x 25 ml). The combined filtrate was washed with H_2O (2 x 50ml), followed by saturated aqueous NaHCO_3 (2 x 100 ml) then dried (MgSO_4). The

solvent was evaporated under vacuum and the residue purified by semi-preparative HPLC (high performance liquid chromatography) in an hexane:ethyl acetate (9:1) eluant. ES-MS m/z (relative intensity): 223(MH^+). 1H NMR: 8.29 (dd, J 8.1/8.1, 1H), 7.99 (s, 1H), 7.66 (t, J 7.0, 1H), 7.55–7.34 (m, 7H); ^{13}C NMR ($CDCl_3$): 176.2, 156.2, 153.0, 133.6, 131.8, 128.9, 128.5, 128.2, 126.4, 125.4, 125.2, 124.6, 118.0. Melting point: 135-136.5°C, literature reference 134-135°C (Singh *et al.*, 1999). Yield: 0.33g. Extinction coefficient: 9266 M^{-1} at 310nm.

2.1.d.2 - Thioflavone (2-Phenyl-4*H*-chromene-4-thione) (Abdou *et al.*, 1994)

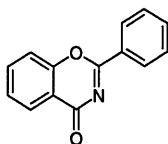


Compound 14

Lawesson's reagent was used for this simple substitution of oxygen by sulfur: Lawesson's reagent (0.6 equiv.) was added to flavone (2.23g, 10 mmol) dissolved in toluene (100 ml) and the reaction mixture was refluxed overnight. The reaction was followed by TLC. The solvent was evaporated and the residue purified by silica column chromatography using a hexane:ethyl acetate gradient as eluent followed by further purification by preparative TLC using hexane:ethyl acetate (70:30) as eluents to give a red solid. ES-MS m/z (relative intensity): 238.01 (M). 1H NMR: 8.55 (dd, J 8.25/8.25, 1H), 7.93 (dd, J 2.01/2.01, 2H), 7.73 (s, 1H), 7.65 (m, 1H), 7.5 (m, 4H), 7.35 (m, 1H); ^{13}C NMR ($CDCl_3$): 202, 154.2, 151.5, 134.15, 131.8, 131.1, 129.9, 129.2, 128.6, 126.5, 126.2, 120.3, 118.4. IR: 2924.8, 2853, 1743, 1597, 1501, 1460, 1261, 1121.4, 928.5, 769. IR (cm^{-1}): 2924.8, 2853.1, 1743.3, 1597.4, 1501.8, 1460, 1261.5, 1124.4, 928.5. Elemental analysis found: C 75.2%, H 4.2%, calculated: C

75.6%, H 4.24%. Yield: 1.65g. Extinction coefficient: 7799 M⁻¹ at 470nm. Melting point: 84-85.5°C, literature reference 85-86° (Abdou *et al.*, 1994).

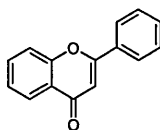
2.1.d.3 - Azaflavone (2-Phenyl-4*H*-benzo[*e*][1,3]oxazin-4-one) (Kemp *et al.*, 1980)



Compound 15

Benzoyl chloride (1 equiv.) was added to a solution of salicylamide (0.685g, 5 mmol) in toluene (30 ml). The reaction mixture was refluxed till no further change by TLC was observed. p-TSA was added, the solution refluxed and 1 equiv. of water was extracted by azeotropic distillation. The remaining solution was washed with saturated aqueous NaHCO₃ (2 x 50 ml), followed by H₂O (2 x 25ml), then dried with MgSO₄. The solvent was evaporated and the residue purified by silica column chromatography using a gradient of hexane:ethyl acetate as eluent. ES-MS *m/z* (relative intensity): 241.84 (M+NH₄⁺), 263 (M+K⁺). ¹H NMR: 8.18 (dd, *J* 7.5/1.03, 2H), 7.5 (m, 5H), 7.3 (t, *J* 7.14, 1H), 6.83 (d, *J* 7.86, 1). ¹³C NMR: 167, 163, 155.1, 134.5, 133.9, 129, 128.6, 128, 126.4, 118.3, 117. Yield: 0.05g.

2.1.d.4 - Flavone (2-Phenyl-4*H*-chromen-4-one) (Ares *et al.*, 1993)

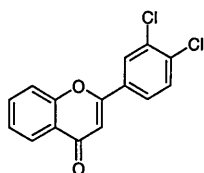


Compound 10

KOBu (1 equiv) was added to dry THF (100ml) under a nitrogen atmosphere. The mixture was cooled to 0-5 °C, and 2-hydroxyacetophenone (0.408g, 3 mmol) in THF (100 ml) was added dropwise, the ice bath was then removed and the mixture allowed to warm to room temperature and stirred for 50 min. The reaction mixture was re-

cooled to 0-5 °C and benzoyl chloride (1 equiv) was added dropwise, the ice bath was removed and the mixture stirred at room temperature for 60 min. The mixture was again recooled to 5 °C and KOBu (1 equiv) was added, stirred at room temperature for 10 min and finally refluxed overnight. The mixture was diluted with water (100 ml) and acidified to pH 2 with 1M HCl, the diketone was extracted into ethyl acetate (3 x 50 ml), washed with saturated sodium hydrogen carbonate (2 x 100 ml), dried with MgSO₄, and evaporated. Crystallization with ethanol afforded white needles. This crystalline diketone was dissolved in glacial acetic acid (30 ml) containing concentrated sulfuric acid (2 ml) and refluxed for 40 min. The acetic acid was removed by high vacuum evaporation, and the residue was poured onto crushed ice (200 ml) and the resulted solid was filtered. The product was purified by silica column using a gradient of hexane:ethyl acetate as eluent to give pure flavone. ES-MS *m/z* (relative intensity): 223.5 (M+H⁺1). ¹H NMR: 8.29 (dd, J 7.95/1.7, 1H), 7.91 (dd, J 8.5/1.03, 2H), 7.68 (m, 1H), 7.55 (m, 4H), 7.35 (t, J 7.1/1.1, 1H), 6.76 (s, 1H); ¹³C NMR: 178, 162, 155, 133.8, 131.6, 129, 126.2, 125.5, 125.2, 118, 107.4. Yield: 15.4% respect to 2-hydroxyacetophenone. Extinction coefficient: 9325.8 M⁻¹ at 313nm. Melting point: 98.5-100°C, literature reference 99°C (Shivhare *et al*, 1985).

2.1.d.5 - 3',4'-Dichloroflavone (3',4'-Dichloro-3-phenyl-4*H*-chromen-4-one) (Singh, 1993)

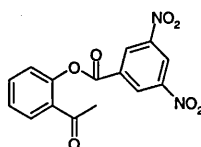


Compound 31

KOBu (1 equiv) was added to dry THF (tetrahydrofuran) (100ml) under nitrogen atmosphere. The mixture was cooled to 0-5 °C, and 2-hydroxyacetophenone (0.408g,

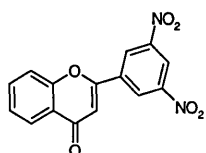
3 mmol) in THF (100 ml) was added dropwise, the ice bath was then removed and the mixture allowed to warm to room temperature and stirred for 50 min. The reaction mixture was re-cooled to 0-5 °C and 3,4-dichloridebenzoyl chloride (1 equiv) was added dropwise, the ice bath removed and the mixture stirred at room temperature for 60 min. The mixture was again re-cooled to 5 °C and KOBu (1 equiv) was added, stirred at room temperature for 10 min and finally refluxed overnight. The mixture was diluted with water (100 ml) and acidified to pH 2 with 1M HCl, the diketone was extracted into ethyl acetate (3 x 50 ml), washed with saturated sodium hydrogen carbonate (2 x 100 ml), dried with MgSO₄, and evaporated. Crystallization with ethanol afforded white needles. This crystalline diketone was dissolved in glacial acetic acid (30 ml) containing concentrated sulfuric acid (2 ml) and refluxed for 40 min. The acetic acid was removed by high vacuum evaporation, and the residue was poured onto crushed ice (200 ml) and the resulted solid was filtered. The product was purified by silica column using a gradient of hexane:ethyl acetate as eluent to give the pure flavone derivative. ES-MS *m/z* (relative intensity): 293 (M+H⁺). ¹H NMR: 8.1 (dd, J 8.04/8.04, 1H), 8.03 (d, J 8.16, 1H), 7.8 (dd, J 8.6/8.6, 1H), 7.7 (t, 1H), 7.65–7.55 (m, 2H), 7.4 (t, 1H), 6.78 (s, 1H). ¹³C NMR: 117.5, 160.46, 155.7, 135.2, 134, 131.2, 131, 127.7, 125.3, 125.2, 125, 123.4, 118, 107.7. Melting Point: 203–205 °C. Yield: 11.5% respect to 2-hydroxyacetophenone. Extinction coefficient: 2439 M⁻¹ at 320nm.

2.1.d.6 - 2-Acetylphenyl-3',5'-dinitrobenzoate



Under argon dry triethylamine (1 equiv) was added dropwise to 2-hydroxyacetophenone (0.408g, 3 mmol) in dry diethylether (50 ml) with stirring and cooling in ice bath. The reaction mixture was allowed to stir for 15 min and 3,5-dinitrobenzoyl chloride (1 equiv) dissolved in dry diethyl ether (50 ml) was added dropwise over 30 min. The reaction mixture was allowed to attain room temperature and the product was used directly for the next procedure.

2.1.d.7 - 3',5'-Dinitroflavone (3',5'-Dinitro-2-phenyl-4*H*-chromen-4-one) (Marder *et al.*, 1997)

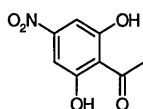


Comound 30

KOBu (1 equiv) was added to dry THF (100 ml) under a nitrogen atmosphere. The mixture was cooled to 0-5 °C and 2-acetylphenyl-3',5'-dinitrobenzoate (0.99g, 3 mmol) in THF (100 ml) was added dropwise. The ice bath was then removed and the mixture allowed to warm to room temperature for 50 min and then refluxed overnight. Upon cooling, the mixture was diluted with water (100 ml), acidified to pH 2 with 1M HCl, and the diketone was extracted into ethyl acetate (3 x 50 ml). The extraction was washed with saturated sodium hydrogen carbonate (2 x 100 ml), dried with MgSO₄, and evaporated. Crystallization with ethanol afforded yellow needles. This crystalline diketone was dissolved in glacial acetic acid (30 ml) and concentrated sulfuric acid (2 ml) and refluxed for 40 min. The acetic acid was removed by high vacuum evaporation, the residue was poured into crushed ice (200 ml) and the product was extracted with ethyl acetate. After evaporation of the solvent, the product was purified by silica column using a gradient of hexane:ethyl acetate as eluent to

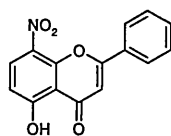
give the pure flavone. ES-MS m/z (relative intensity): 313.03 ($M+H^+$). 1H NMR: 9.8 (d, J 2.2, 1H), 9.1 (t, J 2.01, 1H), 9.04 (d, J 2.01, 2H), 8.17 (dd, J 7.89/1.47/1.47, 1H), 7.7 (m, 1H), 7.4 (dd, J 6.9/1.1/1.1, 1H), 7.01 (s, 1H); ^{13}C NMR: 182.3, 162.5, 159, 149.1, 148.3, 137.3, 134, 132.7, 128.9, 127.5, 126.8, 124.9, 120.1, 109.2, 106.8. IR (cm^{-1}): 3097.3, 1709.7, 1629.4, 1544, 1343, 1160, 756. Melting Point: 127 – 129.5 °C. Yield: 0.4g. Extinction coefficient: 2276 M^{-1} at 403nm.

2.1.d.8 - 2,6-Dihydroxy-3-nitroacetophenone (Cushman *et al.*, 1994)



Nitric acid (density=1.42 mg/ml, 1.2 ml) in glacial acetic acid (2 ml) was slowly added to a solution of 2,6-dihydroxyacetophenone (2.4g, 16 mmol) in glacial acetic acid (13 ml) with stirring and cooling using an ice-water bath. The reaction mixture turned a dark-red colour and was stirred for 40 min at room temperature. The mixture was poured onto ice-water (80 ml) to give a solid product that afforded 2,6-dihydroxy-3-nitroacetophenone by purification with silica column using a gradient of hexane:ethyl acetate as eluent and used directly for the next procedure.

2.1.d.9 - 5-Hydroxy-8-nitroflavone (5-Hydroxy-3',5'-nitro-3-phenyl-4H-chromen-4-one) (Cushman *et al.*, 1994)

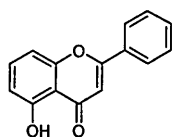


Compound 26

KOBu (1 equivalent) was added to dry THF (100ml) under nitrogen atmosphere. The mixture was cooled to 0-5 °C, and 2,6-dihydroxy-3-nitroacetophenone (0.6g, 3mmol) in THF (100 ml) was added dropwise. The ice bath was then removed and the mixture

allowed to warm to room temperature and stirred for 50 min. The mixture was again cooled to 0-5 °C and benzoyl chloride (1 equiv) was added dropwise, the ice bath was removed and the mixture stirred at room temperature for 60 min. The mixture was recooled to 5 °C and KOBu (1 equiv) was added, stirred at room temperature for 10 min and finally refluxed overnight. The mixture was diluted with water (100 ml) and acidified to pH 2 with 1M HCl. The diketone was extracted into ethyl acetate (3 x 50 ml) and washed with saturated sodium hydrogen carbonate (2 x 100 ml), dried with MgSO₄, and evaporated. Crystallization with ethanol afforded yellow needles. This crystalline diketone was dissolved in glacial acetic acid (30 ml) and concentrated sulfuric acid (2 ml) and refluxed for 40 min. Acetic acid was removed by high vacuum evaporation. The residue was poured onto crushed ice (200 ml) and the solid filtered. The product was purified by silica column using a gradient of hexane:ethyl acetate as eluent to give pure flavone. ES-MS *m/z* (relative intensity): 324 (M+H⁺2/K). ¹H NMR: 8.3 (d, J 9.3, 1H), 7.8 (d, J 2.1, 2H), 7.5 (m, 3H), 6.6 (s, 1H), 6.3 (d, J 9.3, 1H); ¹³C NMR: 182, 169.1, 164.6, 157, 139, 132.3, 131.9, 130.4, 127.9, 126.5, 121.6, 119.5, 117, 107.8. Yield: 0.37g. Extinction coefficient 3355.3 M⁻¹ at 410nm.

2.1.d.10 - 5-Hydroxyflavone (5-Hydroxy-3-phenyl-4*H*-chromen-4-one) (Ares *et al.*, 1993)

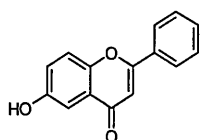


Compound 20

KOBu (1 equiv) was added to dry THF) (100ml) under nitrogen atmosphere. The mixture was cooled to 0-5 °C, and 2,6-dihydroxyacetophenone (0.456g, 3 mmol) in

THF (100 ml) was added dropwise, the ice bath was then removed and the mixture allowed to warm to room temperature and stirred for 50 min. The reaction mixture was re-cooled to 0-5 °C and benzoyl chloride (1 equiv) was added dropwise, the ice bath removed and the mixture stirred at room temperature for 60 min. The mixture was again re-cooled to 5 °C and KOBu (1 equiv) was added, stirred at room temperature for 10 min and finally refluxed overnight. The mixture was diluted with water (100 ml) and acidified to pH 2 with 1M HCl, the diketone was extracted into ethyl acetate (3 x 50 ml), washed with saturated sodium hydrogen carbonate (2 x 100 ml), dried with MgSO₄, and evaporated. Crystallization with ethanol afforded pale yellow needles. This crystalline diketone was dissolved in glacial acetic acid (30 ml) containing concentrated sulfuric acid (2 ml) and refluxed for 40 min. The acetic acid was removed by high vacuum evaporation, and the residue was poured onto crushed ice (200 ml) and the resulted solid was filtered. The product was purified by silica column using a gradient of hexane:ethyl acetate as eluent to give pure flavone. ES-MS *m/z* (relative intensity): 238.75 (M+H⁺). ¹H NMR: 12.58 (s, 1H, OH), 8.2 (m, 2H), 7.9 (m, 2H), 7.55 (m, 2H), 6.8 (dd, J 8.25/8.25, 1H), 6.4 (d, J 8.2, 1H), 6.7 (s, 1H); ¹³C NMR: 183.4, 163.7, 162.9, 158.9, 137.8, 136.8, 136.2, 135.5, 132.1, 129.1, 126.4, 111.26, 107.2, 105.8. Melting Point: 148 – 150.5 °C. Yield: 0.06g. Extinction coefficient: 2396.8 M⁻¹ at 330nm.

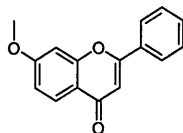
2.1.d.11 - 6-Hydroxyflavone (6-Hydroxy-3-phenyl-4*H*-chromen-4-one) (Aksnes *et al.*, 1996)



Compound 19

KOBu (1 equiv) was added to dry THF (100ml) under nitrogen atmosphere. The mixture was cooled to 0-5 °C, and 2,5-dihydroxyacetophenone (0.456g, 3 mmol) in THF (100 ml) was added dropwise, the ice bath was then removed and the mixture allowed to warm to room temperature and stirred for 50 min. The reaction mixture was re-cooled to 0-5 °C and benzoyl chloride (1 equiv) was added dropwise, the ice bath removed and the mixture stirred at room temperature for 60 min. The mixture was again re-cooled to 5 °C and KOBu (1 equiv) was added, stirred at room temperature for 10 min and finally refluxed overnight. The mixture was diluted with water (100 ml) and acidified to pH 2 with 1M HCl, the diketone was extracted into ethyl acetate (3 x 50 ml), washed with saturated sodium hydrogen carbonate (2 x 100 ml), dried with MgSO₄, and evaporated. Crystallization with ethanol afforded yellow needles. This crystalline diketone was dissolved in glacial acetic acid (30 ml) containing concentrated sulfuric acid (2 ml) and refluxed for 40 min. The acetic acid was removed by high vacuum evaporation, and the residue was poured onto crushed ice (200 ml) and the resulted solid was filtered. The product was purified by silica column using a gradient of hexane:ethyl acetate as eluent to give pure flavone. ES-MS *m/z* (relative intensity): 238.85 (M+H⁺). ¹H NMR: 11.6 (s, 1H), 7.8 (m, 2H), 7.4 (m, 3H), 7.3 (d, J 8.1, 1H), 7.2 (dd, J 7.49/1.5, 1H), 7.1 (d, J 2.5, 1H), 6.7 (s, 1H). ¹³C NMR: 179.4, 163.9, 155.1, 154.7, 150.3, 148.7, 131.4, 128.8, 126.2, 123.7, 119.2, 107.7, 106. MP: 145 – 147 °C. Yield: 0.070g.

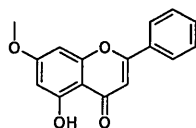
2.1.d.12 - 7-Methoxyflavone (7-Methoxy-3-phenyl-4*H*-chromen-4-one) (Shin *et al.*, 1999)



Compound 24

Methyl iodide (1 equiv) was added dropwise to 7-hydroxyacetophenone (0.714g, 3mmol) in dry THF (100ml) with stirring at 50°C in presence of K₂CO₃ (3 equiv). The reaction mixture is allowed to stir till no further change was observed by TLC. The product was purified by silica column using a gradient of hexane:ethyl acetate as eluent. ES-MS *m/z* (relative intensity): 253.3 (M+H⁺). ¹H NMR: 7.9 (d, J 8.4, 1H), 7.74 (m, 2H), 7.39 (m, 3H), 6.84 (d, 2.37, 1H), 6.8 (dd, J 8.72/2.3, 1H), 6.6 (s, 1H), 3.78 (s, 3H). ¹³C NMR: 177.8, 164, 162.9, 157.9, 131.3, 128.9, 126.9, 126, 117.7, 114.3, 107.4, 100.3, 55.72. Melting Point: 111 – 112.8 °C. Yield: 0.67g. Extinction coefficient: 27255 M⁻¹ at 310nm.

2.1.d.13 - 5-Hydroxy-7-methoxychrysin (5-Hydroxy-7-methoxy-3-phenyl-4*H*-chromen-4-one) (Shin *et al.*, 1999)

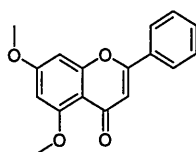


Compound 25

Methyl iodide (1 equiv) was added dropwise to chrysin (0.766. 3mmol) in dry THF (100 ml) with stirring at 50°C in the presence of K₂CO₃ (3 equiv). The reaction mixture was allowed to stir till no further change was observed by TLC. The product was purified by silica column using a gradient of hexane:ethyl acetate as eluent. ES-MS *m/z* (relative intensity): 269 (M+H⁺). ¹H NMR: 12.65 (s, 1H, OH), 7.77 (m, 2H), 7.43 (m, 3H), 6.54 (s, 1H), 6.48 (d, J 2, 1H), 6.25 (d, J 2, 1H), 3.77 (s, 3H). ¹³C NMR:

182.3, 165.5, 163.8, 163.8, 162, 157.6, 131.7, 128.9, 126.1, 125.4, 105.6, 98.1, 92.6, 55.7. Elemental analysis, found: C 72.09%, H 5.17%, calculated: C 71.64%, H 4.51%. Yield: 0.48g. Extinction coefficient: 5478 M⁻¹ at 340nm.

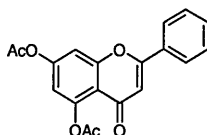
2.1.d.14 – 5,7-Dimethoxychrysin (5,7-Dimethoxy-3-phenyl-4H-chromen-4-one)
(Shin *et al.*, 1999)



Compound 22

Sodium hydride (2 equiv) was added to 5-hydroxy-7-methoxychrysin (0.81g, 3mmol) in dry THF (100 ml) with stirring at 50°C. Methyl iodide (1 equiv) was added dropwise to the reaction mixture, which was allowed to stir till no further change was observed by TLC. The product was purified by silica column using a gradient of hexane:ethyl acetate as eluent. ES-MS *m/z* (relative intensity): 283.51 (M+H⁺). ¹H NMR: 7.77 (m, 2H), 7.4 (m, 3H), 6.58 (s, 1H), 6.48 (d, J 2.2, 1H), 6.28 (d, J 2.2, 1H), 3.86 (s, 3H), 3.82 (s, 3H). ¹³C NMR: 177.5, 163.9, 160.8, 160.5, 131.09, 128.8, 125.8, 108.9, 96, 92.7, 56.3, 55.7. Elemental analysis, found: C 72.13%, H 4.96%, calculated: C 72.33%, H 5.00%. Yield: 0.24g. Extinction coefficient: 11494.9 M⁻¹ at 320nm.

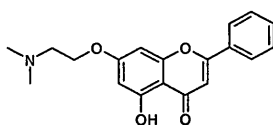
2.1.d.15 – 5,7-Diacetoxychrysin (5,7-Diacetoxy-3-phenyl-4H-chromen-4-one)
(Shin *et al.*, 1999)



Compound 23

Acetic anhydride (2 equiv) was added dropwise to chrysin (0.762 g, 1mmol) in dry pyridine (50 ml). The reaction mixture was allowed to stir under reflux till no further change was observed by TLC. The product was purified by silica column using a gradient of hexane:ethyl acetate as eluent ES-MS m/z (relative intensity): 338 ($M+H^+$). 1H NMR: 7.78 (m, 2H), 7.45 (m, 3H), 7.3 (d, J 2.4, 1H), 6.79 (d, J 2.4, 1H), 6.59 (s, 1H), 2.35 (s, 3H), 2.29 (s, 3H). ^{13}C NMR: 184.9, 164.5, 163.9, 163, 158.5, 157, 149, 131.6, 128.7, 125.9, 124.4, 123.6, 113.5, 109, 108, 57, 39.7. Melting Point: 196.2 – 197 °C. Yield: 0.68g. Extinction coefficient: 3577.8 M^{-1} at 315nm.

2.1.d.16 - 7-(2-(Dimethylamino)ethoxy)-5-hydroxy-3-phenyl-4H-chromen-4-one
(Briggs *et al.*, 1982)



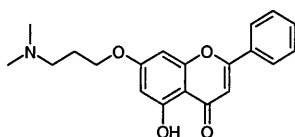
Compound 27

N,N-Dimethylethanolamine (1 equiv) was added to chrysin (1.52g, 6mmol) in dry THF (30 ml) in the presence of triphenylphosphine (1.1 equiv); sonication at 40 kHz was carried out till the materials were soluble. DIAD (1.3 equivalent) was added dropwise and sonication carried out for 60 min. The solvent was evaporated and the product poured into acidic water (100 ml). Dichloromethane (50 ml) was used to extract the triphenyl oxide and hydrazine derived product. The aqueous layer was neutralized (pH 7), extracted with ethyl acetate (3 x 20 ml), the extract washed with a saturated solution of $NaHCO_3$ (3 x 25 ml), dried with $MgSO_4$ and the solvent evaporated. The product was purified by silica column using a gradient of hexane:ethyl acetate:isopropanolamine as eluent. ES-MS m/z (relative intensity): 325.48 ($M+H^+$ 4). 1H NMR: 12.5 (s, 1H), 7.8 (d, J 2.2, 2H), 7.4 (m, 3H), 6.6 (s, 1H),

6.4 (d, J 2.2, 1H), 6.3 (d, J 2.2, 1H), 4.07 (t, J 5.6, 2H), 2.7 (t, J 5.7, 2H), 2.3 (s, 6H).

^{13}C NMR: 182.4, 164.7, 164, 162, 158, 132, 131.3, 129, 126.3, 106, 98.6, 93.2, 66.7, 58, 45.9. Melting Point: 126 - 126.8 °C. Yield: 0.55g. Extinction coefficient: 10229 M^{-1} at 309nm.

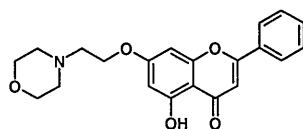
2.1.d.17 - 7-(3-(Dimethylamino)propoxy)-5-hydroxy-3-phenyl-4H-chromen-4-one



Compound 28

N,N-Dimethylpropanolamine (1 equiv) was added to chrysin (1.52g, 6mmol) in dry THF (30 ml) in the presence of triphenylphosphine (1.1 equiv); sonication at 40 kHz was carried out till the materials were soluble. DIAD (1.3 equivalent) was added dropwise and sonication carried out for 60 min. The solvent was evaporated and the product poured into acidic water (100 ml). Dichloromethane (50 ml) was used to extract the triphenyl oxide and hydrazine derived product. The aqueous layer was neutralized (pH 7), extracted with ethyl acetate (3 x 20 ml), the extract washed with a saturated solution of NaHCO_3 (3 x 25 ml), dried with MgSO_4 and the solvent evaporated. The product was purified by silica column using a gradient of hexane:ethyl acetate:isopropanolamine as eluent. HRMS m/z (relative intensity): found 340.1543, calculated 340.1544. ^1H NMR: 7.8 (dd, J 1.65/ 2.2, 2H), 7.4 (m, 3H), 6.6 (s, 1H), 6.4 (d, J 2.2, 1H), 6.3 (d, J 2.2, 1H), 4.07 (t, J 5.6, 2H), 2.7 (t, J 5.7, 2H), 2.3 (s, 6H), 1.03 (q, J 6.6, 2H). ^{13}C NMR: 187, 169.7, 168.4, 162.4, 136.5, 133.7, 130.8, 128.7, 126.4, 118.4, 110.2, 103.3, 97.63, 71.53, 60.7, 37.2, 31.9. Yield: 0.52g. Extinction coefficient: 2476 M^{-1} at 370nm.

2.1.d.18 - 7-(2-(mMorpholinoethoxy)-5-hydroxy-3-phenyl-4*H*-chromen-4-one



Compound 29

2-Morpholinoethanol (1 equiv) was added to chrysin (1.52g, 6mmol) in dry THF (30 ml) in the presence of triphenylphosphine (1.1 equiv); sonication at 40 kHz was carried out till the materials were soluble. DIAD (1.3 equivalent) was added dropwise and sonication carried out for 60 min. The solvent was evaporated and the product poured into acidic water (100 ml). Dichloromethane (50 ml) was used to extract the triphenyl oxide and hydrazine derived product. The aqueous layer was neutralized (pH 7), extracted with ethyl acetate (3 x 20 ml), the extract washed with a saturated solution of NaHCO₃ (3 x 25 ml), dried with MgSO₄ and the solvent evaporated. The product was purified by silica column using a gradient of hexane:ethyl acetate:isopropanolamine as eluent. HRMS *m/z* (relative intensity): found 368.1492 calculated calc 368.1494. ¹H NMR: 7.8 (dd, *J* 1.65/2.2, 2H), 7.4 (m, 3H), 6.6 (s, 1H), 6.4 (d, *J* 2.2, 1H), 6.3 (d, *J* 2.2, 1H), 4.09 (t, *J* 5.6, 2H), 3.64 (t, 4H), 2.7 (t, *J* 5.7, 2H), 2.5 (t, 4.74, 4H). ¹³C NMR: 182, 164.3, 163.6, 161.6, 157.3, 131.7, 131.5, 130.7, 128.7, 128.3, 128.1, 125.9, 105.4, 98.3, 92.8, 66.4, 53.6, 53.3, 39.9. Yield: 0.50g. Extinction coefficient: 5495 M⁻¹ at 314nm.

2.1.e: Tumour cell lines

Clonal populations of the MCF7 cell line and the CCRFCM cell line were used for cell viability, flow cytometry and Comet assay experiments; they were donated by the

University of Nottingham. They were cultured in an initial concentration of 5×10^6 cells per well and used 24 hours later. These cells were routinely grown in RPMI (Roswell Park Memorial Institute) - glutamax (SIGMA Aldrich, United Kingdom) supplemented with 5%, respectively of heat-inactivated foetal calf serum (GIBCO, United Kingdom) at 37°C, and 6% CO₂ in air. The cells were subcultured twice a week.

2.2.a.1: Methods

Drug - DNA ligand associations can be achieved via a combination of electrostatic forces, hydrogen-bonding, hydrophobic interactions, van der Waals forces, etc. Other factors, like neighbour exclusion and cooperativity, also play a role. The result of these interactions is the formation of a nucleic acid – drug complex.

The interactions of salmon testes DNA, polynucleotides, DNA triple helix and DNA quadruplex structures with a range of compounds were studied using a range of physicochemical techniques such as spectrophotometric analysis, thermal denaturation and competition dialysis. These techniques allow us to study the strength of binding, mode of action and stability. Biological techniques, such as nucleic acid damage assay and footprinting, make it possible to identify the sequence specificity of the drugs towards nucleic acids structures. Some nucleic acid intercalators have been shown (Liu, 1989) to alter topoisomerase activity. Therefore topoisomerase I / II inhibition assays were performed to elucidate any activities of our compounds as verified by DNA unwinding. CYP1A1 belongs to the Cytochrome P450 family, and is involved in detoxification – metabolic pathways. An analytical assay has thus been

performed in order to find possible metabolites resulting from the metabolism of some of our compounds by CYP1A1.

Cell work on breast cancer (MCF7) and leukemia (CCRFCEM) cell lines was performed for certain compounds in order to evaluate biological activity.

2.2.a.2 – Spectroscopic methods for the study of DNA-drug interactions

There are several available methods for the study of the intercalation process, allowing the determination of the nature and affinity of the binding. Intercalation is an equilibrium binding process. To determine the association constant for this process, the concentration of free and bound drug in the DNA-drug mixture must be determined. This can be done by a number of techniques including spectrophotometric methods and equilibrium dialysis. Intercalation also causes changes in the physical properties of the molecules. These changes include the stabilization of the DNA double helix against thermal denaturation and the unwinding of the double helix, which can be monitored through changes in the absorbance of the DNA during melting.

2.2.a.3 - Temperature denaturation studies

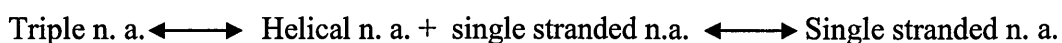
When the temperature of a solution containing helical nucleic acid is raised sufficiently, strand separation occurs, through a process called melting. The temperature that marks the midpoint of the melting process is termed the melting temperature (T_m), it is defined as the point where 50% of the DNA is in duplex form and 50% of the DNA is denaturated into single strands. Single strand DNA absorbs

more UV light than double strands and as the bases unwind an hyperchromic shift can be observed in the absorbance at 260 nm during the melting assay.

The equilibrium for this is:



For triple helix, two T_m values can be found; the equilibria are as follow:



Association of ligands to nucleic acids can have dramatic effects on the helix – coil transition, leading to an increase or decrease in the melting temperature. The bonding between AT bases is the first to break (as these bases are connected through two hydrogen bonds), followed by the CG pairs (as they have three); the ionic strength of the buffer also plays an important role, as salts can shield repulsion of negatively charged phosphate groups. The melting curve is sigmoid, which is an indication of a cooperative process; this increase in absorbance is because of the reduction in electronic interactions through base stacking and the final absorbance therefore approaches that of the nucleic acid bases taken as monomers. The inflection point in the curve is the T_m .

To determine the drug – NA (nucleic acid) complex stability, the drugs were evaluated for their ability to stabilise or destabilise STDNA and polynucleotides against thermal denaturation. A positive result in this experiment indicates a stabilization of the nucleic acid through the drug interaction, while a negative result indicates that the drug destabilises the DNA structure.

Optical thermal denaturation experiments were performed in stoppered quartz cuvettes using a UVIKON spectrophotometer fitted with a temperature control unit and a programmable heated cell holder capable of maintaining the temperature to within $\pm 0.1^\circ\text{C}$ over a temperature range of 25 to 98°C in a 1 cm pathlength, 3 ml quartz cell. DNA–drug solutions were prepared by addition of the ligand compound to give a final drug concentration of $2 \times 10^{-6}\text{ M}$ and a final DNA concentration of 10^{-5} M in the appropriate buffer. A fixed DNA:drug molar ratio of 5:1 was used. Heating was applied at $1^\circ\text{C}/\text{min}$ until the denaturation process was completed, the optical absorbance at 260 nm was recorded throughout the process. The data were plotted using the software program Origin (Microcal, USA) giving a sigmoid curve, the first derivative was used to identify the maximum which is the T_m (melting temperature; T_{complex}). In each case the drug – DNA complex was compared with DNA alone and ΔT_m were obtained, where $\Delta T = T_{\text{bound DNA}} - T_{\text{free DNA}}$.

2.2.a.4 – UV titrations

When light – either visible or ultraviolet – is absorbed by valence (outer) electrons these electrons are promoted from their normal (ground) states to higher energy (excited) states (Sheffield, 2004). Absorption of ultraviolet and visible radiation by organic molecules is restricted to certain functional groups (chromophores) that contain valence electrons of low excitation energy. The spectrum of a molecule containing these chromophores is complex because the superposition of rotational and vibrational transitions on the electronic transitions gives a combination of overlapping lines appearing as a continuous absorption band. Most absorption spectroscopy of organic compounds is based on transitions of n or π electrons to the

π^* excited state (200 - 700 nm). These transitions need an unsaturated group in the molecule to provide the π electrons (<http://www.cem.msu.edu>, 20/07/2006).

The majority of flavones and flavonols exhibit two major bands in the UV/Vis region. Band I is in the 320-385 nm range representing B-ring absorption, and band II is in the 250-285 nm range representing the A-ring absorption. An increase in the number of hydroxyl groups induces a red shift, for instance baicalein (with hydroxyl groups in the 5-, 6- and 7-positions) has a maximum at 359 nm whereas quercetin (3-, 5-, 7-, 3'-, 4'-positions) has a maximum of absorbance at 375 nm. The absence of a 3-OH group in flavones (which distinguish flavones from flavonols) means that band I is always at a shorter wavelength by about 20–30 nm. O-Methylation and glycosylation produce hypsochromic shifts (Markham, 1989).

2.2.a.5: Data fitting and experimentation

Measurement of NA-drug interactions using spectroscopic methods is based on the fact that electronic absorption spectrum of the unbound drug is altered upon binding to the nucleic acid. The optical changes, due to the binding process, can be quantitatively measured by performing a titration and a binding curve can be plotted (Connors, 1987). It is relevant to consider the drug's absorption spectrum; as it would need to be in the UV/Visible region, but outside the range of 200 – 300 nm, where the nucleic acid absorbs, so any changes in the spectrum are attributed solely to changes in the drug spectrum (McGhee, 1974).

For most spectra, the sample solution obeys Beer's law, which states that the light absorbed is proportional to the number of absorbing molecules (concentration of

absorbing molecules); this is true for dilute solutions. A second law, Lambert's law, says that the fraction of radiation absorbed is independent of the intensity of the radiation. The Beer – Lambert law is expressed as:

$$A = \epsilon cl = \log_{10} I_0 / I$$

where A is the absorbance, ϵ is the extinction coefficient, l is the cell path length (in this project it will be considered as 1cm) and c is the concentration of the analyte, I_0 is the intensity of the incident radiation and I is the intensity of the transmitted radiation. The absorbance of the free drug and NA must be linearly dependent upon concentration, and the extinction coefficient must be invariant. The flavonoid compounds and the NA obey the Beer - Lambert law in the range between $10^{-6} - 10^{-3}$ M. Considering this fact, any changes observed during the titration can be related to the drug-DNA binding process.

The data obtained by this assay have been fitted in the following equation (Missailidis *et al.* 2002, Arrowsmith, 1999), using automated fitting in the Origin program:

$$Abs_c = \frac{(Abs_f - Abs_0) \left\{ 1 + KnD + KAbs_0 - \sqrt{(1 + KnD + KAbs_0)^2 - 4KKnDAbs_0} \right\}}{2KnD} + Abs_0nD$$

where:

Abs_c is the absorbance calculated (by the above equation); Abs_f is the final absorbance of the drug after titration (parameter 1, P1); Abs_0 is the initial absorbance of the drug before titration (parameter 2, P2); K is the binding constant which

indicates the strength of binding (parameter 3, P3); D is the drug concentration in the solution (parameter 4, P4); n is the number of drugs per base pair when fully bound (parameter 5, P5; see Figure 11 for an explanation)

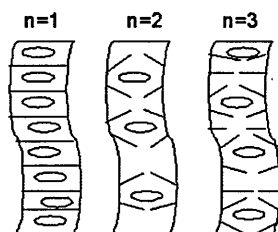


Figure 11: DNA binding sites. The drug is represented by the green ball, and the binding site (n) is the number of base pairs per drug when fully bound, base on the nearest neighbour model. For $n=1$, the drug intercalates on each base pair, that situation would make the DNA to extend 100%, a very unstable situation.

Absorption spectra of the compounds were obtained using a UVIKON UV/Visible spectrophotometer. The Beer–Lambert law was obeyed within the concentration ranges used for both drug and DNA solutions. The extinction coefficients of the compounds were determined using the following procedure: measurement of intensity of absorbed light for solutions with various concentrations of the test drug; a plot of A vs c was constructed and the line-of-best-fit through the experimental points was obtained. The slope of the line passing through the origin (this intercept is zero) was taken as the molar absorptivity. To study the changes in the UV–visible absorption spectra of the drugs upon interaction with NA, the following general method was used for a fixed volume (1 ml for each compound in appropriate buffer) of an aqueous drug solution (unless stated differently, the concentration were made up to give an absorbance between 0.5 – 1, this resulted in values of 50 μM for duplexes and 25 μM for triplexes and tetraplexes). The concentration of the nucleic

acids was increased by sequentially adding 2 µl of a 0.02M nucleic acid stock solution. The concentration of the drug in the cuvette consequently varies and the absorbance was therefore corrected using a standard formula: $Abs_{corr} = Abs_{orig} \times (1000 + V) / 1000$; where V is the volume of nucleic acid added. The UV spectrum of the free drug was initially measured and its UV absorbance was included in the calculations of association binding constants as the initial titration point. The final titration point was the absorbance recorded as the completely bound ligand; experimentally, this point was obtained by adding volumes of nucleic acid till there was no further observed change in the absorbance or any increase in the absorbance was solely due to the nucleic acids' absorbance.

2.2.a.4 - Fluorescence titrations

Absorption of UV radiation by a molecule excites it from a vibrational level in the electronic ground state to one of the many vibrational levels in the electronic excited state; this excited state is usually the first excited singlet state. A molecule in a high vibrational level of the excited state will fall to the lowest vibrational level of this state by losing energy to other molecules through collision. Fluorescence occurs when the molecule returns to the electronic ground state, from the excited singlet state, by emission of a photon, see Figure 12.

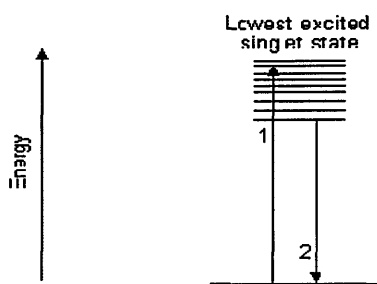


Figure 12: Electronic states during different fluorescence processes. The blue line 1 is the absorption process and the blue line 2 is the fluorescence process. (Modification of kerouac.pharm.uky.edu/ASRG/HPLC/fluorescence.html, 20/07/2006).

To study the changes in the fluorescence emission spectra of the drugs upon interaction with NA, the following general method was used for a fixed volume (3 ml for each compound in appropriate buffer) of an aqueous drug solution in a 3 ml quartz cuvette with 1 cm path length ; the excitation and emission slit widths were set at 5 nm; the excitation and emission values were set by scanning of the free drug and emission wavelengths were chosen where there was no overlap with emission from STDNA or the buffer A. The concentrations of the nucleic acids were increased by adding 6 μ l of a stock solution. The concentration of the drug in the cuvette varies and the emission was corrected using: $Abs_{corr} = Abs_{orig} \times (3000 + V) / 3000$; where V is the volume of nucleic acid added. Fluorescence intensity values were monitored at the emission maximum of the free drug, the change in the emission maximum was followed during the titration and the values were recorded in a FluoromaxP (Jobin Yvon, Japan) equipment. The fluorescence emission of the free drug was initially measured and was included in the calculations of association binding constants as the initial titration point. The final titration point was the emission recorded as the completely bound ligand; experimentally, this point was obtained by adding volumes

of nucleic acid till no further change in the emission was observed. Data were plotted to obtain binding constants as explained in 2.2.c.2.3

2.2.a.5: Competition dialysis

The competition dialysis is based on the thermodynamic principle of equilibrium dialysis. In the competition dialysis experiment, a volume of NA is dialysed against a solution containing the drug under study. After equilibrium is reached (usually in 24 hours), the amount of drug bound to NA is measured by UV absorbance.

The amount of analyte bound is directly proportional to the association constant for ligand binding to a particular structure. In 200 ml of buffer D containing 1 μM of the test drug, a disposable dialyser membrane (DispoDialyzer® cat: 135506, cut off of 1000 MW) was placed with 0.5 ml of 75 μM concentration of nucleic acids. The beaker was covered with Parafilm and wrapped in foil, and its contents were allowed to equilibrate with continuous stirring at 4 °C overnight. At the end of the equilibration period, nucleic acid samples were carefully removed to microcentrifuge tubes, and were made to a final concentration of 1 % (w/v) SDS (sodium dodecyl sulfate) by the addition of appropriate volumes of a 10 % stock solution of SDS up to 1 ml. The total concentration of each test sample (C_t) was determined spectrophotometrically, the free ligand concentration (C_f) was determined spectrophotometrically using an aliquot of the dialysate solution. The amount of bound drug (C_b) was determined by difference, $C_b = C_t - C_f$

2.2.b: Determination of pK_a in an automatic titrator

Many of the interactions between drugs and receptors are dependent on the ionization state of the functional groups involved in the interactions, the protonation state of an amino group will change the type of hydrogen bonding interactions it can be involved in, as well as allow for it to be involved in ionic or ion dipole interactions. The protonation state will also affect the solubility and availability.

Determination of the pK_a values of the drugs was realized according the method developed by Serjeant, 1984. The measures were performed in an ETS822 end-point titration system (Radiometer, Copenhagen). The titrations started at approximately $pH=2$, with a concentration of each drug at 0.001 M and were performed using aliquots of 0.1 ml from a stock solution of 0.01M NaOH. After reaching the pK_a , the titrations were continued till a basic pH was reached and no further change was observed. pK_a values were calculated by plotting pH vs [NaOH] in Origin 6.0, the inflection point being the pK_a value.

2.2.c: Nucleic acid damage

Oxidative DNA damage appears to play an important role in carcinogenesis, commonly as a result of mutations. This damage can become apparent as alterations in base pairs, adduct formation, strand breaks, and cross linkages. The most common is the DNA single strand break. In an agarose gel, circular and open NA runs with different speed. Open nucleic acid runs faster than nicked nucleic acid, and they can be seen as separate bands. Different band lengths in a same gel will allow us to identify interactions between the nucleic acids and the compounds.

The samples were incubated for 30 min at 37°C. Standard solutions of STDNA, polydAdT, poly(dAdT)₂, polydGdC, poly(dGdC)₂ and polydAdTdT at 10⁻⁵M in buffer A and in buffer B for triple helix, were mixed with the various drugs (2 x 10⁻⁶M). The gel was 1% agarose, stained with ethidium bromide (2µg/ml) in buffer TAE, visualized under UV light and photographed. Gel electrophoresis was performed at room temperature at 75 volts in an electrophoretic tank (model Passed MPSU-125/200 submarine gel unit). The gel was photographed using Polaroid Black& White film #667.

2.2.d - Linear Taq polymerase stop PCR and Footprinting assays

Footprinting analysis provides a means of identifying the sites of equilibrium binding drugs on DNA. The most frequently used probe in footprinting studies is the endonuclease DNase I. The enzyme not only reports the sites of ligand binding but, since it is sensitive to local changes in DNA structure, it has also been used to determine the sites of ligand-induced structural changes in DNA. These are reflected in enhancements in the DNase I cleavage rate, appearing as sites on the DNA lattice bind ligand. The rate of cleavage by DNase I at a phosphodiester linkage of DNA, is governed by rate expression. In the drug-DNA footprinting experiment, the drug may influence the cleavage rate by blocking the enzyme from cleaving at certain sites, altering DNA structure away from the sites of binding, or causing redistribution of the enzyme to regions where no drug binding is occurring. The redistribution of enzyme should lead to increases in the rate of cleavage associated with all sites not involved in binding. If the total amount of cleavage on the fragment remains constant as drug loading occurs, the amount of enzyme on the fragment is also constant. Thus,

drug binding shifts enzyme to unblocked sites, increasing DNase I concentration at these sites. This mechanism predicts that all unblocked sites will exhibit the same fractional enhancement, the magnitude of which is related to the fraction of the total number of enzyme cleavage sites which are blocked by drug (Ward *et al.*, 1988).

The DNaseI footprinting protocol is based on the principle that DNaseI digests the DNA that is not bound to the drug. The result is gaps on the sequence of the DNA. A basic protocol is: incubation with the drugs, incubation with the DNaseI and loading of samples into a denaturing polyacrylamide gel for reading. In Figure 13 a footprinting scheme is shown.

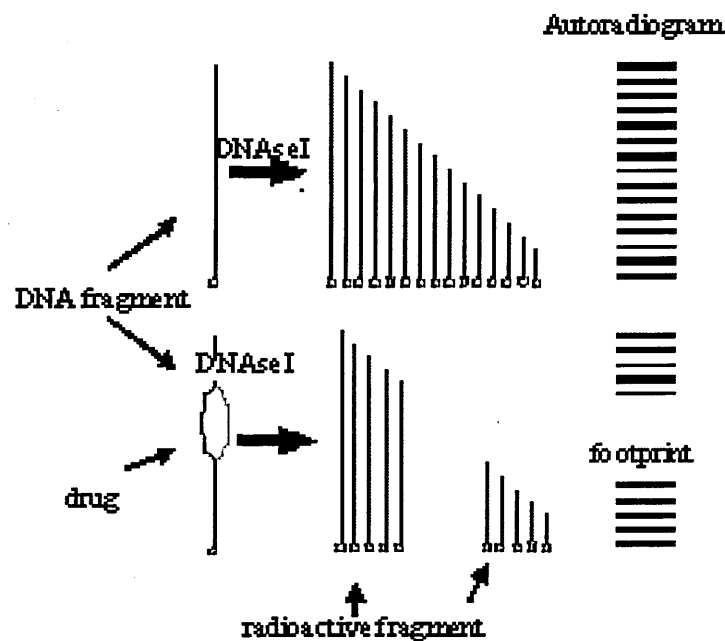


Figure 13: Dnase I footprinting representation. The drug is incubated with the DNA and the complex is digested with DNaseI that after radiography shows a gap in the bases when run in a polyacrylamide gel; this gap is called a footprint and represents the drug – DNA binding site (Musciatti, 1995).

DNA polymerase assay also determines the specificity of binding of drugs for DNA sequences. In this procedure the drug is incubated with the DNA and then the DNA is extracted from an agarose gel in order to remove any unwanted drug and buffer. A PCR (polymerase chain reaction) cycle is performed on the sample using a DNA polymerase (ex: Sequenase); after the sample is load in a denaturing polyacrylamide gel, the result is similar to the one obtained by footprinting as it is shown in Figure 13. Topo 2.1 plasmid (390 µg) was linearised with EcoR1 restriction enzyme (10 Units) in 10x reaction buffer SH (50µl) and water (450µl), 1 hour at 37°C. The sample was precipitated with NaOAc (3M) and ethanol 95%. Linearised DNA (0.5 µg) was incubated with 50 and 100 µM of each drug for 30 minutes at 37°C, in buffer A. The DNA was extracted from a 1% agarose gel using the gel extraction Qiagen Kit. Linear amplification was performed in a premix total volume of 17 µl containing 0.5 µg of DNA, primer M13 Forward -21 (5'-TGTAACGACGGCCAGT-3') (1µl), primer M13 Reverse (5'-CAGGAAACAGCTATGACC-3') (1µl), 3.5x sequencing PCR buffer (7.2µl) and Sequenase (1µl); 4 µl of this premix was divided in 4 and added in a 0.2 ml eppendorf containing each one 2 µl of dATP – dCTP – dGTP – dTTP. The amplification procedure was carried out for 30 cycles, each consisting of 30 sec denaturation at 94°C, 15 sec annealing at 48°C and 1 minute chain elongation at 72°C. The samples were taken up in formamide dye (5 µl), denaturated at 95°C (4 min) and removed onto ice. The DNA fragments were separated on 0.4 mm, 41 cm, 6% polyacrylamide gels with buffer TBE at 50°C, 3000V for approx. 10 hours. Results were observed on LI COR 4200 sequencing series. The sequence specificity of covalent DNA modification by the drugs has been determined using footprinting assays. Oligonucleotides were purchased from SIGMA

Genomics (United States) on a scale of 0.2 μ M. Duplex DNA fragments were prepared by PCR reaction. Linear amplification was performed in a total volume of 100 μ l containing 0.5 μ g of DNA (5'-GGGAGACAAGAATAAACGCTCAAGCAGTTGATCCTTTGGATACCCTG GG CCTGTTGTGAGCCTCCTGTCGAA-3'), primer M13 Forward -21 (5'-GGGAGACAAGAATAAACGCTCAA-3') (1 μ l), primer M13 Reverse (5'-GCCTGTTGTGAGCCTCCTGTCGAA-3') (1 μ l), 10x PCR buffer (10 μ l), 0.4 mM dNTP mix, 0.6 μ l $MgCl_2$ and 2U Taq polymerase. The amplification procedure was carried out for 35 cycles, each consisting of 1 minute denaturation at 94°C, 1 minute annealing at 48°C and 1 minute chain elongation at 72°C, with a final step of 10 minutes at 72°C. The DNA was extracted by ethanol precipitation and incubated with 100 μ M of each drug for 60 minutes at 37°C, in 10mM phosphate buffer. DNase I digestion was performed for 5 minutes at 37°C using 2 μ l DNase I diluted solution to achieve 0.01units/ml. The solution was stopped with DNase I stop solution (3 μ l) and the DNA was heated to 95°C for 10 minutes and frozen immediately in liquid nitrogen. The samples were stored at -20°C.

Ladder: permanganate oxidizes the C5-C6 double bond in thymines and renders the DNA backbone sensitive to cleavage by piperidine. The 40 mM $KMnO_4$ solution is prepared in 0.01 M phosphate buffer and stored on ice. $KMnO_4$ stop solution consists of 20 mM Tris pH 7.4, 20 mM NaCl, 40 mM EDTA, 1% SDS, 0.4M β -MeOH and stored at room temperature so the SDS doesn't precipitate. DNA (0.5 μ g) was mixed with 10 μ l of ice cold 40 mM $KMnO_4$ and incubated for 2 minutes. The reaction was finished by adding 20 μ l of stop reaction. The DNA is extracted by ethanol

precipitation. The DNA was subsequently resuspended in 10 µl of 10% piperidine and incubated at 95°C for 30 minutes. The digested DNA was extracted by ethanol precipitation and resuspended in 2 µl of 0.05% bromophenol blue [w/v]; 20 mM EDTA in formamide) and 8 µl of distilled water.

Gel electrophoresis: the smallest glass plate was treated with 4 µl of PlusOne Bind Silane (Amersham Pharmacia Biotech, Sweden), in 1 ml of acidic ethanol (0.5% glacial acetic acid in 95% ethanol) to covalently attach the gel onto the glass plate, and let to dry for 5 min and remove the excess using a paper tissue moistened with 95% ethanol. The larger glass plate was treated with 1 ml of a 2% solution of PlusOne Repel-Silane ES (Amersham Pharmacia Biotech, Sweden) to assure gel release and let to dry for 5 min. A solution was prepared for 8% polyacrylamide sequencing gel; 7 M urea; 15 ml of RapidGel, 4 ml of formamide, 7.5 ml of 5X TBE with 525 µl of freshly prepared 10% ammonium persulfate and 112.5 µl of TEMED; and distilled ultra pure water added to make 50 ml of solution. The gel solution was applied to the assembled gel plates (0.4 mm thickness) and allowed 120 min for the gel to polymerize. The sequencing gel run at 80 W (42 mA; 1500 V) for 20 min or until the gel temperature reaches 55°C in 1 X TBE) 2 µl of 0.05% bromophenol blue [w/v]; 20 mM EDTA in formamide was added to the 10 µl reaction. The samples were denaturated for 10 min at 94°C in the thermocycler and placed on ice. Samples (5 µl) were loaded onto and run at 50 W for 80-100 min at 50-55°C.

Silver staining: the gel apparatus was disassembled carefully, separating the glass plates. The glass plate with the bound gel was placed onto a plastic tray. 1 L fixing solution (10% ethanol, 1% acetic acid) was applied and shaken gently for 10 min.

The gel was washed with distilled H₂O for 1 min. The oxidised gel was pretreated with 1 L of 1.5% nitric acid for 3 min, shaking gently. The gel was rinsed with 1000 ml distilled H₂O for 1 min. The gel was impregnated with 1 L of 0.2% AgNO₃ solution for 20 min, shaking gently. The gel was rinsed with 1 L distilled H₂O for 30 s, twice. The gel was developed by applying 1 L of developing solution (30 g/l Na₂CO₃; 0.54 ml 37% formaldehyde) and gently shaken until the solution is dark. The developing solution was subsequently removed. The developing reaction was stopped by adding 1 L of 5% acetic acid for 5 min. The gel was air dried overnight and scanned.

2.2.e : Topoisomerase I and II inhibition – DNA unwinding

DNA topoisomerases are a class of enzymes involved in the regulation of DNA supercoiling. Type I topoisomerases change the degree of supercoiling of DNA by causing single-strand breaks and re-ligation (see Figure 14). Type II topoisomerases cause double-strand breaks (see Figure 15). The different roles of DNA topoisomerase I and II may indicate an opposing pair of roles in the regulation of DNA supercoiling. Both activities are crucial during DNA transcription and replication, when the DNA helix must be unwound to allow proper function of large enzymatic machinery, and topoisomerases have been shown to maintain both activities. Inhibition of any of them would interrupt the processes of transcription and replication. Compounds like camptothecin and ureas are known inhibitors of these enzymes (Esteves-Souza, 2005)

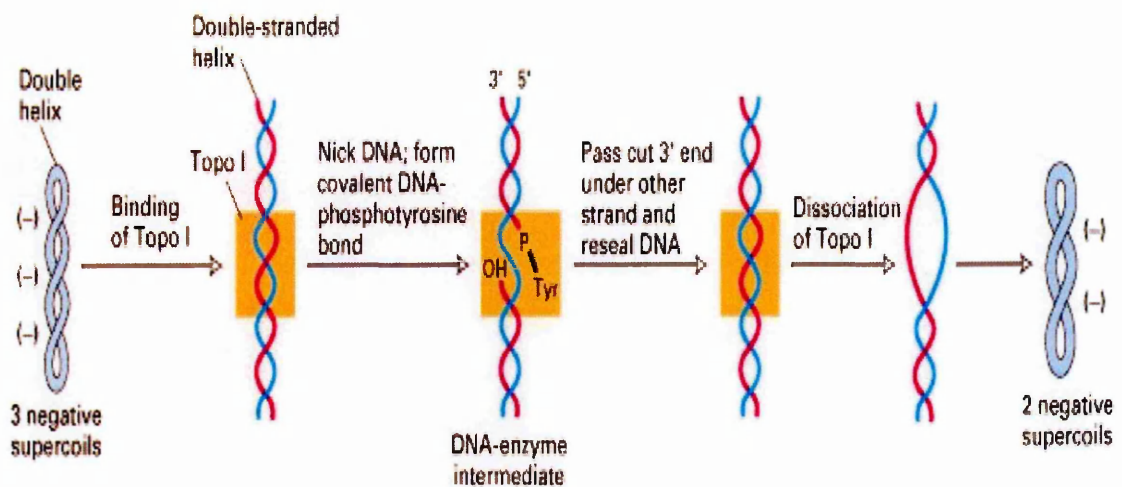


Figure 14: DNA binds to topoisomerase I and the double strand is nicked allowing resealing passing under the other way. Dissociation of topoisomerase I gives rise to a different supercoil DNA (<http://bioweb.wku.edu/courses/biol22000/14Topoisomerase/default.html>, 19/07/2006)

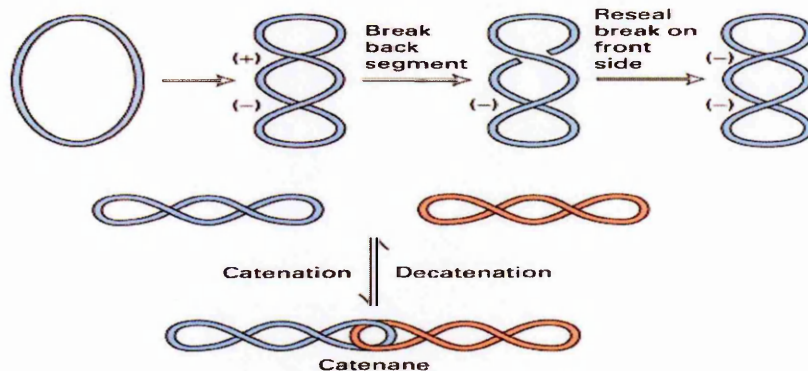


Figure 15: Topoisomerase II interconverts topological isomers of DNA by breaking and resealing phosphodiester bonds (<http://bioweb.wku.edu/courses/biol22000/14Topoisomerase/default.html>, 9/07/2006)

The topo I and II inhibition assays were carried out according to the manufacturer's protocol of the topo I and topo II assay kit (TopoGen Inc., USA).

The kits used for these experiments were:

TopoGEN Topo I Drug Screening Kit (representative for 100 assay kit size: supercoiled plasmid substrate DNA, 25 µg; relaxed and nicked plasmid DNA markers; 10X Topoisomerase I assay/cleavage buffer, 300 µl; sodium dodecyl sulfate (SDS) termination buffer (10%); 10X gel loading dye). Purified human topoisomerase was purchased from TopoGen and used according to the protocol provided by TopoGen. The control inhibitor was camptothecin, purchased by SIGMA Aldrich (United Kingdom), in a final concentration of 100 µM. Proteinase K was purchased by SIGMA Aldrich (United Kingdom).

TopoGEN Topo II Drug Screening Kit (representative for 100 assays: supercoiled DNA [pRYG DNA] 25 µg; markers are linear pRYG DNA and open circular DNA; 10X Topoisomerase II relaxation assay buffer; 10X Topoisomerase II cleavage buffer; sodium dodecyl sulfate (10%); 10X Gel loading buffer (bromophenol blue, glycerol); control inhibitor, etoposide. Purified human topoisomerase II was purchased from TopoGen (USA) and used according to the protocol provided in the kit. Proteinase K was purchased by SIGMA Aldrich (United Kingdom). For topoisomerase II, cleavage as well as relaxation experiments were performed. kDNA / topoI and pRYG DNA / topo II were incubated at 37°C for 60 minutes with different concentrations of the drugs: 50 µM, 75 µM and 100 µM.

The reactions were stopped by adding 2 µl of SDS 10% and were followed by digestion with proteinase K, with an incubation time of 15 min at 37°C. The samples were run on a 1% agarose gel in TAE buffer, visualized under UV light and photographed. Gel electrophoresis was performed at room temperature at 75 volts in an electrophoretic tank (model Passed MPSU-125/200 submarine gel unit). For topoI

drug screening assay, the gel was stained after running in a solution of EtBr 5 µg/ml and destained in distilled water prior to be photographed using Polaroid Black%&White film #667.

For topo II drug screening assay, the agarose and buffer gel were containing EtBr (ethidium bromide) 5 µg/ml during running.

2.2.f.1: Evaluation of compounds in tumour models

The preclinical screening of potential anticancer drugs in tumour models involves *in vitro* and *in vivo* systems. This screening is based on the assumption that a correlation exists between the activity of a compound against human cancer cell lines and its therapeutic effect in human cancer.

2.2.f.2: Flow cytometry

The term "flow cytometry" derives from the measurement (meter) of single cells (cyto) as they flow past a series of detectors. The concept is that cells flow one at a time through a specific region where biophysical properties of each cell can be measured at rates of over 1000/sec. These biophysical properties are then correlated with biological and biochemical properties of interest. The cells are stained with fluorescent dyes which bind specifically to cellular constituents and the dyes are excited by the laser beam, emitting light at a longer wavelength. This emitted light is picked up by detectors, and these analogue signals are converted to digital so that

they may be stored, for later display and analysis (Jaroszeski, 1997). Light scatter is utilized to identify the cell population of interest, while the measurement of fluorescence intensity provides specific information about individual cells. The measurement of the DNA content of cells was one of the first major applications of flow cytometry, the DNA content of the cell can provide information about the cell cycle, apoptosis, etc and consequently the effect of drugs on the cell cycle. This technique also provides percentages of cells on each cycle stage. The percentage of cells in the S-phase gives an indication of the proliferative activity of that cell population, as in this stage the cell synthesizes DNA. Another major stage is preG1, during which the cells prepares for RNA and protein synthesis and grows in size.

The ability of four structurally related flavonoids (baicalein, baicalin, daidzein and quercetin) to affect chemotherapy-induced apoptosis and cell cycle arrest of breast cancer MCF7 and leukemia cancer CCRFCM cell lines was studied. The antitumour ability of flavonoids has been extensively documented, but the effect on cell cycle distribution is still unclear. Flow cytometry has been performed in order to elucidate the effect of our compounds to the cell cycle stages and induction of apoptosis.

MCF7 breast cancer and CCRFCM leukemia cell lines were grown in 6 well-plates in an initial concentration of 3×10^5 cells/ml in the appropriate medium for 24 hours at 37°C and 6% CO₂ in air. A period of 24 hours of incubation with 100 µM of the test compounds and similar concentration of DMSO, followed the initial step. MCF7 cells were trypsinised, and both cell lines were collected in FACS tubes. After a centrifugation period of 8 minutes at 1200 rpm and decantation of supernatant, the cells were kept at 4°C overnight in a Fluorochrome solution (0.1 % Triton X100,

0.1% Na-citrate, 50 µg/ml Propidium Iodide, 0.1 mg/ml RNaseA), this solution is used as a dye for the DNA content in cells (the propidium iodide intercalates into the major groove of the DNA and produces a highly fluorescent adduct that can be excited at 488 nm with a broad emission around 600 nm) the samples were read in a Beckam Coulter Epics XL equipment employing a EXPO32 (Applied Cytometry Systems) software.

2.2.f.3: MTS cell proliferation assay

Viability assays measure the percentage of a cell suspension that is viable. This is generally accomplished by a dye exclusion stain, where cells with an intact membrane are able to exclude the dye while cells without an intact membrane take up the coloring agent. The MTT/S cell proliferation assay is a colorimetric assay system which measures the reduction of a tetrazolium component into an insoluble formazan product by the mitochondria of viable cells. After incubation of the cells with the reagent, a detergent solution is added to lyse the cells and solubilize the colored crystals. The samples are read using an ELISA plate reader at a wavelength of 570 nm. The amount of color produced is directly proportional to the number of viable cells. The system is a quantitative test, and because there is a linear relationship between cell activity and absorbance, the growth or death rate of cells can be measured. The Cell Titer 96® AQueous Non Radioactive Cell Proliferation Assay (Promega, United Kingdom) is a colorimetric method for determining the number of viable cells in proliferation. The tetrazolium compound (3-(4,5-dimethylthiazol-2-yl)-5-(3-carboxymethoxyphenyl)-2-(4-sulfophenyl)-2H-tetrazolium, inner salts) was

dissolved in buffer PBS and electron coupling reagent (phenazine methosulfate) was added according to the protocol supplied. MCF7 breast cancer and CCRFCM leukemia cell lines were grown in 96 well-plates in an initial concentration of 1×10^4 cells/ml – 0.2 ml in the appropriate medium for 24 hours at 37°C and 6% CO₂ in air. A period of 24, 48 and 72 hours of incubation with 0, 1, 5, 10, 50, 100, 500 and 1000 µM of the test compounds followed the first step. According to the protocol 40 µl of MTS – PMS solution was added and incubated at 37°C and 6% CO₂ in air for 2 hours prior to reading. Readings were recorded at 490 nm in a plate reader (model Anthos Labtec 2001), employing a Deltasoft3 (Biometallics Inc) software.

2.2.f.4: COMET ASSAY – Alkaline electrophoresis

Analysis of Oxidative DNA damage using the Comet assay: Oxidative DNA damage was measured in both cell lines using the Trevigen Comet assay. The assay is a sensitive technique for detection of DNA damage.

The samples are treated for 24 hours with the test drugs and for positive control, H₂O₂ is used. When the samples are loaded in an agarose gel and electrophoresis is carried out, the DNA (negatively charged) will run towards the positive pole. The cells will remain in their position. If the DNA has been damaged, a smear band (like comet) will be observed coming out of the cell representing the various DNA fragments. In a negative result, the cell remains intact.

An explanation of the comet assay is shown in Figure 16.

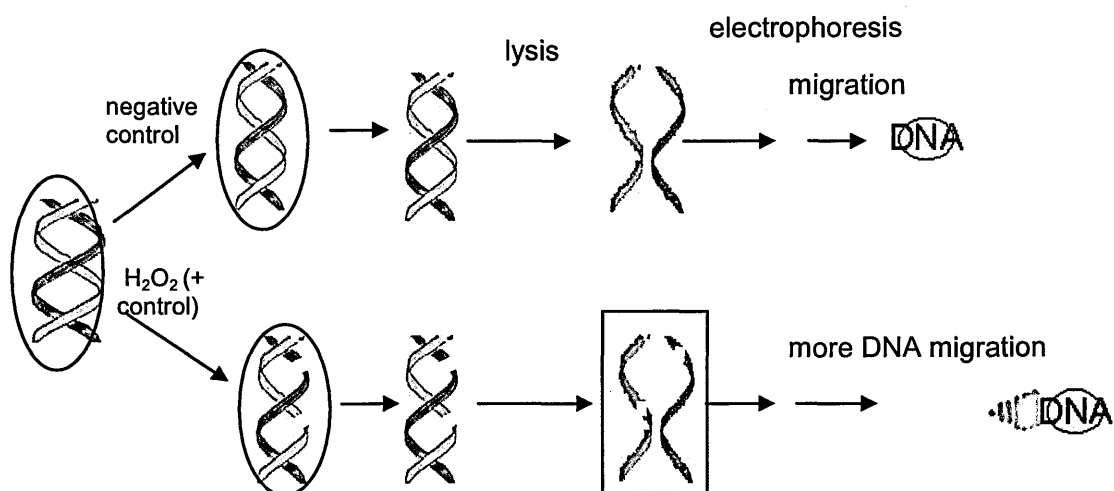


Figure 16: Comet Assay. In presence of a DNA damage agent (like hydrogen peroxide) the nucleus experience a retardation when the cell is run in an agarose gel, giving rise to a shape of a comet tail.

Protocol was based on the Trevigen Comet Assay manufacturer's specifications provided in the respective kit. Briefly, both cell lines were grown overnight in an initial concentration of 3×10^5 cells/ml in the appropriate medium for 24 hours at 37°C and 6% CO₂ in air. A period of 24 hours of incubation with 100 µM of the test compounds followed the initial step. Treatment with H₂O₂ was used as positive control. Cells were suspended in LM Agarose, 10µl of sample per 70µl low melting Agarose (Trevigen) and pipetted (75µl) onto each sample well of Trevigen Comet Slides. Subsequently, all slides were refrigerated at 4°C for 1 hour to allow adherence of the agarose to the slide, then immersed in lysis solution (Trevigen). Following lysis, all slides were placed in alkali buffer (0.3 M NaOH, 200mM EDTA, pH>13) for 40 minutes at 4°C to unwind the DNA. Next, the slides were electrophoresed at 25V, 300mA for 30 minutes. After electrophoresis, slides were neutralized in 0.4M Tris-HCl buffer (pH 7.4), deionized water / ethanol and allowed to dry overnight.

Slides were then stained with SYBR green in buffer TE pH 7.4. Samples were viewed on a fluorescent microscope with FITC filters (excitation 494 nm, emission 521 nm).

2.2.g: CYP1A1: Analytical assay for metabolites products

The cytochrome (CYP) P450 family of enzymes is responsible for the metabolism of the majority of drugs and xenobiotics, consisting in subfamilies of CYP1A, 2C, 2D and 3A. P450s most commonly catalyse monohydroxylation, but other reactions can be catalysed as well. CYP1A1 is an extrahepatic enzyme responsible for bioactivating several classes of food or environmental procarcinogens (polycyclic aromatic hydrocarbons (PAHs)) like cigarette smoking products and other products of combustion. The CYP1A enzymes are substrate inducible; and this induction occurs at the level of transcription and is mediated by the cytosolic aryl hydrocarbon receptor. Ligand binding to the receptor induces conformational changes (named transformation) which allow the AhR to translocate to the nucleus and dimerize with the AhR nuclear translocator protein. The complex AhR-ARNT functions as a transcriptional activator by binding to consensus sequences present in the 5' flanking DNA of numerous genes (Williams, 2001). Decreased activation of carcinogens due to modulation of the CYP1A enzymes has been proposed as a possible chemopreventive mechanism. Flavonoids are present in the daily diet, therefore we studied the possible number of hydroxylations for compounds 3, 4, 6 and 8 after incubation with CYP 1A1, as this enzyme is the one responsible for the majority of flavonoid metabolism in the human body. Solutions of substrates were prepared in DMSO at a concentration of 10 mM. Microsomal fractions of CYP1A1 were incubated in the

presence of a NADPH-generating system at 37°C for 60 min in test tubes. The incubation mixture consisted of 0.2 g/L microsomal protein, 0.1 M potassium phosphate buffer (pH = 7.4), 0.066 mol/L glucose 6-phosphate, 0.026 M NADP⁺, 0.065 M MgCL₂6H₂O, 40 IU/ml glucose 6-phosphate dehydrogenase and concentrations of 0, 25, 50 and 100 µM of test compounds in final volume of 0.5 ml. The metabolic reaction was initiated by the addition of microsomal protein. After incubation for 60 min, the reactions were stopped by cooling on ice and the mixtures were vortexed for 1 min, centrifuged at 12,000 g for 10 min and the reaction supernatants were transferred to a clean tube and freeze dried. Samples required to be derivatised with BFTSA (N-methyl-N-(trimethylsilyl)-trifluoroacetamide) to enable analysis by GC-MS; as carbohydrates cannot withstand derivatisation, baicalin underwent acid hydrolysis prior to treatment with BFTSA.

Acid hydrolysis: H₂SO₄ (0.5 M) (1 ml) was added to each sample of baicalin. The solutions were incubated at 37 °C for 1 h. Double distilled water (1.0 ml) was added and the solutions were acidified by addition of concentrated HCl (20 ml) and extracted twice with diethyl ether (2.0 ml). Diethyl ether was removed under a reduced pressure. **Derivatisation:** dried samples were derivatized by addition of BSTFA (100 µl) at 80°C for 12 hours.

Gas chromatography coupled with mass spectrometry (GC–MS): Analyses were performed using a HP 5973 mass spectrometer coupled to a HP 6890 gas chromatograph. Separation of the analytes was achieved using an HP 5MS capillary column, (30 m x 0.25 mm I.D., 0.25 mm film thickness). Helium was used as carrier gas with a linear velocity of 0.9 ml/s. The oven temperature program was: initial

temperature 100°C, 100–270°C at 4°C/min, 270°C for 20 min. The GC injector temperature was 250°C; the transfer line temperature was held at 280°C. The mass spectrometer parameters for EI mode were: ion source temperature: 230°C; electron energy: 70 eV; filament current: 34.6 mA; electron multiplier voltage: 1200 V.

2.2.h: Hemin sesquiterpenes interactions

The mechanism of action of artemisinin is still unclear, but most likely involves the formation of free radical intermediates, originating from the direct interaction of the endoperoxide group with the heme iron (Messori, 2003). Artemisinin becomes cytotoxic in the presence of ferrous iron. Since iron influx is high in cancer cells, artemisinin and its analogs selectively kill cancer cells under conditions that increase intracellular iron concentrations.

Solutions of 1 ml of hemin 18×10^{-6} M in buffer E were titrated with 0.01 M stock solutions of STDNA, artesunate and artemisinin in different ratios; with and without stock solutions of FeCl_2 0.01M. Absorption spectrums of the complexes were obtained with a UVIKON UV/Visible spectrophotometer. Data were plotted to analyse interactions.

Chapter 3: Preliminary results

3.1: Screening of natural compounds

As explained in Chapter 1, a group of compounds isolated from herbal extracts was selected for biophysical and biological testing in order to establish if there is an interaction between these compounds and DNA.

3.2: Drug - DNA interactions

3.2.a: Melting temperature

A stabilising DNA agent would increase the melting point of a DNA motif, a process that would interfere with the replication of DNA and would not allow the cell to synthesise DNA and replicate, eventually leading the cell to apoptosis. On the other hand a destabilising agent would shift the melting point to lower temperatures promoting the DNA structure to open. For STDNA and polynucleotides polydAdT and poly(dAdT)₂, one transition from double helix to single stranded is present. In the case of triple helix polydAdTpolydT, two transitions are observed, from triple to double helix, and from double to single strands.

The experiments were conducted at pH 7.4 (physiological conditions) and pH 6.5 for purine triplex motif (environment required to facilitate the triple structure formation) and in the appropriate buffer according to the nucleic acid used; buffer A for duplexes, buffer B for polydAdTdT, buffer C for purine triplex motif and buffer D for quadruplex DNA (see section 2.2.a.1); all structures were monitored by melting denaturation to assess formation (refer to Figures 17 a , 17 b and Appendix). Melting

points have been calculated as the maxima of the first derivative (or differential) of the sigmoide curve observed when measuring the UV spectra of DNA at various temperatures and fitting the data in Origin 6.0 (Figure 17). The results are shown in Table 1.

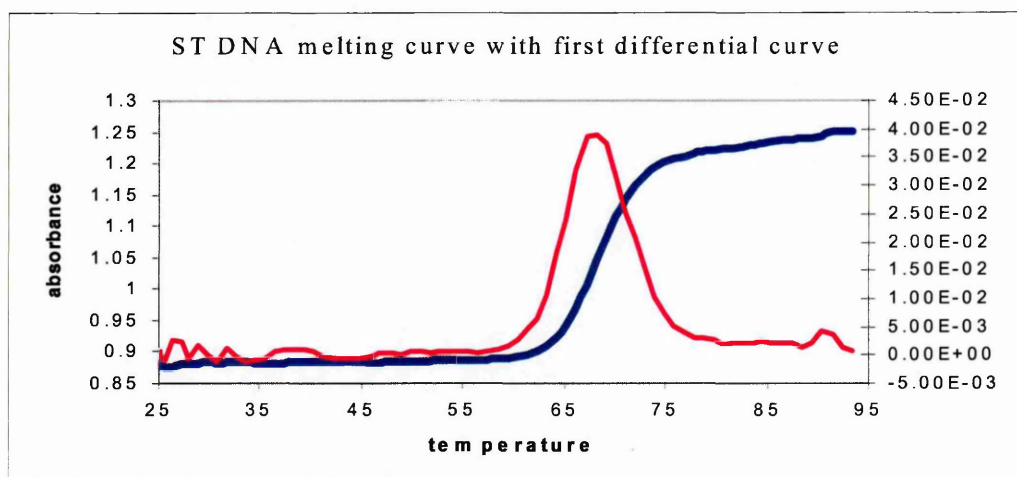


Figure 17a: Representation of STDNA alone melting curve and the first differential indicating the maxima in the curve (pink) is the inflexion point in the melting curve (blue).

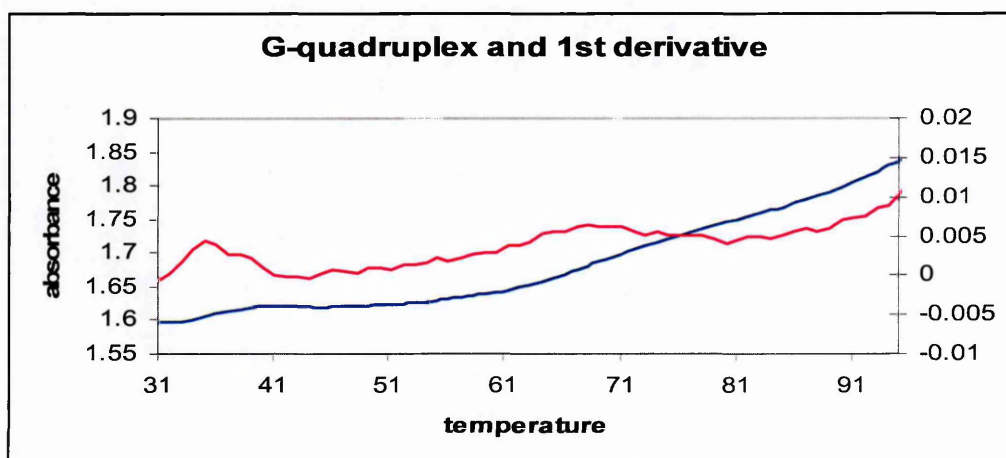


Figure 17b: Representation of G-quadruplex alone melting curve and the first derivative (1st differential) indicating the maxima in the curve (pink) is the inflexion point in the melting curve (blue). The first inflexion point is the transition of the TTA bases belonging to the loop of the tetraplex and the second point is the transition of the G-tetrads in the tetraplex.

Melting points for polydGdC and poly(dGdC)₂ could not be calculated as the strength of the GC bonds is so high that denaturing points can not be measured in the range of 25 - 98°C. For STDNA quercetin and rutin showed a slight destabilising effect. In the case of polydAdT, none of the drugs showed any activity. For polydAdT-dAdT the drugs proved to be non-effective (Figure 18). Quercetin (Figure 19) and baicalein showed to stabilised the triplex helix polydAdTdT in the first transition, by 3.2°C for baicalein and 7.3°C for quercetin. However, the drugs provoked a slight destabilisation of the second transition (Figure 19 and Table 1). An acridine derivative was used as the positive control for melting stabilisation of STDNA ($\Delta T=12^{\circ}\text{C}$).

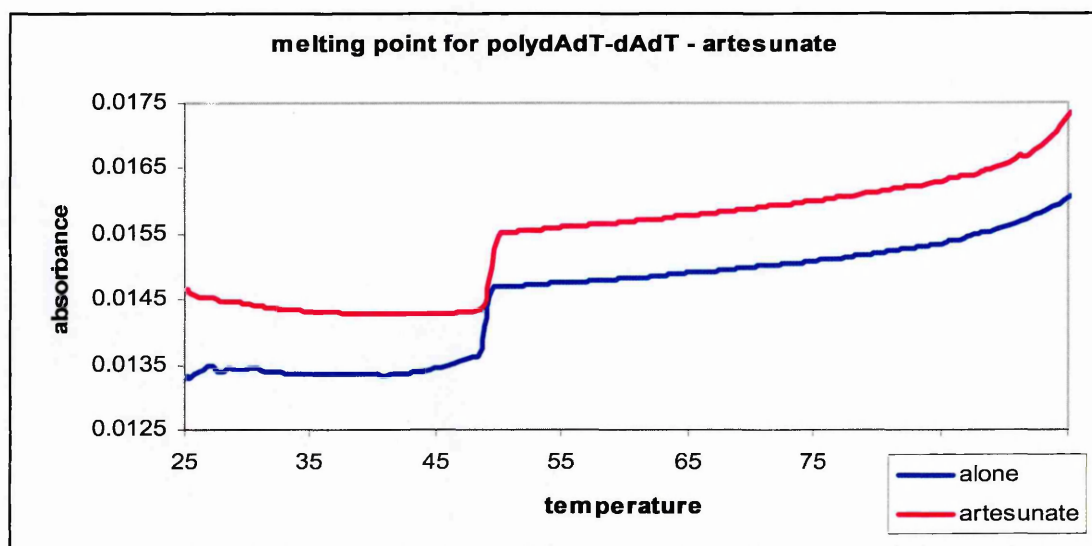


Figure 18: The results of the temperature denaturation studies for polydAdT-dAdT – artesunate show how artesunate (pink) does not affect the double helix melting profile

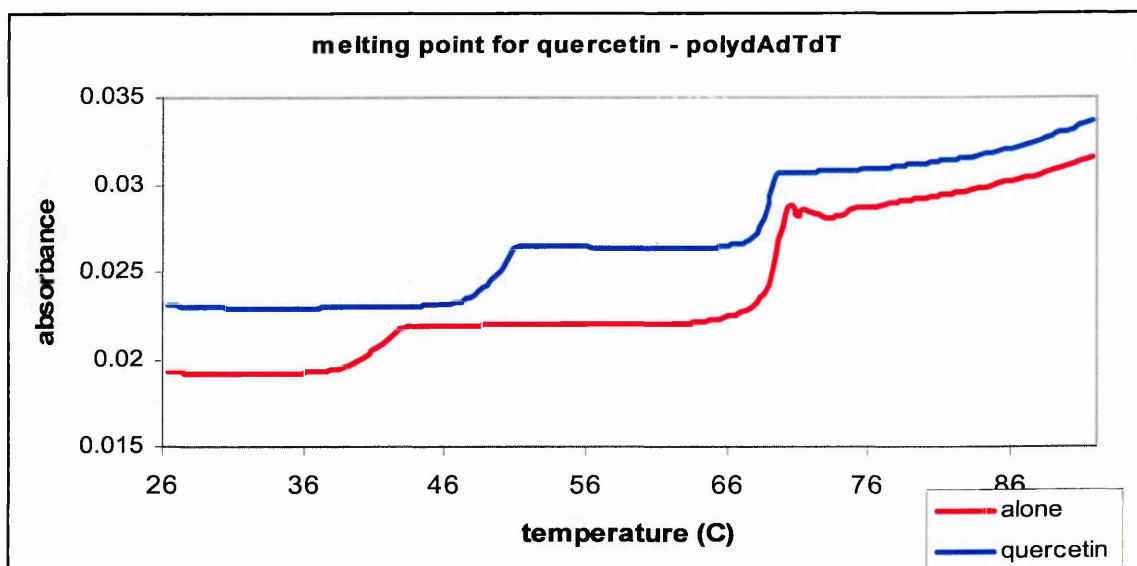


Figure 19: The results for the temperature denaturation studies for polydAdTdT – quercetin show clearly that quercetin stabilises the first transition from triplex to double strand.

G-quadruplex oligonucleotides presented two transitions, the opening of the TTA loop, with a first melting point at 35.9°C and the opening of the G-bases forming the tetraplex structure with a second melting at 69.1°C. Artesunate, artemisinin, cantharidin and rutin do not have an effect on the stability of any DNA structure. Baicalein made the first melting point of the G-quadruplex disappear but did not affect the second, which indicates that baicalein binds preferentially to the TTA sequence. Baicalin and daidzein destabilised the G-quadruplex and caused its denaturation at a lower temperature. Puerarin did not affect the first transition of the G-quadruplex but stabilised the second one, implying a preference for the G-bases forming the quadruplex structure. Quercetin did not affect considerably the melting points of the G-quadruplex but it affected the denaturation pattern, producing the appearance of a third melting point (refer to Appendix).

Table 1: The results of the temperature denaturation assay and our original set of compounds are shown. In the case of polydAdTdT, all the compounds appeared to interact, in some cases stabilising the first transition point (like baicalein and quercetin) and in some cases distabilising the first transition point (like artesunate, artemisinin, baicalin, cantharidin, daidzein and rutin). In the case of G-quadruplex, the flavonoids baicalein, baicalin, daidzein, puerarin, quercetin and rutin showed remarkable effects in different points of the tetraplex, stabilising or destabilising the two transitions observed, or adding a third one, in the case of quercetin.

Nucleic acid	ΔT_m								
	Artesunate	Artemisinin	Baicalein	Baicalin	Cantharidin	Daidzein	Puerarin	Quercetin	Rutin
ST DNA	0.1	-1	0.2	0.3	-0.8	-0.7	-0.3	-1.2	-1.2
T(68.1°C)									
polydAdT	0.6	0	0.6	0.1	0.2	0.1	0.7	0.7	1.2
T(47.5°C)									
Poly(dAdT) ₂	-0.2	0.1	0	0	0.5	0	-0.4	-0.1	0.3
T(48.9°C)									
polydAdTdT	-5.1/-1.8	-6.4/-2.2	3.2/-2.4	-6.9/-2.3	-6.7/-2.3	-5.8/-2.7	0.6/0.2	7.3/-1.5	-4.3/-1.9
T(41.5/69.4°C)									
G-quadruplex	-7.7/0	-6.8/-3	--/0	-1.9/--	-4.9/1	0.2/--	0.2/14.9	-2.9/0.3/--	-0.9/0.5
T(35.9/69.1°C)									

3.2.b.1: Association binding constants

Artesunate, artemisinin and cantharidin have no UV/visible spectrum and fluorescence emission; thus this experiment was performed only for the remaining compounds. Extinction coefficients were determined for those peak maxima that lay outside the range of the absorbance of nucleic acids.

Compound	Wavelength (nm)	Extinction coefficient (M^{-1})
Baicalein	359	14898
Baicalin	315	15556
Daidzein	310	15639
Puerarin	340	14572
Quercetin	375	11806
Rutin	365	16956

Table 2: Extinction coefficients for baicalein, baicalin, daidzein, puerarin, quercetin and rutin in buffer A.

The appropriate concentration of drug for binding interactions was obtained after titrations were performed using different drug concentrations, based on a range of absorbance/drug concentrations. The best results were obtained for values of 0.5 of absorbance giving a general concentration of 5×10^{-5} M.

To examine the DNA binding properties, we performed UV/Vis and fluorescence titrations (see section 2.2.a.2. to 2.2.a.4). In practice, a solution containing the test compound is placed into a quartz cuvette, an initial spectra is recorded (Abs_0), nucleic acid aliquots are added and stirred into the test solution and a spectra is recorded after each addition; aliquots are added till no further change in the absorbance. The results are initially plotted into Excel (Figure 20, 22). Absorption measurements at the absorption maxima wavelength vs. DNA

concentration were fitted into the binding equation (see section 2.2.a.3) to result in a binding curve points and a best fitted curve corresponding to a binding constant value (full line) (Figure 21).

A bathochromic shift was found in all cases, except for baicalein which exhibited a hypochromic shift. Isosbestic points are an indication of a two-state situation, one involving the drug unbound and the other the drug–DNA complex (drug bound); poorly defined isosbestic points may indicate an interaction involving more than two states (multiple binding motifs). For our preliminary set of compounds we observed the following isosbestic points: baicalein (312, 413 nm), daidzein (297, 365 nm), quercetin (302, 464 nm) and rutin (311, 420 nm).

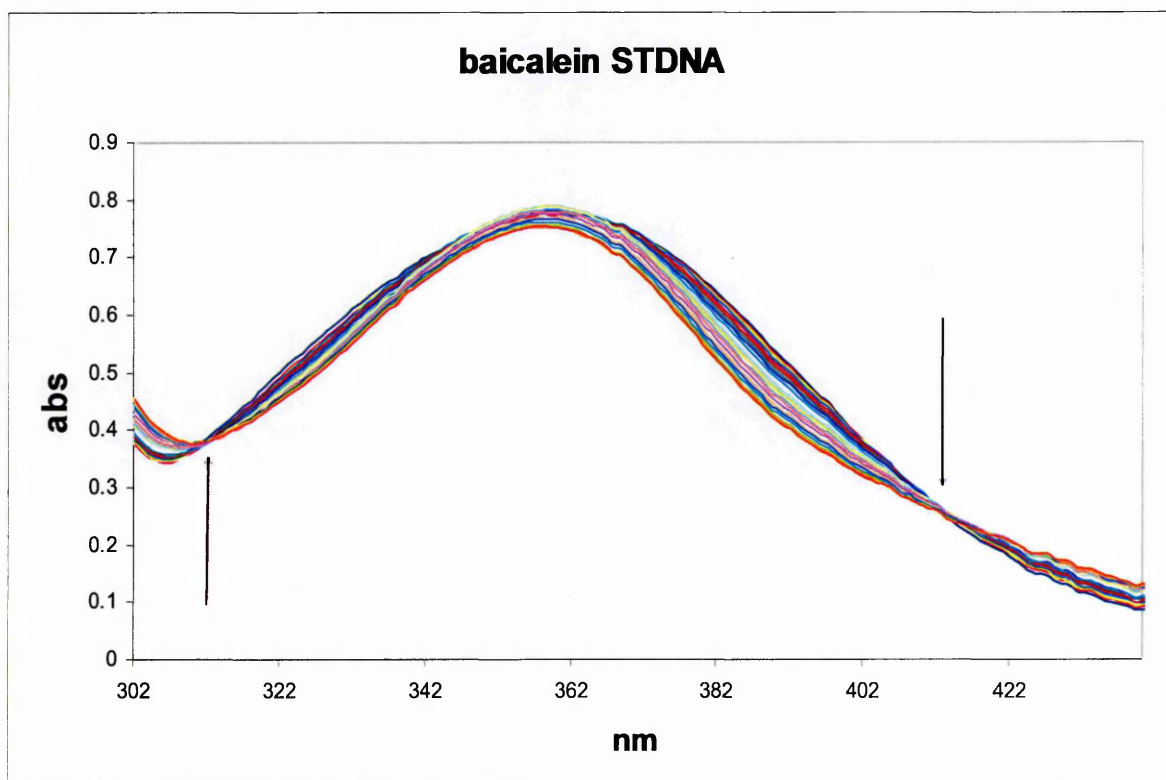


Figure 20: The results of the titration of baicalein with STDNA is shown and the arrows indicate two defined isosbestic points; a clear indication of the formation of a single drug

- DNA complex.

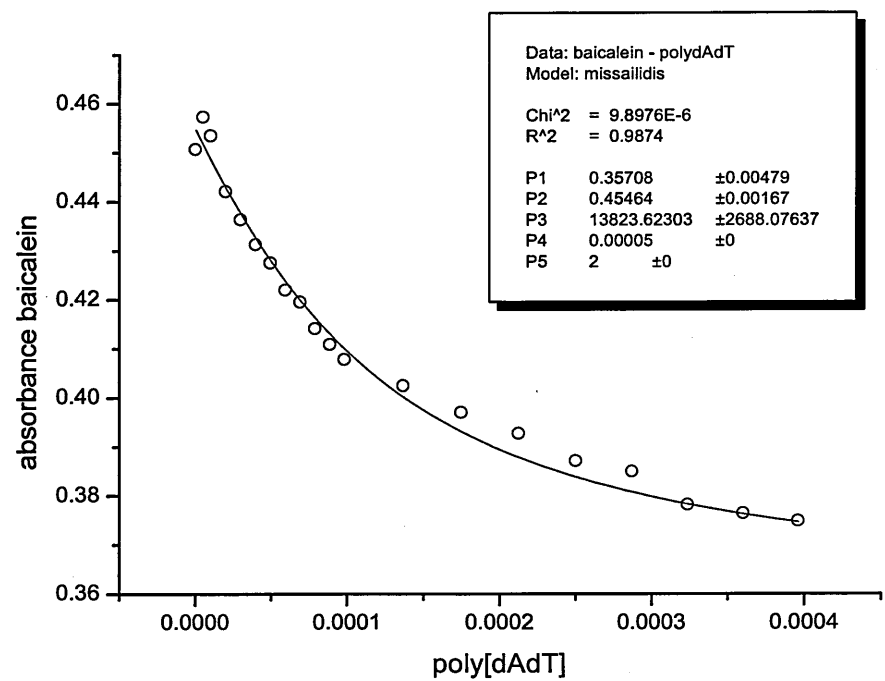


Figure 21: The results of fitting the data into the binding association equation is shown for baicalein – STDNA complex. Please refer to see section 2.2 in Methods for an explanation of the parameters and the formula used.

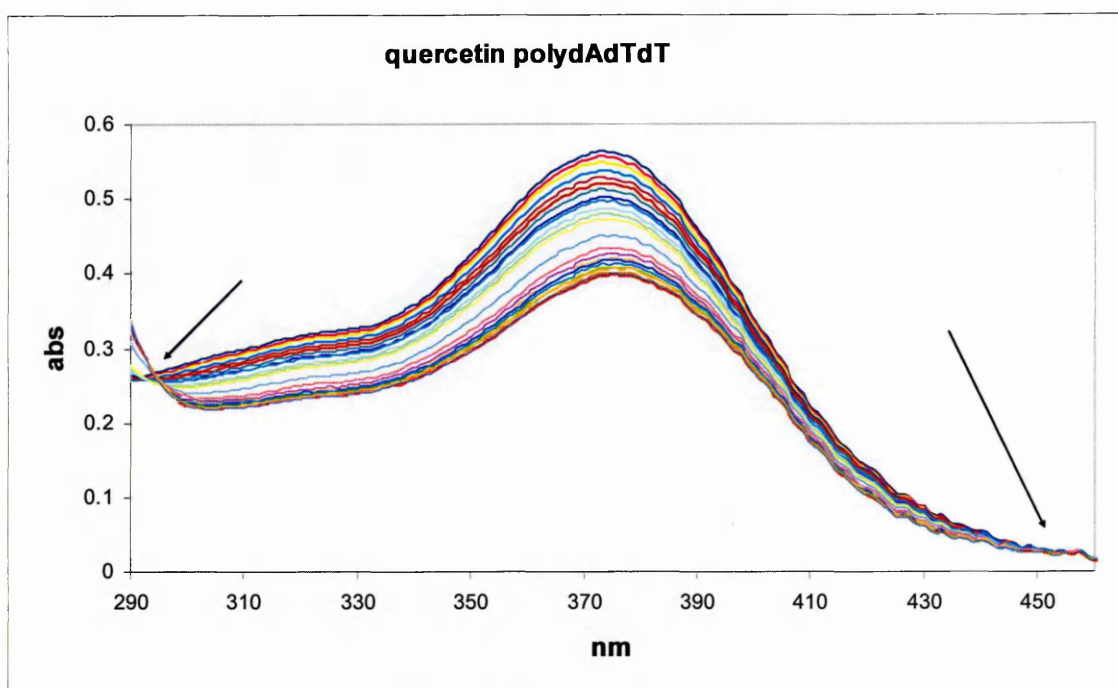


Figure 22: The results of the titration of quercetin with polydAdT-dT show two clear isosbestic points indicating a single binding of the drug to DNA triplex.

3.2.b.2: Duplex binding

The compounds do not have a strong binding affinity to any sequence A-T / G-C, with association constants in the range of 10^4 M^{-1} . These results are in agreement with the melting temperature studies, where the ΔT of compounds for STDNA was not found to be $> 1^\circ\text{C}$. The duplex binding data are presented in Table 3 for duplex binding constants and Figures 20a and 20b for fitting curves. All figures are shown in the Appendix section.

An acridine derivative was used as positive control for binding to STDNA ($K \times 10^6 \text{ M}^{-1}$) (Missailidis, 2002).

Other techniques besides UV/Vis titrations were employed in order to assess the binding association constants, like ethidium bromide displacement and quenching but they did not

provide conclusive results. Another technique that would provide information is fluorescence (see section 2.2.a.4), this technique requires the compound to have fluorescence properties. For the fluorescence titrations with STDNA, the following excitation and emission wavelengths were used respectively: baicalein, daidzein and puerarin were excited at 450 nm and emitted at 530 nm, baicalin and rutin were excited at 450 nm and emission was recorded at 531 nm, quercetin was excited at 450 nm and the emission recorded at 532 nm.

Table 3: The binding association for a range of compounds and different duplex DNA motifs are shown. K is expressed in M^{-1} , n is the number of base pairs per drug, R^2 is correlation coefficient. Fluorescence was used to compare the STDNA association binding value for the UV titrations, it can be noticed that the K values are similar for all compounds except for puerarin that did not present any activity; only the n values can not be compared; possibly as the binding constants are so low it gets harder to assess a real value. Baicalein and quercetin showed to be the compounds with the highest binding constant for all duplexes.

Compound	dAdT (UV)			dAdT dAdT (UV)			dGdC (UV)			dGdC (UV)			STDNA (UV)			STDNA (Fluoresce)		
	K/ M^{-1}	n	R^2	K/ M^{-1}	n	R^2	K (M^{-1})	N	R^2	K/ M^{-1}	n	R^2	K/ M^{-1}	n	R^2	K/ M^{-1}	n	R^2
Baicalein	13823.6	2	0.98	12530.6	2	0.99	13839.3	2	0.99	12143	2	0.97	10027.9	2.1	0.99	15329.6	7	0.97
Baicalin	1358.9	2.1	0.97	1191.2	2.2	0.97	1175.8	2	0.98	445.8	1.9	0.94	1791.9	2	0.98	1287.8	2	0.95
Daidzein	1221.7	2.2	0.98	5681.3	2	0.99	5507.1	3	0.98	3987.5	2	0.99	1521	2	0.91	952.2	3	0.94
Puerarin	6086.2	2	0.98	1263.5	2	0.98	6309.3	3	0.93	6895.1	2.3	0.95	957.8	2	0.98	No interaction observed		
Quercetin	23658.3	1	0.95	12311.4	2	0.99	10966.7	2	0.99	14924.5	2	0.96	12098.6	2	0.99	11417.1	3	0.92
Rutin	5612.3	3	0.98	6587.7	3	0.99	3397.1	4	0.90	3274.8	4	0.98	1183.6	2.1	0.95	1974.4	2	0.95

Baicalein and quercetin presented similar values in magnitude for the different duplex forms in the order of 10^4M^{-1} , with quercetin showing a slight preference for polydAdT. Baicalin, daidzein, puerarin and rutin presented low values for association constants, in the order of 10^3M^{-1} , only rutin and puerarin presenting slightly higher values. With the results obtained from the duplex binding experiments we decided to investigate further the activity of the compounds on other DNA structures. Alternative DNA structures offer significant differences in terms of shapes and rigidity, compared to double stranded DNA. Specific recognition of higher order DNA, such as triplexes and quadruplexes by small ligands has been demonstrated in a number of studies (Ren, 1999).

3.2.b.3: Competition dialysis

To evaluate the selectivity of the drugs for different DNA structures, we performed a competition dialysis experiment using eight nucleic acid structures against a common drug solution. It is possible to correlate the amount of the bound dye to a given structure with the affinity of the dye for that sample (Ren, 2000), this means that the more drug found to be bound to the nucleic acid the more this drug will prefer that structure over the others. Each solution compound was placed in a beaker with the eight different nucleic acid structures (each structure was placed into a membrane in where the drug can cross the membrane freely but the nucleic acid will remain inside) and left to reach equilibrium for 24 h at 4°C. After this period of time the bound drug (the amount of drug inside the dialysis membrane) was measured by UV/Vis absorbance.

Amongst the group of compounds, baicalein and quercetin proved to have the strongest activity when related to the amount of bound drug. Baicalein bound to all the structures in the same proportion while baicalin showed a slight preference for polydAdT and polydAdTdT. Daidzein and puerarin showed strongest selectivity for G-triplex, possibly due to the isoflavone skeleton penetrating easily the base pairs by having the B ring in position C-3. From these results we can presume that hydroxyl groups in the A and B ring help to improve the binding; and sugar substitutions as in the case of baicalin and rutin, decrease the binding activity. In the case of the isoflavonoids, the B ring situated in C-2, decreases the binding activity. See Figures 23 a, b, c, d, e, f for results.

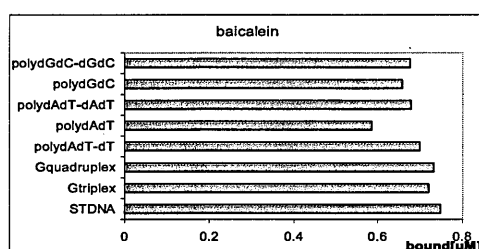


Figure 23 a: Competition dialysis for baicalein showed preference for STDNA, this indicates a lack of selectivity of this compound for any precise sequence.

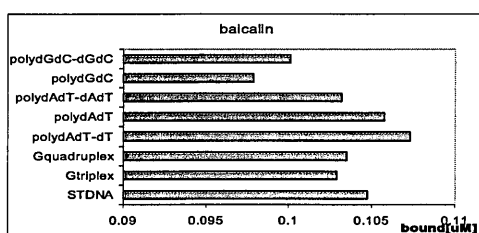


Figure 23 b: Competition dialysis for baicalin showed preference for polydAdTdT and polydAdT.

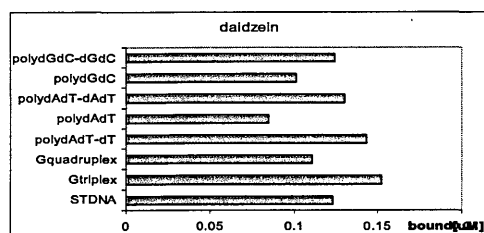


Figure 23 c: Competition dialysis for daidzein showed preference for purine triplex and polydAdTdT. It might be triple structures can accommodate a plain isoflavonoid scaffold with the B ring facing outwards.

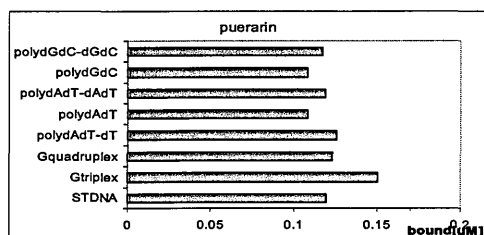


Figure 23 d: Competition dialysis for puerarin showed preference for triplex purine. Puerarin has a similar structure that daidzein, indicating that isoflavonoids can interact better with G-triplex structures.

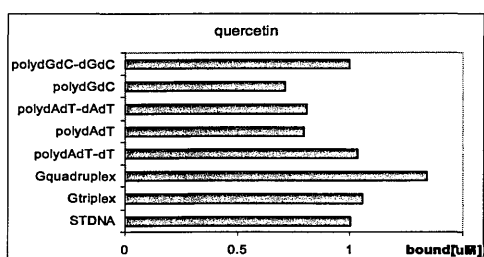


Figure 23 e: Competition dialysis for quercetin showed a high preference for G-quadruplex, this coincides with the binding constant this compound has exhibited for this structure.

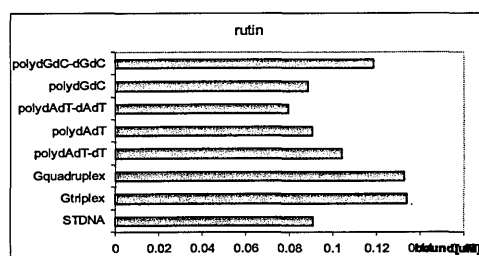


Figure 23 f: Competition dialysis for rutin showed preference for triplex purine, G-quadruplex and polydGdC-polydGdC. This compound seems to prefer GC sequences at any structure, as rutin is similar to quercetin except for rutinoside segment in OH-3 we can presume this sugar substituent plays a relevant role in binding to different DNA isoform.

3.2.b. 4: Triplex binding

Baicalein and quercetin showed higher affinity for both purine and pyrimidine triplexes therefore we selected these two compounds for binding studies to triplex and quadruplex DNA. Temperature denaturation studies confirm the hypothesis that these two flavonoids stabilize the triplex DNA structures. In the case of polydAdT, no significant increase on ΔT was observed, but when we performed the experiment with polydAdTdT, we found an increase of 3.2°C for baicalein and 7.3°C for quercetin (Table 2; see also Table 4 for binding constants). Baicalein presented similar values for both structures, which are similar to the one of quercetin for polydAdTdT; but quercetin exhibited very low binding for the GAG triplex.

Table 4: The results of the binding constants for triplexes structures show baicalein and quercetin to have similar values

Compound	dAdTdT (UV)			GAG triplex (UV)		
	K (M ⁻¹)	n	R ²	K (M ⁻¹)	n	R ²
Baicalein	22704.5	4	0.98	23361.8	3	0.94
Quercetin	27058.1	3	0.99	2446.1	1.4	0.98

3.2.b.5: G-quadruplex binding

G-quadruplexes are a family of high order DNA structures formed in the presence of cations and consist of four strands of guanines stabilized in quartets. The 3' terminal region of the G-rich strand of human telomeres is single stranded and may adopt a G-quadruplex conformation. This structure has been shown to inhibit telomerase elongation activity *in vitro*. Telomerase is expressed in germinal, but not somatic cells, as well as almost 80% of all cancers. Therefore, stabilization of G-quadruplex could interfere with telomerase elongation and replication of cancer cells. Competition dialysis suggests that some of the flavonoids interact with tetraplexes. To confirm this observation we performed UV-visible titrations for baicalein and quercetin. The chosen oligonucleotide mimics the repeats of human telomeric motif, and is supposed to adopt an intramolecular quadruplex structure (Sen, 1988). Titrations were performed using quercetin that showed moderate activity in the magnitude of near 10⁵M⁻¹ for the G quadruplex which is in agreement with quercetin's stabilising effect to the melting denaturation pattern of the tetraplex structure. Baicalein

presented a lower binding activity with a K of 19012.3 M⁻¹, similar to the values obtain for the triplex structures. See Table 5 for binding constants.

Table 5: The results of the binding constants for G quadruplex show quercetin to be the more active compound.

Compound	Quadruplex (UV)		
	K /M ⁻¹	n	R ²
Baicalein	19012.3	2	0.98
Quercetin	85417.6	2	0.96

3.2.b.6: DNA-drug-metal interactions

In nucleic acids there are two classes of binding sites available for metal interaction: the heterocyclic bases and the negatively charged phosphate groups. As metals are positively charged we would expect them to interact with the phosphate groups. However, metal ions have been shown to interact also directly with the DNA base or through hydrogen bonding via water molecules (Anastopoulou, 2003). Quercetin has shown to interact with copper and produce DNA damage (Yamashita *et al.*, 1999). We decided to investigate if the carbonyl bond and hydroxyl group in the ortho position really produces this effect, or at least increase the binding activity. Four compounds from our original group have been investigated for their binding to STDNA (see section 2.2.a.2 and 2.2.a.3) in the presence of metal ions. Baicalein, baicalin, quercetin and rutin all have at least one OH group in the ortho position respectively to the carbonyl in C4 (for structures please refer to Introduction). Six cations (as oxides) were investigated as these are commonly found in the cell environment: Fe²⁺: as part of haems (Grandorri *et al.*, 2000); Fe³⁺: as part of the

transferrin family (Lambert *et al.*, 2005); Cu^{2+} : already described in drug – DNA interactions (Asadi *et al.*, 2005); Mg^{2+} : as the second most abundant intracellular cation modulating many processes (Mooren *et al.*, 2005); Mn^{2+} : active role in mitogen activated protein (MAP) kinase dependent pathways (Touyz *et al.*, 2003); Zn^{2+} : as part of the zinc finger DNA binding proteins (Sepp *et al.*, 2005). Monovalent cations like Na^+ and K^+ do not bind directly to the DNA, they bind by the inner water sphere and they are also less reactive than divalent cations (Anastopoulou, 2003); for this reason we decided to study only divalent and trivalent cations. Spectrophotometry was the methodology of choice and we performed UV-Vis titrations as described before. We approached these experiments in two main ratios: metal – drug, ratio 1:1 and then titrated with STDNA and metal – drug, ratio 2:1 (when two unsubstituted hydroxyls are in ortho position) and then titrated with STDNA, in this way we saturated all the possible hydroxyl groups in the ortho positions of the drugs.

Results are presented in Table 6. For quercetin the binding was not improved overall compared with the binding to the STDNA alone, but it is possible that the hydroxyl in position 3 interacts with the carbonyl and the hydroxyl in position 5 forms a complex with the metal cation. In the case of rutin, the binding was increased dramatically for interactions with Fe^{2+} / Fe^{3+} / Zn^{2+} in ratios 1:1, probably due to the interaction of the metals in position 7; it is also possible the rutinoside sugar in position 3 would allow the carbonyl to interact alone with the hydroxyl in position 5 and form a complex with the cation. The binding of baicalein to DNA was decreased in all situations, which shows that hydroxyls in ortho position of the A ring clearly form complexes with the metal that does not allow the molecule to intercalate the double helix; only with Fe^{2+} in ratio 2:1 did the binding constant

for STDNA remained unchanged. Baicalin maintained in the same value for STDNA binding constant in presence or not of any metal cation.

Table 6: The results of the titrations of the metal – drug – DNA complexes. The ratios of drug: metal are indicated under the name of the drug, the binding association constants are expressed in M^{-1} , the n value appears between brackets.

Cation	Baicalein 1:1, K /M ⁻¹	Baicalein 1:2, K /M ⁻¹	Baicalin 1:1, K /M ⁻¹	Quercetin 1:1, K /M ⁻¹ ₁	Quercetin 1:2, K /M ⁻¹	Rutin 1:1, K /M ⁻¹	Rutin 1:2, K /M ⁻¹
Cu ²⁺	2395 (2.2)	1388 (2.3)	1674 (2)	12132 (2)	16222.6 6.6)	1202.7 (2.7)	No interaction observed
Fe ²⁺	1117 (2.7)	15385 (2.3)	2027 (2)	12899 (2)	14447.8(8.4)	130794 (2.6)	1049.2 (2)
Fe ³⁺	1258 (2)	1164 (2.1)	2794 (2)	9504 (2.7)	10868 (7.7)	75787 (3.2)	1154 (2.1)
Mg ²⁺	1139 (2.5)	1334 (2.2)	1523(2.6)	10959 (2)	7413 (4.8)	1121 (2.5)	1119.3 (2.4)
Mn ²⁺	1210 (2.5)	1235 (2.3)	1086 (1.9)	7885(3.3)	11307 (6.9)	10129 (2)	1091.9 (2.3)
Zn ²⁺	1625 (2.1)	1170 (2.2)	1884 (2.1)	10739(2.1)	10101.3 3.3)	46157 (2.5)	927 (2.1)

3.2.c: Nucleic acid damage assay

Nucleic acid damage was examined by gel electrophoresis. This experiment would allow us to see if there is any interaction between the different nucleic acid structures and all the compounds, including artesunate, artemisinin and cantharidin that could not be tested by UV/Vis spectroscopy. Samples of complexes formed between the different nucleic acid isoforms and the test drugs were incubated for 30 minutes at 37°C (see section 2.2.c).

For artesunate and artemisinin, we used Fe²⁺/Fe³⁺ redox couple (ratio 1:1:1, metal:metal:DNA) to allow a possible mechanism of strand break as was postulated by Dr

Efferth (recommendation by personal communication). Unfortunately, the redox couple damages the nucleic acid by itself and no further improvement was found when the drugs were added. We tested all the compounds with all the nucleic acid isoforms and no remarkable interaction was found for the different nucleic acid structures. In Figure 24 an example can be seen for the case of polydAdTpolydT.

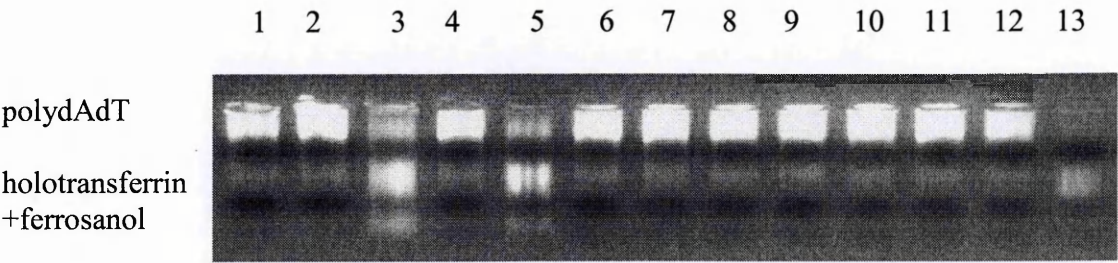


Figure 24: The results of the nucleic acid damage of the drugs on polydAdTdT are shown in this figure with no apparent positive results. 1- NA; 2- NA+artesunate; 3- NA+artesunate+ $\text{Fe}^{2+}/\text{Fe}^{3+}$; 4- NA+artemisinin; 5- NA+artemisinin+ $\text{Fe}^{2+}/\text{Fe}^{3+}$; 6- NA+baicalein; 7- NA+baicalin; 8- NA+cantharidin; 9- NA+daidzein; 10- NA+puerarin; 11- NA+quercetin; 12- NA+rutin; 13- holotransferrin+ferrosanol

3.2.d: Linear Taq Polymerase stop PCR and Footprinting assays

The study using the Taq stop PCR (see section 2.2.f) polymerase assay did not produce positive results. Different PCR conditions and different treatments for purification were performed in order to get appropriate result. Two conclusions can be drawn, either the drugs are taq DNA polymerase inhibitors in the concentrations tested, or the strength of binding between the drugs and the plasmidic DNA is not strong enough to remain bound during the consecutive purification steps.

Footprinting (section 2.2.f) provides the identification of the binding sites between the drugs and the DNA. We used Dnase I footprinting to allocate the interaction between the

drugs and the bases. Dnase I digests the DNA that is not protected by bound drug, through cleaving of the phosphodiester bonds. The bound sites will appear as holes in the photographed gel. We used KMnO_4 and piperidine cleavage for the ladder as they cleave thymidine bases. As positive control we used acridine, that shows preference for $(\text{dAdT})_2$ and dGdC . Our oligo was designed to have dGdC and dTdA sequences. Unfortunately radioactive footprinting could not be performed, which would provide a clear gel; and silver staining was used to replace this technique. As shown in Figure 25, the quality of the gel is really poor, and no precise results were obtained.

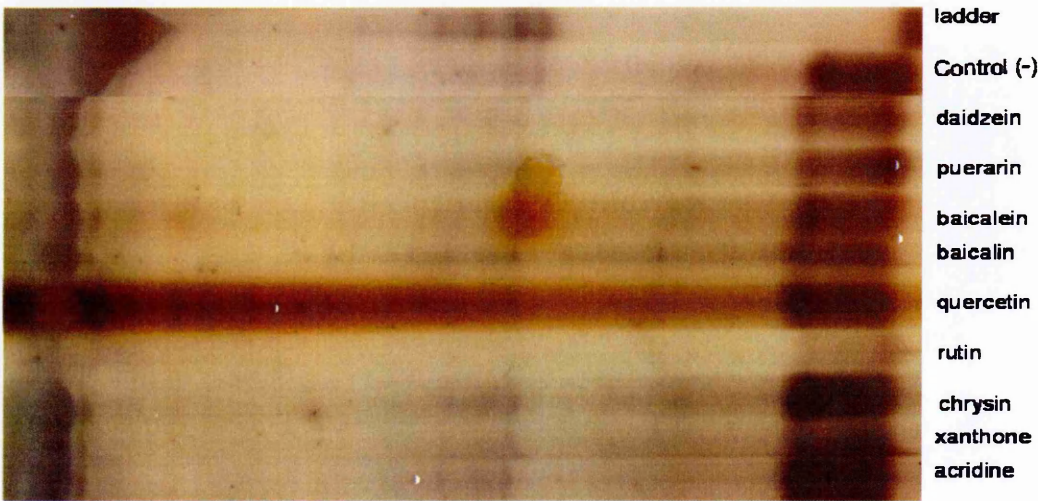


Figure 25: The results of the footprinting assay showed silver staining is not an appropriate technique to use in this experiment. Two more compounds were added in this experiment, xanthone and chrysin, which will be explained in Chapter 4.

3.23.e: Topoisomerase I & II inhibition assay

We tested all the compounds for inhibition of both enzymes. The samples were tested at different concentrations of the test drug (50, 75 and 100 μ M) for both enzymes. As in the case of the nucleic acid damage, the samples were run in agarose gels and they were visualised as bands under UV light with ethidium bromide staining. Different lengths in the bands are an indication of inhibition processes. Negative controls were taken as samples with the same volume of DMSO used in order to demonstrate the solvent has no effect by itself on inhibiting the enzymes. For the topo I inhibition assay camptothecin was used as positive control and etoposide was used for topo II. For topo II positive result, we should find 3 bands in the gel (open circular DNA, linear DNA and form I DNA) and the medium band should be in the same length as the linearised DNA. In the topo II inhibition test, we tested cleavage (if then drug affects the cleavage relegation cycle) and relaxation activities (section 2.2.g, Figures 14 and 15).

The results showed the drugs are not topo I inhibitors. Artesunate, artemisinin and baicalein appeared to have inhibition for topo II cleavage activity (appearing as the two upper lines in the gel). The rest of the compounds showed negative results.

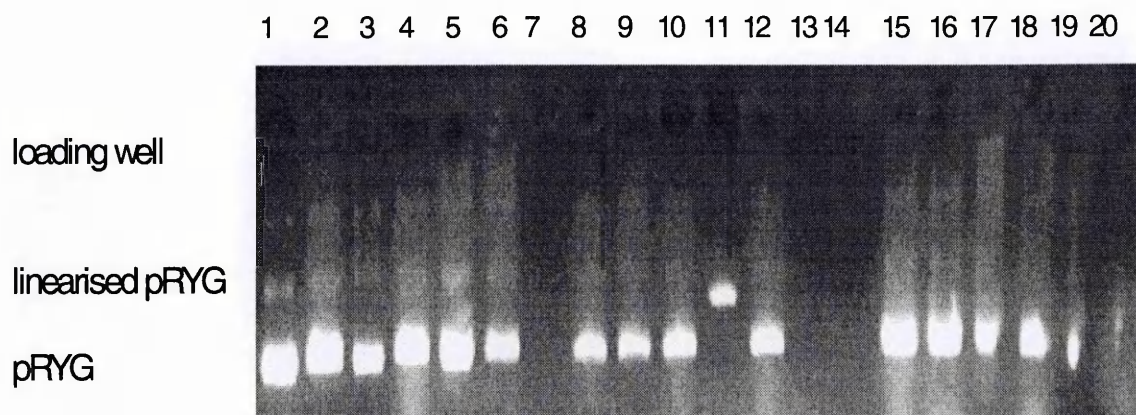


Figure 26a: The results of topoisomerase II cleavage activity showed a light activity of artesunate and artemisinin.

1: artesunate 50 μM + pRYG + topoII. 2: artesunate 75 μM + pRYG + topoII. 3: artesunate 100 μM + pRYG + topoII. 4: artemisinin 50 μM + pRYG + topoII. 5: artemisinin 75 μM + pRYG + topoII. 6: artemisinin 100 μM + pRYG + topoII

7: free.

8: pRYG + topoII. 9: pRYG + 0.5 μL DMSO. 10: pRYG + topoII + 0.5 μL DMSO. 11: linearised pRYG. 12: pRYG + topoII + VP-16 (etoposide, inhibitor). 13: free. 14: free. 15: baicalein 50 μM + pRYG + topoII. 16: baicalein 75 μM + pRYG + topoII. 17: baicalein 100 μM + pRYG + topoII. 18: baicalin 50 μM + pRYG + topoII. 19: baicalin 75 μM + pRYG + topoII. 20: baicalin 100 μM + pRYG + topoII

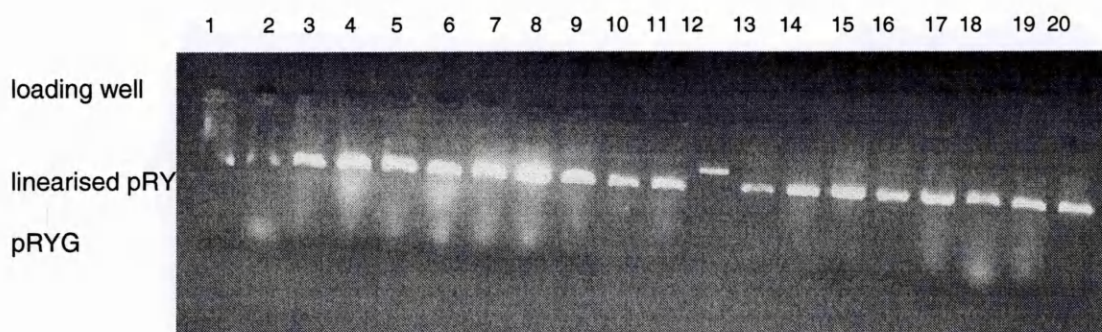


Figure 26b: The results of topoisomerase II cleavage second part.

1: cantharidin 50 μ M + pRYG + topoII. 2: cantharidin 75 μ M + pRYG + topoII. 3: cantharidin 100 μ M + pRYG + topoII. 4: daidzein 50 μ M + pRYG + topoII. 5: daidzein 75 μ M + pRYG + topoII. 6: daidzein 100 μ M + pRYG + topoII

7: puerarin 50 μ M + pRYG + topoII. 8: puerarin 75 μ M + pRYG + topoII. 9: puerarin 100 μ M + pRYG + topoII. 10: pRYG + topoII. 11: pRYG + topoII + 0.5 μ L DMSO 12: linearised pRYG + 0.5 μ L DMSO.

13: pRYG + topoII + VP-16 (etoposide, inhibitor). 14: quercetin 50 μ M + pRYG + topoII. 15: quercetin 75 μ M + pRYG + topoII. 16: quercetin 100 μ M + pRYG + topoII. 17: rutin 50 μ M + pRYG + topoII. 18: rutin 75 μ M + pRYG + topoII. 19 rutin 100 μ M + pRYG + topoII. 20: pRYG + topoII + VP-16 (etoposide, inhibitor)

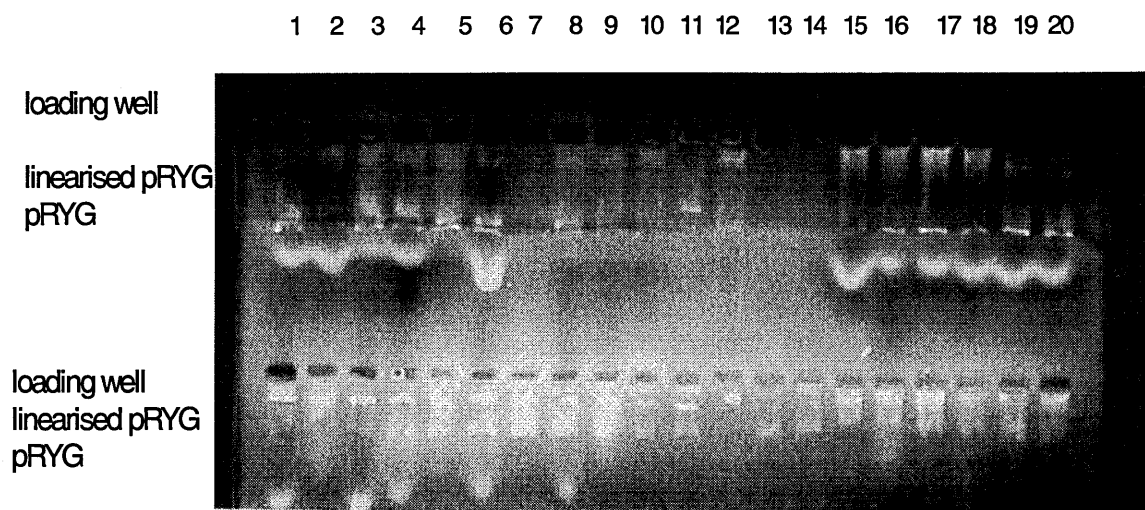


Figure 26c: The results of topoisomerase II relaxation activity showed non conclusive results for any compound.

1: artesunate 50 μ M + pRYG + topoII. 2: artesunate 75 μ M + pRYG + topoII. 3: artesunate 100 μ M + pRYG + topoII. 4: artemisinin 50 μ M + pRYG + topoII. 5: artemisinin 75 μ M + pRYG + topoII. 6: artemisinin 100 μ M + pRYG + topoII

7: free.

8: pRYG + topoII. 9: pRYG + 0.5 μ L DMSO. 10: pRYG + topoII + 0.5 μ L DMSO. 11: linearised pRYG. 12: pRYG + topoII + VP-16 (etoposide, inhibitor).

13: free. 14: free. 15: baicalein 50 μ M + pRYG + topoII. 16: baicalein 75 μ M + pRYG + topoII. 17: baicalein 100 μ M + pRYG + topoII. 18: baicalin 50 μ M + pRYG + topoII. 19: baicalin 75 μ M + pRYG + topoII. 20: baicalin 100 μ M + pRYG + topoII. 21: cantharidin 50 μ M + pRYG + topoII. 22: cantharidin 75 μ M + pRYG + topoII.

23: cantharidin 100 μ M + pRYG + topoII. 24: daidzein 50 μ M + pRYG + topoII. 25: daidzein 75 μ M + pRYG + topoII. 26: daidzein 100 μ M + pRYG + topoII. 27: puerarin 50 μ M + pRYG + topoII.

28: puerarin 75 μ M + pRYG + topoII. 29: puerarin 100 μ M + pRYG + topoII. 30: pRYG + topoII. 31: pRYG + topoII + 0.5 μ L DMSO. 32: linearised pRYG + 0.5 μ L DMSO. 33: pRYG + topoII + VP-16 (etoposide, inhibitor). 34: quercetin 50 μ M + pRYG + topoII. 35: quercetin 75 μ M + pRYG + topoII. 36: quercetin 100 μ M + pRYG + topoII. 37: rutin 50 μ M + pRYG + topoII. 38: rutin 75 μ M + pRYG + topoII. 39: rutin 100 μ M + pRYG + topoII. 40: pRYG + topoII + VP-16 (etoposide, inhibitor)

3.2.f: Flow Cytometry

Within the cell cycle, before cells can multiply and divide, they have to make copies of their DNA. Normally, most cells are not actively growing and dividing and are in the G₀ or resting phase of the cell cycle and have a diploid (two series of chromosomes, 2N DNA) content. Cells in G₁ phase are cycling, and also have diploid content. A smaller percentage of cells are undergoing DNA synthesis during S phase (having between 2N and 4N DNA content). A few cells completed their DNA synthesis and are in G₂ phase (having 4N DNA content). After cells double their DNA, they undergo mitosis (M phase) dividing into two daughters (Weinberg *et al.*, 1996).

The ability of four structurally related flavonoids (baicalein, baicalin, daidzein and quercetin) to affect chemotherapy-induced apoptosis and cell cycle arrest of breast cancer MCF7 and leukemia cancer CCRFCM cell lines was studied. The antitumour ability of flavonoids has been extensively documented (Efferth *et al.*, 1996; Gerhauser *et al.*, 2003; Wong *et al.*, 2001), but the effect on cell cycle distribution is still unclear. Flow cytometry (see section 2.2.f.1) has been used in order to define in which step of the cell cycle the flavonoids induce apoptosis. Treatment of MCF7 breast cancer cells with the drugs showed that baicalein, baicalin and daidzein block in phase G₁ and quercetin blocks in phase G₂.

The same treatment with CCRFCM leukemia cell lines proved that baicalein and daidzein act as blockers for phase G₁, daidzein also affects preG₁ stage and quercetin acts on preG₁ and G₂ stages. See Table 7 for results.

It is noticeable these flavonoids block during the steps where the proteins are being synthesised (G₁) implying they can bind to earlier steps of protein cascades (by binding

proteins and receptors) or DNA (duplex and triplex forms – during replication). Even more, our postulation of these flavonoids binding DNA can be explained by the fact that quercetin is affecting G2 phase in MCF7 and CCRFCCEM cell lines. During this stage the content of DNA in the nucleus is double, and this means more DNA available to be targeted; if a drug is said to bind preferentially DNA it will possibly do so during the stage where more DNA is available.

Table 7: The results of flow cytometry on both cell lines showed quercetin to be a G2 blocker in MCF7 cell line, baicalin a preG1 blocker in CCRFCCEM cell line and daidzein a G1 blocker in both cell lines.

Stages	Baicalein	Baicalin	Daidzein	Quercetin	Blank with DMSO
MCF7					
Pre G1	3.8%	5.0%	5.7%	6.4%	8.5%
G1	57.3%	57.2%	48.5%	20.9%	58.3%
S	21.0%	20.5%	21.9%	10.3%	18.1%
G2/M	18.3%	17.7%	24.2%	62.6%	15.4%
Stages					
CCRFCCEM					
Pre G1	21.4%	53.9%	1.3%	29.6%	38.3%
G1	29.3%	22.0%	49.5%	19.5%	16.6%
S	35.4%	19.8%	30.1%	33.4%	30.5%
G2/M	14.9%	4.8%	19.8%	18.2%	15.1%

3.2.g: MTS Cell Proliferation Assay

MCF7 breast cancer cell line is an epithelial cell line while CCRFCCEM is a cancer cell line in suspension; the interest of testing our compounds in these two cell lines relies also on the interest of studying if the compounds prefer epithelial cancer cell lines or cells in suspension (leukemias and lymphomas). Cell proliferation assay (see section 2.2.f.2) measures the cell proliferation rate and conversely, when metabolic events lead to apoptosis

or necrosis, the reduction in cell viability. Data obtained from the present study indicate that flavonoids with very similar structures may not produce an identical biological response. At 24 hours of incubation, the compounds have IG_{50} near 100 μM in both cell lines. When the incubation period was prolonged to an incubation of 48 hours, the IG_{50} values dropped to around 65 μM for baicalein and baicalin on MCF7, and 50 μM for baicalin and daidzein on CCRFCM cell line. The incubation period of 72 hours showed that baicalein has some activity against MCF7 (33.12 μM) but not CCRFCM cancer cell lines. Baicalin has activity in both cell lines at 72 h (63 and 44 μM for MCF7 and CCRFCM cell lines respectively). Daidzein promotes growth of MCF7, something that could be expected as this line expresses estrogenic receptors and daidzein has estrogenic structure; moreover the compound does not have a strong anticancer activity on CCRFCM. Quercetin showed to have anticancer activity on both cell lines when the incubation period was 72 hours (83.6 μM for MCF7 and 38.15 μM for CCRFCM cell lines). The results are shown in Table 8.

Table 8: The results of the MTS proliferation assay demonstrated that the compounds are not good anticancer drugs in both cell lines. Baicalein proved to have some activity in MCF7 cell line at 72 h of incubation and quercetin showed some antiproliferation activity on CCRFCM cell line after 72 h of exposure.

Compound	IG_{50} MCF7 (μM)	IG_{50} CCRFCM (μM)
Baicalein	> 100 (24); 69.65 (48); 33.12 (72)	>100 (24); >100 (48); >100 (72)
Baicalin	>100 (24); 78.83 (48); 63.3 (72)	>100 (24); 63.98 (48); 44.56 (72)
Daidzein	93.14 (24); >100 (48); >100 (72)	59.66 (24); 44.5 (48); >100 (72)
Quercetin	>100 (24); >100 (48); 83.6 (72)	>100 (24); >100 (48); 38.15 (72)

Good anticancer drugs have IC₅₀ values in the order of 1 - 5 μ M (Czyz, 2005), this group of compounds clearly do not show a remarkable anticancer activity, it is possible they are metabolised to a less active compound, or they can't reach properly the DNA inside the nucleus.

3.2.h: COMET ASSAY – Alkaline electrophoresis

The experiment (see section 2.2.f.3) has been performed in both cell lines. Daidzein showed no result on MCF7 cell line, but baicalein and quercetin showed to be active in this cell line indicating these compounds entered into the nucleus and produced some DNA damage. For CCRFCM cell line, only quercetin showed to be active and entered into the nucleus while baicalein, baicalin and daidzein were negative. Comparing with the results obtained from the cell proliferation assay and flow cytometry we can stipulate that quercetin may effect its anticancer activity in both cell lines by entering into the nucleus and affecting the DNA, this hypothesis could also apply for baicalein on MCF7 cell line but not on CCRFCM, which may indicate this compound binds to another target rather than DNA in this cell line. Baicalin was negative on both cell lines for the comet assay, but it produced significant anticancer activity when compared to the other compounds, this can be explained either because baicalin does not enter into the nucleus and / or it has another target in the cells rather than DNA. See Figures 27 a, b and c for examples.

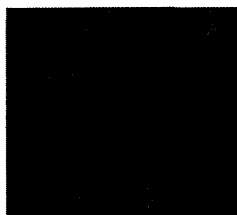


Figure 27 a: MCF7 cell line control, no modification in shape is found.



Figure 27 b: MCF7 cell line positive control, the presence of hydrogen peroxide produces comet tails in the cells, a clear indication of entrance into the cell and DNA damage.



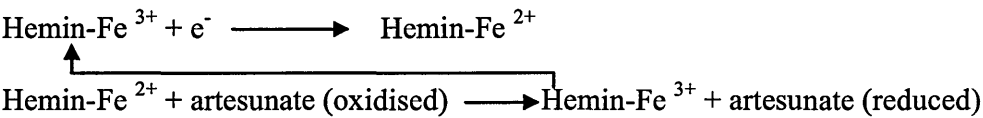
Figure 27 c: MCF7 cell line in the presence of baicalein produces comet tails in the cells, a clear indication of entrance into the cell and DNA damage

3.2.i: Hemin sesquiterpenes interactions

The mechanism of action of artemisinin is still unclear. Most likely it involves the formation of free radical intermediates, originating from the direct interaction of the

endoperoxide group with the heme iron (Messori, *et al.* 2003). Artesunate and artemisinin have no UV spectra, and it is reported that they interact with hemin as a mechanism of action for their antimalarial activity (Meschnick *et al.*, 1991). We have, thus, decided to use hemin as a revealing agent for any DNA – drug interaction. Hemin has a main peak at 385 nm that shifts to 414 nm in oxidizing conditions and to 529 – 565 nm when the ferric ion is in low spin (Grandori *et al.*, 2000). Therefore, we expected that any shift in the UV spectrum of hemin would be an indication of a binding between DNA and artesunate / artemisinin if the mechanism of action involved the drugs acting as peroxides.

With artesunate (or artemisinin), hemin acts as a catalyst, reducing artesunate (or artemisinin) in the same way it reduces hydrogen peroxide by cleaving the oxygen-oxygen bond (Chen *et al.*, 1998)



We used hemin as a revealing agent of any activity between artesunate / artemisinin and DNA. Titrations were performed between: drug – hemin, hemin – DNA, hemin – DNA- Fe²⁺, hemin – drug – Fe²⁺, hemin – drug – DNA – Fe²⁺, hemin – DNA – drug. From the results we obtained we can conclude that artesunate / artemisinin interacts with hemin in the presence or absence of Fe²⁺, but the complexes formed do not show any interaction with DNA in the conditions used here. In Figures 28 a, b, c, d, e the results for artesunate binding titrations are shown.

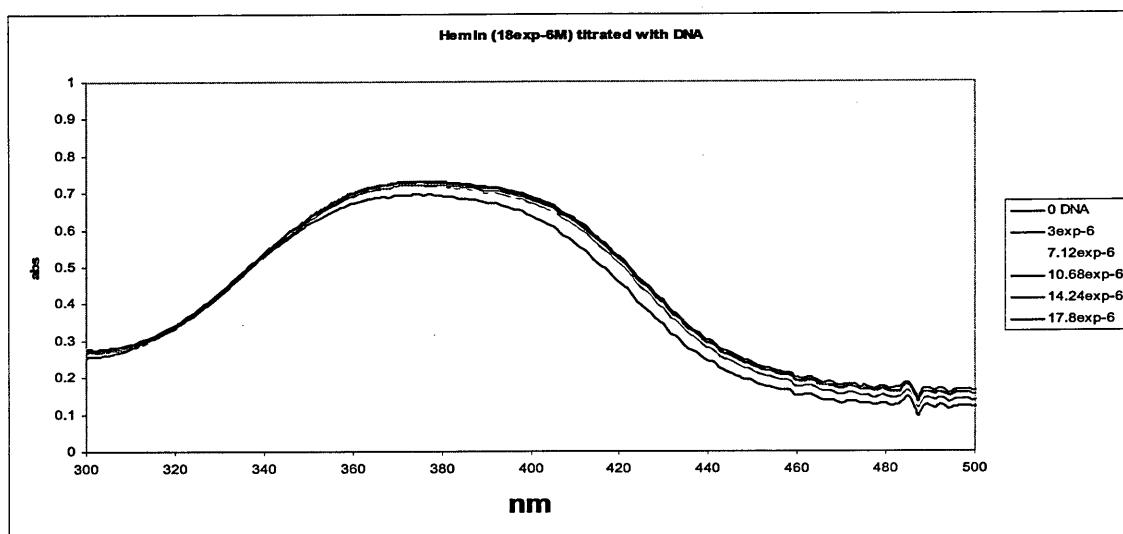


Figure 28a: Hemin titrated with DNA, there is a small increase in the absorbance upon the first addition of DNA and no more changes after it.

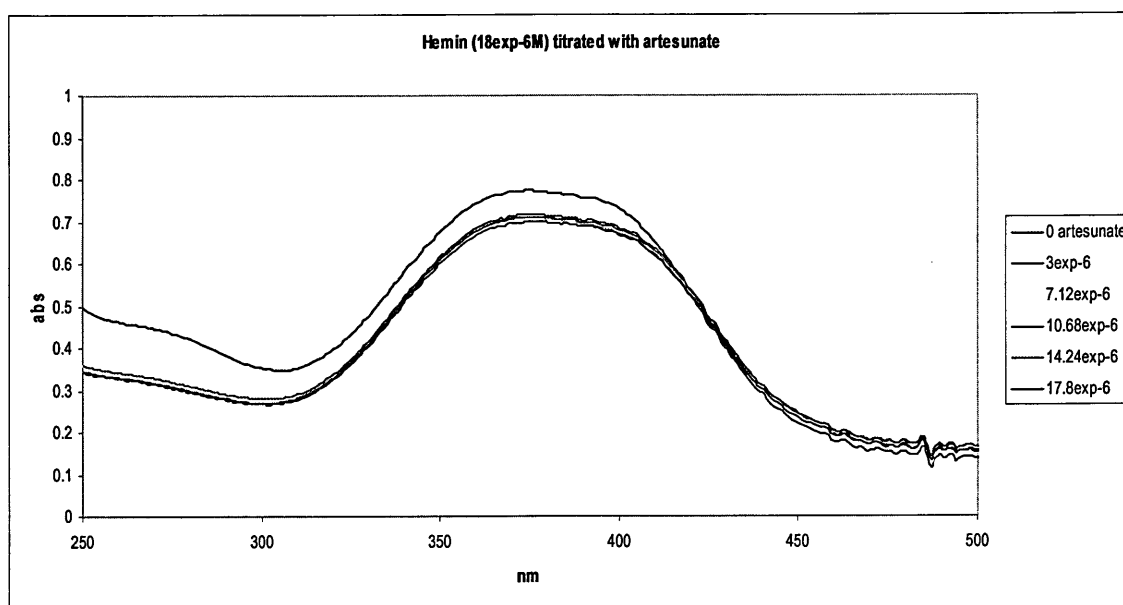


Figure 28 b: Hemin titrated with artesunate, interaction is observed as a decrease in the absorbance of hemin.

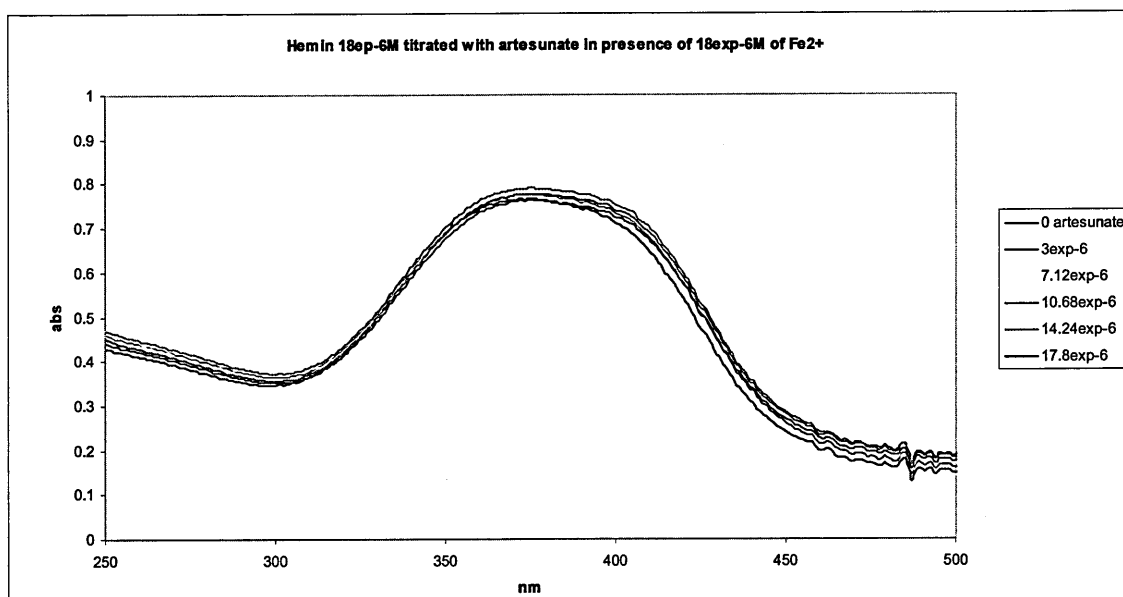


Figure 28 c: Hemin titrated with artesunate in presence of Fe, moderate interaction is observed but not the one expected as a shift in the hemin absorbance spectrum.

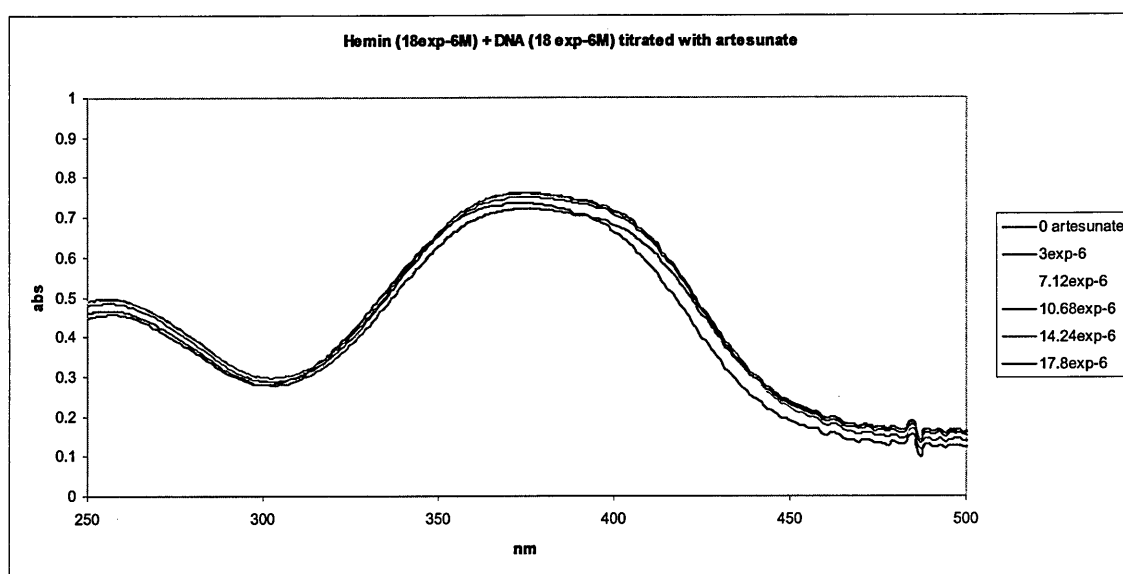


Figure 28 d: Hemin titrated with DNA in presence of artesunate, only a random interaction is observed.

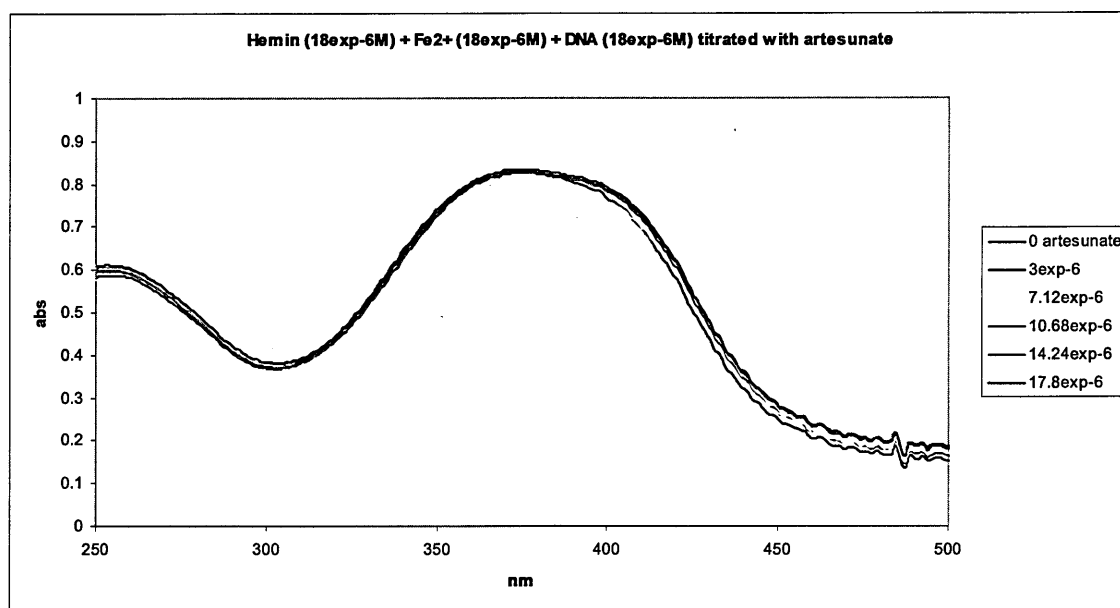


Figure 28 e: Hemin in presence of Fe²⁺ and artesunate titrated with DNA, no defined interaction is observed.

3.3.j: CYP1A1 metabolites assay

Flavonoids are known for inhibiting the CYP family of enzymes (Chan *et al.*, 2002), and as explained in section 2.2.g, CYP1A1 is responsible of bioactivating a vast amount of compounds of the daily diet.

We decided to study the effect this enzyme has on our group of four flavonoids and to investigate a possible mechanism of metabolization for baicalein, baicalin, daidzein and quercetin.

We found that at high concentration of drug (>50 μ M) the enzyme CYP1A1 (see section 2.2.g for methodology) is inhibited and no metabolites are found. While baicalein, daidzein and quercetin gave a positive response at a concentration of 25 μ M; baicalin gave a positive

response at a concentration of 50 μ M, probably because the carbohydrate hinders the interaction with the substrate pocket of CYP1A1.

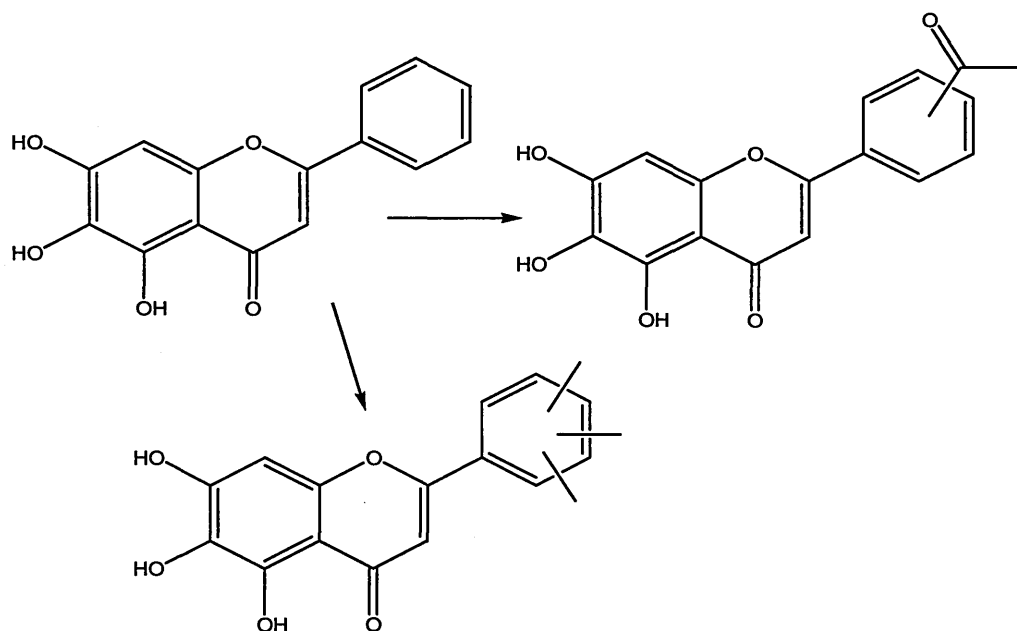
Table 9 shows the results obtained in this experiment. Derivatisation of flavonoids with BSTFA produces a main peak that is the molecular weight of the compound minus 15, a methyl group of the derivatising agent, and a second peak that is the molecular weight (Owen *et al.*, 2003).

Table 9: CYP1A1 results for baicalein, baicalin, daidzein and quercetin. All compounds showed some kind of interaction after being incubated with the enzyme.

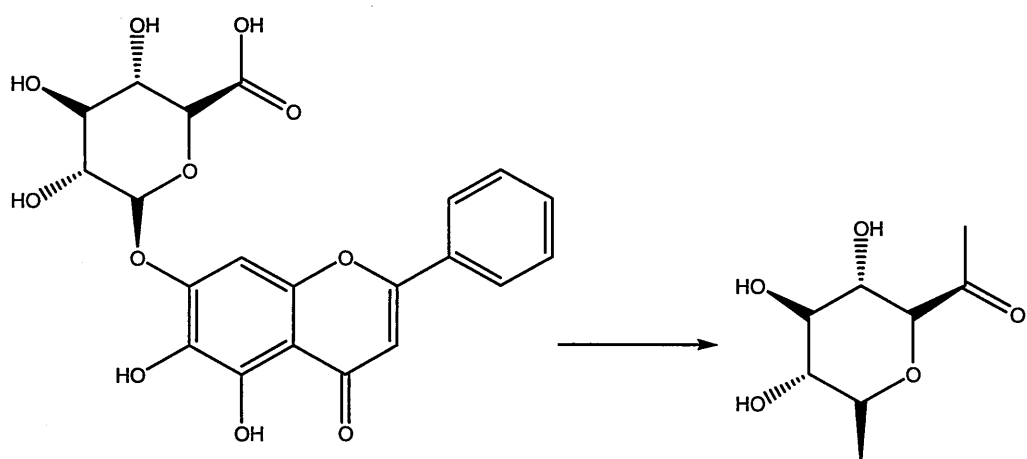
Compound	Retention time (min)	Main peak (M-15)	Second peak(M)	Concentration of drug with positive response	Main peak (M-15)	Second peak(M)
Baicalein	15.3	471	486	25 μ M	441	456
Baicalin	34.3	471	486	50 μ M	247	262
Daidzein	18.5	383	398	25 μ M	345	360
Quercetin	17.5	647	661	25 μ M	264	279

Hydroxylation is the main metabolic pathway to follow, but other possibilities can be contemplated; in our experiment baicalein seems to follow methylation or addition of an acetyl group, see Scheme 2. Baicalin does not seem to follow any specific pattern and the only peak we can assign would be the one for the carbohydrate, which contradicts the fact that carbohydrates can not be derivatised by BSTFA (Owen *et al.*, 2003), see Scheme 3. Daidzein seems to undergo double hydroxylation, see Scheme 4. Quercetin did not show any proper hydroxylation or transformation pattern in the whole molecule. This could be

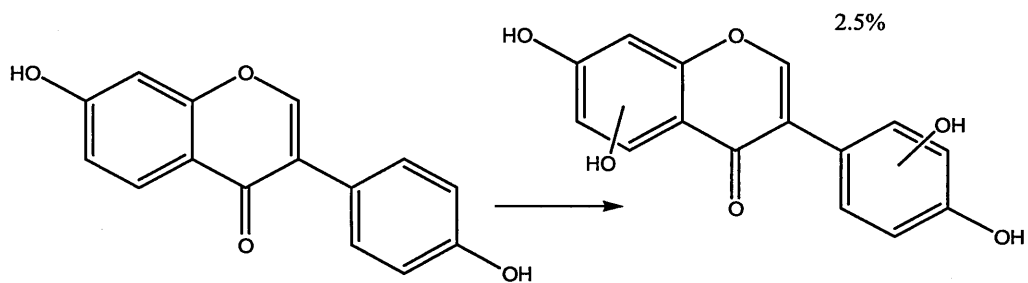
due to the high hydroxylation pattern it already has. Interestingly, the peak we obtained seems to be some sort of modification in one ring, Scheme 5 shows different possibilities explaining the result obtained.



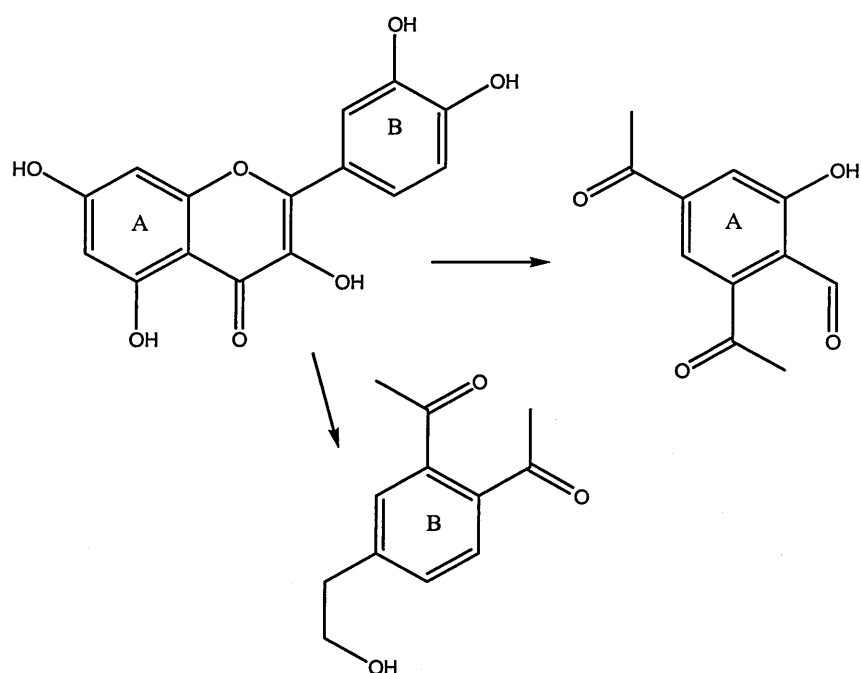
Scheme 2: baicalein after CYP1A1, methylation is a possible process.



Scheme 3: baicalin after CYP1A1, it is possible that CYP1A1 would act on the sugar.



Scheme 4: daidzein after CYP1A1 produced hydroxylation



Scheme 5: quercetin after CYP1A1 seemed to have produced different patterns of modifications in either A ring or B ring.

None of these results can be definitive as we would also need NMR spectra of each metabolite to define the real structure of the peaks. Unfortunately the material left from the incubation was not enough to perform an NMR assay. We could only presume based on the results of the mass spectrometry and literature. The binding studies showed that the number of hydroxyls is extremely relevant when considering the interaction with STDNA; the more number of hydroxyls a flavonoid has, the higher the binding constant. In the case of daidzein, hydroxylation seems to follow as metabolic pathway; but for quercetin, baicalein and baicalin this pathway seems to not appear. These results could explain the fact that some of the compounds (like baicalein and quercetin) can bind reasonably tight to DNA but not show a strong anticancer activity, even though they may enter to the nucleus; we can assume these compounds are subjected to some kind of inactivation before entering into the

nucleus or binding some other target. Baicalin showed to be slightly active in the cell work when cells were exposed for 72 h, but the binding to STDNA was quite weak. According to our results from the CYP1A1 assay, baicalin is metabolised by the enzyme and loses the carbohydrate. It is possible that the metabolism of baicalin results in a more reactive agent as anticancer agent against MCF7 and CCRFCM cell lines, through binding to a different target than DNA.

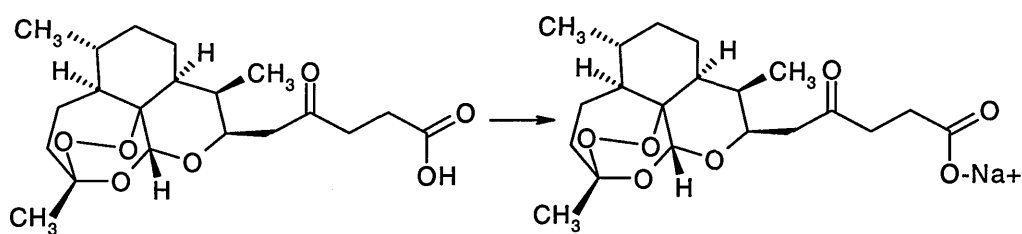
3.2k: Determination of pK_a

DNA is a molecule negatively charged. We would therefore that assume a positively charged compound would be favoured for DNA binding. In order to know if our compounds are protonated or not in the conditions we used for our binding studies we performed appropriate studies to determine the pK_a of our compounds. Artemisinin and cantharidin have no ionisable protons, so the experiment was performed for artesunate, baicalein, baicalin, daidzein, puerarin, quercetin and rutin (see section 2.2.b). According to the results obtained, the flavonoids are neutral at physiological pH ($pH=7.4$). This would improve its binding to a negatively charged molecule such as DNA. Therefore, all our experiments are being conducted at pH 7.4, except in the case of the purine triplex ($pH6.5$) that requires a light acid pH for the conformation. In Table 10 the results of the pK_a experiments are shown.

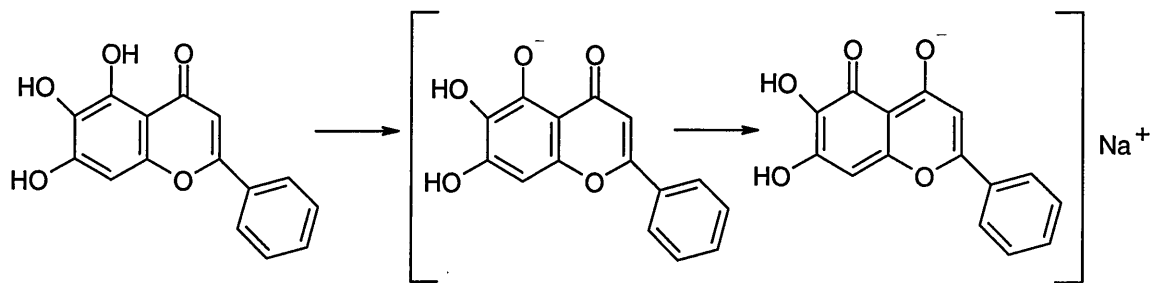
Table 10: The data obtained by the pK_a determination assay are presented. The compounds showed to be protonated at physiological pH, with the exception of artesunate and baicalin.

	Artesunate	Baicalein	Baicalin	Daidzein	Puerarin	Quercetin	Rutin
pK_a	5.67	7.57	6.33	8.42	8.57	10.3	8.02
percentage of neutral molecule at pH 7.4 (%)	5.0	50.0	10.0	90.0	90.0	99.0	80.0

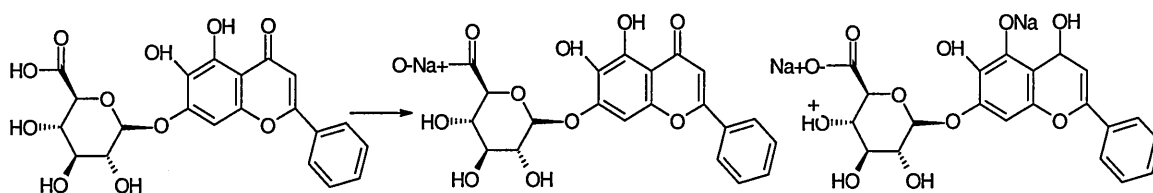
The possible aqueous equilibrium for the compounds when titrated with NaOH are shown in Schemes 6.



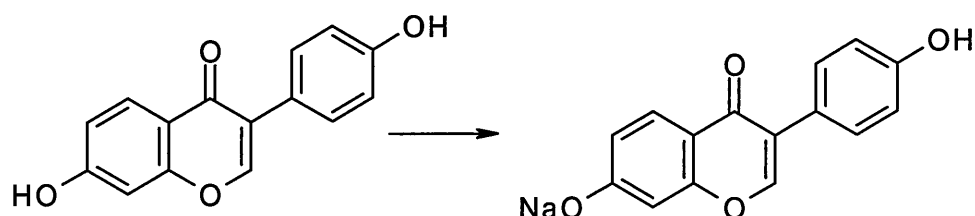
Scheme 6 a: artesunate loses the acidic proton



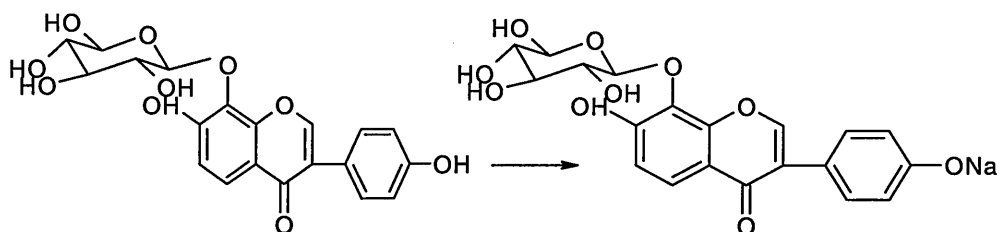
Scheme 6 b: baicalein loses the more acidic proton



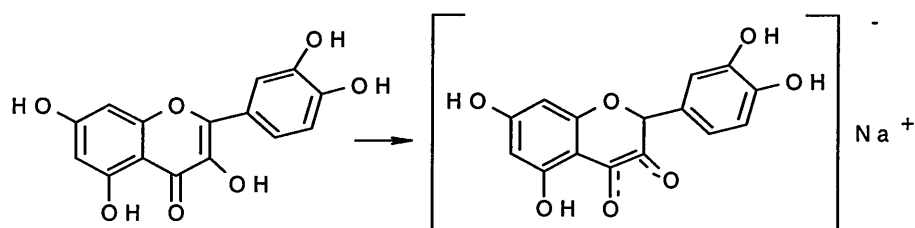
Scheme 6 c: baicalin loses the more acidic proton



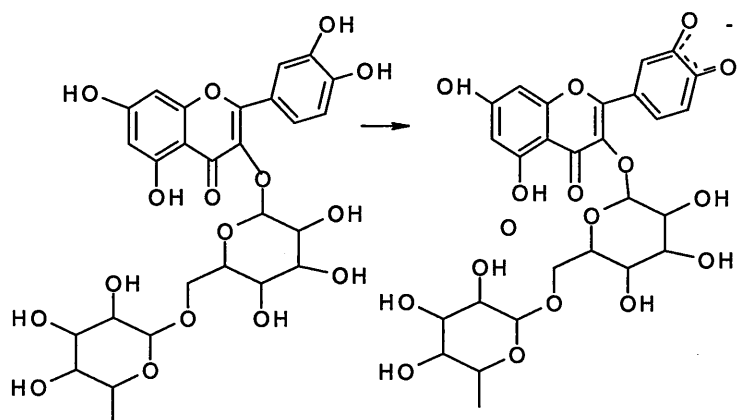
Scheme 6 d: daidzein loses the more acidic proton



Scheme 6 e: puerarin loses the more acidic proton



Scheme 6 f: quercetin loses the more acidic proton. On position 4, probably we can find an enolic equilibrium with arrangement (in presence of an alkali like NaOH), on positions 3', 4' we can find resonance structures in the same medium



Scheme 6 g: rutin loses the more acidic proton

3.3 Conclusions for the foundation compounds

This study has provided a quantitative molecular basis for the DNA binding behaviour and biological activity of the types of intercalating compounds that formed our initial set of compounds. Stabilisation studies by temperature denaturation demonstrated that the compounds interfere mainly with the stabilization of triplex polydAdTdT and G-quadruplex. While the majority of the compounds destabilise the structure by approximately 6°C for the first melting transition point in polydAdTdT, baicalein and quercetin stabilized this structure by 3.2 and 7.3°C respectively. In the case of G-quadruplex, baicalein stabilised the first melting point transition and allowed the G-quadruplex to melt in a single transition. Baicalin and daidzein destabilised the structure and while quercetin affected the denaturation pattern.

Many techniques were employed to study the drug-DNA binding interactions in addition to the UV-Vis and fluorescence titrations. Ethidium bromide displacement and quenching were used but they did not provide any result, possibly due to the low affinity these compounds have for DNA. Nuclear magnetic resonance was also considered as an option, unfortunately this kind of experiment requires high concentrations of DNA and drug; the drugs need to be solubilised in DMSO prior to dilution into the aqueous buffer and at the concentration required for NMR studies the percentage of DMSO was over 10% in final volume. As this would affect the DNA (personal communication Dr. Gary Parkinson), this series of experiments had to be abandoned. Binding constants obtained by UV spectrophotometry were in the order of $10^3 - 10^4 \text{ M}^{-1}$. The results indicate that baicalein and quercetin emerge as the most potent among the set of flavonoids, with the binding constants in the range of $2-8 \times 10^4 \text{ M}^{-1}$. Interaction with DNA is thought to involve the planar ring

structures. The double bond of the O in C4, gives planarity to the molecule, and this allows the molecule to intercalate the bases in the different nucleic acid structures. The number of hydroxyl groups in the flavonoid also plays an important role, 3 or more hydroxyl groups seem to allow a better binding to different forms of nucleic acids and the position of them is also relevant as quercetin, with two hydroxyl groups in the B ring, showed a remarkable binding activity to G-quadruplex.

Competition dialysis provided us with data on the affinity of the dyes for triplex, quadruplex and duplex structures. We confirmed with this study the observation that baicalein and quercetin binds preferentially to triplexes and quadruplex by UV-visible titrations. Baicalein shows specificity for the AT bases, triplex and quadruplex and proved to be active in MCF7 cell line by arresting in G1 phase. Baicalin and Rutin have activity towards AT bases and baicalin arrests the preG1/G1 phase in CCRFCM cell line. Daidzein and Puerarin are weak binders with specificity for GC bases. Daidzein is considered a phytoestrogen, promotes activity where estrogen receptors are located; that would explain the promotion of growth effected on MCF7 cell line.

Quercetin has interaction with tetraplex and triplex, presented activity on CCRFCM cell line by arresting in G2 stage. The hydroxyl groups in positions 5, 7, 3' and 4' seem to have a strong influence on the interaction with the nucleic acids.

There is no strong correlation between the DNA – binding and antiproliferative activity against the two cell lines. These facts clearly indicate that binding to DNA is not the only determinant for anticancer action, but other factors such as cellular uptake and protein inhibition may also contribute. In conclusion, quercetin can be chosen as a leading

compound from our original set of compounds and the flavone skeleton has been considered for the design of a new generation of higher order DNA binding agents.

The results for topo I and II assay showed the drugs are not topo I inhibitors, and only artesunate and artemisinin appeared to have inhibition for topo II cleavage activity. The rest of the compounds showed negative results.

The employment of metal cations did not appear to improve the binding association constant in most cases. Moreover, they decreased by 10 fold the binding association constant of baicalein on STDNA; probably by reacting with some centre in the molecule that is involved in the binding. In the case of rutin, however, when the ratio is 1:1 the cations Fe (II), Fe (III), Mn and Zn improved the binding from 10 to 10^3 fold depending on the metal.

pK_a values obtained for the family of flavonoids showed that they are weakly acidic which means they are predominantly neutral at pH 7.4 (cellular environment).

CYP1A1 metabolites experiments gave a positive response for a hydroxylation pattern in daidzein and a possible methylation for baicalein. For quercetin and rutin, no definitive response could be interpreted.

4.1: Obtaining DNA intercalating ligands

In order to get a successful DNA intercalating agent, some properties need to be taken into account:

- degrees of freedom: the major requirement for intercalating agents is the planar aromatic ring structure. This structure fits between adjacent base pair planes and can have some, rotational freedom within the plane of the ring. The ligand itself may have flexibility of structural parts outside the DNA binding site and may contain more than one intercalating side chain (Laughton *et al.*, 1999)
- role of base pair sequence: base pair sequence does not play a large role on the specific nature of most intercalating complexes, but some affinity has been found for some intercalating agents, as in the case of acridines for GC bases. (Belousov *et al.*, 2004)
- counter ion effect: DNA is a negatively charged polyanion attracting counter ions, positively charged Na^+ , or Ca^{2+} and Mg^{2+} ions as well as protonated basic residues of proteins. The presence of small counter ion affect drug binding, since the counter ions can screen and shield the negative backbone surface allowing non electrolytes as well as positively charged ligand to interact more strongly with the DNA target. High ionic strength, however, reduces non-covalent interaction mediated by hydrogen bonds and electrostatic interactions. (Olmsted *et al.*, 1996)
- role of solvent: there are three general classes of interactions to be considered during binding

- ligand solvent interaction
 - DNA solvent interaction
 - ligand-DNA complex with solvent interaction (Blankenship *et al.*, 2002)
- rational drug design: when a compound intercalates into nucleic acids, there are changes that occur on the DNA and the compound during the complex formation that can be used to study the ligand DNA interaction. The binding is an equilibrium process because no covalent bond formation is involved and the binding constant can be determined by measuring the free and DNA bound forms of the ligand. In the present project the intercalating substrates are aromatic chromophores, therefore the binding constants were obtained spectroscopically.

In addition to these properties, a consensus definition of an intercalator (Ashbey, 1985) requires molecules having a combination of several of the following groups: benzene ring, heterocyclic ring (both aromatic and aliphatic), aliphatic amine (preferably tertiary), carboxamide group, alcoholic hydroxyl group, carboxy ester, keto group.

We decided to further investigate chromophores constituted by a flavonoid skeleton with substitutions in the A and B ring for studying the mode and affinity as DNA binding ligands; some other chemical forms, such as isoflavonoids, flavones and 3 aromatic fused rings were also studied on DNA binding interactions. The data obtained allowed us to formulate some structure-activity relationships for this second generation of compounds.

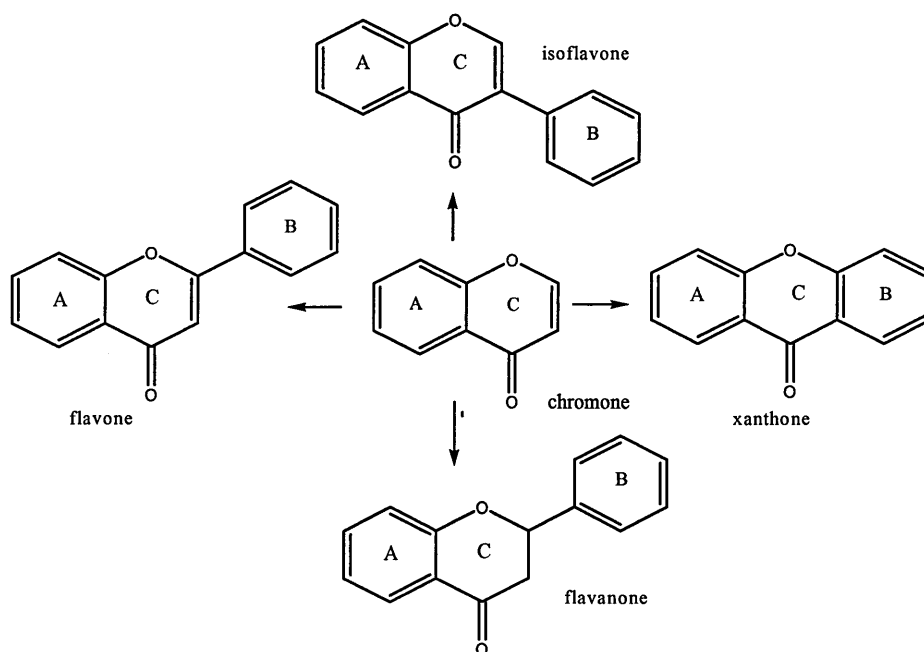
Amongst the steric constraints that control the interactions, the presence of methoxy or acetoxy substituents on the molecule is relevant as far as the drug – DNA binding is concerned.

For a general study, we decided to use primarily STDNA, as it contains both A-T and G-C sequences, and would provide preliminary information about the changes in the binding. The techniques used were UV-Vis absorbance and fluorescence spectrophotometric titrations, as they can give an indication of the binding affinity, and orientate in the mode of binding of the molecule, as well as information on which specific moiety plays a major role during the interaction. For this part of the project some compounds were purchased from Sigma Aldrich (United Kingdom), Acros (United Kingdom) and Lancaster Chemicals (United Kingdom) and some others were synthesized and characterized by NMR (nuclear magnetic resonance), mass spectroscopy and IR (infrared) Spectroscopy.

4.2: Organic synthesis

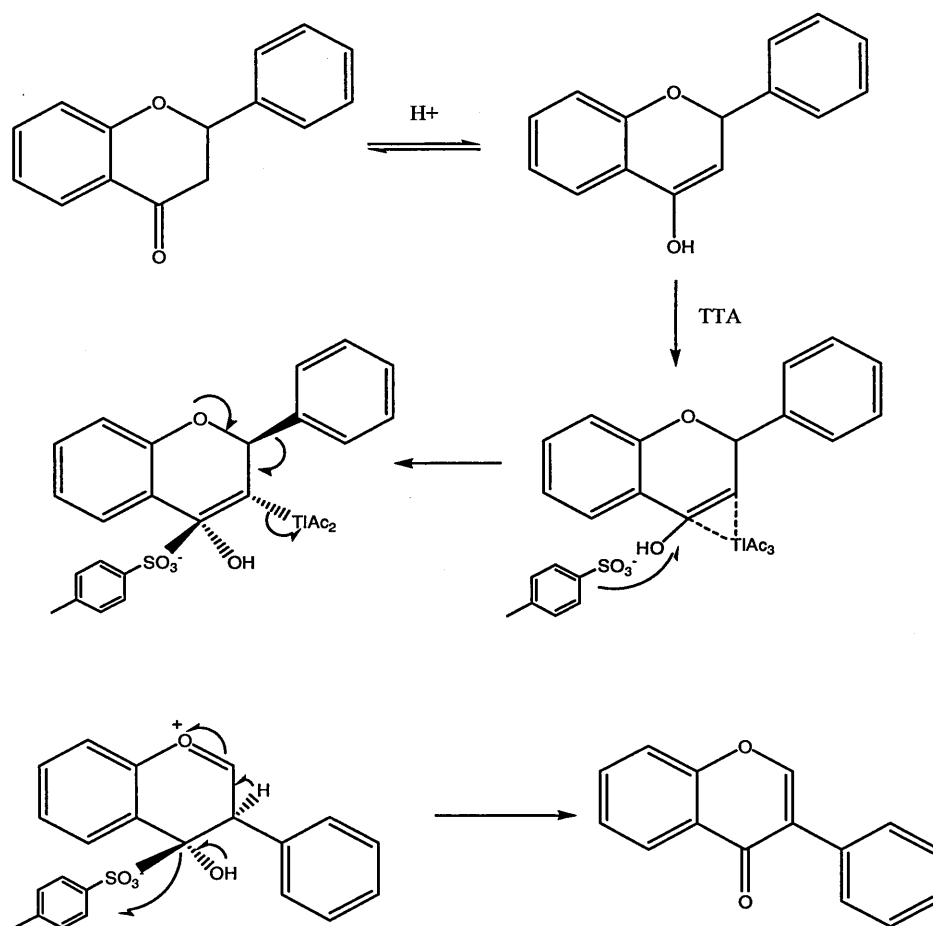
With the intention of deciphering the way of binding, we modified our chosen scaffold by placing substituents at different positions in the three rings.

From the preliminary results we concluded that a flavone skeleton would be suitable and this should enable us to gain an insight into the binding interactions with DNA. Consequently, we envisaged a model composed by the parent chromone (A and C rings) in which the B ring is appended in different positions and in which the level of saturation of the chromone is changed. These are described in Scheme 7.



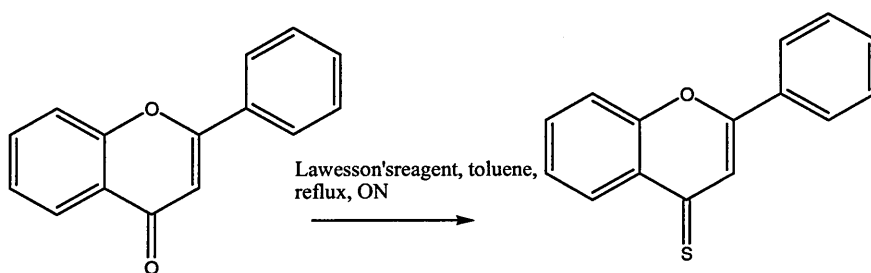
Scheme 7: Different chromone possibilities. Rings A and C are fused to provide a planar molecule that could intercalate between stacked nucleic acid bases. Flavone has the B ring located at C-2, while isoflavone has the B ring in C-3. Xanthone has a C-2 / C-3 ring fusion, maintaining a planar system. In the case of flavanone, a distortion appears as a result of the saturation of the C ring.

Flavanone, xanthone and flavone were purchased; the synthesis of isoflavone (Scheme 8) employed thallium (III) acetate (TTA) and 4-toluenesulfonic acid. The product was easily purified by HPLC.



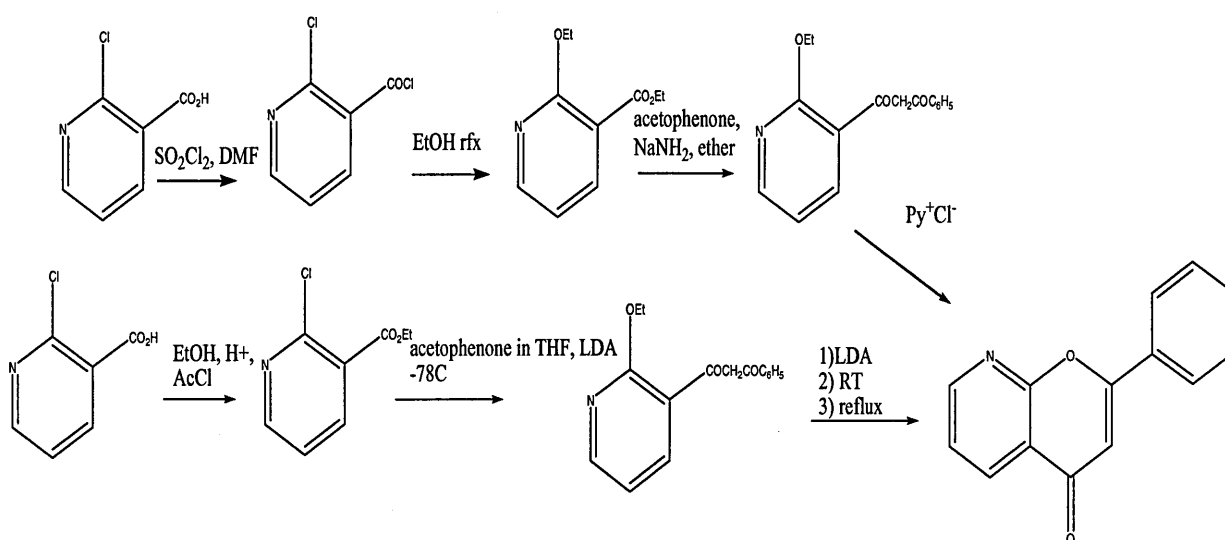
Scheme 8: Isoflavone synthesis. Acid catalysed enolization of flavanone followed by alkoxythallation leads to two unstable intermediate thallium adducts (*syn* and *anti* to the aryl group). The *anti* adduct is predominant and dethallation proceeds via migration of the aryl group resulting in the formation of isoflavone.

To examine the role of the carbonyl group we proposed to synthesise flavothione (Hafez 1991; Kataoka, 2004). We used 2,4-bis(4methoxyphenyl)-1,2,3,4-dithiophosphetan-2,4-disulfide (Lawesson's reagent) as a thiating agent as shown in Scheme 9. The reaction was straightforward and the product was easily purified by preparative TLC plates giving a red powder.



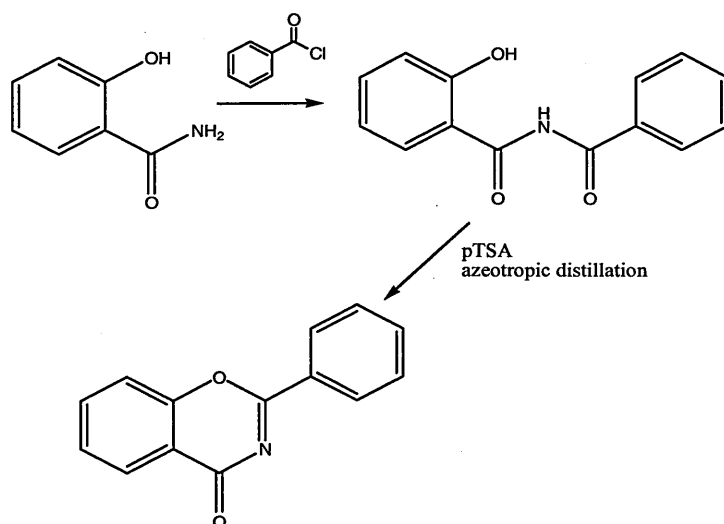
Scheme 9: Flavothione synthesis. The carbonyl in position 3 is replaced by sulfur.

We also investigated the role of nitrogen, as many DNA binding agents have nitrogen in their scaffold (Wang *et al.*, 1994). We used several protocols, as shown in Schemes 10, and 11.



Scheme 10: Nitrogen introduction in A ring. The upper reaction uses sulfonyl dichloride to produce substitution in the acid; the reaction did not pass step 3. The lower reaction employed ethanol and acetyl chloride to produce acid chloride and ethyl acetate as first step, but the reaction did not proceed as expected.

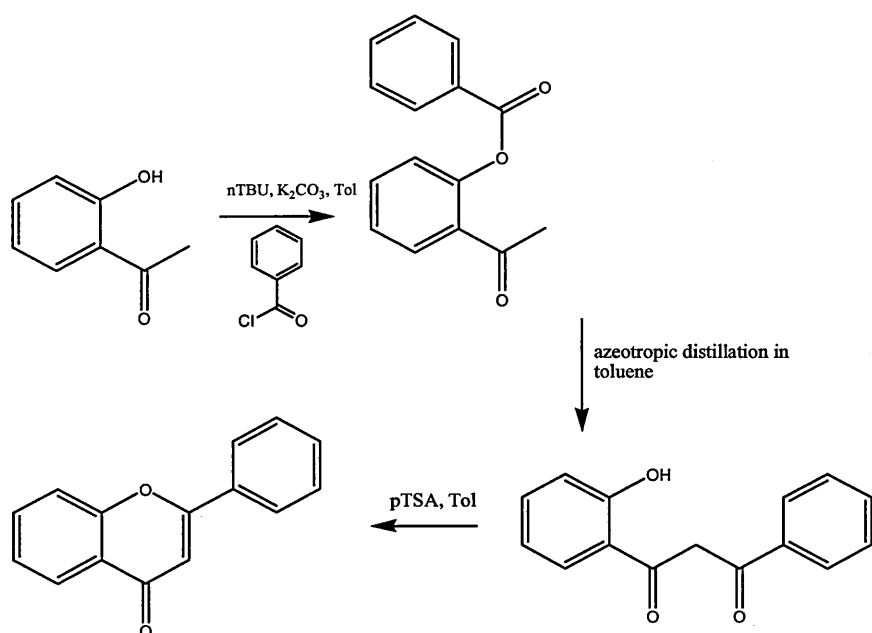
For the C ring, salicylamide was mixed with benzoyl chloride in toluene, the generation of HCl provided the acid environment needed for the O- to N- rearrangement to proceed; the addition of p-toluenesulfonic acid led to dehydration that resulted in the desired product (Scheme 11). The water of the dehydration step was collected in the Dean-Stark apparatus.



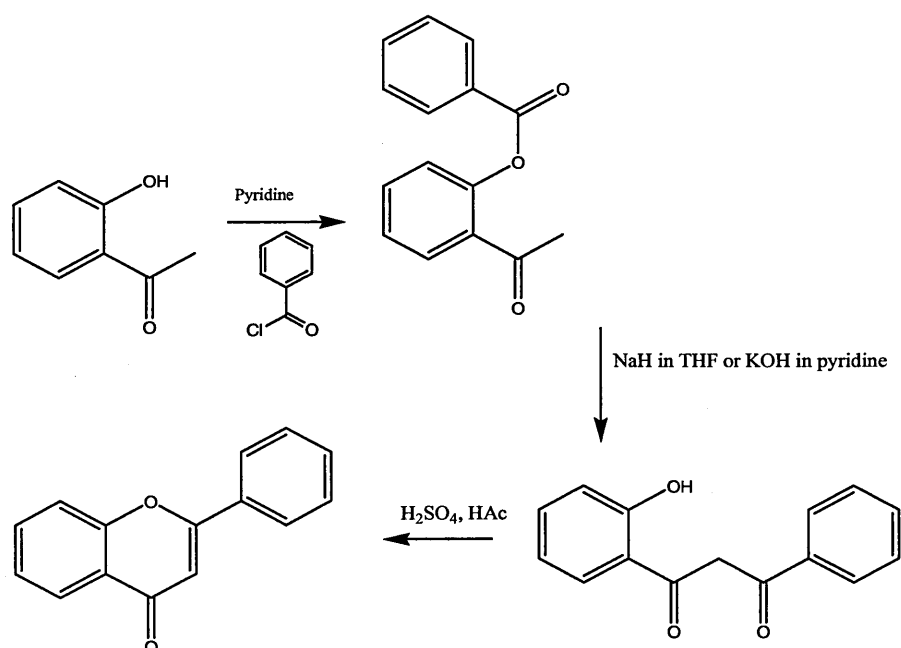
Scheme 11: Synthesis of 3-azaflavone.

4.2.a: Flavone and its derivatives

The literature regarding flavonoids synthesis is vast, but not all protocols prove to be effective, in the presence of hydroxyl and chloride substituents. We tried a range of methodologies as shown in Schemes 12, 13 and 14.

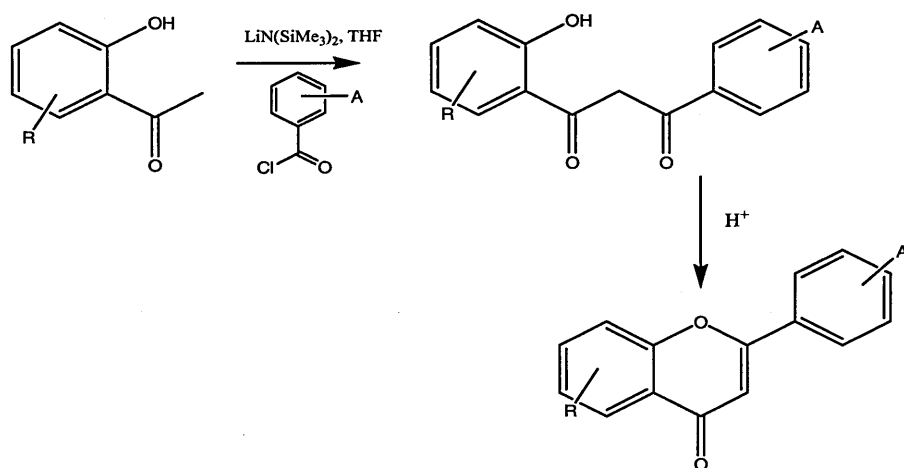


Scheme 12: The Baker-Venkatarao approach. This scheme is appropriate for MeO or unsubstituted systems, but in the case of $-\text{OH}$ groups the main product is an over benzoylated derivative that interferes with the rearrangement process (Jain, 1982). Yields of the desired product were typically in the range of 1 – 2 %.



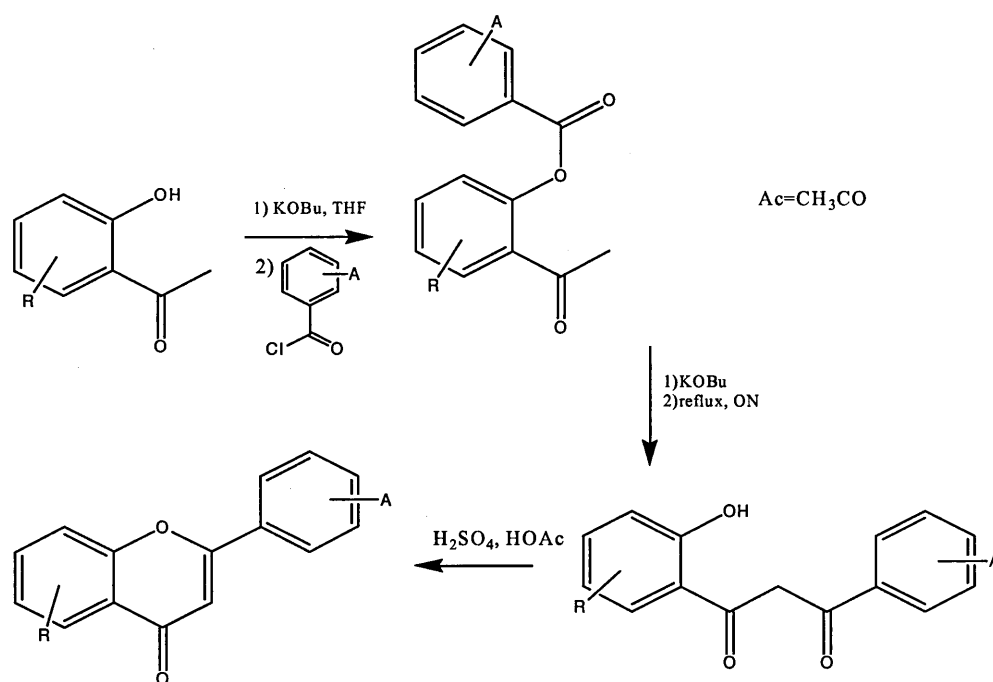
Scheme 13: Another possibility that would replace toluene with pyridine, acting as catalyst too (Ares *et al.*, 1995). This scheme works with a high yields (total 60 %) on unsubstituted systems or with MeO substitutions. The second step can be performed with NaH in THF giving higher yields than the variant KOH in Py. Rearrangement in acidic conditions leads to 50% of yield in this last step.

Cushman resolved in part the problem of -OH or other substituents in the 2-hydroxy acetophenone as starting materials by employing 4 equivalents of lithium bis(trimethylsilyl)amide (Cushman *et al.*, 1994). This forms lithium enolate from the acetyl group in the 2-hydroxyacetophenone. Treatment of the lithium enolate with 1 equivalent of aryl chloride affords a 1,3-diketone that is subsequently cyclised in acidic conditions (Scheme 14). Unfortunately we found this methodology to be inconvenient due to the low yield when scaling up.



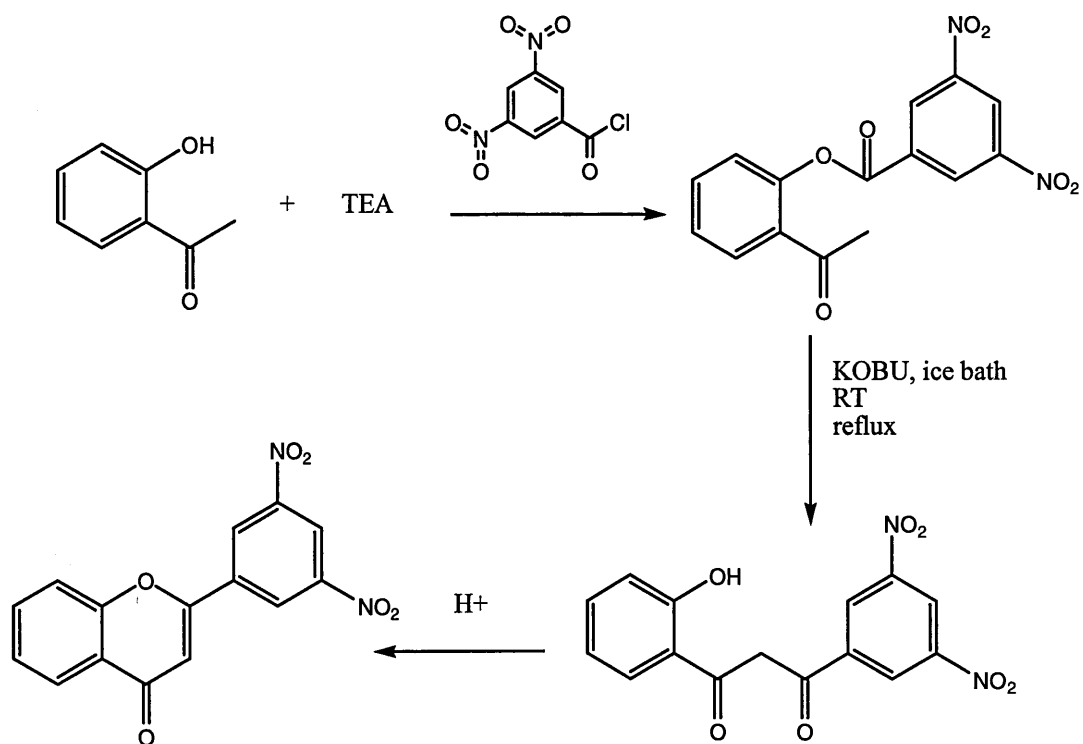
Scheme 14: Cushman's approach for synthesis of flavones.

Ares resolved the scale up problem by using potassium tert-butoxide (Ares *et al.*, 1993). The first equivalent of KOBu forms a potassium aroxide anion and treatment with benzoyl chloride forms the benzoyl ester; a second equivalent of KOBu promotes rearrangement to the diketone by forming an intermediate enolate as shown in Scheme 15. Treatment of the diketone with sulfuric acid and acetic acid gives the flavone (general yield after purification 10%).

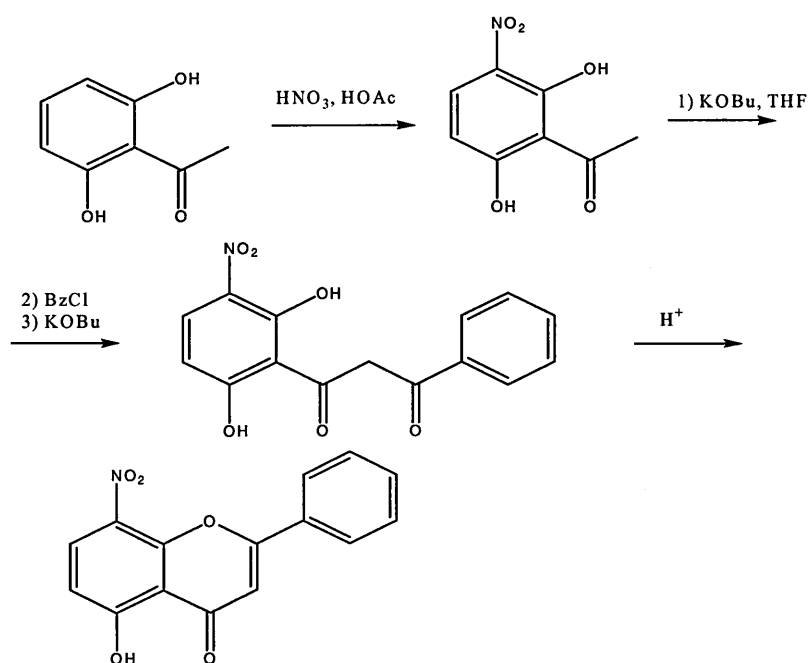


Scheme 15: Ares' approach for synthesis of flavones.

We used this protocol successfully for several compounds (6) and we also used an adaptation for introducing nitro substitutions as shown in Schemes 16 and 17. In the case of 3',5'-dinitroflavone, the 3,5-dinitrobenzoyl chloride would react in any conditions forming 3,5-dinitrobenzoic acid and would not react later on with the 2-hydroxyacetophenone. To overcome this problem we reacted the 2-hydroxyacetophenone with triethylamine (TEA) and then with 3,5-dinitrobenzoyl chloride forming 2-acetylphenyl-3,5-dinitrobenzoate and triethylamine chloride which precipitated as white pellets. For 5-hydroxy-8-nitroflavone, we first reacted the 2-hydroxyacetophenone with nitric acid in glacial acetic acid forming 2,5-dihydroxy-3-nitroacetophenone as a yellow powder. We tried to nitrate flavone and 7-hydroxyflavone in order to reduce them and to form amino flavones, but we had no success as the yields were extremely low (< 1%) only detectable as traces in mass spectrometry.



Scheme 16: 3',5'-Dinitroflavone synthesis. In this synthesis the first step was carried in presence of triethylamine (TEA) to replace the first equivalent of KBuO as following the complete Ares approach did not work when benzoyl chloride has nitro substitutions. The rest of the synthesis follows Ares' approach.



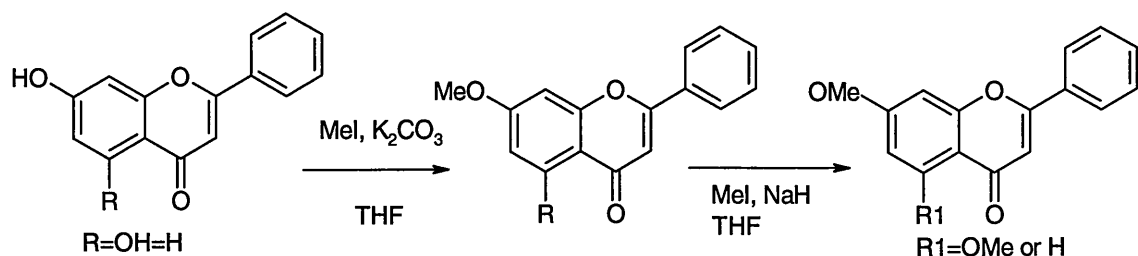
Scheme 17: 5-Hydroxy-8-nitroflavone synthesis. In this synthesis we first nitrated the 2,5-dihydroxyacetophenone with HNO_3 in HOAc . The purified 2,5-dihydroxy-3-nitroacetophenone was reacted with benzoyl chloride following Ares' approach.

Since hydroxyl groups are likely to be extremely relevant for the binding of the compounds to the DNA, as they are essential for intercalating the bases and form complexes (Yamashita *et al.*, 1999), we decided to study different hydroxyl positions in the A and B rings. Chrysin (5,7-dihydroxyflavone), 7-hydroxyflavone and 3'4'-dihydroxyflavone were purchased from Sigma–Aldrich UK Ltd and Lancaster Chemicals UK. 5-Hydroxyflavone and 6-hydroxyflavone were synthesised by Ares' protocol using 2,5-dihydroxyacetophenone and 2,4-dihydroxyacetophenone respectively; 5-hydroxyflavone was also synthesised as in Scheme 14 but the yield was so low ($< 1\%$) it could not be enough for the binding studies; fortunately the use of KOBu helped to increase the yield. 6-Hydroxyflavone was also synthesised by using the Scheme 14 but the yield was so low we had to try another protocol; as the same case as 5-hydroxyflavone, the employment of KOBu helped to

increase the yield and to obtain the desired product. Unfortunately we could not obtain flavones with hydroxyl groups in positions 8 and 7 & 8; most likely due to the formation of unreactive species. Different approaches involving protecting groups were tried but no success was had.

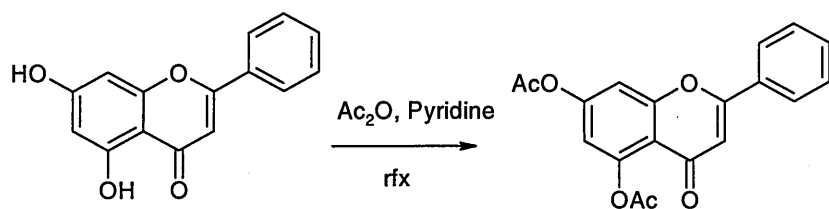
Chlorine atoms can provide an electronegative environment in a flavone while enhancing lipophilicity. We used Ares' approach to synthesise 3'4'-dichloroflavone. We also tried to synthesise 2'6'-dichloroflavone, but the chlorines in 2,6-dichlorobenzoyl chloride would not allow the reaction to proceed; we were always obtaining 2,6-dichlorobenzoic acid that would not react with the 2-hydroxyacetophenone. Different approaches were employed but with no success.

One or two methoxy groups, similarly, could provide a lipophilic environment and, moreover, may remove important interactions present in the parent hydroxy groups that are relevant to the binding of the flavone to DNA. Therefore, we employed a methylation strategy (Scheme 18) for chrysin and 7-hydroxyflavone. Position 7 proved to be easily methylated as it is the most acidic. The hydroxyl group in position 5 forms a hydrogen bond with the carbonyl in position 4, this bond decreases the acidity of the hydroxyl making it less likely to react to extract the proton and accept substitutions; to overcome this problem we employed a second step using sodium hydride in tetrahydrofuran to increase the acidity of position 5 and make it able to react.



Scheme 18: Methylation of ring A hydroxylated flavones.

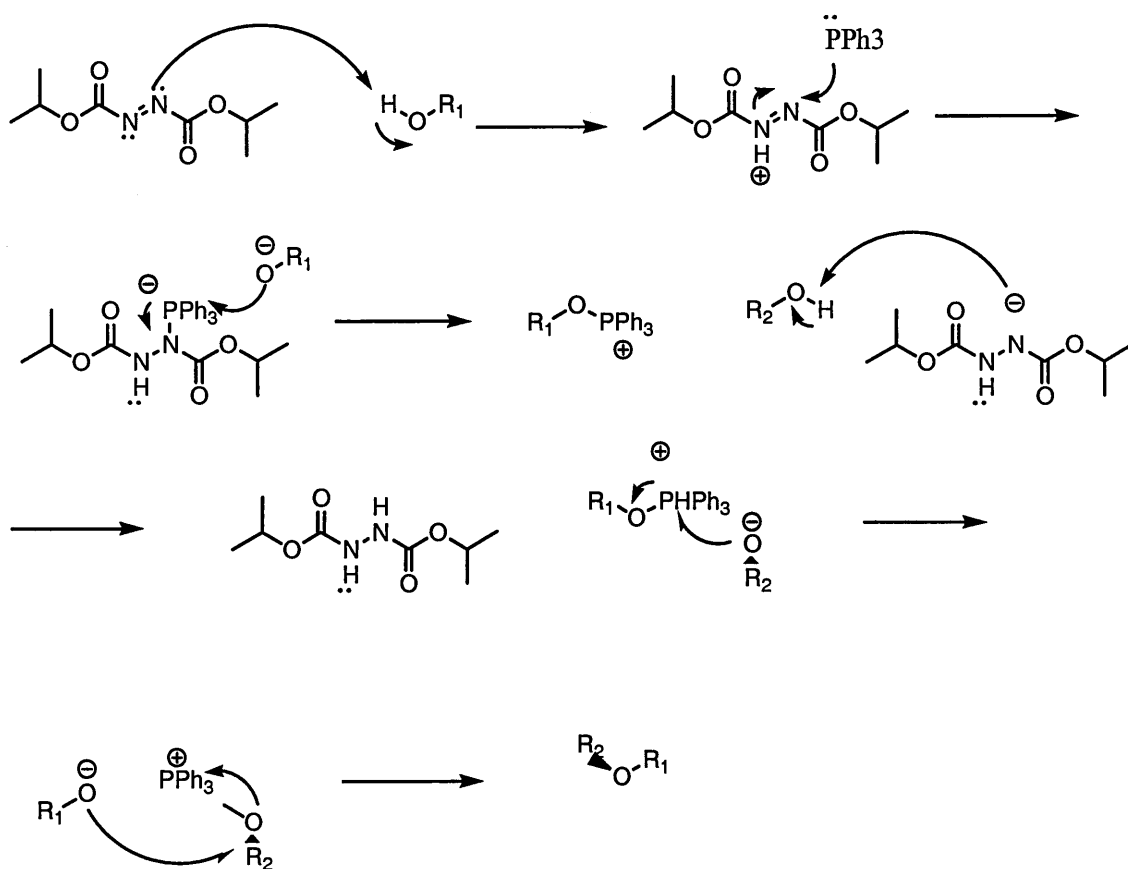
Adding extra carbonyl groups could provide some more information about steric impediments as well as selectivity of DNA for certain groups. We used acetoxylation in chrysin in order to obtain an acetoxy derivative.



Scheme 19: Acetoxylation synthetic route

Tertiary amines could provide a completely different environment, as at pH 7.4 they would be protonated, making them more suitable for binding to the negatively charged phosphates of the DNA. For tertiary amines we used dimethylaminoethanol, dimethylaminopropanol and morpholinoethanol as substituent agents for chrysin. Only position 7 could be substituted.

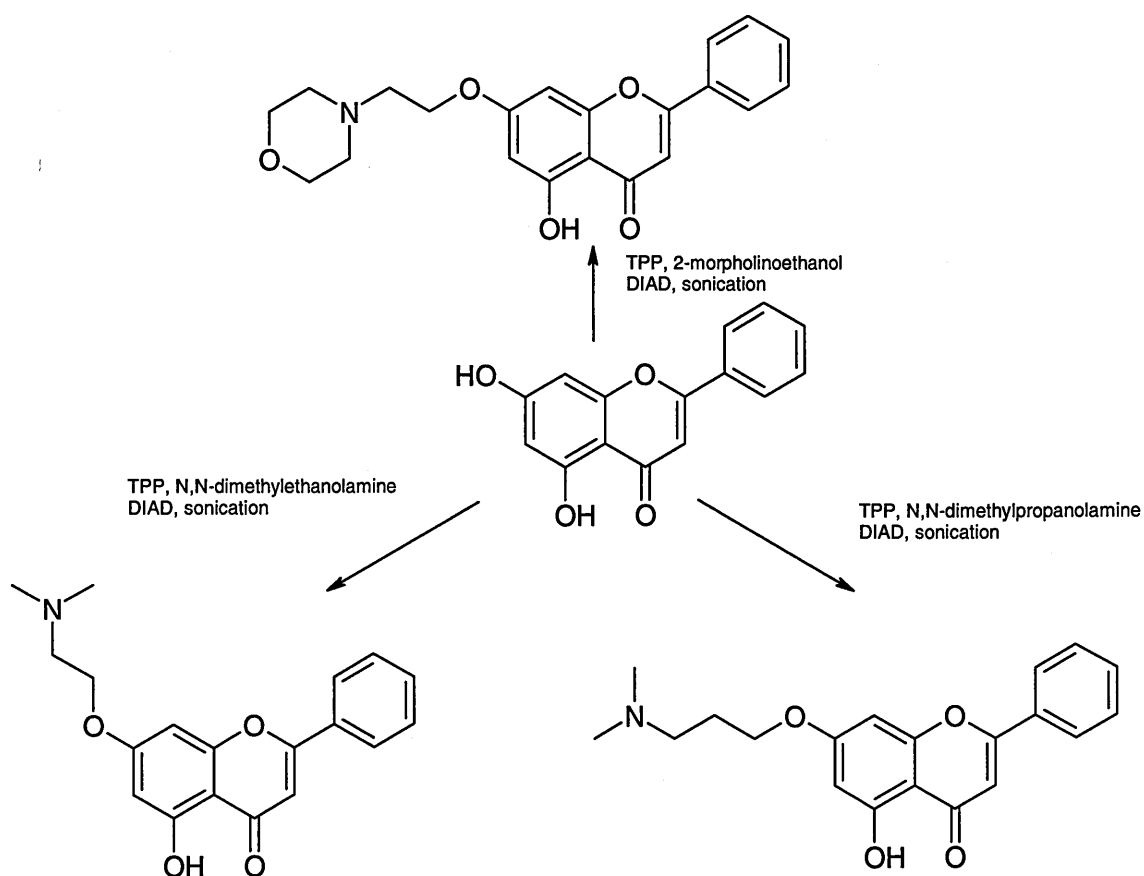
Mitsunobu reaction was used with chrysin as starting material in order to create other possibilities for studying DNA - drug interactions. An insight of the process is shown in scheme 20.



R_1 is the 5,7-dihydroxychrysin, and R_2 is the substituent

Scheme 20: Mitsunobu reactions. The reactions were carried out under sonication where TPP (or PPh_3) (triphenylphosphine) combines with DIAD (diisopropyl azodicarboxylate) to generate a phosphonium intermediate that binds to the alcohol oxygen, activating it as a leaving group. Substitution by a nucleophile completes the process.

With this reaction we employed chrysin as a flavone starting material to produce 3 compounds, as shown in scheme 21.



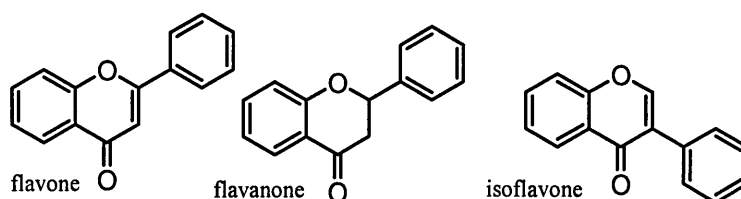
Scheme 22: Tertiary amine derivatives

4.3: Obtaining binding association constants

In order to choose an appropriate scaffold to make modifications and study suitable substituents, we employed UV-Vis and fluorescence titrations (see section 2.2.c.2 to 2.2.c.4) to get binding constants and to be able to determine which structure preferentially binds to STDNA. We also used these same methodologies to assess if the addition of cations assists on the binding to nucleic acids of flavonoids with hydroxyl groups in close positions to the carbonyl. As well as studying binding constants, we also studied the thermal stability of this new batch of compounds with STDNA using thermal denaturing studies (see section 2.2.c.1). To assess an improvement in the biological activity we studied some of the compounds for cell proliferation activity (see section 2.2.h.2)

4.3.a: Localization of the B ring and the relevance of the double carbon bond in the C ring

The B ring can be either in C-2 forming the flavonoid family or in C-3 forming the isoflavonoid family, and these structures can affect the mode of binding. The double bond C-2 to C-3 makes a small distortion in the molecule, and also changes the saturation of the C ring. See compounds 10, 11, 12.



Compounds 10, 11, 12: The different possibilities of localization of the B ring are shown, in flavone (10) the B ring is in C2, as is in flavanone (11) but with a saturated C ring; in isoflavone (12) the ring is in C3.

The binding constants obtained are shown in Table 11. From these results we can conclude that the binding constants are quite similar and at such low values that we can not rely on this method to choose a scaffold. However, if we consider the results in chapter 3 and we based our choices in the results of the binding constants, of the initial compounds the flavone scaffold appears to be the preferred choice for further structure activity relationship studies.

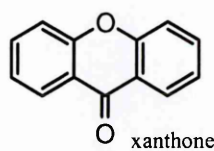
Table 11: The results of the binding association constants for flavone, flavanone and isoflavone proved to be quite similar in the magnitude of 10^3 M^{-1} . Flavone and isoflavonoid presented fluorescence properties, but showed no measurable change in the emission signal upon titration with DNA.

Compound	STDNA (UV)	STDNA (Fluorescence)		
	K (M ⁻¹)	N	K(M ⁻¹)	N
Flavone	1221.7	2.6	No interaction observed	
Flavanone	1237.8	2.5	1238.92 (exc 300, emis 375)	2.04
Isoflavonoid	1767	10	No interaction observed	

4.3.b: Three fused rings

Intercalating agents share the common feature of the planar polyaromatic systems which bind by insertion between the DNA base-pairs, with preference for 5'-pyrimidine-purine-3' steps. The chromophores are linked to basic chains that might also play a role in the affinity and selectivity shown by this class of agents. The planar structure of acridines (Hutchins, 2003) confers to the molecules the ability to bind DNA by intercalation. A large number of

synthetic acridine derivatives have been tested as anticancer agents and only a few molecules have entered clinical trials and have been approved for chemotherapy. Based on this premise, we tested a compound with three fused rings, see compound 13, maintaining the central structure of the C ring (see Compound 13). This molecule is known as xanthone and has been found to act as antimalarial agent (Dua, 2004), antidepressant working as a MAO (monoamine oxidase) inhibitor (Núñez *et al.*, 2004), anticancer agent on HL60 leukemia cell line (Matsumoto *et al.*, 2004) and chemopreventative agent (Jiang *et al.*, 2003).



Compound 13: Xanthone with its three fused rings.

The binding constant of xanthone with DNA, was measured by UV-Vis spectroscopy and fluorescence quenching, and the results are shown in Table 12.

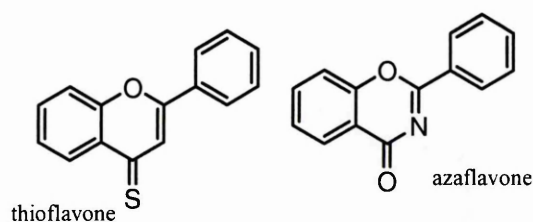
Table 12 : The binding association constants for xanthone proved to be similar to the one for flavone.

Compound	STDNA (UV)	STDNA (Fluorescence)		
	K (M ⁻¹)	N	K	n
Xanthone	2323.31	2	2283.7 (exc 340 emis390)	2.1

From the analysis of the plain molecules, we can conclude the strength of binding for STDNA is the same for the system with three fused rings (xanthone) as for the system with the third aromatic ring (B ring) in C-2 (flavone) or in C-3 (isoflavone). Therefore, we will retain the flavone structure as the scaffold for our further modifications.

4.3.c: Sulfur and nitrogen in the 3-ring system

Nitrogen, sulfur and electronegative atoms, added into a naked scaffold would produce a small distortion into the planar structure and a charged molecule when it is tested at pH 7.4; see compounds 14 and 15. In the case of aza-3-flavone (azaflavone), no interaction was observed by UV-Vis spectroscopy, but a binding association constant was obtained by fluorescence spectroscopy, giving a very low value, see Table 13. For flavothione (or thioflavone) we observed in the UV-Vis spectrum an isosbestic point at 304 nm, see Figure 29, further on the curves end on a single line without showing any clear isosbestic point. This could indicate a two binding mode for this compound and STDNA. The fitting of the UV-Vis results gave a sigmoid curve (Figure 30) that could not be fitted into our one mode of binding equation, possibly other binding models would be able to fit this results. On the other hand, fluorescence titrations gave a general binding association constant for flavothione on STDNA which showed that flavothione had the highest binding association constant for an unsubstituted compound, with an association constant of 15550 M^{-1} .



Compounds 14, 15: Thioflavone (14) has a sulfur anion in C4 while azaflavone (15) has a nitrogen replacing C3.

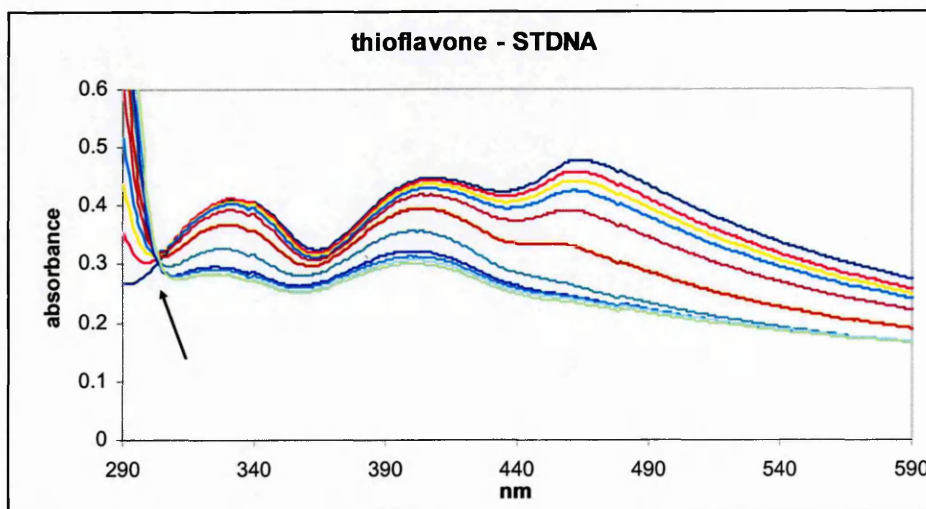


Figure 29: The results of the titration of thioflavone on STDNA shows an isosbestic point at 304 nm.

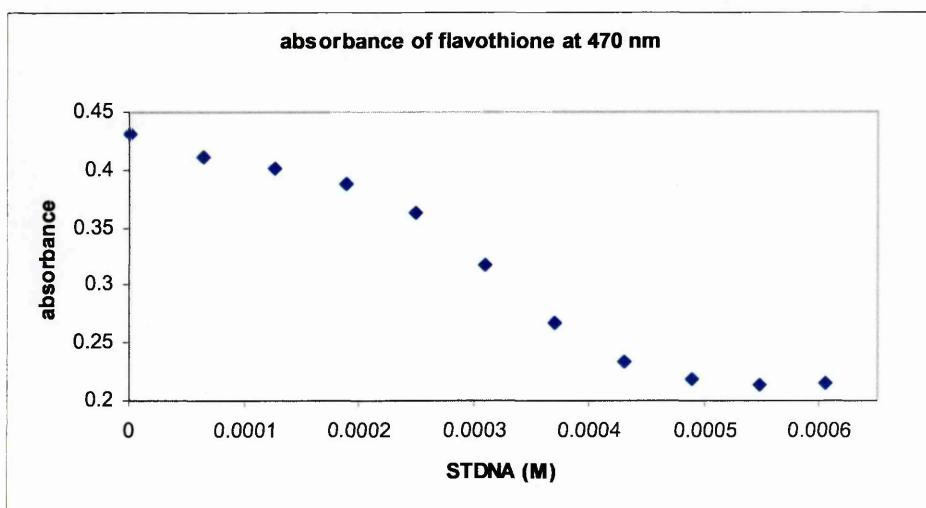


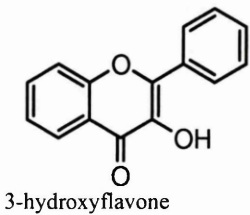
Figure 30: The titration of flavothione on STDNA produced a sigmoid curve when the absorbance at a specific wavelength was plotted against the concentration of STDNA.

Table 13: The results of the binding association constants for flavothione and aza-3-flavone are shown, indicating a very high binding constant for flavothione.

Compound	STDNA (UV)	STDNA (Fluorescence)	N
	K (M ⁻¹)	K(M ⁻¹)	
Flavothione	Not defined	15538.7 (exc 420 , emis 464)	9.3
Azaflavanone	No interaction observed	876.9 (exc 340, emis 422)	2.1

4.3.d: The difference between flavones and flavonols

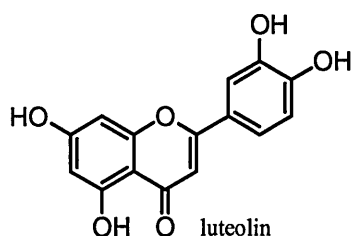
Flavonoids are polyphenolic secondary metabolites widely dispersed throughout the plant kingdom. In plant tissues, flavonols and flavones are found conjugated to sugars, primarily glucose, rhamnose and rutinose, and most conjugation occurs at the 3 position of the B ring. The main difference between these two families is the presence of one hydroxyl group in C-3, see compound 16. We tested the relevance of this hydroxyl for the binding to STDNA, and we found that 3-hydroxyflavone is not soluble in phosphate buffer, even in presence of 10% of DMSO (dimethylsulfoxide).



Compound 16: 3-hydroxyflavone is not soluble in buffer A at a 10% DMSO concentration

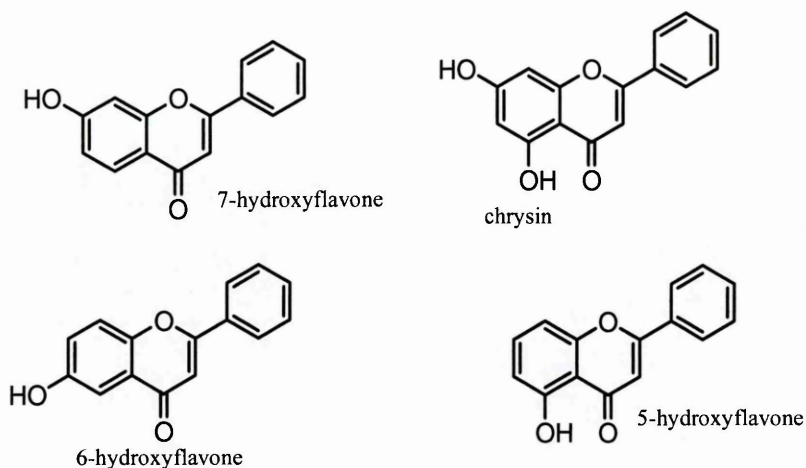
4.3.e: Modifications on the A ring

The basic flavonoid structure originates from two sources: The 'A' ring is formed from three acetate units (via the malonic acid pathway) and the 'B' ring with the 3-carbon bridge is constructed of a phenylpropane unit via the shikimic acid pathway. As antioxidants, these phytochemicals can donate an electron, accompanied by a hydrogen nucleus, from the -OH groups attached to their phenolic rings, to a free radical. This electron stabilizes and inactivates the damaging radical, in the process, the polyphenolic reducing agent becomes an aroxyl radical which is considerably more stable than the free radical that it has reduced; the result is the cessation of damaging oxidative chain reactions (Skaper *et al.*, 1997). From our previous results, we found hydroxyl groups in flavonoids were crucial for promoting DNA binding. Some compounds such as luteolin, see compound 17, already have reported DNA binding activities, have been found to have antioxidant properties by neutralizing peroxides, as well as work as anti-inflammatory, anticancer, antiallergic agents and have immune-modulating properties (Hyuncheol *et al.*, 2004).



Compound 17: luteolin has two hydroxy groups in each of the A and B rings.

We studied the importance of key positions of hydroxyl groups like in positions 5, 6 and 7, see compounds 18, 19, 20, 21.

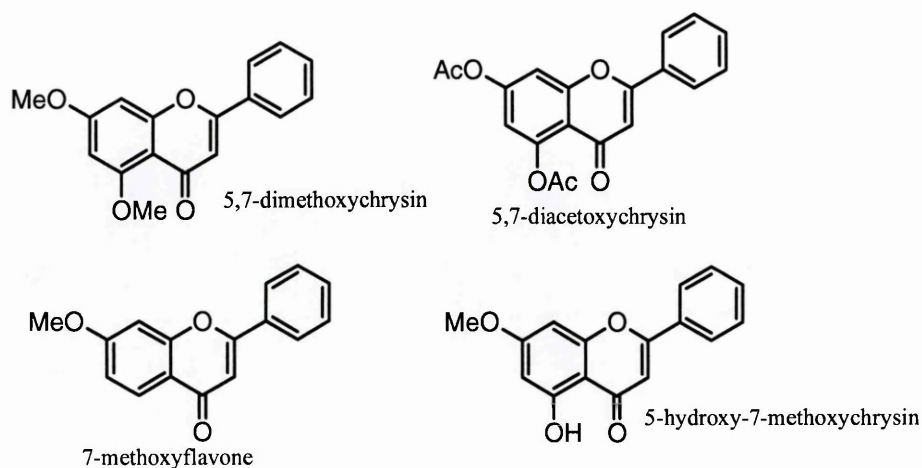


Compounds 18, 19, 20 and 21: 7-hydroxyflavone (18), 6-hydroxyflavone (19) and 5-hydroxyflavone (20) have one hydroxyl in the A ring. Chrysin (21) has two hydroxyls in positions 5 and 7.

As a further step, we studied substitution in the A-ring, and we postulated some specific positions with hydroxyl groups.

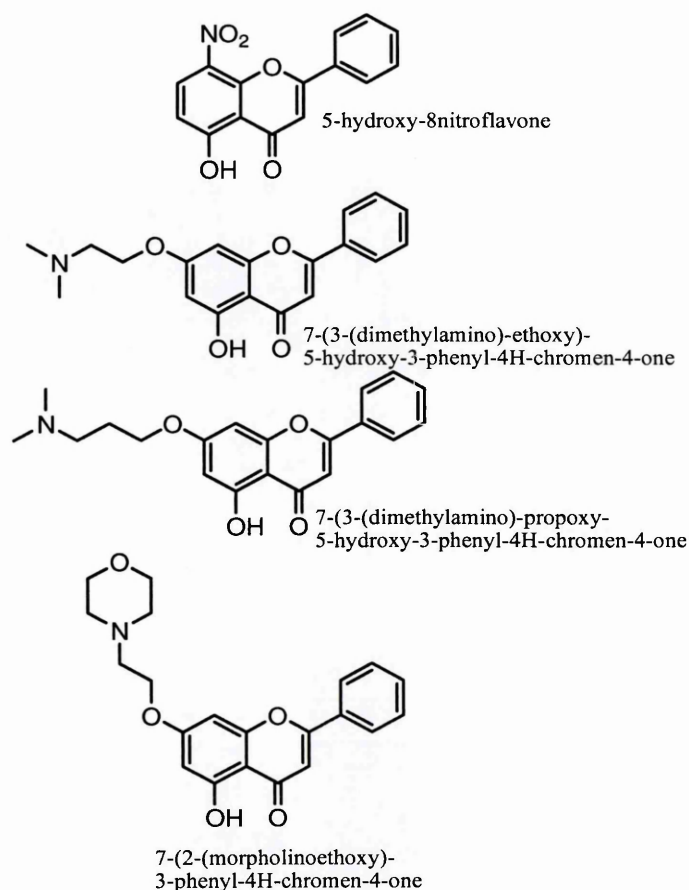
We also investigated the relevance of hydroxyl groups as electron donors by methylating and acetylating the hydroxyls, see compounds 22, 23, 24, 25; this study would give an indication of :

- the presence of a group increases the binding and helps to the intercalation
- the chemical characteristic of the substituted promotes stability and binding to the complex.



Compounds 22, 23, 24 and 25: We approached studied substitutions, substituting in the case of 5,7-dimethoxychrysin (22) the two hydroxyls with methoxy groups, as well as in the case of 5,7-diacetoxychrysin with the acetoxy groups (23). In 7-methoxyflavone (24) and 5-hydroxy-7-methoxyflavone (25) we have substituted only the position 7.

As the DNA is negatively charged a protonated drug would bind stronger or the complex would be more stable, a tertiary amine would be protonated in an environment of pH 7.4, offering the drug a positive charge. Therefore we studied the substitution of 7 hydroxyl with N,N-dimethylethanolamine, N,N-dimethylpropanolamine and 2-morpholinoethanol (by Mitsunobu reactions); as well as the position 8 with a nitro substitution, see compounds 26, 27, 28, 29.



Compounds 26, 27, 28 and 29: We studied the relevance of a nitro group in the A ring with 5-hydroxy-8-nitroflavone (26). In the group of tertiary amines we studied an ethyl chain in 7-dimethylaminoethoxy-5-hydroxyflavone (27), a propyl chain in 7-dimethylaminopropoxy-5-hydroxyflavone (28) and morpholine substitution in 7-morpholinoethoxy-5-hydroxyflavone (29).

In Table 14 we can see the results obtained for this group of compounds with modifications in the A ring. The highest association binding constants for 7-dimethylaminoethoxy-5-hydroxyflavone and 7-morpholinoethoxy-5-hydroxyflavone clearly show a tertiary amine with a two carbon chain is really appropriate for the binding increasing the binding of the unsubstituted molecule (chrysin) by 100 fold. It also showed that two methyl groups joined to the tertiary amine assist to the binding in a more favourable way than a morpholine substitution. In contrast, 7-dimethylaminopropoxy-5-hydroxyflavone in which the tertiary

amine was on a three carbon chain, show a binding in the order of 10^3 M^{-1} , this could indicate that the flavone intercalates the base pairs of the DNA by positions 7 and 8. A two carbon chain could probably seal this intercalation, but a three carbon chain would inhibit the binding probably by steric hindrance. Chrysin, considering it only has two hydroxyls (in positions 5 and 7) also showed a strong binding activity (10^4 M^{-1}) when compared to other flavones with the same number of hydroxyls but in different positions. Considering that 7-hydroxyflavone presents only one third of the binding of chrysin and 5-hydroxyflavone did not show any binding activity, we can conclude the most relevant position in the A ring is position 7. 5-Hydroxyflavone did not show any interaction with STDNA, but when we added a nitro group in position 8, the binding increased giving a binding constant of 7781.4 M^{-1} . Hydroxyl groups in position 6 did not help the binding to STDNA. Methoxy and acetoxy substitutions inhibit the binding to the DNA as it was shown by the decrease of the binding constant of the unsubstituted parent compound (chrysin) when methoxy and acetoxy groups were added. Some compounds did not provide identical results in the UV-Vis calculated binding association constants and fluorescence association constants, but this is possibly due to the fact that the equation is not appropriate for very low binding constants, obtained by compounds such as the one in the order of 10^3 M^{-1} , like 5-hydroxy-7-methoxychrysin, 5,7-diacetoxychrysin, chrysin and luteolin.

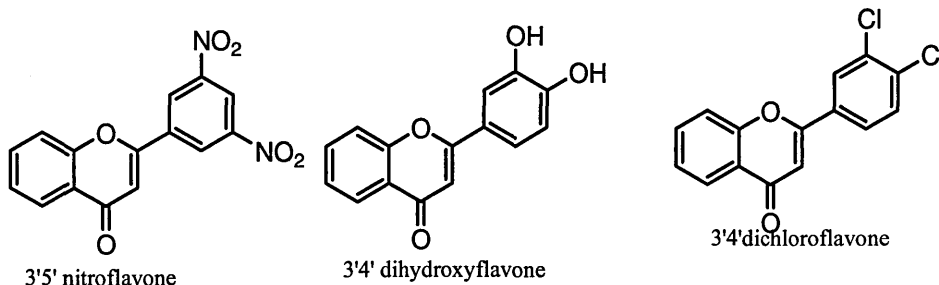
Table 14: The results of the binding association constants show 7-dimethylamino-ethoxy-5-hydroxyflavone and 7-morpholino-ethoxy-5-hydroxyflavone as the strongest binders followed by chrysin and luteolin. These results clearly show the relevance of a substituent in the 7 position.

*Nio: no interaction observed.

Compound	Uv –Vis K (M-1)	N	Fluorescence K (M-1)	N
5-hydroxyflavone	N i o*		N i o*	
6-hydroxyflavone	1155.4	2.6	1266.8 (exc 420, emis 481)	2
7-hydroxyflavone	8134.9	3.4	N i o*	
7-methoxyflavone	1567.4	2	1575.9 (exc 340, emis 534)	2.6
5-hydroxy-7-methoxychrysin	714.2	1.7	5865.4 (exc 340, emis 442)	2
5,7-methoxychrysin	1474.6	2.3	1947.4 (exc 340, emis 442)	2
5,7-acetoxychrysin	3200	2.7	1695.4 (exc 340, emis 528)	2
chrysin	28460.5	4	7499.4 (exc 340, emis 442)	3
5-hydroxy-8-nitroflavone	N i o*		7781.4 (exc 340, emis 383)	4
luteolin	11193.8	12.9	2214.6 (exc 340, emis 383)	4
7-dimethylamino-ethoxy-5-hydroxyflavone	189714.6	2.3	N i o*	
7-dimethylamino-propoxy-5-hydroxyflavone	2189.5	1.5	1728.2 (exc 420, emis 490)	3.3
7-morpholino-ethoxy-5-hydroxyflavone	110679.3	0.85	N i o*	

4.3.f: Modifications on the B ring

In quercetin, the B ring seems to play an important role when bound to the DNA (Yamashita, 1999) so we studied different substitutions on this ring. Electron-withdrawing groups are present in many anticancer drugs (Chu, 1980) so we studied other substituents like Cl^- and NO_2^- . See compounds 30, 31 and 32.



Compounds 30, 31, 32: We studied nitro substitutions in 3',5'-dinitroflavone (30), hydroxyl groups in 3',4'-dihydroxyflavone (31) and chloride groups in 3',4'-dichloroflavone (32).

In Table 15 we can appreciate the results of the binding association constants. We would expect hydroxyl groups in the B ring to be responsible of a reasonable part of the DNA-drug interaction. However, after analyzing results from luteolin and chrysin we can conclude that hydroxyl groups in 3' and 4' positions decrease the binding. Moreover, if we extend the assumption to the original set of compounds we can speculate that the hydroxyl in position 3 in quercetin helps to improve the binding or does not affect the binding in any way. Chlorine and nitro substitutions did not improve the binding as it would be expected.

Table 15: The results of the binding association constants show clearly that substitutions in the B ring do not assist in a remarkable way the interaction with STDNA.

Compound	STDNA (UV)	STDNA (Fluorescence)		
	K (M ⁻¹)	N	K(M ⁻¹)	n
3',5'-dinitroflavone	1138.9	2.2	1181.1 (exc 340 , emis 384)	2
3',4'-dihydroxyflavone	1978.9	7.2	1217.9 (exc 320, emis 467)	3
3',4'-dichloroflavone	763.6	1.9	1345 (exc 420, emis 464)	5.4

4.3.g: DNA – drug – metal interactions

Drugs can bind to metals directly or indirectly by using the hydration water; and metal cations have preferences for the bases in the DNA, helping the selectivity of the drug for the nucleic acid structure and modifying its conformation from B to Z or A – DNA (Anastassopoulou, 2003).

From the structural related studies we have two main groups with hydroxyl groups that show relatively high binding association constants:

- tertiary amines, with the substituted chrysin
- chrysin, luteolin and 7-hydroxyflavone with free hydroxyl groups.

From these two groups, the second one provided compounds with hydroxyl groups in ortho position to the carbonyl in position 4 and hydroxyl groups in position 7 which showed to be relevant to binding with DNA; these 3 drugs were studied for metal – drug – DNA interactions (see section 3.3.b.4). Chrysin and luteolin have hydroxyl groups next to the carbonyl, but 7-hydroxyflavone has not, so that would be possible to have a negative

control in this study if it corroborates what Yamashita (*et al.*, 1999) observed about copper interacting first with quercetin and then with DNA. As the drugs have only one hydroxyl next to the carbonyl we used a ratio 1:1 of drug:metal. In Table 16 the results for this study are shown, and they indicate that Fe^{3+} , Mg^{2+} and Mn^{2+} increase by 1000 times the binding constants of 7-hydroxyflavone for DNA. This clearly shows the metals bind to the drug and allow it to better interact the DNA. For chrysin Cu^{2+} , Fe^{2+} , Fe^{3+} , Mn^{2+} and Mg^{2+} helped to increase 100 times the binding constant, but Zn^{2+} increased only by 75%. In the case of luteolin, no metal helped with the bindings. These results indicate the flavones bind preferentially using the 7-hydroxy position and metal cations improved remarkably this process. The fact that chrysin has stronger binding than 7-hydroxyflavone can be due to the hydroxyl in position 5, which could interact forming bonds with a metal joined to the carbonyl. Only crystallization of this complex would elucidate the actual structure.

Table 16: The results of the titrations of the metal – drug – DNA complexes. The binding association constants are expressed in M^{-1} , the n value appears between brackets.

Cation	7-hydroxyflavone 1:1, K (M^{-1})	Chrysin 1:1, K (M^{-1})	Luteolin 1:1, K (M^{-1})
Cu^{2+}	10541 (2.29)	136723 (1.9)	1390.4 (2.3)
Fe^{2+}	10932.3 (2.1)	589632 (4)	1428.4 (2.4)
Fe^{3+}	200550 (2.09)	448189.5 (2.5)	1366.2 (2.6)
Mg^{2+}	1032439 (1.4)	1179875 (1.5)	1518.4 (2.8)
Mn^{2+}	107741 (2)	251482 (2.7)	1372.7 (2.2)
Zn^{2+}	9935.5 (2.18)	74901 (5)	1447.6 (3)

4.4: Selectivity for different structures

4.4.a: Competition dialysis

Selectivity for different isoforms of DNA is always relevant when drug – nucleic acid interactions are under study. We studied this second set of compounds on 8 different isoforms of nucleic acids (STDNA, polydAdT, poly[dAdT]₂, polydGdC, poly[dGdC]₂, polydAdT-dT, purine triplex, G-tetraplex) using competition dialysis (see Chapters 2 and 3) Figures 31 a – s show the results of these experiments. Thioflavone showed remarkable preference for G-quadruplex and polydGdC-dGdC. It is possible that thioflavone prefers quadruplex DNA as these structures present more available space for intercalation and the sulfur in thioflavone could possibly play an important role in the stabilization of the complex. For duplex DNA structures, thioflavone clearly prefers GC sequences. Flavone also showed preference primarily for G-quadruplex, with high affinities for poly[dGdC]₂ and purine triplex (GCG). This is a clear indication of preference for GC. Presence of a nitrogen as part of the ring, as in the case of azaflavone, changed the preference for G-quadruplex to GCG triplex and polydAdT-dAdT. It appears that the flavone scaffold interacts preferentially with high order DNA structures. However, when the skeleton changes, the marked preference for GC bases also changes to AT bases. As well as thioflavone and flavone, 3',4'-dichloroflavone, luteolin, 3',5'-dinitroflavone, chrysin, 7-morpholinoethoxy-5-hydroxyflavone, 7-dimethylaminoethoxy-5-hydroxyflavone and 7-dimethylaminopropoxy-5-hydroxyflavone showed a remarkable preference for G-quadruplexes in first place, followed by preference for GCG triplex and polydGdC-dGdC for second place. 5-Hydroxy-8-nitroflavone showed preference for polydGdC-dGdC and secondly for G-quadruplex, in this case the preference was inverted when compared with

the previously described compounds. 3',4'-Dihydroxyflavone showed preference for G-quadruplex followed by equal preferences for GCG triplex, polydGdC-dGdC, polydGdC and polydAdT-dAdT. Adding two methoxy groups in chrysin started to change the preference for G-quadruplex to STDNA, but adding only one methoxy group kept the initial preference for G-quadruplex and added a remarkable preference for polydAdT. Introduction of two acetoxy groups in chrysin inverted the preference of G-quadruplex and polydGdC-dGdC to polydGdC-dGdC primarily and G-quadruplex secondly. 7-hydroxyflavone and 5-hydroxyflavone showed a clear preference for STDNA, but when we added a methoxy group to 7-hydroxyflavone the preference changed dramatically to polydAdTdT. 6-Hydroxyflavone showed preference for poly[dGdC]₂ and polydAdT. It appears that any preferential binding to GC rich duplex DNA is for the alternating purine-pyrimide GC step and not for the polydGpolydC homopurine-homopyrimidine strands, in agreement with previous data of intercalators showing a preference for GC steps (Ren and Chaires, 1999).

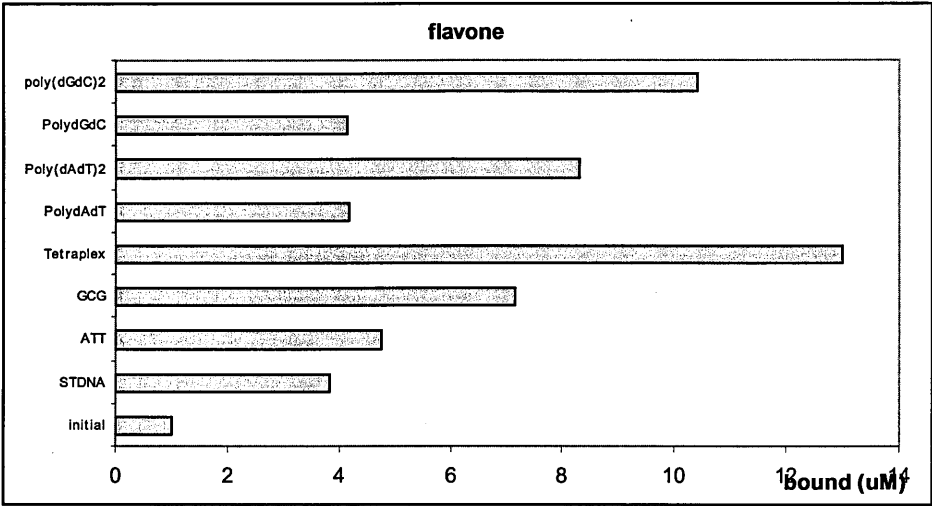


Figure 31 a: Flavone shows preference for G-quadruplex and poly[dGdC]₂

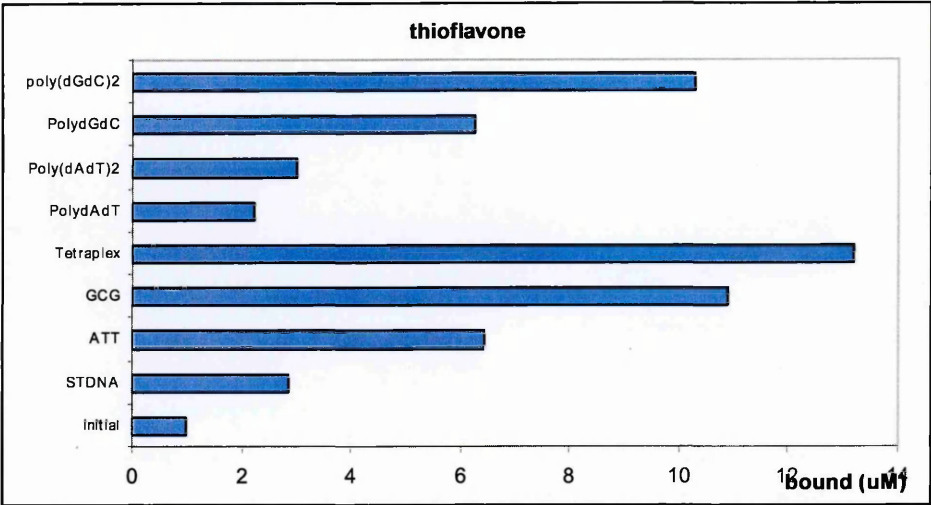


Figure 31 b: Thioflavone shows preference for G-quadruplex, poly[dGdC]₂ and purine triplex.

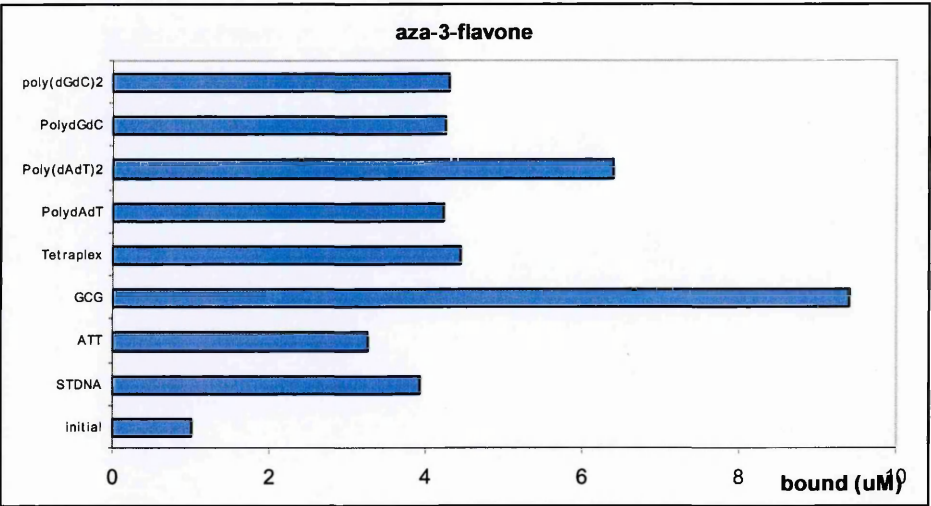


Figure 31 c: Aza-3-flavone shows preference for purine triplex and poly[dAdT]₂

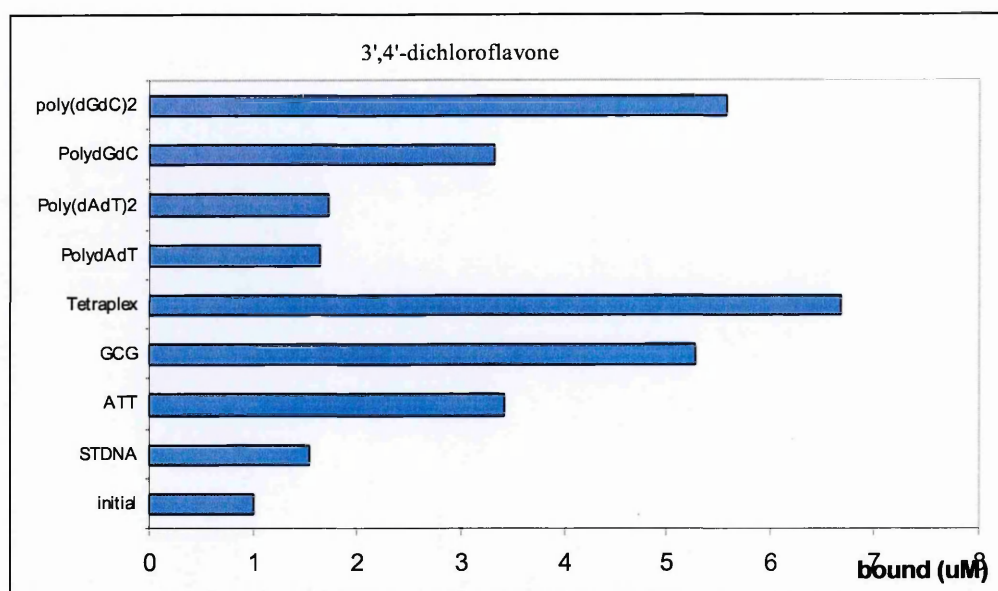


Figure 31 d: 3',4'-Dichloroflavone shows preference for G-quadruplex, poly[dGdC]₂ and purine triplex.

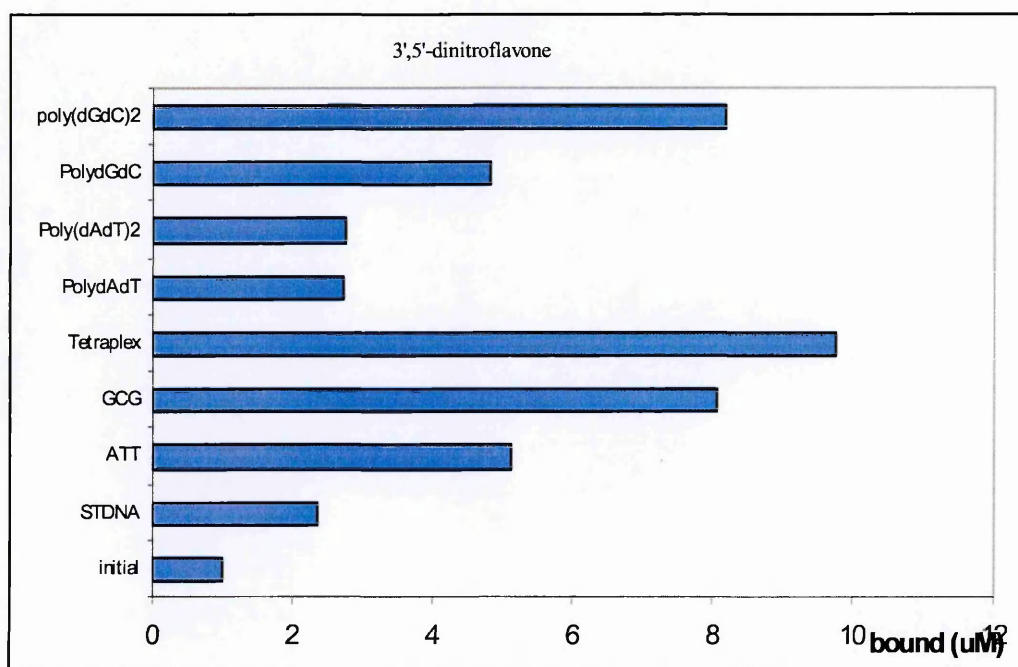


Figure 31 e: 3',5'-Dinitroflavone shows preference for G-quadruplex, poly[dGdC]₂ and purine triplex.

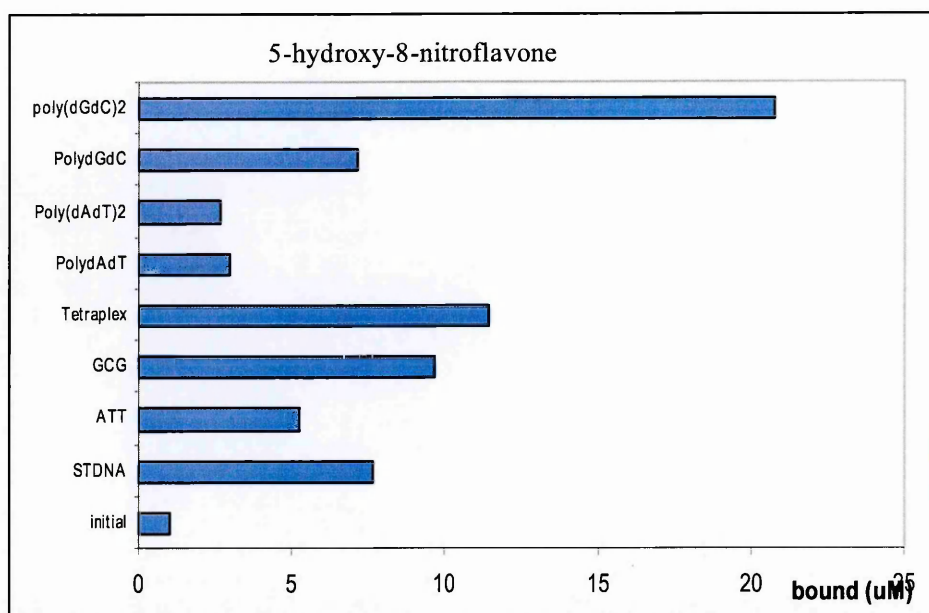


Figure 31 f: 5-Hydroxy-8-nitroflavone shows preference for poly[dGdC]₂ and G-quadruplex.

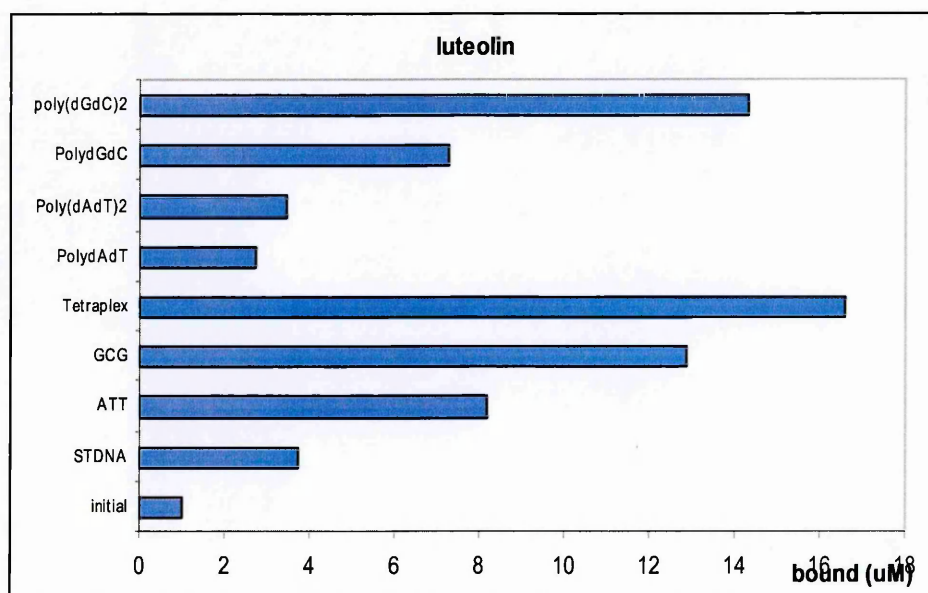


Figure 31 g: Luteolin shows preference for G-quadruplex, poly[dGdC]₂ and purine triplex.

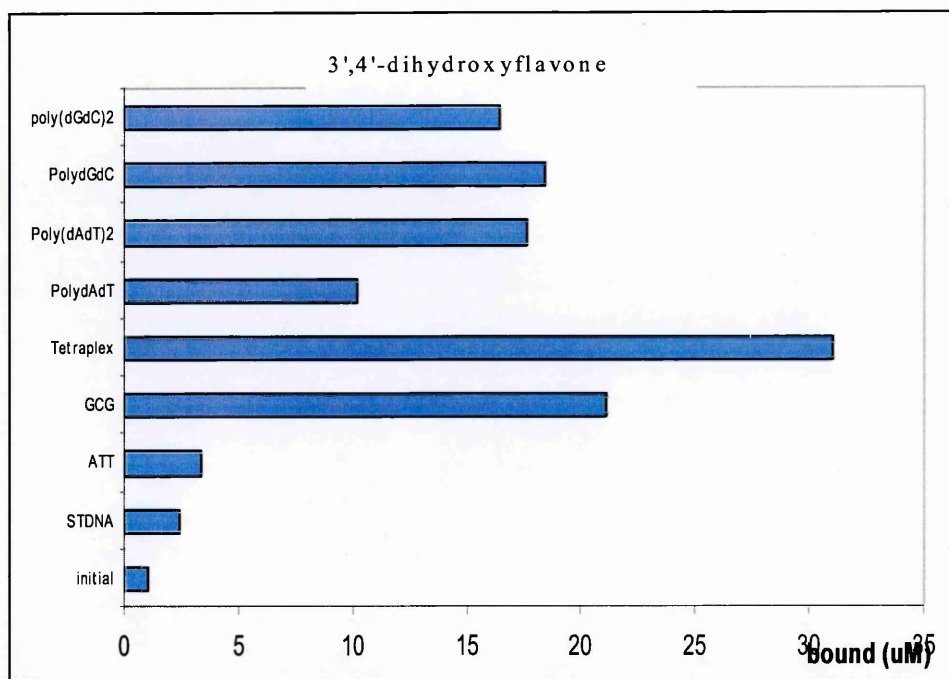


Figure 31 h: 3',4'-Dihydroxyflavone shows preference for G-quadruplex and purine triplex.

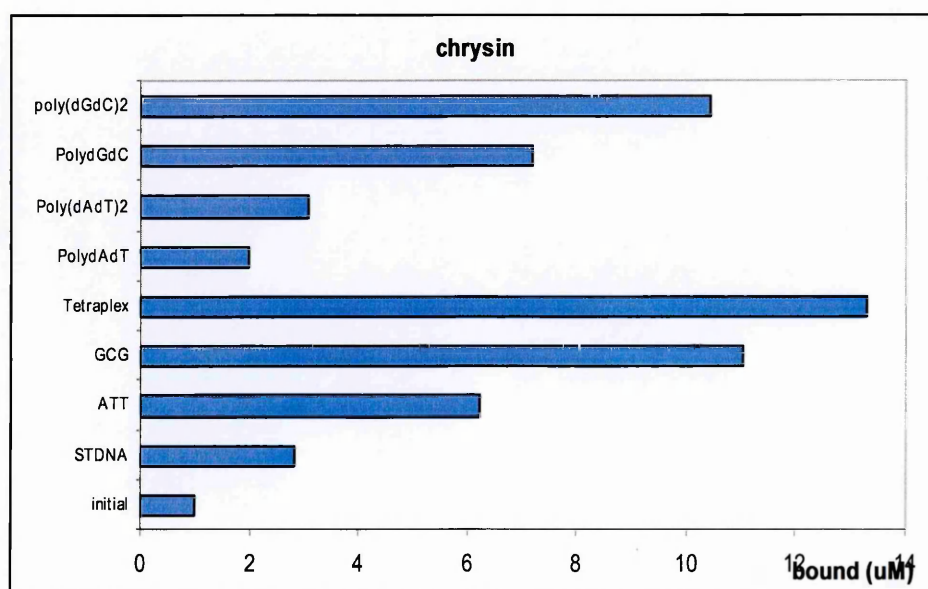


Figure 31 i: Chrysin shows preference for G-quadruplex, purine triplex and poly[dGdC]₂.

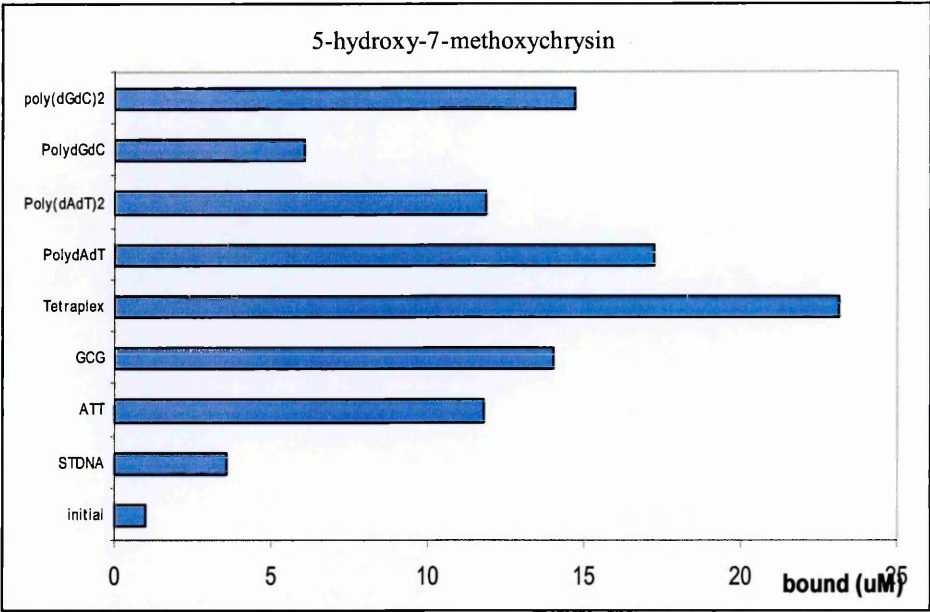


Figure 31 j: 5-Hydroxy-7-methoxyflavone shows preference for G-quadruplex, polydAdT, poly[dGdC]₂ and purine triplex.

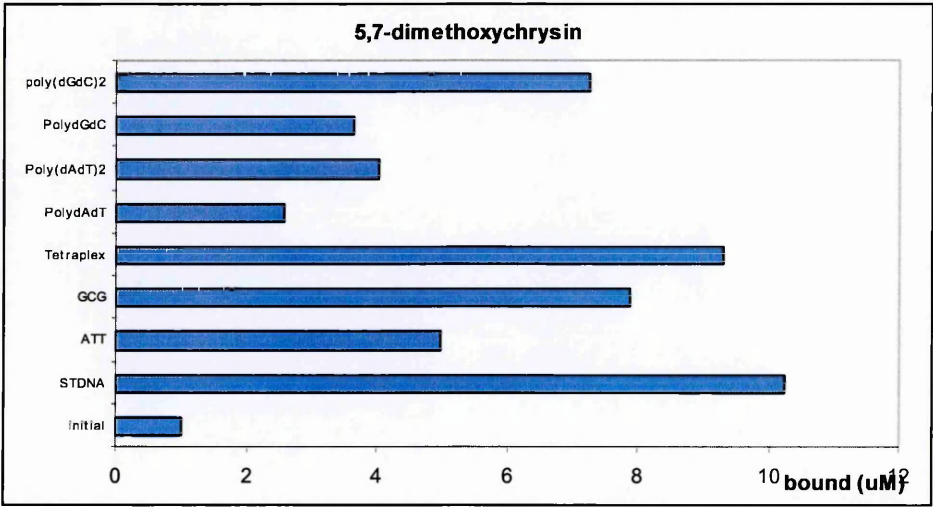


Figure 31 k: 5,7-Dimethoxychrysin shows preference for STDNA, G-quadruplex and purine triplex.

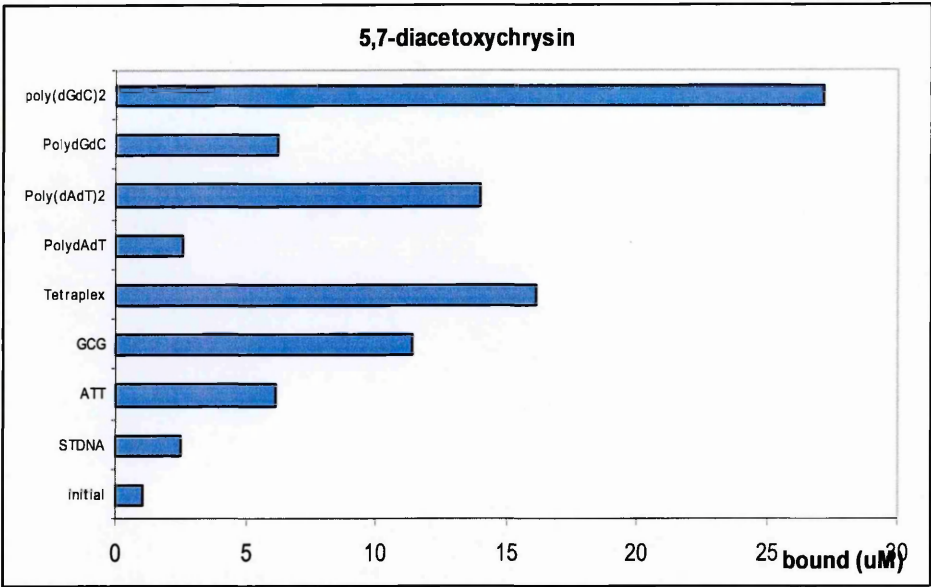


Figure 31 l: 5,7-Diacetoxychrysin shows preference for poly[dGdC]₂.

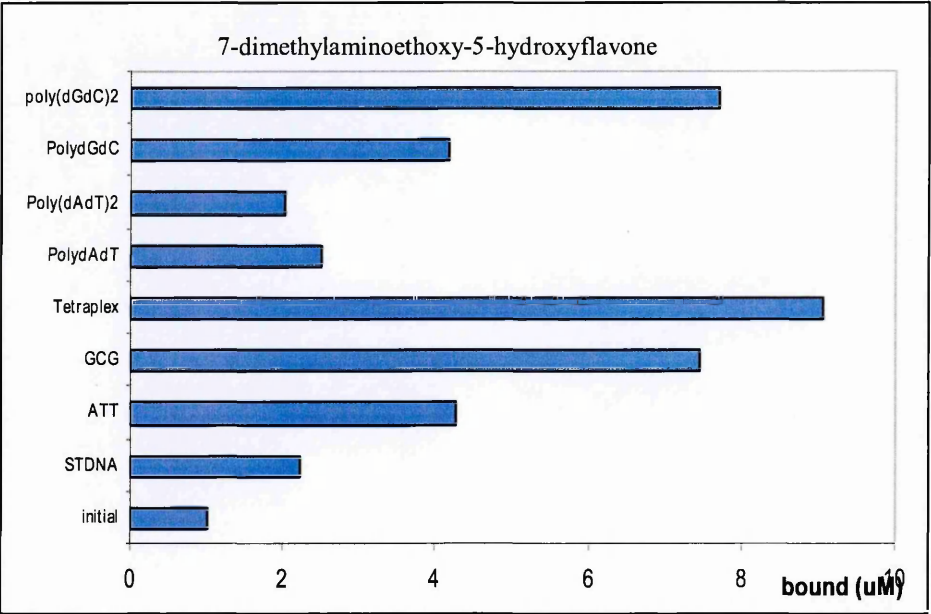


Figure 31 m: 7-Dimethylaminoethoxy-5-hydroxyflavone shows preference for G-quadruplex, poly[dGdC]₂ and purine triplex

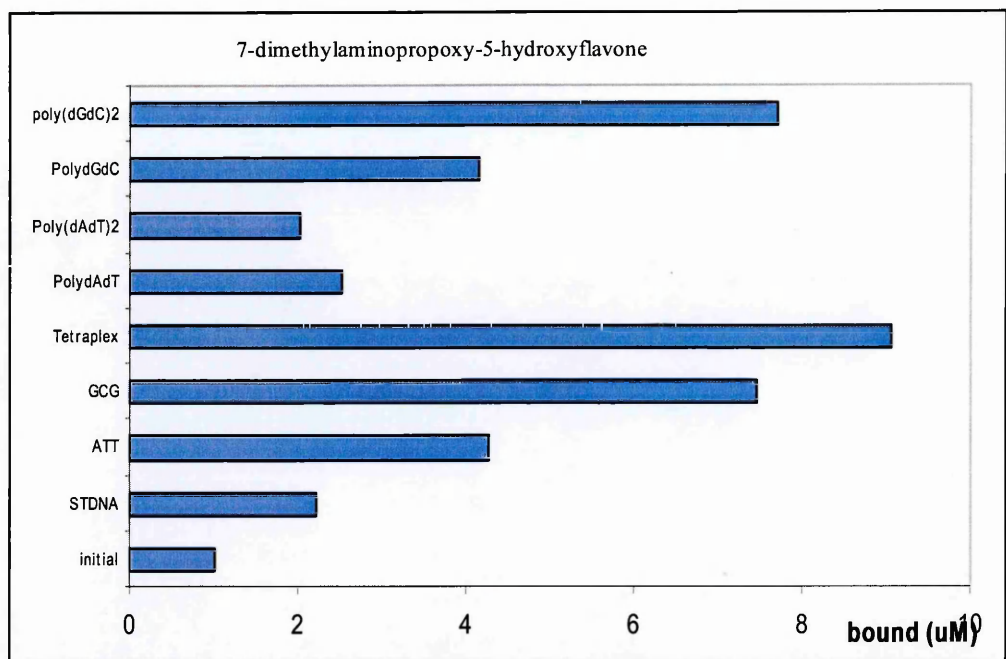


Figure 31 n: 7-Dimethylaminopropoxy-5-hydroxyflavone shows preference for G-quadruplex, poly[dGdC]₂ and purine triplex

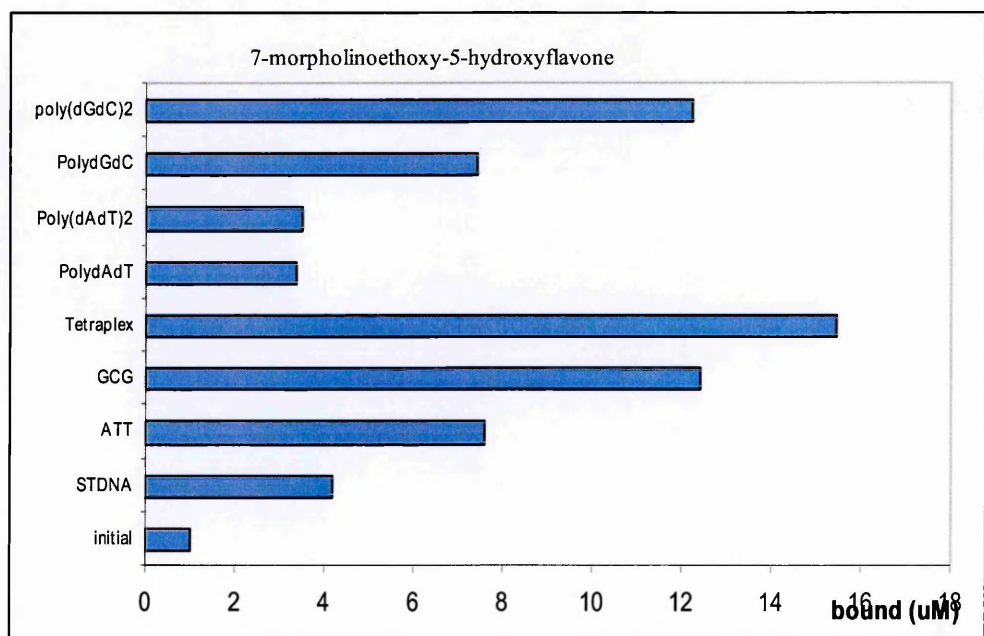


Figure 31 o: 7-Morpholinoethoxy-5-hydroxyflavone shows preference for G-quadruplex, poly[dGdC]₂ and purine triplex.

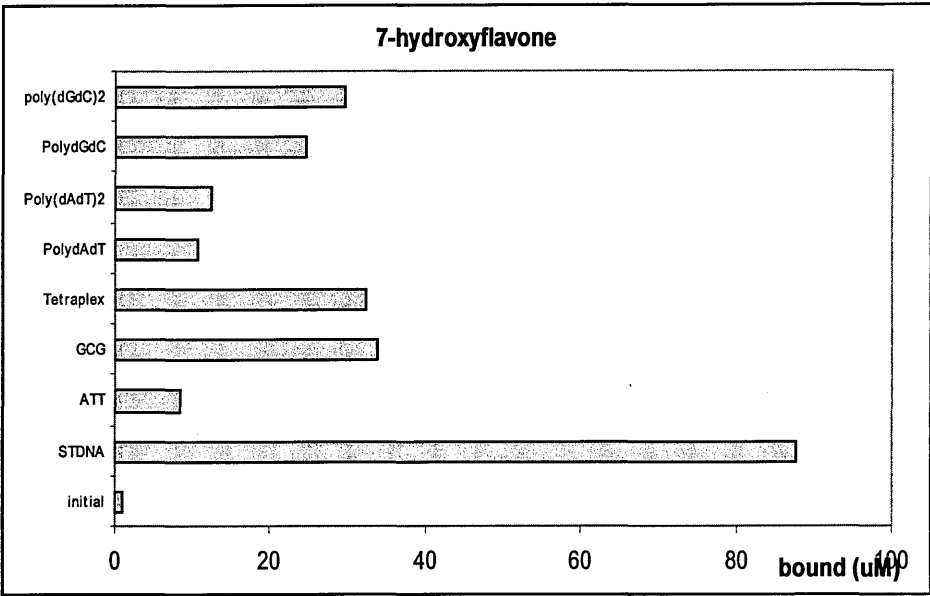


Figure 31 p: 7-Hydroxyflavone shows preference for STDNA.

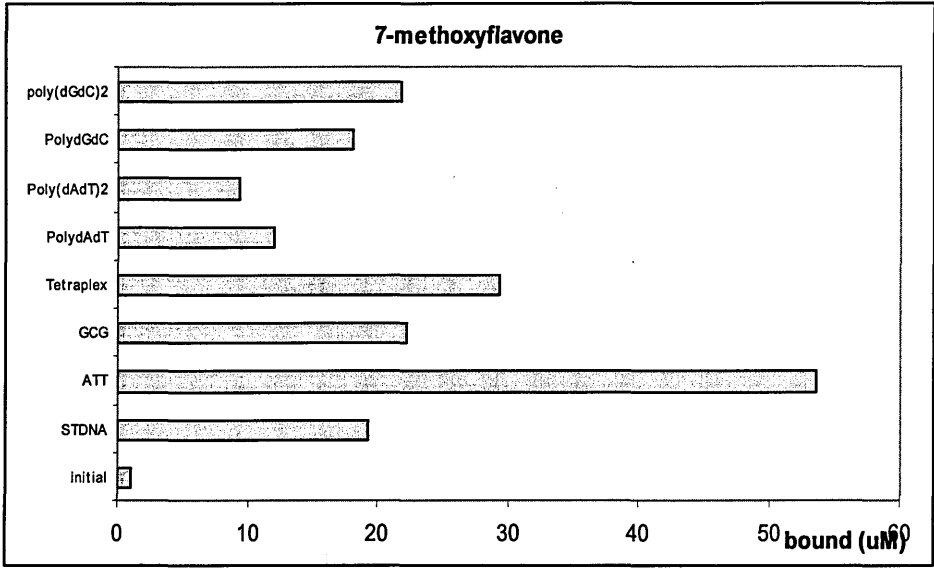


Figure 31 q: 7-Methoxyflavone shows preference for polydAdTdT.

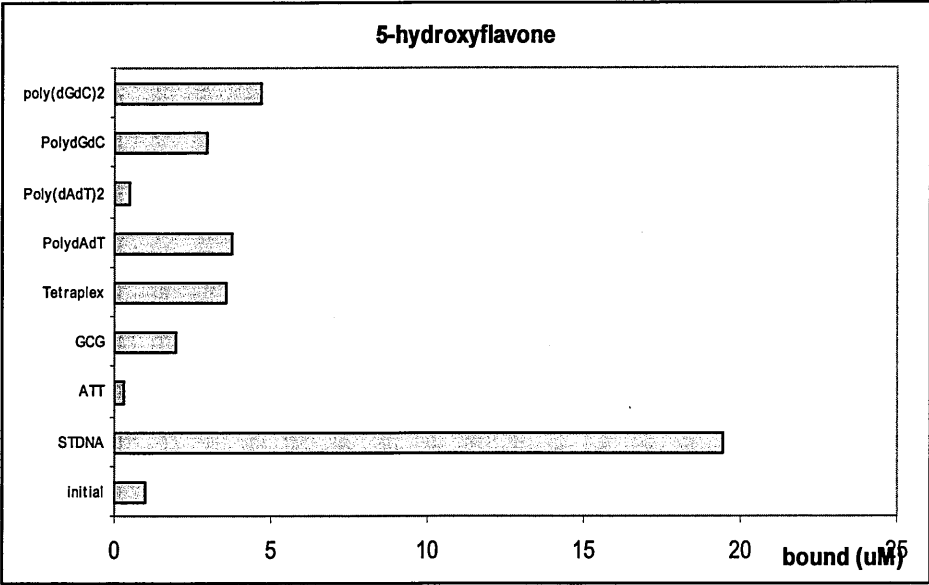


Figure 31 r: 5-Hydroxyflavone shows preference for STDNA.

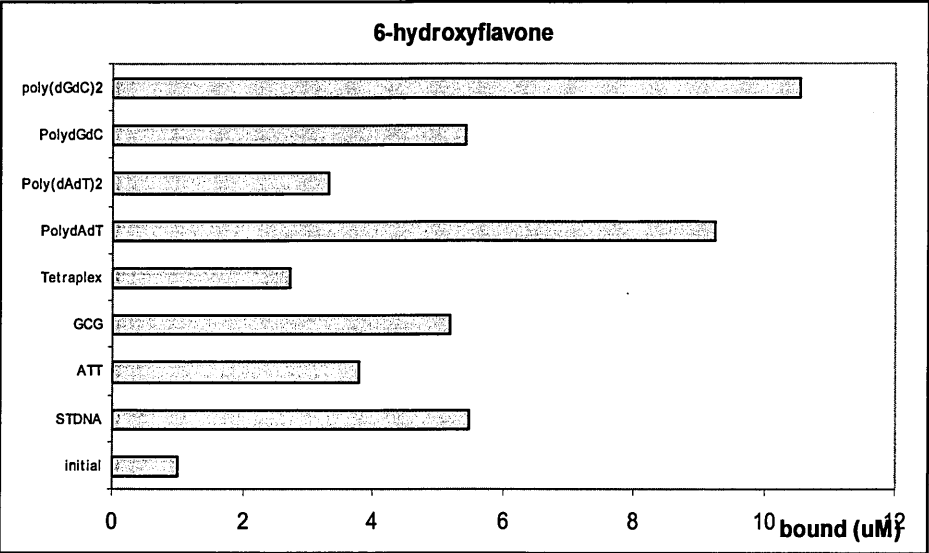


Figure 31 s: 6-Hydroxyflavone shows preference for poly[dGdC]₂ and polydAdT.

4.5: Stabilisation of the double helix

4.5.a: Melting points

Alongside binding association constants binding preference and metal contributions to the binding, we studied the effect of the modified set of compounds on the stabilization of STDNA. 6-Hydroxyflavone, luteolin and azaflavone showed extremely low binding constants, but these 3 compounds stabilised the DNA by an average of 2 – 3 °C, demonstrating that association binding does not correlate with DNA stabilisation. 5-Hydroxy-7-methoxyflavone, 5,7-dimethoxyflavone, 5-hydroxy-8-nitroflavone, 7-dimethylaminopropoxy-5-hydroxyflavone, 3'4'-dichloroflavone and flavothione destabilise the duplex helix of STDNA. 7-Dimethylaminoethoxy-5-hydroxyflavone, 7-morpholinoethoxy and 3'5'-dinitroflavone produced some effect in the STDNA that affected its melting profile, resulting in an inability to accurately calculate melting points, see Figure 32.

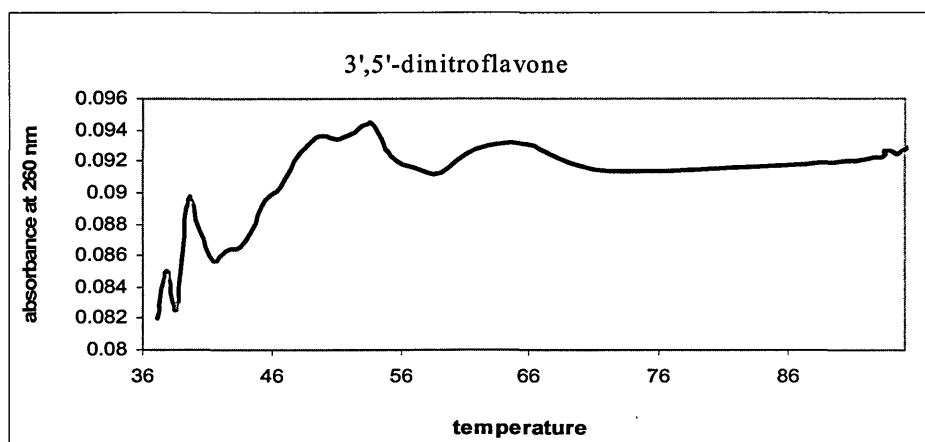


Figure 32: The result of the melting point of 3',5'-dinitroflavone on STDNA showed the drug to destabilise the double helix in a way not possible to measure or produce colloids in the test solution.

The results from the temperature denaturation studies are shown in Table 17 and indicate that the compounds do not have a clear effect on the double helix.

Table 17: The results of the melting points for these compounds show luteolin and aza-3-flavone have a small stabilisation effect on the double helix while the rest of the compounds do not affect it. 7-Dimethylaminoethoxy-5-hydroxyflavone, 7-morpholinoethoxy-5-hydroxyflavone and 3',5'-dinitroflavone produced some effect in the STDNA that made the assay impossible to perform.

Compound	ΔT (°C)
5-hydroxyflavone	0
6-hydroxyflavone	2.5
7-hydroxyflavone	0
7-methoxyflavone	0
5-hydroxy-7-methoxychrysin	-3
5,7-dimethoxychrysin	-1
5,7-diacetoxychrysin	-1.9
5-hydroxy-8nitroflavone	-1.5
luteolin	3.4
7-dimethylaminoethoxy-5-hydroxyflavone	No defined interaction
7-dimethylaminopropoxy-5-hydroxyflavone	-1.5
7-morpholinoethoxy-5-hydroxyflavone	No defined interaction
3',5'-dinitroflavone	No defined interaction
3',4'-dihydroxyflavone	0.4
3',4'-dichloroflavone	-1.5
flavothione	-0.6
azaflavanone	3.4

4.6: Biological evaluation

4.6.a: Cell viability results

To evaluate the anticancer activity of these compounds we tested the most relevant ones against the two cell lines studied in chapter 3, MCF7 breast cancer cell line and CCRFCM leukemia cell line. We compared the results obtained here with flavone in order to see if we could get some improvement based in our rational drug design studies. We studied the inhibition of growth by 50 % of the population of cells at 24, 48 and 72 hours of incubation of the cells with the test drugs at 0, 1, 5, 10, 50, 100, 500 and 1000 μM . Unfortunately none of the compounds proved to be an effective anticancer drug with the majority of them having a $\text{IG}_{50} > 100 \mu\text{M}$. Only 7-dimethylaminoethoxy-5-hydroxyflavone and 7-dimethylaminopropoxy-5-hydroxyflavone presented IG_{50} in the order of 65 – 85 μM . It is worth noting that nitro substitutions promote growth in these two cell lines, possibly by forming some metabolites that assist cell growth. This effect does not appear to be related to estrogenic activity, previously seen by daidzein (see Chapter 3), as the molecules have a similar effect on both cell lines tested. In Table 18 the results are shown.

Table 18: The results of the MTS proliferation assay showed the compounds are not cytotoxic in both cancer cell lines. 7-Dimethylaminoethoxy-5-hydroxyflavone proved to have some activity in CCRFECM cell line at 72 h of incubation and 7-dimethylaminopropoxy-5-hydroxyflavone showed some antiproliferation activity on both cell lines after 72 h of exposure. 5-Hydroxy-8-nitroflavone, 3',5'-dinitroflavone and flavone promote growth.

	IG ₅₀ MCF7 (μM) at 72 hours	IG ₅₀ CCRFCEM (μM) at 72 hours
5-hydroxy-8-nitroflavone	Promotes growth	> 100
luteolin	> 100	> 100
7-dimethylaminoethoxy-5-hydroxyflavone	> 100	69.9
7-dimethylaminopropoxy-5-hydroxyflavone	88.6	65.9
7-morpholinoethoxy-5-hydroxyflavone	> 100	> 100
3',5'-dinitroflavone	Promotes growth	Promotes growth
3',4'-dihydroxyflavone	> 100	> 100
3',4'-dichloroflavone	> 100	> 100
flavothione	> 100	> 100
azaflavanone	> 100	> 100
flavone	Promotes growth	> 100

4.7: Conclusions to Chapter 4

Several protocols can be employed with the purpose of synthesizing flavonoids, unfortunately majority of them work given rise to very small yields or do not work at all, and this is even worse when some hydroxyl groups are present in the flavone scaffold. The employment of potassium *tert*-butoxide as catalyst did help for getting better yields in the synthesis of the study compounds. Other synthetic routes like Mitsunobu reactions, methoxylation and acetoxylation were employed with successful results. Drug design can be employed to understand analogues of drugs which best utilise a particular feature of the DNA structure to maximise the interactions. The rational design has indicated the overall order of DNA affinity, suggesting that the intercalation model has relevance for the mode of action and tertiary amines are the most appropriate groups, by giving binding constants in the order of 10^6 M^{-1} . The length of the carbon chain in the substituted chrysin for obtaining the amine derivatives plays a major role when binding to DNA, demonstrating that this particular position (7) binds directly to the DNA bases and with a particular length; it resulted to be more important having a length of 2 carbons instead of 3 carbons, rather a morpholino group replacing a dimethylamine group. The relevance in the introduction of hydroxyl groups into the flavone skeleton could not be analysed by denaturation melting studies, as almost all flavonoids did not show any stabilisation of the double helix. Introduction of chloride and nitro groups did not improve the binding or stability in the duplex helix of STDNA. The competition dialysis experiments showed a remarkable preference for high order structures of DNA (like G-quadruplexes and triplexes) in majority of the cases as it was already found for the group of compounds in chapter 3. Metal cations

did assist on improving the binding of the drugs to DNA when the compounds have hydroxyls in position 7. The results for the cell viability assay showed the anticancer activity could not be improved even though the binding has been improved by 100 folds. Other factors such as metabolism, cellular uptake, drug persistency, cytotoxicity, and other possible reactions with cellular components could be responsible of the apparent lack of anticancer activity on the cell lines tested.

Chapter 5: Conclusions and further work

Cancer chemotherapeutic drugs may be classified according to their mechanism of action into several classes: hormones, immunological agents, radiosensitisers, antimetabolites, mitotic agents and those that interact with nucleic acid. The choice of a feasible target has been made considering a big diversity of treatments for antitumour cells and nucleic acids showed to be a workable target for antitumour activity. DNA interactive agents can bind to the nucleic acids in different ways. We have studied the mode of action of a group of compounds on nucleic acids and their biological anticancer activity and we have used different approaches to improve both their binding to the nucleic acids and their antitumour activity.

For that purpose we have chosen two families of herbal extracts (sesquiterpenes and flavonoids) and studied their binding to different isoforms of DNA in order to assess any sequence or structural preference and strength of binding.

Our group of sesquiterpenes was composed of artesunate, artemisinin and cantharidin; unfortunately these compounds did not have any UV-Vis spectrum or fluorescence; therefore we were limited to a small set of techniques we could employ to test any DNA-drug activity. Amongst these methodologies we used denaturing points, footprinting, DNA damage, topoisomerase I & II, and hemin as an indicator of any activity between artesunate and artemisinin on STDNA. Unfortunately none of these compounds appeared to interact with STDNA in any way. Artesunate and artemisinin, however, showed to have some inhibition of topoisomerase II activity, maybe by acting on the enzyme topoisomerase rather than the nucleic acid.

From our preliminary set of compounds, the flavonoids baicalein, baicalin, daidzein, puerarin, quercetin and rutin demonstrated preference for higher order DNA structures like G-quadruplex, and purine and pyrimidine triplexes; with baicalein and quercetin giving binding association constant values in the order of $2-8 \times 10^4 \text{M}^{-1}$. In the cell work, the compounds baicalein, baicalin, daidzein and quercetin proved not to be active anticancer agents by giving very high values of GI_{50} for the two cell lines employed (MCF7 breast cancer and CCRFCM leukaemia cell lines). Baicalin showed very low binding constants for the nucleic acids, but had the slowest GI_{50} values on both cell lines, possibly by acting as an anticancer agent in these two cell lines through binding to some other target or by being metabolised to a more active intermediate. In the metabolite CYP1A1 assay only baicalein and daidzein gave results that would allow speculation of hydroxylation and methylation patterns. Baicalin and quercetin proved to be unstable during the assay or to produce results that we could not interpret in our assay.

From this screening of activities we could conclude that the flavonoids are DNA intercalator agents and the flavone skeleton is a useful scaffold to explore binding sites on the DNA.

The synthesis of flavones is not an easy task as it is shown in the literature or in the design of a mechanism of reaction. Different approaches were considered and the use of a strong base as potassium tert-butoxide helped to drive the reaction to completion. In the case of the substitutions with tertiary amines, the employment of Mitsunobu reactions helped to produce some novel compounds as 7-dimethylaminopropoxy-5-hydroflavone and 7-morpholinoethoxy-5-hydroflavone and the known 7-dimethylaminoethoxy-5-hydroflavone.

In this second generation of compounds, the majority of the compounds kept the preference for higher order of DNA structures like G-quadruplexes, purine triplex and the duplex poly[dGdC]₂. Unfortunately the anticancer activity in the cell lines used (MCF7 and CCRFCM cell lines) did not appear to improve. We can speculate that this class of compounds is metabolised inside the cell and are thus not able to bind to DNA inside the nucleus and effect their anticancer activity. Furthermore, molecules they also possibly bind to protein or receptor targets inside the cell.

The binding association constants provided invaluable information about the mode of binding of the flavonoids to the STDNA, which can be summarised as follow:

- the binding is improved when the B ring is located in the C3 position
- insertion of nitrogen into the skeleton did not improve the binding, but insertion of sulphur improved the binding 6-fold
- substitutions of nitro and chloride moieties did not improve the binding, but substitutions of nitro plus hydroxyl groups in the same molecule improved the binding
- methoxylation and acetoxylation reduced the original binding association constants
- tertiary amines helped to improve the binding association constants, when associated in a two carbon chain like is the case of 7-morpholinoethoxy-5-hydroflavone and 7-dimethylaminoethoxy-5-hydroflavone where the binding was improved 100-fold, but in the case of 7-dimethylaminopropoxy-5-hydroxyflavone where the carbon chain is 3 carbon atoms, the binding was reduced 10-fold

- position 7 in the A ring is the most important for interacting with STDNA; and when position 5 is added the binding is improved 4 folds, even though the binding of position 5 alone is non-existent
- substitution in B ring did not prove to be too effective
- metal cations did improve the binding when added to 5,7-dihydroxyflavone (chrysin) and to 7-hydroxyflavone; which agrees with the speculation of position 7 as extremely relevant in the binding.

More studies are needed in order to get a better understanding of the interaction between flavones and DNA and to improve this binding, some possibilities to explore are:

- substitutions with amino groups
- substitutions with piperazine groups
- substitutions with fluoride
- running the same panel of compounds but with a flavothione scaffold
- running similar panel of compounds but with a xanthone scaffold
- exploring substitutions in the B ring employing Mitsunobu reactions
- formation of dimers in different positions (like in 7, 3 and 3')
- test of the drugs in other cell lines

All the information provided by this project and all the information that would be provided by the suggested items, could assist in the design of novel agents with improved bioavailability and anticancer activity.

REFERENCES

- Adams P, Berman P, Egan T, Marsh P, Silver J: "The iron environment in heme and heme-antimalarial complexes of pharmacological interest", *J. Inorganic Biochemistry*, **63**, 69-77; 1996
- Aerssens J, Armstrong M, Gilissen R, Cohen, N: "The Human Genome: an introduction" *The Oncologist* **6**: 100-109; 2001
- Albert A, Serjeant E: "The determination of ionization constants", Chapter 3, 3rd edition, 1984
- Alberts B, Bray D, Lewis J, Raff M, Roberts K, Watson, J: "The molecular biology of the cell", 3rd edition, Garland Publishing Inc, NY, 1992
- Anastossopoulou J: "Metal – DNA interactions", *J. of Molecular Structure*, **653**, 19-26; 2003.
- Ares J, Outt P, Kakodkar S, Buss R, Geiger J: "A convenient large scale synthesis of 5-methoxyflavone and its application to analog preparation", *J. Organic Chemistry*, **58**, 7903-7905, 1993
- Ares J, Outt P, Randall J, Murray P, Weisshaar P: "Synthesis and biological evaluation of substituted flavones as gastroprotective agents", *J. Medicinal Chemistry*, **38**, 4937-4943; 1995
- Armstrong N, Ernst E.: "The treatment of eczema with Chinese herbs: a systematic review of randomized clinical trials". *British J. Clinical Pharmacology*; **48**, 262-264; 1999.
- Arrowsmith J, Missailidis S, Stevens M: "Antitumour imidazotetrazines. Part 37. Conjugation of the DNA major-groove alkylating imidazotetrazine mitozolomide to peptide motifs recognising the minor groove", *Anticancer Drug Design*, **14**, 205-end page; 1999
- Asadi M, Safaei E, Ranjbar B: "A study on the binding of two water – soluble tetrapyridinoporphyrinato copper (II) complexes to DNA", *J. of Molecular Structure*, **754**, 116-123; 2005
- Ashby J: "Fundamental structural alerts to potential carcinogenicity and noncarcinogenicity", *Environmental Mutagenesis*, **7**, 919-921; 1985
- Aksnes D, Standnes A, Andersen O: "Complete Assignment of the 1H and 13C NMR Spectra of Flavone and its A-Ring Hydroxyl Derivatives", *Magnetic Resonance Chemistry*, **34**, 820-823; 1996
- Avila M, Velasco J, Cansado J, Notario V: "Quercetin mediates the down regulation of mutant p53 in the human breast cancer cell line MDA MB 468", *Cancer Research*, **54**, 2424-2428; 1994
- Baguley B; Denny W: "Potential antitumour agents 34. Quantitative relationships between DNA binding and molecular structure for 9-anilinoacridines substituted in the aniline ring" *J. Medicinal Chemistry*, **24**, 170-177; 1981

- Batty K., Davis T., Thu L., Binh T., Anh T., Ilett K.: "Selective HPLC determination of artesunate and α - and β - dihydroartemisinin in patients with *falciparum malaria*", *J. of Chromatography B*, **677**, 345-350; 1996
- Becker S: "Treatment by Chinese medicine: semen anomalies". *J. Chinese Medicine*, **62**, 46-51; 2000
- Beekman A, Barentsen A, Woerdenbag H: "Stereochemistry-dependent cytotoxicity of some artemisinin derivatives", *J. Natural Products*, **60**, 325-330; 1997.
- Belousov Y, Welch R, Sanders S, Mills A, Kulchenko A, Dempcy R, Afonina I, Walburger D, Glaser C, Yadavalli S, Vermeulen N, Mahoney W: "Single nucleotide polymorphism genotyping by two colour melting curve analysis using the MGB Eclipse Probe System in challenging sequence environment", *Human Genomics*, **1**, 209-17; 2004
- Bernstein C, Bernstein H: "DNA repair with emphasis on single-strand damages", *Aging, Sex and DNA Repair*, 173-207; 1991
- Bertram, J: "The molecular biology of cancer", *Molecular Aspects of Medicine*, **21**, 167-223; 2001
- Binsack R, Boersma B, Patel R, Kirk C: "Enhanced antioxidant activity after chlorination of quercetin by HCl;", *Alcoholism Clinical Experimental Research*, **25**, 434-443; 2001
- Blackburn, E: "Telomere states and cell fates", *Nature*, **408**, 53-56; 2000
- Blankenship J, Balambika R, Dawson P: "Probing backbone hydrogen bonds in the hydrophobic core of GCN4", *Biochemistry*, **41**, 15676-15684, 2002
- Boerner L, Zaleski J: "Metal complex – DNA interactions: from transcription inhibition to photoactivated cleavage", *Current Opinion in Chemical Biology*, **9**, 135-144; 2005
- Boveri, T: "Zur Frage der Entstehung Maligner Tumoren" (The Origin of Malignant Tumours) Jena: Gustav Fisher, 1914
- Briggs M, Duncan G, Thornber C: "The preparation of flavones and their derivatives. Part I. Flavone and 4-thioflavone" *J. of Chemical Research Miniprint*, **9**, 2461-2487, 1982
- Brown A, Stanley T: "Mechanism of quercetin oxygenation a possible model for haem degradation", *Tetrahedron Letters*, **22**, 4331-4334; 1981
- Campanale N, Nickel C, Daubenberger C, Wehlan D: "Identification and characterization of heme-interacting proteins in the malaria parasite, *Plasmodium falciparum*", *J. Biological. Chemistry*, **278** (30), 27354-27361; 2003
- Chan F, Choi H, Chen Z: "Induction of apoptosis in prostate cancer cell lines by a flavonoid, baicalin" *Cancer Letters*, **160**, 219-228; 2000
- Chan H., Chen Z., Tsang D., Leung L: "Baicalein inhibits DMBA-DNA adduct formation by modulating CYP1A1 and CVYP1B1 activities", *Biomed. Pharm.*, **56**, 269-275; 2002

- Charron J, Breton G, Danyluk J, Muzac I, Ibrahim R, Sarhan F. :“Molecular and biochemical characterization of a cold-regulated phosphoethanolamine N-methyltransferase from wheat”. *Plant Physiology*, **129**, 363-73, 2002
- Chen Y, Zhu S, Chen H, Li Y: “Artesunate interaction with hemin”, *Bioelectrochemistry and Bioenergetics*, **44**, 295-300; 1998
- Chen, A; Kuo, W: “ Photochemical synthesis of 2,2’biflavones from flavone”, *J. of Chinese Chemical Society*, **50**, 123-127; 2003
- Cheng A: “Oligodeoxyribonucleotide length and sequence effect on intramolecular and intermolecular G quartet formation”, *Gene* **197**, 253-260; 1997
- Chu K: “The quantitative analysis of structure-activity relationships” *The Basis of Medicinal Chemistry/Burger’s Medicinal Chemistry*, 393-418, John Willey, 1980
- Cipak L, Rauko P:” Effects of flavonoids on cisplatin induced apoptosis of HL60 and L1210 leukemia cells”, *Leukemia Research*, **27**, 65-72; 2003
- Collins E, Berkoff N: “Everything you need to know about echinacea and immunity” *Roseville, CA, Prima Publishing*, 85-86; 1999
- Connors K: “Binding constants: the measurement of molecular complex stability”, Chapter 2, *John Wiley & Sons, USA*, 1987
- Cook N, Samman S: “Flavonoids – Chemistry, metabolism, cardioprotective effects and dietary sources”, *The J. of Nutritional Biochemistry*, **7**, 66-76; 1996
- Craig G, Nexman D: “Discovery and development of antineoplastic agents from natural sources”, *Cancer Investig.*, **17**, 153-63; 1999
- Creste, Tulmann, Figueira: “Detection of Single Sequence Repeat Polymorphisms in Denaturing Polyacrylamide Sequencing Gels by Silver Staining”, *Plant Molecular Biology Reports*, **19**, 299–306; 2001
- Cushman M, Zhu H, Geahlen R: “Synthesis and biochemical evaluation of a series of aminoflavones as potential inhibitors of protein tyrosine kinases p56, EGFR and p60”, *J. Medicinal Chemistry*, **37**, 3353-3362; 1994
- Czyz M, Szulawaska A, Bednarek A: “Effects of anthracycline derivatives on human leukemia K562 cell growth and differentiation”, *Biochemical Pharmacology*, **70**, 1431-1442, 2005
- Desmaze, C, Soria, J: “Telomere – driven genomic instability in cancer cells”, *Cancer Letters*, **194**, 173-182; 2003
- Dewick, P: “Medicinal Natural Products – Biosynthetic Approach”, 2nd edition, 149-151; 2001
- Dixon R, Steele C: “Flavonoids and isoflavonoids – a gold mine for metabolic engineering”, *Trends in Plant Science*, **4**, 394-400, 1999
- Dua V, Roy R, Joshi B, Valecha N: “Anti-malarial activity of some xanthenes isolated from the roots of *Andrographis paniculata* “, *J of Ethnopharmacology*, **95**, 247-251, 2004

- Efferth T, Dunstan H, Sauberbrey A, Miyachi H, Chitambar C: "The antimalarial artesunate is also active against cancer", *International J. Oncology*, **18**, 767-773; 2001
- Efferth T, Marshall M, Wang X, Huong S, Hauber I, Olbrich A, Kronschnabl M, Stamminger T, Huang E: "Antiviral activity of artesunate towards wild type, recombinant and ganciclovir resistant human cytomegaloviruses", *J. Molecular Medicine*; **80**, 233-242; 2002
- Efferth T, Rucker G, Falkenberg M, Manns D, Olbrich A, Fabry U, Osieka R: "Detection of apoptosis in KG-1a leukemic cells treated with investigational drugs", *Arzneim Forsch DrugRes*, **46**, 196-200; 1996
- Engin H, Celik I. "Treatment of classical Kaposi's sarcoma with visceral involvement by weekly paclitaxel", *Clinical Oncology* , **14**, 178-185; 2002
- Esteves-Souza A, Pissinate K, Nascimiento M, Echevarria A: "Synthesis, cytotoxicity , and DNA-topoisomerase inhibitors activity of new asymmetric ureas and thioures", *Bioorganic & Medicinal Chemistry*, **14**, 492-499; 2006
- Evgeny N, Kaido P: "Molecular pathogenesis of bilateral breast cancer", *Cancer Letters*, **191**, 1-7; 2003
- Ferriola P, Cody V: "Protein kinase C inhibition by plant flavonoids, kinetic mechanisms and structure-activity relationships" *Biochemical Pharmacology*; 1989
- Fox K: "Drug – DNA interaction protocols" *Methods in Molecular Bioogy*", Humana Press, 1997, chapter 14: "Optical absorbance and fluorescence techniques for measuring DNA – Drug interactions" by T. Jenkins).
- Gao Y, Wang A: "Crystal Structure of Four Morpholino-doxorubicin Anticancer Drugs Complexed with d(CGTACG) and d(CGATCG): Implications in Drug-DNA Crosslink." *J. Biomolecular Structural Dynamics* **13**, 103-117, 1995
- Gawron A: "Effect of quercetin on the growth of mouse fibroblast cells in vitro", *Polish J. Pharmacology*, **6**, 531-535; 1995
- Gerhauser K, Klimo C: "Mechanism based in vitro screening of potential cancer chemo preventive agents", *Mutation Research*, **523**, 163-172; 2003
- Grandori R, Schwarzingen S, Müller N: "Cloning, overexpression and characterization of micro-myoglobin, a minimal heme-binding fragment", *European J. Biochemistry* **267**, 1168-1172, 2000
- Green M, Mount D, Wirtz R, White N: "A colorimetric field method to assess the authenticity of drug sold as the antimalarial artesunate", *J. Pharmacology Biomolecular. Analysis*, **24**, 65-70; 2000
- Guerra M, Speroni E, Broccoli M, Cangini M, Pasini P: "Comparison between chinese medical herb pueraria lobata crude extract and its main isoflavone puerarin. Antioxidant properties and effects on rat liver CYP-catalysed drug metabolism", *Life Science*, **67**, 2297-3006; 2000

- Guo Q, Rimbach G, Moini H: "ESR and cell culture studies on free radical scavenging and antioxidant activities of isoflavonoids", *Toxicology*, **179**, 171-180; 2002
- Hafez T, El-Khoshniesh Y, Mahran M: "Organophosphorus chemistry. The behaviour of certain pyrone derivatives toward 2,4-bis-(4methoxyphenyl)-1,2,3,4-dithiophosphetan-2,4-disulphide (Lawesson reagent)", *Phosphorus, Sulfur and Silicon*, **56**, 165-171; 1991
- Hahn, W; Counter, C; Lundberg, A; Beijersbergen, R; Brooks, M; Weinberg, R; "Creation of human tumour cells with defined genetic elements" *Nature*, **400**: 464-468; 1999
- Hahnfeldt, P; Panigrahy, D: "Tumour development under angiogenic signalling: a dynamical theory of tumour growth, treatment response, and postvascular dormancy" *Cancer Research*, **59**, 4770-4775; 1999
- Hanahan, D; Weinberg, R: "The hallmarks of cancer", *Cell*, **100**, 57-70; 2000
- Hansen R, Oesterrich S, Lemieux P, Sarge K, Fuqua S: "Quercetin inhibits heat shock protein induction but not heat shock factor DNA-binding in human breast carcinoma cells", *Biochemical Biophysical Research. Communication*, **239**, 851-856; 1997
- Hiipaka R, Zhang H, Dai W, Dai Q, Liao S: "Structure-activity relationships for inhibition of human 5 α -reductases by polyphenols", *Biochemical Pharmacology*, **63**, 1165-1176, 2002
- Ho C., Chen Q., Shi H.: "Antioxidative effect of polyphenol extract prepared from various Chinese teas", *Prevention Medicine*, **21**, 520-525; 1992
- <http://www.books.md/M/dic/mitosis.php>
- <http://www.looneyware.com/pchem/files/terpenoids.php>
- Hurley L: "DNA and its associated processes as targets for cancer therapy", *Nature Reviews Cancer* **2**, 188-200; 2000
- Hutchins R, Crenshaw J, Graves D, Denny W: "Influence of substituent modifications on DNA binding energetics of acridine-based anticancer agents", *Biochemistry*, **42**, 13754-13761; 2003
- Hyuncheol O, Do-Hoon K, Jung-Hee C: "Hepatoprotective and free radical scavenging activities of phenolic petrosins and flavonoids isolated from *Equisetum arvense*", *J. of Ethnopharmacology*, **95**, 421-424; 2004
- Ibrahim A, Takamatsu S, Galal A, Ross S, Ferreira D, ElSohly M, El-Ferally S: "Antioxidant effect of flavonoids", *Phytotherapy Research*, **17**, 963-966, 2002
- Jain, K; Makrandi, J: "A facile Baker-Venkataram synthesis of flavones using phase transfer catalysis", *Synthesis*, **3**, 221-223; 1982
- Janbaz A, Saeed S: "Protective effect of rutin on paracetamol and CCl₄ induce hepatotoxicity in rodents", *Fitoterapia*, **73**, 557-563; 2002

- Jaroszeski M, Heller R: "Flow Cytometry Protocols", *Methods in Molecular Biology B*, **91**, 288-295, 1997
- Jenkins, T: "Targeting multi stranded DNA structures", *Current Medicinal Chemistry*, **7**, 99-115; 2000
- Jiang D, Hu G, Jiang J, Xiang H: "Relationship between protective effect of xanthone on endothelial cells and endogenous nitric oxide synthase inhibitors", *Bioorganic & Medicinal Chemistry*, **11**, 5171-5177; 2003
- Kamenetskii L: "Triplex DNA structures" *Annu. Rev. Biochem.*, **64**, 65-95; 1995
- Kataoka T, Watanabe S, Mori E, Kadamoto R: "Synthesis and structure activity relationships of thioflavone derivatives as specific inhibitors of the ERK_MAP kinase signaling pathway", *Bioorganic & Medicinal Chemistry*, **12**, 2397-2407; 2004
- Kemp D, Vellacio F: "Structure of anhydridoacetylsalicylamide", *Journal Organic Chemistry*, **46**, 1804-1807; 1981
- Kimchi-Sarfaty C, Gripar J, Gottesman M: "Functional characterization of coding polymorphisms in the human MDR1 gene using a vaccinia virus expression system". *Mol. Pharmacology*, **62**, 1-6; 2002
- Kimura Y, Kubo M, Tani T, Arichi S, Ohminami H, Okuda H: "Studies on *scutellariae radix* III. Effects on lipid metabolism in serum, liver and fat cells of rats", *Chemical Pharmaceutical Bulletin*, **29**, 2308-2312; 1981
- Knudson, A: "Two genetic hits (more or less) to cancer" *Nature Reviews Cancer* **1**, 157-162; 2001
- Kopach, Klechek: "Luminescent characteristics of some flavonoids", *Zh. Org. Khim.*, **16**, 1721-1724; 1980
- Kosmas C, Tsavaris N, Kalofonos H. "Salvage chemotherapy with the gemcitabine/docetaxel combination in non-small cell lung cancer: an overview of recent phase II studies". *Medicinal Science Monitoring* , **8**, 58-63; 2002
- Krontiris, T: "Oncogenes: Molecular Medicine" *New England J. of Medicine*, **333**, 303-306; 1995
- Kudo T, Naito K, Yokoyama H: "Effects of quercetin and sunphenon on responses of cancer cells to heat shock damage", *Experimental Molecular Pathology*, **66**, 66-75; 1999
- La Casa C, Villegas I, "Evidence for protective and antioxidant properties of rutin, a natural flavone, against ethanol induced gastric lesions", *J. Ethnopharmacology*, **71**, 45-53; 2000
- La E, Kern J, Atarod E, Kehrer J: "Fatty acid release and oxidation are factors in lipoxigenase inhibitor induce apoptosis", *Toxicology Letters*, **138**, 193-203; 2003
- Lambert L, Perri H, Halbrooks P, Mason A: "Evolution of the transferring family: conservation of residues associated with iron and anion binding", *Comparative*

Biochemistry and Physiology Part B: Biochemistry and Molecular Biology, **142**, 129-141; 2005

- Latunde -Dada G, Klinder T, Becker A, Hermann T, Voigt U: "Iron overload induces oxidative DNA damage in the human colon carcinoma cell line HT29 clone 129A" *Mutation Research.*, **519**, 151-161; 2002
- Laughton C, Luisi B: "The mechanics of minor groove width variation in DNA, and its implications for the accommodation of ligand", *J. Molecular Biology*, **288**, 953-63; 1999
- Lee C, Hong H, Shin J, Jung M, Shin I, Yoon J, Lee W: "NMR studies on novel antitumour drug candidates, deoxoartemisinin and carboxypropyl deoxoartemisinin", *Biochemical Biophysical Research Communication*, **274**, 359-369; 2000
- Lee MS, Yang KH, Huh HJ: "Qi therapy as an intervention to reduce chronic pain and to enhance mood in elderly subjects: a pilot study". *J. Chinese Medicine* , **29**, 237-245; 2001
- Lee, J; Burkholder, G: "Immunofluorescent staining of mammalian nucleic and chromosomes with a monoclonal antibody to triples DNA", *Chromosoma*, **97**, 185-187; 1988
- Lei B, Roncaglia V, Vigano, Cremonini, De Maria, del Buono, Manenti, Villa: " Phytoestrogens and liver disease", *Molecular Cell Endocrinology*, **193**, 81-84; 2002
- Levine, A: "p53, the cellular gatekeeper for growth and division", *Cell*, **88**, 323-331; 1997
- Lin H., Chen Y: "Differential inhibitory mechanisms of flavones on LPS and LTA induced NO and PGE2 productions in RAW264.7 macrophages" *The Sixteenth Joint Annual Conference of Biomedical Sciences*, 285; 2001
- Lin M-Shiau, Lin S: "Induction of apoptosis by apigenin and related flavonoids through cytochrome c release and activation of caspase 9 and caspase 3 in leukaemia HL-60 cells", *European J. Cancer*, **35**, 1517-1525; 1999
- Lin R, Guthrie S, Xie C, Mai K: "Isoflavonoid Compounds Extracted From Pueraria Lobata Suppress Alcohol Preference In A Pharmacogenetic Rat Model of Alcoholism", *Alcoholism: Clinical and Experimental Research*, **20**, 659-663, 1996
- Lingner, J; Hughes, T: "Reverse transcriptase motifs in the catalytic subunit of telomerase", *Science*, **276**, 561-567, 1997
- Lipsett, M: "Complex formation between polycytidilic acid and guanine oligonucleotides", *J. Biological Chemistry*, **239**, 1256-1281; 1964
- Liu: "DNA Topoisomerase as Anticancer drugs", *Annual Review of Biochemistry*, **58**, 351-375; 1989
- Marder M, Zinckezink J, Colombo M: "Synthesis of haslogenated/nitrated flavone derivatives and evaluation of their affinity for the central benzodiazepines receptors" *Bioorganic & Medicinal Chemistry Letter*, **7**, 2003-2008; 1997

- Markham K: "Flavones, flavonols and their glycosides", *Methods in plant biochemistry*. Plant phenolics, NY, Academic Press, 197-235; 1989
- Marks L, DiPaola R: "PC-SPES: herbal formulation for prostate cancer" *Urology*, **54**, 369-375; 2002
- Martens S, Forkmann G: "Genetic control of flavone synthase II activity in flowers of gerbera hybrids", *PII S0031-9422*, 345-348; 1998
- Maser, R; DePinho, R: "Connecitng chromosomes, crisis, and cancer", *Science*, **297**, 565-569; 2002
- Matsumoto K, Akao Y, Yi H, Ohguchi K: "Preferential target is mitochondria in α -mangostin-induced apoptosis in human leukemia HL60 cells", *Bioorganic & Medicinal Chemistry*, **12**, 5799-5806; 2004
- Mauelera W, Bassilia G, Rudiger A: "The (gt)n(ga)m containing intron 2 of *HLA-DRB* alleles binds a zinc-dependent protein and forms non B-DNA structures", *Gene*, **226**, 9-23; 1999
- Mc.Cluskey A: "Anhydride modified cantharidin analogues. Is ring opening important in the inhibition of PP2A?" *European J. Medicinal Chemistry*, **35**, 957-964; 2000
- McCluskey A, Taylor D: "Inhibition of PP2A by cantharidin analogues", *Bioorganic & Medicinal Chemistry Letters*, **6**, 1025-1028; 1996
- McCluskey A, Walkom C, Bowyer M, Ackland, Gardiner, Sakoff: "Cantharimides: a new class of modified cantharidin analogues inhibiting PP1 and 2A" *Bioorganic & Medicinal Chemistry Letters*, **11**, 2491-2496; 2001
- McGhee, von Hippel: "Theoretical aspects of DNA – protein interactions: cooperative and non cooperative binding of large ligands to a one dimensional heterogenous lattice" *J. Molecular Biology*, **86**, 469-489; 1974
- Mergny J, Duval-Valentin G, Nguyen C: "Triple helix specific ligands", *Science* **256**, 1691-1694; 1992
- Meshnick S, Thomas A, Ranz A, Xu C, Pan H: "Artemisinin: the role of intracellular hemin in its mechanism of antimalarial action" *Molecular Biochemical Parasitology*, **49**, 181-196, 1991
- Messori L, Piccioli F, Eitler B, Bergonzi M, Bilia R: "Spectrophotometric and ESI-MS/HPLC studies reveal a common mechanism for the reaction of various artemisinin analogues with hemin", *Bioorganic & Medicinal Chemistry Letters*, **13**, 4055-4057; 2003
- Mischiati C, Feriotto G: "A non radioactive automated footprinting study", *European. J. Pharmacology*, **290**, 85-93; 1995
- Missailidis S, Stanslas J, Modi C, Ellis M, Robins R, Laughton C, Stevens M: "Antitumour polycyclic acridines. Part 12. Physical and biological properties of 8,13-diethyl-6methylquino[4,3,2-kl] acridinium iodide: a lead compound in anticancer drug design", *Oncology Research*, **13**, 175-189; 2002

- Moore J, Lai H, Li J, Ren R, McDougall A, Singh N, Chou C: "Oral administration of dihydroartemisinin and ferrous sulphate retarded implanted fibrosarcoma growth in the rat", *Cancer Lett.*; 83-87; 1995
- Mooren F, Golf S, Lechterman A: "Alterations of ionized Mg (II) in human blood after exercise", *Life Science*, **77**, 1211-1225; 2005
- Motoo Y, Sawabu N: "Antitumour effects of saikosporins, baicalin and baicalein on human hepatoma cell lines", *Cancer Letters*, **86**, 91-95; 1994
- Murnane, J, Sabatier, B, Marder, W: "Telomere dynamics in an immortal human cell line", *EMBO J.*, **13**, 4953-4962; 1994
- Murthi K, Dubay M, McClure C, Brizuela L, Boisclair M, Worland P, Mansuri M, Pal K.: "Structure-activity relationship studies of flavopiridol analogues". *Bioorganic & Medicinal Chemistry Letters*, **10**, 1037-1041; 2000
- Nakahata N, Kyo R, Kutsuwa M., Ohizumi Y:"Inhibition of mitogen activated protein kinase cascade by baicalein, a flavonoid of natural origin", *Nippon Yakuragaku Zasshi*, **1**, 215-219; 1999
- Nestler G.: "Traditional Chinese medicine", *Medicinal Clinical North America*, **86**, 63-73; 2002
- Nose, M: "Inhibition by flavonoids of RNA synthesis in permeable WI-38 cells and of transcription by RNA polymerase II", *Biochemical Pharmacology*, **33**, 3823-3827; 1984
- Núñez M, Maguna F, Okulik N, Castro E: "QSAR modeling of the MAO inhibitory activity of xanthenes derivatives", *Bioorganic & Medicinal Chemistry Letters*, **14**, 5611-5617; 2004
- O'Hagan R, Chang S: "Telomere dysfunction provokes regional amplification and deletion in cancer genomes", *Cancer Cell*, **2**, 149-157; 2002
- Ohtani H, Koyabu N, Juichi Y, Iwase C: "Inhibition of p-glycoprotein by flavonoid derivatives in adriamycin resistant human myelogenous leukaemia (K562/ADM) cells", *Cancer Letters*, **177**, 89-93; 2002
- Olmsted M: "The effect of nucleic acid geometry on counterion association", *J Biomolecular Structural Dynamics*, **13**, 885-902; 1996
- Overstreet D, Lee Y, Rezuani A: "Suppression of Alcohol Intake following Administration of the Chinese Herbal Medicine (NPI-028) and Its Derivatives". *Alcoholism: Clinical and Experimental Research*, **20**, 221-227; 1996
- Owen R, Haubner R, Hull W, Haber B: "Isolation and structural elucidation of the major polyphenoles in carob fibre", *Food & Chemical Toxicology*, **41**, 1727-1738; 2003
- Parker L, Anderson F, O'Hare C: "Synthesis of novel DNA cross-linking antitumour agents based on polyazamacrocycles", *Bioorganic & Medicinal Chemistry*, **13**, 2389-2395; 2005

- Perrem K, Bryan T: "Repression of an alternative mechanism for lengthening of telomeres in somatic cell hybrids", *Oncogene*, **18**, 3383-3390; 1999
- Posner G, Northrop J, Paik I, Borstnik K, Dolan P, Kensler T, Xie S, Shapito T: 'New chemical and biological aspects of artemisinin derived trioxane dimmers", *Bioorganic & Medicinal Chemistry*, **10**, 227-232; 2002
- Qinglei Z, Aixia H, Huirong H: "Puerarin: a scavenger of reactive oxygen species and inhibitor of LDL oxidation, has potential effect to prevent atherosclerosis" <http://www.cmj.org/7qw/zhuqinglei2.htm>
- Rajagopal, P; Feigon, J: "Triple strand formation in the homopurine :homopyrimidine DNA oligonucleotides d(GA)₄ and d(TC)₄ " *Nature*, **339**, 637-640; 1989
- Reddel, R: "Alternative lengthening of telomeres, telomerase and cancer", *Cancer Letters*, **194**, 155-162; 2003
- Reizenstein P: "Iron, free radical and breast cancer" *Medicinal Oncology Tumour Pharmacology*, **8**, 229-233; 1999
- Ren J, Baily C, Chaires J: "NB-506, an inolocarbazole topoisomerase I inhibitor, binds preferentially to triplex DNA", *FEBS Letters*, **470**, 355-359; 2000
- Ren J, Chaires J: "Sequence and structural selectivity of nucleic acid binding ligands", *Biochemistry* **38**, 16067-16075; 1999
- Rice-Evans C., Miller N.: "Structure-Antioxidant activity relationships of flavonoids and phenolic acids", *Free Radical Biology & Medicine*, **20**, 933-956; 1996
- Rodgers E, Grant M: "The effect of flavonoids, quercetin, myricetin and epicatechin on the growth and enzyme activities of MCF7 human breast cancer cells", *Chemical Biological Interactions*, **116**, 213-228; 1998
- Rossi M., Meyer R., Constantinou P., Caruso F., Castelbuono D., O'Brien M., Narasimhan V: "Molecular structure and activity toward DNA, baicalin a flavone constituent of the Asian Herbal Medicine Sho-saiko-to", *J. Natural Products*, **64**, 26-31; 2001
- Sadava D., Philips T, Lin C, Kane S: "Transferrin overcomes drug resistance to artemisinin in human small cell lung carcinoma cells", *Cancer Letters*, **179**, 151-156; 2002
- Sawa T, Nakao M, Akaike T, Ono K, Maeda H: "Alkylperoxyl radical-scavenging activity of various flavonoids and other phenolic compounds: implications for the anti-tumor-promoter effect of vegetables", *J. Agriculture Food Chemistry*, **47**, 397-402; 1999
- Scambia G, Ranelletti F, Benedetti P: "Synergistic antiproliferative activity of quercetin and cisplatin on ovarian cancer cell growth", *Anticancer Drugs*, **1**, 45-48; 1990
- Scheel C, Schaefer K: "Alternative lengthening of telomeres is associated with chromosomal instability in osteosarcomas", *Oncogene*, **20**, 3835-3844; 2001

- Schultes C, Guyen B, Cyuetsa J, needle S: "Synthesis, biophysical and biological evaluation of 3,6-bis-amidoacridines with extended 9 anilino-substituents as potent G-quadruple-binding telomerase inhibitors", *Bioorganic & Medicinal Chemistry Letters*, **14**, 4347-4351; 2004
- Segura-Aguilar J: "Quercetin may act as a cytotoxic prooxidant after its metabolic activation to semiquinone and quinoidal product", *Free Radical Biology Medicine*, **26**, 107-116; 1999
- Sen D, Gilbert W: "Formation of parallel four stranded complexes by guanine rich motifs in DNA and its implication for meiosis", *Nature*, **334**, 364-366; 1988
- Sepp A, Choo Y: "Cell free selection of zinc finger DNA binding protein using in vitro compartmentalization", *J. of Molecular Biology*, **354**, 212-219, 2005
- Serjeant E, Albert A: "The determination of ionization constants", 3rd eddition, Chapman and Hall; 1984
- Shen G, Weber F: "Synergistic action of quercetina and genistein in human ovarian carcinoma cells", *Oncology Research*, **9**, 597-602; 1997
- Shin J, Kim K, Kim M, Jeong J, Bak K: " Synthesis and hypoglacemic effect of chrysin derivatives" *Bioorganic & Medicinal Chemistry Letter*, **8**, 869-874; 1999
- Shivhare A, Kale A, Berge D: "Synthesis and oxidation studies of some flavone N-salicyloyl hydrazones with selenium dioxide", *J. Acta Chimica Hungary*, **120**, 107-110, 1985
- Singh N., Lai H.: "Selective toxicity of dihydroartemisinin and holotransferrin toward human breast cancer cells", *Life Science*; **70**, 49-56; 2001
- Singh, O: "Oxidative 1,2 aryl rearrangement in flavanones using Thallium (III) pToluensolphonate (TTS): a new route to isoflavones", *Tetrahedron Letters*, **31**, 2747-2750, 1990
- Singh, O: "Oxidative 1,2 aryl rearrangements in flavanones using Thallium (III) p-Toluene sulphonate: a new route to isoflavones", *Tetrahedron Letters*, **31**, 2747-2750, 1990
- Skaper S, Fabris M: "Quercetin protects cutaneous tissue associated cell types including sensory neurons from oxidative stress induced by glutathione depletion: cooperative effects of ascorbic acid", *Free Radical Biology and Medicine*, **22**, 669-78; 1997
- Slemeczi K; Robert A; Clarapols C: "Alkylation of human haemoglobin A₀ by the antimalarial drug artemisinin", *FEBS Letters*, **27976**, 1-4; 2003
- So F, Guthrie N, Chambers A, Carroll K: "Inhibition of proliferation of estrogen receptor positive MCF-7 human breast cancer cells by flavonoids in the presence and absence of excess estrogen" *Cancer Letters*, **112**, 127-133; 1997
- So F, Guthrie N: "Inhibition of human breast cancer cell proliferation and delay of mammary tumorigenesis by flavonoids and citrus juices" *Nutritional Cancer*; 1996

- Solimani R: "Quercetin and DNA in solution: analysis of the dynamics of their interaction with a LD study", *International J. Biological Macromolecules*, **18**, 287-295; 1996
- Sorensen I, Kristiansen E, Mortensen A: "The effect of isoflavones on the development of intestinal neoplasia in Apc^{min} mouse", *Cancer Letters*, **130**; 217-225; 1998
- Spampinato C, Pairoba C, Benediktsson I, Andreo C: "Properties of DNA – polymerase from petunia Mitchell chloroplast – inhibitory effects of flavonoids", *Bioscience Biotechnology and Biochemistry*, **58**, 822-825; 1994
- Spitzner J, Chung I, Muller M: "Determination of 5' and 3' DNA triplex interference boundaries reveals the core DNA binding sequence for topoisomerase II), *J. Biological Chemistry*, **270**, 5932-5943; 1995
- Sprung C, Sabatier L, Murnane J: "Telomere dynamics in a human cancer cell line", *Experimetal Cell Reseach*, **247**; 29-37; 1999
- Stewart S, Hahn W, O'Connor B: "Telomerase contributes to tumorigenesis by a telomere length – independent mechanism", *Proceeding Natura. Acad. Sc.USA*, **99**, 12606-12611; 2002
- Stockmana B, Dalvit C: "NMR screening techniques in drug discovery and drug design", *Progress in Nuclear Magnetic Resonance Spectroscopy*, **41**, 187–231; 2002
- Sun X, Hu C: "Mannich reaction of baicalein", *Chinese J. Organic Chemistry*, **23**; 81-85; 2003
- Tatarov E, Tkachev A: " Synthesis of norhydroperoxides from natural triterpenic acids", *Collection of Czechoslovak Chemical Communications*, **66**, 1753-1763; 2001
- Tobe T, Komiyama M, Maruyama K: " Daidzein stimulation of bone resorption in pit formation assay", *Bioscience Biotechnology and Biochemistry*, **61**, 370-371; 1997
- Touyz R, Yao G: "Modulation of vascular smooth muscle cell growth by magnesium – role of mitogen activated protein", *J. Cell Physiology* **197**, 326-335; 2003
- Traganos, Ardelt, Halko, Bruno, Darzynkiewicz: "Effects of genistein on the growth and cell cycle progression of normal human lymphocytes and human leukemic MOLT-4 and HL-60 cells", *Cancer Research*, **52**, 6200-6208; 1992
- Tucker, G: "Nutritional enhancement of platn", *Current Opinion in Biotechnology*, **14**, 221-225, 2003
- Vourc'h C, Taruscio D: "Cell Cycle-Dependent Distribution of Telomeres, Centromeres, and Chromosome-Specific Subsatellite Domains in the Interphase Nucleus of Mouse Lymphocytes", *Experimental Cell Research*, **205**, 142-151; 1993

- Wang C, Wu C, Hsieh K, Yen K, Yang L: "Cytotoxic effects of cantharidin on the growth of normal and carcinoma cells", *Toxicology*, **147**, 77-87; 2000
- Wang G, Zhang H, Xie Y: "Effects of genistein and daidzein on the cell growth, cell cycle and differentiation of human and murine melanoma cells", *J. Nutritional Biochemistry*, **13**, 421-426; 2002
- Wang J: "DNA topoisomerases: why so many?" *J. Biological Chemistry*, **266**, 6659-6662; 1991
- Wang W, Jia Z, Yao S, Fan B, Zheng R: "Fast repair of purine deoxynucleotide radical cations by rutin and quercetin", *Science China*, **44**, 610-617; 2001
- Wang W, Liu L, Higuchi C, Chen H: "Induction of NADPH: quinine reductase by dietary phytoestrogens in colonic colo 205 cells", *Biochemical Pharmacology*, **56**, 189-195; 1998
- Ward, Reh fuss, Goodisman, Dabrowiak : "Rate enhancements in the DNase I footprinting experiment"; *Nucleic Acids Research* , **16**, 1359-1369; 1988
- Watanabe S, Uesugi S: "Isoflavones for prevention of cancer, cardiovascular diseases, gynaecological problems and possible immune potentiation", *Biomedical Pharmacology*, **56**, 302-312; 2002
- Welton A, Tobias L: "Effect of flavonoids on arachidonic acid metabolism", *Progress Clinical Biology Research*, **213**, 231-242; 1986
- Westwell A: "Monitor: molecules and profiles", *Drug Discovery Today*, **6**, 1176-1177; 2001
- Williams S: "Comparative studies on the effects of green tea extracts and individual tea catechins on human CYP1A gene expression" *Chemical Biological Interactions* **128**, 211-229; 2000
- Wong R, Sagar C, Sagar S: "Integration of Chinese medicine into supportive cancer care: a modern role for an ancient tradition". *Cancer Treatment Reviews*, **27**, 235-246; 2001
- Xu H, Wan M, Dong H: "Inhibitory activity of flavonoids and tannins against HIV – 1 proteases" *Biological Pharmaceutical. Bulletin*, **23**, 1072-1076; 2000
- Yamashita N, Tanemura H, Kawanishi S: "Mechanism of oxidative DNA damage induced by quercetin in the presence of Cu II", *Mutation Research*, **425**, 107-115; 1999
- Youwen Z, Luoxiu Y: "Blocking effect of puerarin on calcium channel in isolated guinea pig ventricular myocytes", *Chinese Medicine J*, **112**, 787-789; 1999
- Yuan R, Lin Y.: "Traditional Chinese medicine: an approach to scientific proof and clinical validation". *Pharmacology Therapies*, **86**, 191-198; 2000.
- Zhao C, Shi Y: "Fast repair activities of quercetin and rutin toward dGMP hydroxyl radical adducts" *Radiation Physical Chemistry*, **63**, 41-44; 2002

- Zhao J, Zhang Z, Chen H, Zhang X, Chen X: "Synthesis of baicalin derivatives and evaluation of their antihuman immunodeficiency virus activity" *YaXueXueTao*, **33**, 22-27; 1998
- Zheng G, Kenney P, LamL: "Sesquiterpenes from clove (*Eugenia caryophyllata*) as potential anticarcinogenic agents" *J Natural Products*, **55**, 999-1003; 1992
- Zhu, A; Can, L; Li, N: "Eletrochemical studies of quercetin interacting with DNA", *Microchemical Journal*, **71**, 57-63; 2002

Appendix

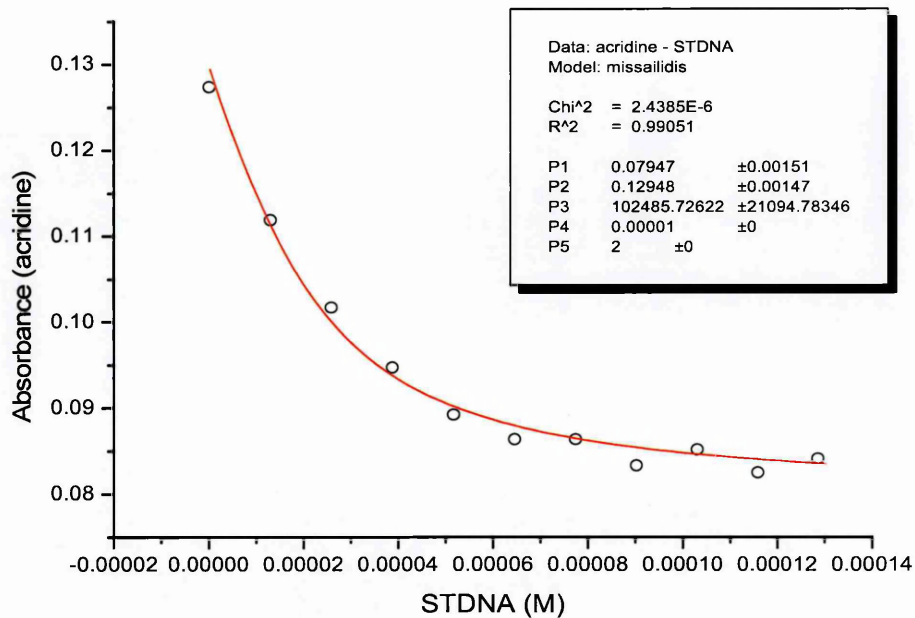


Figure 33: Acridine – STDNA (UV-Vis)

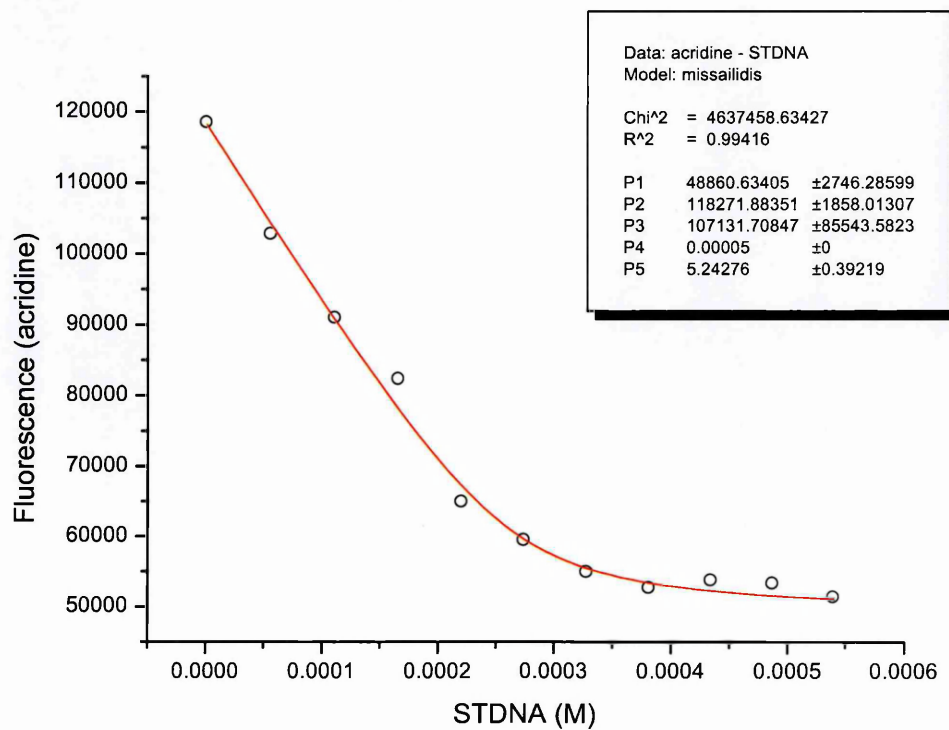


Figure 34: Acridine – STDNA (fluorescence)

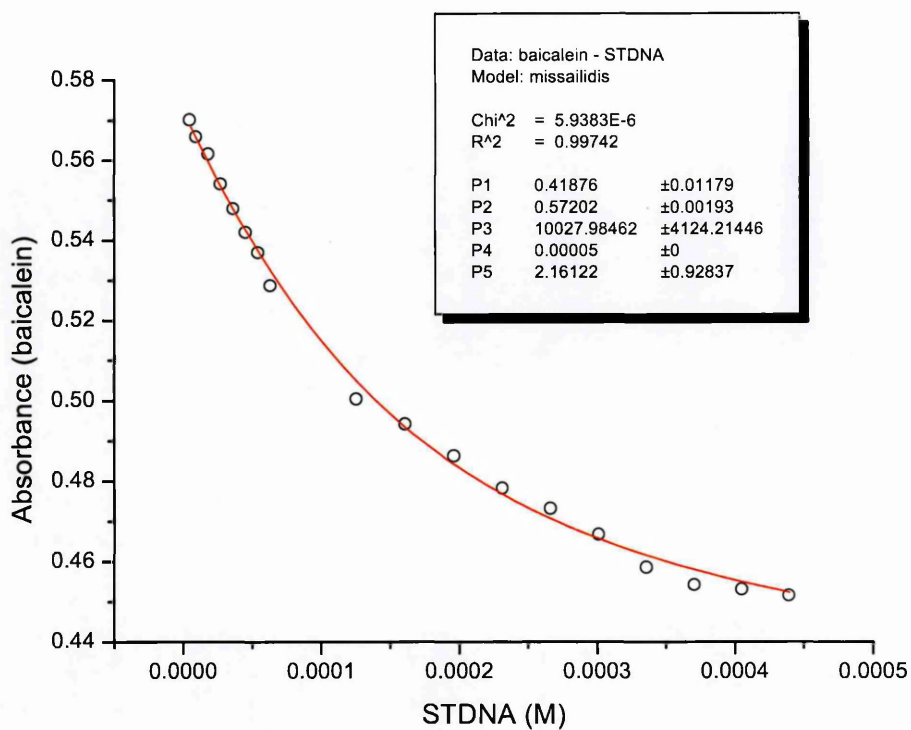


Figure 35: Baicalein - STDNA (UV-Vis absorbance)

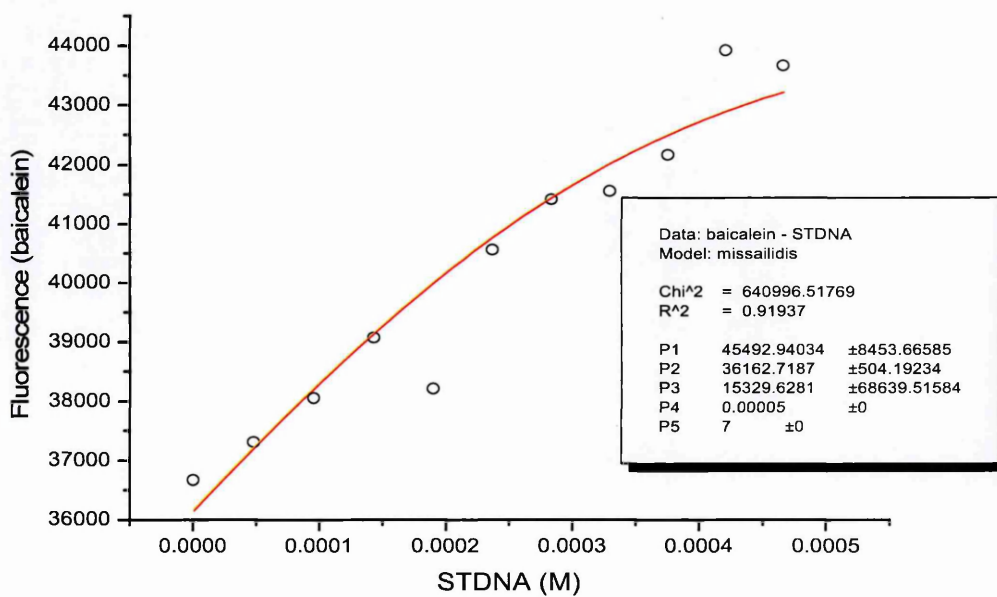


Figure 36: Baicalein - STDNA (fluorescence)

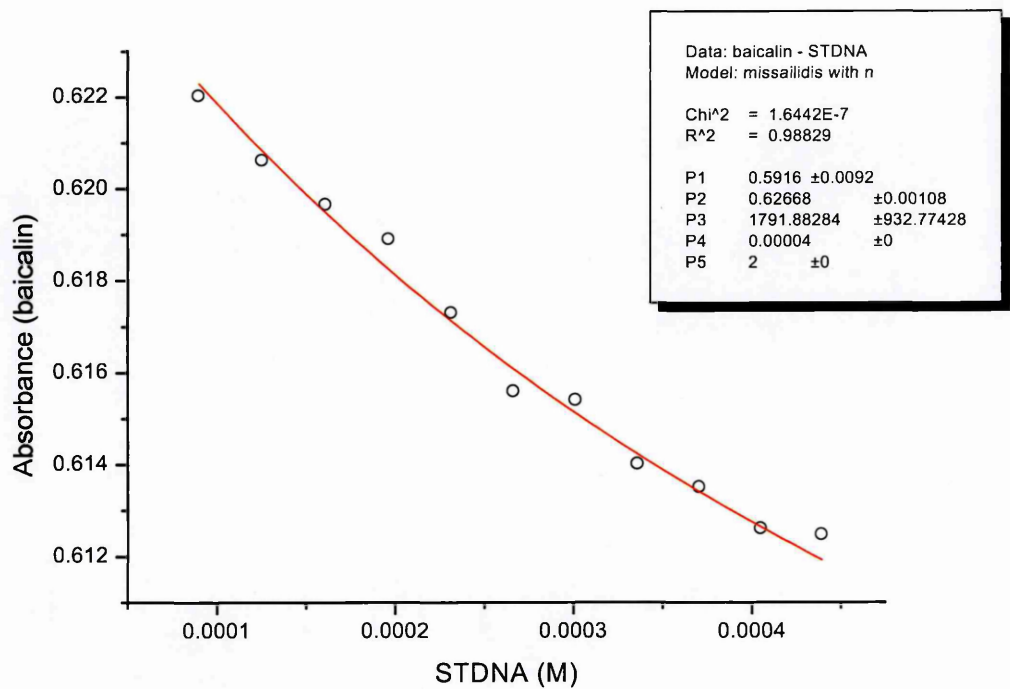


Figure 37: Baicalin - STDNA (UV-Vis)

Fi

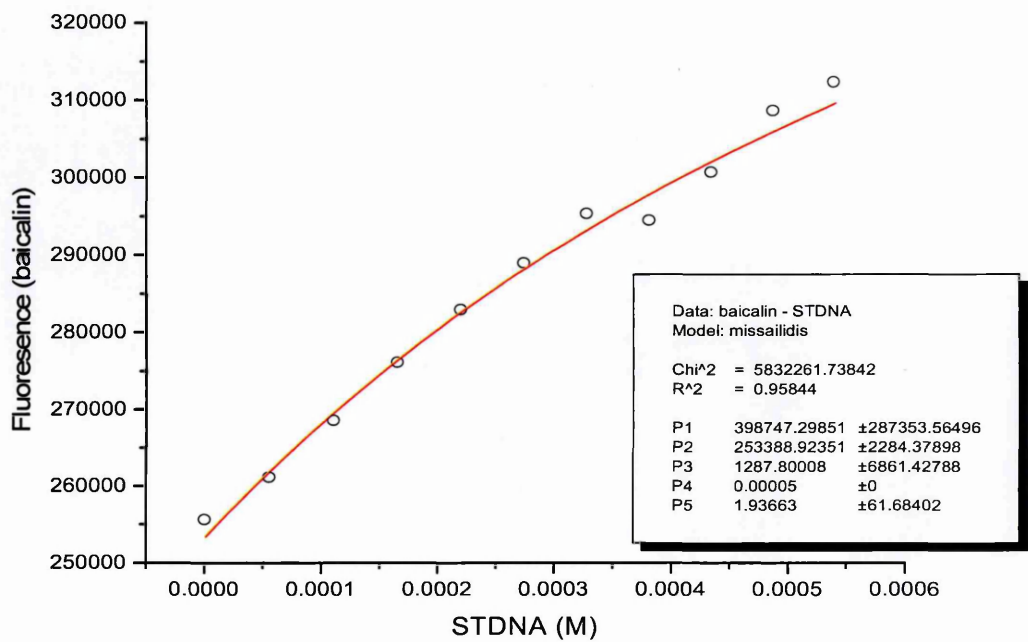


Figure 38: Baicalin - STDNA (fluorescence)

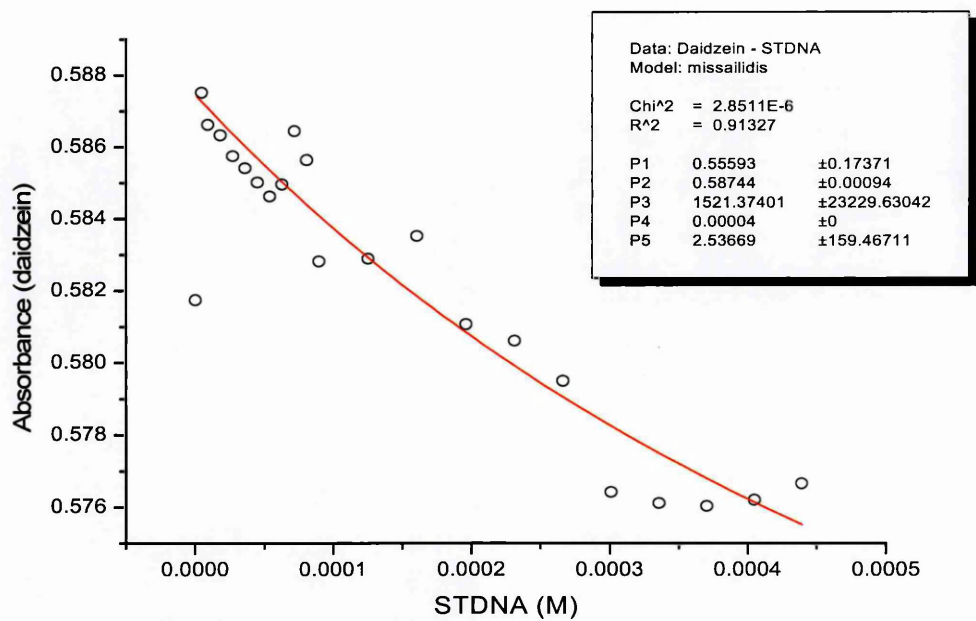


Figure 39: Daidzein - STDNA (UV-Vis)

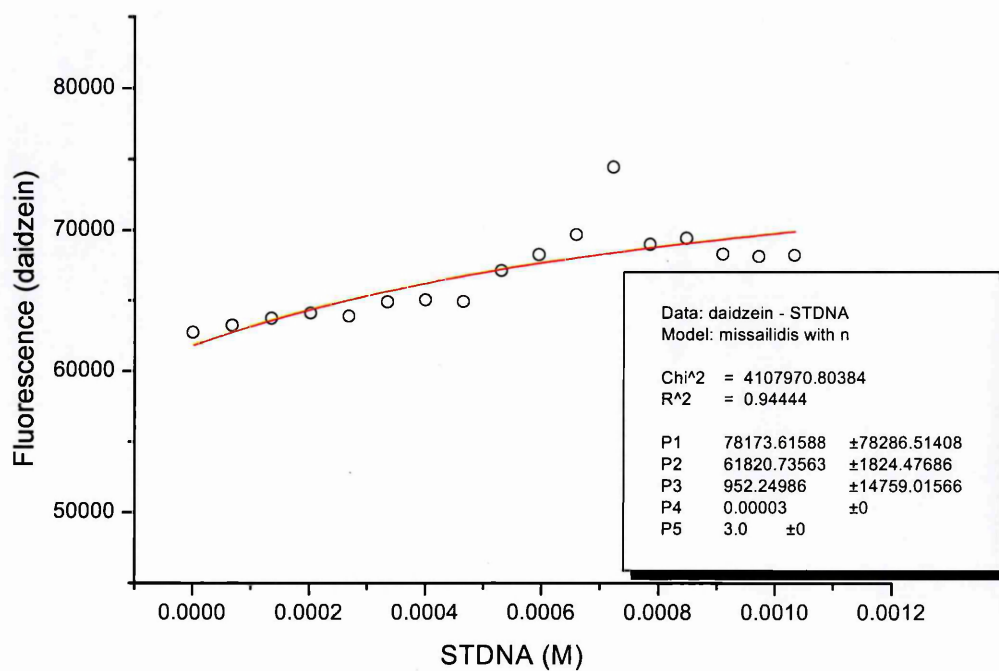


Figure 40: Daidzein - STDNA (fluorescence)

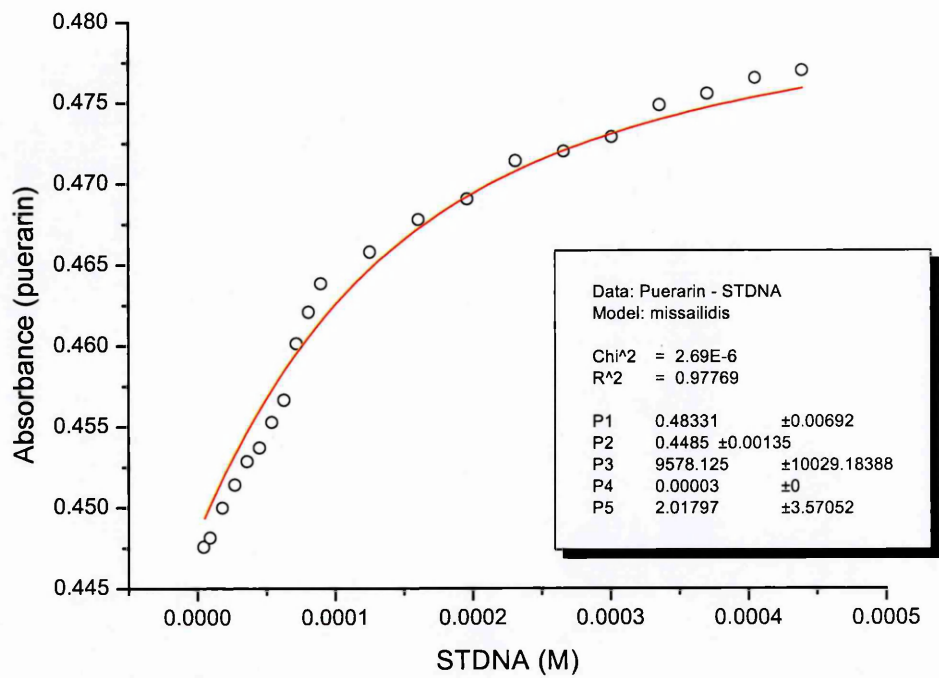


Figure 41: Puerarin - STDNA (fluorescence)

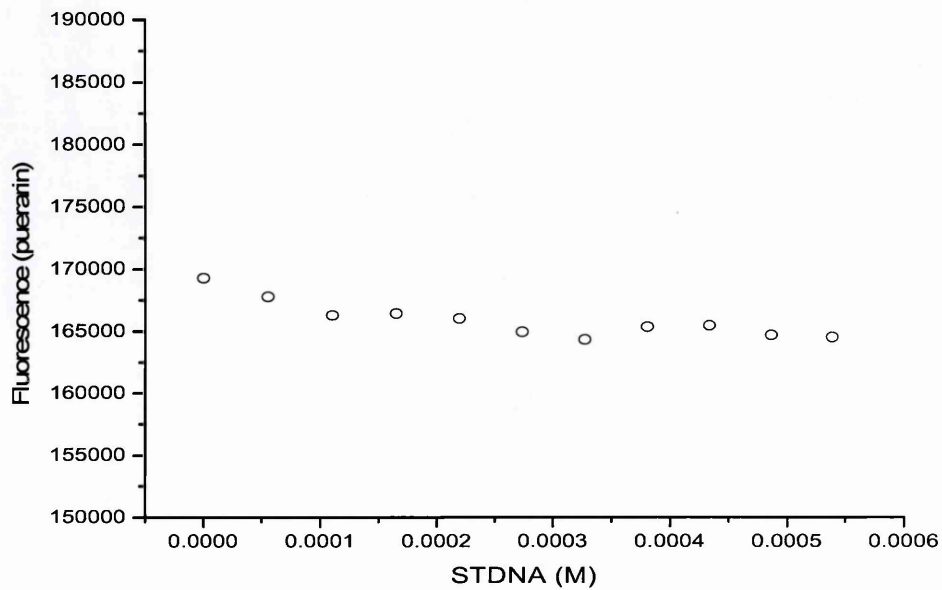


Figure 42: Puerarin - STDNA (fluorescence)

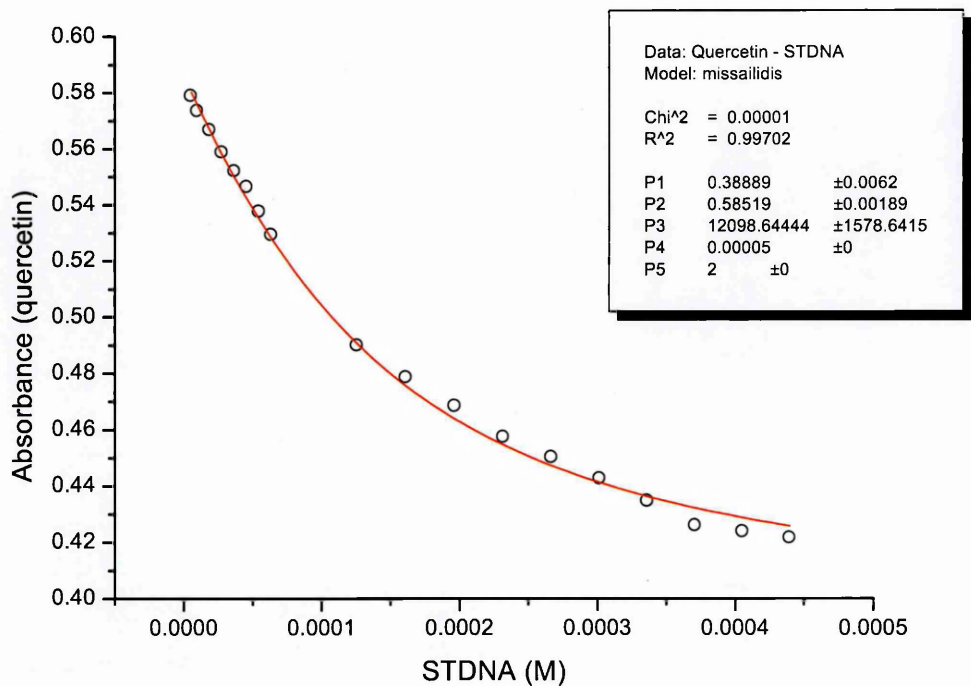


Figure 43: Quercetin - STDNA (UV-Vis)

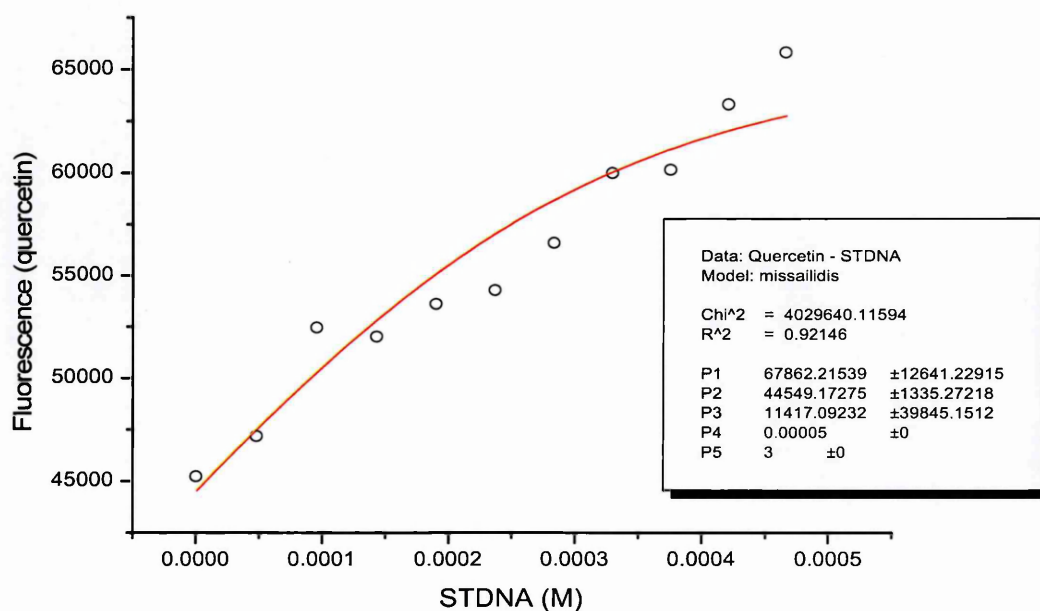


Figure 44: Quercetin - STDNA (fluorescence)

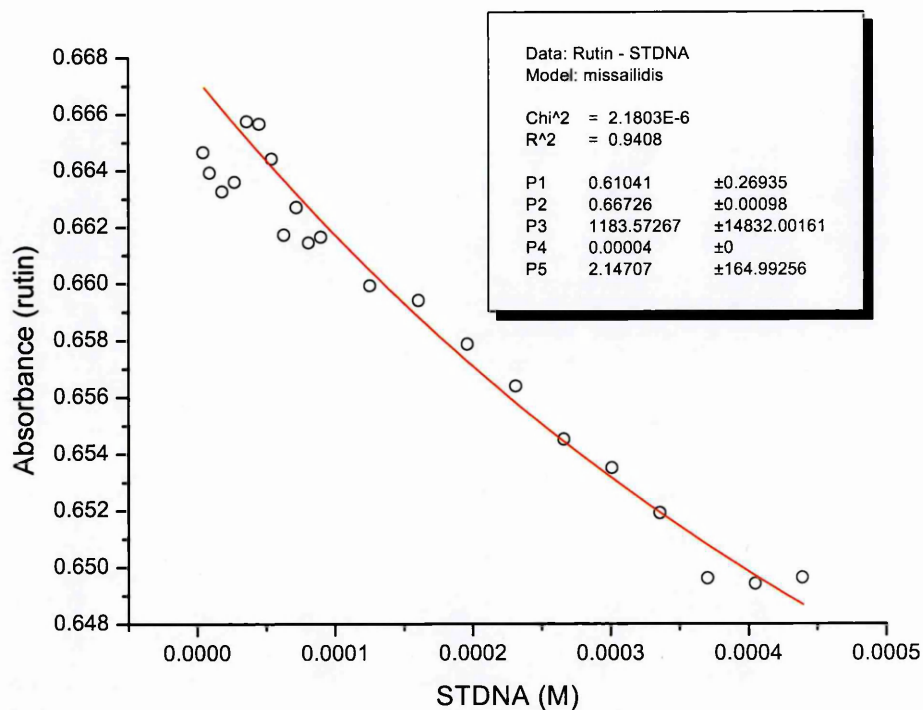


Figure 45: Rutin - STDNA (UV-Vis)

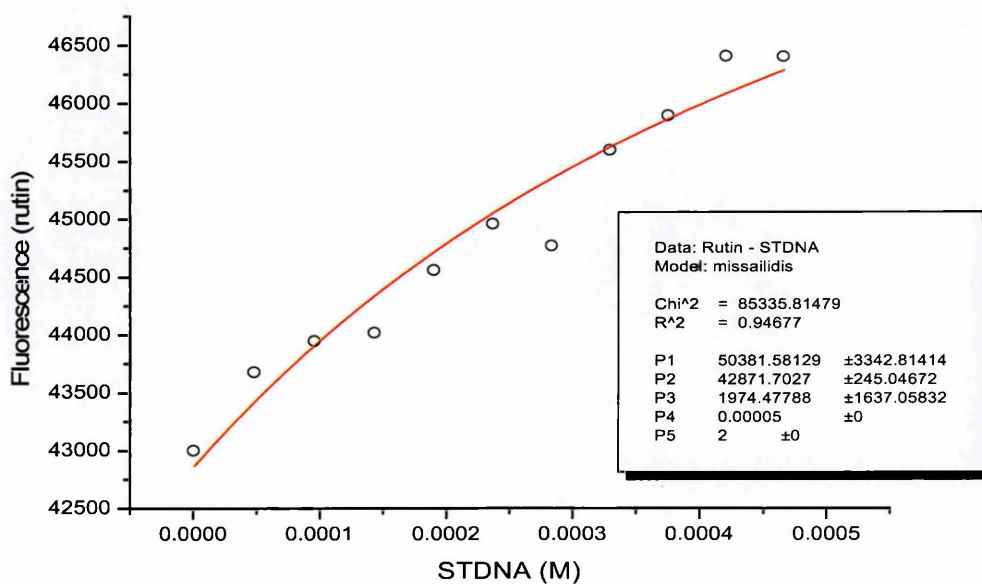


Figure 46: Rutin - STDNA (fluorescence)

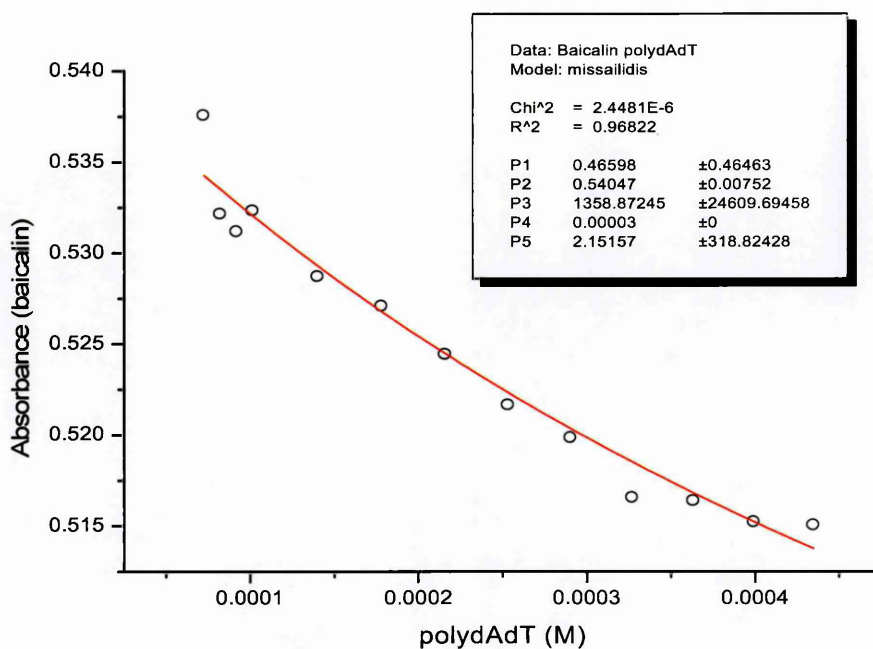


Figure 47: Baicalin - polydAdT

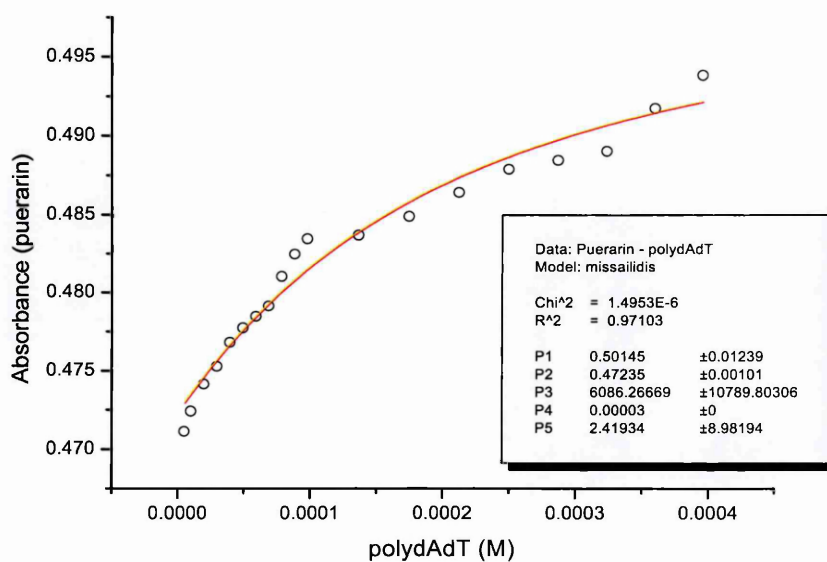


Figure 48: Puerarin - polydAdT

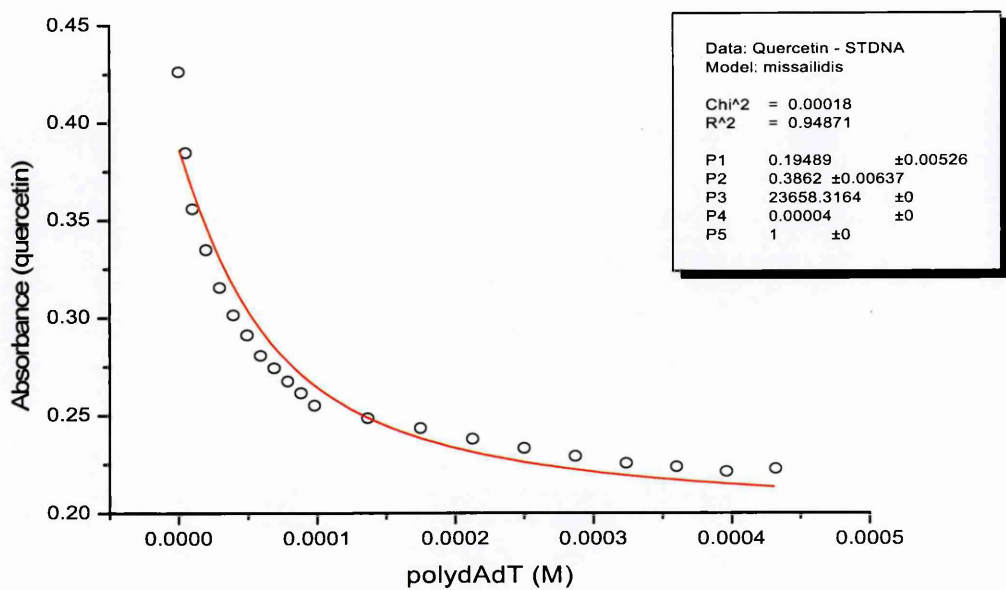


Figure 49: Quercetin - polydAdT

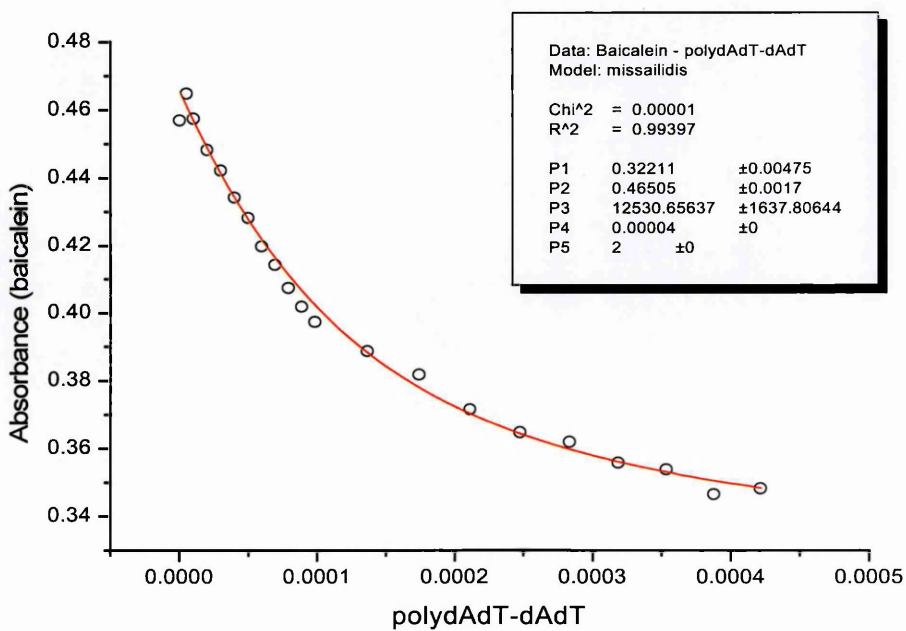


Figure 50: Baicalein polydAdT-dAdT

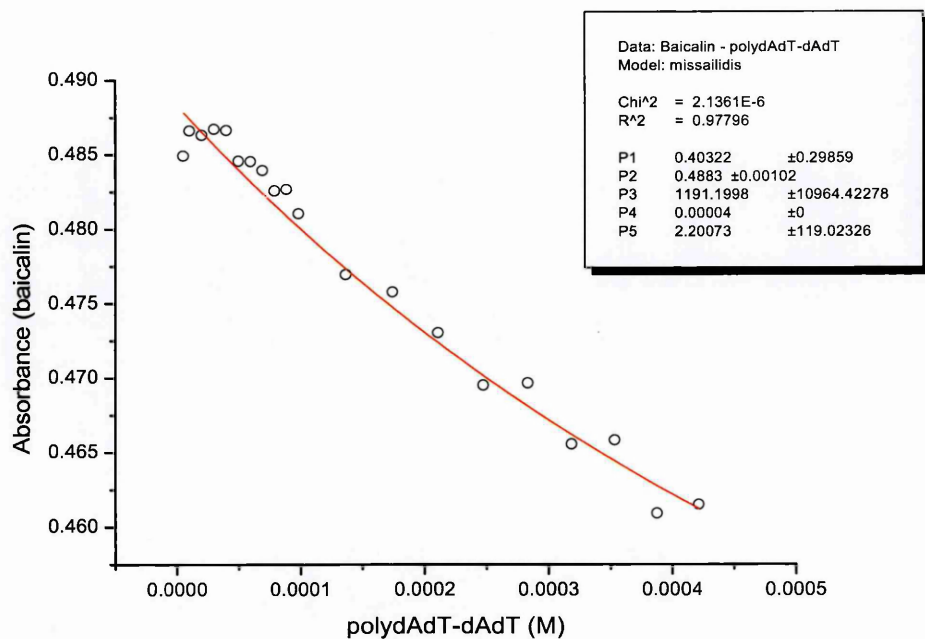


Figure 51: Baicalin – polydAdT-dAdT

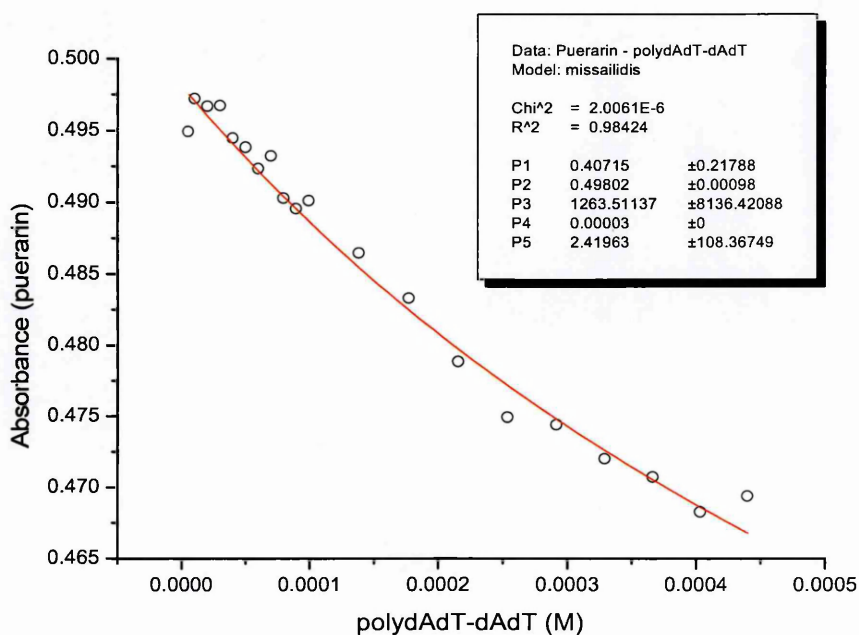


Figure 52: Puerarin – polydAdT-dAdT

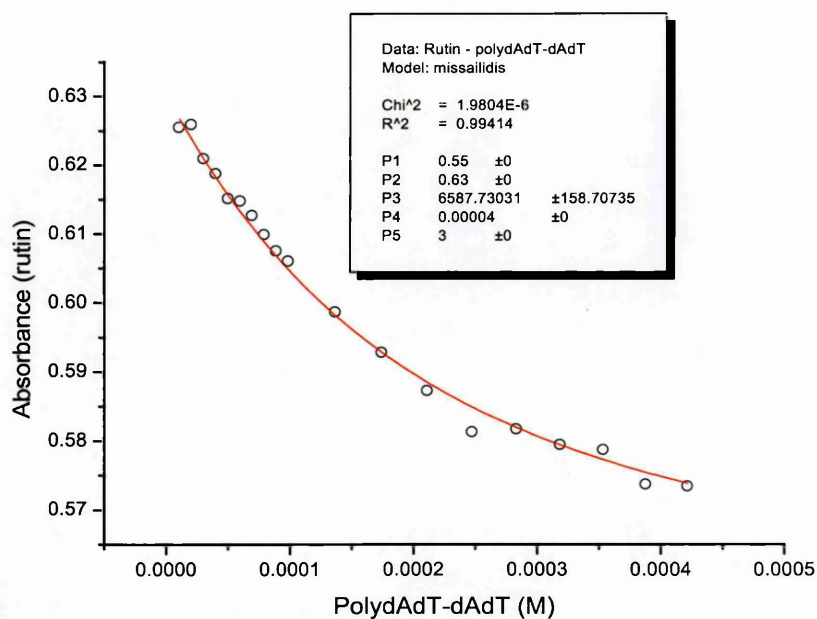


Figure 53: Rutin - -PolydAdT-dAdT

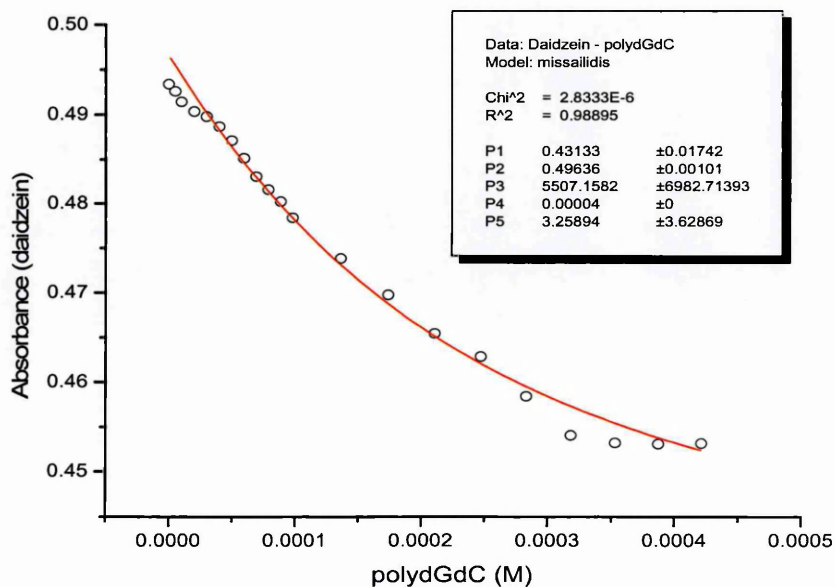


Figure 54: Daidzein - PolydGdC

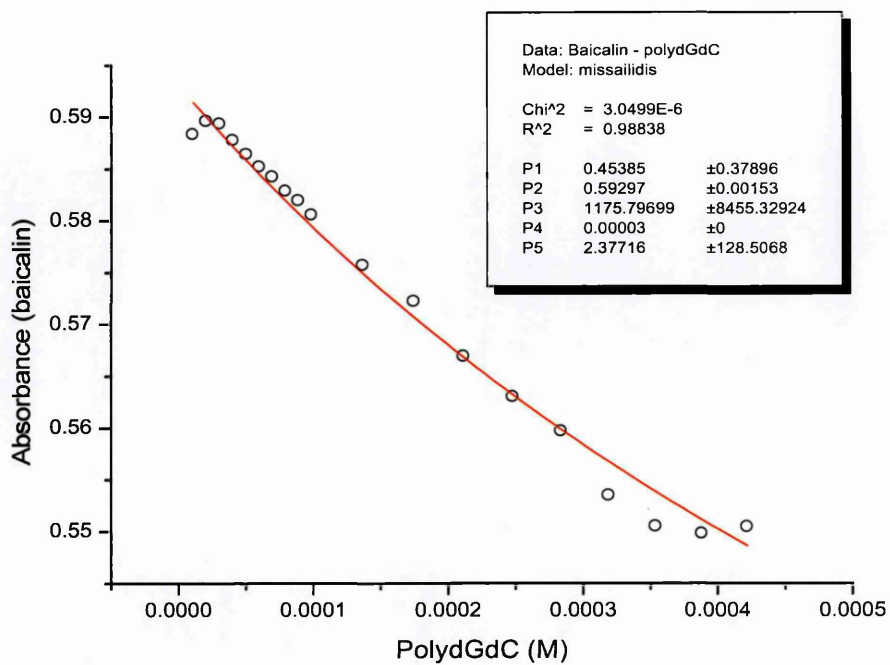


Figure 55:Baicalin - PolydGdC

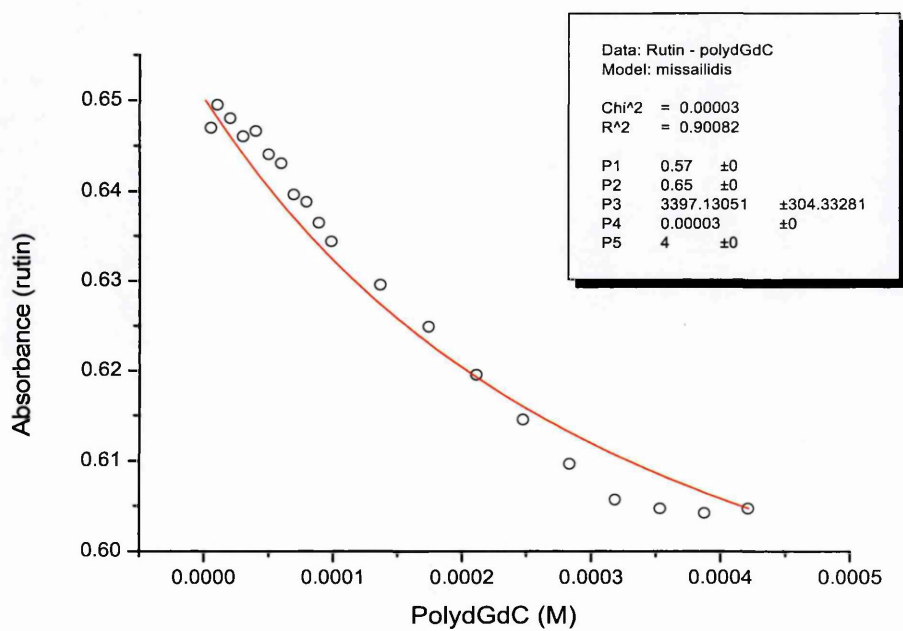


Figure 56: Rutin – PolydGdC

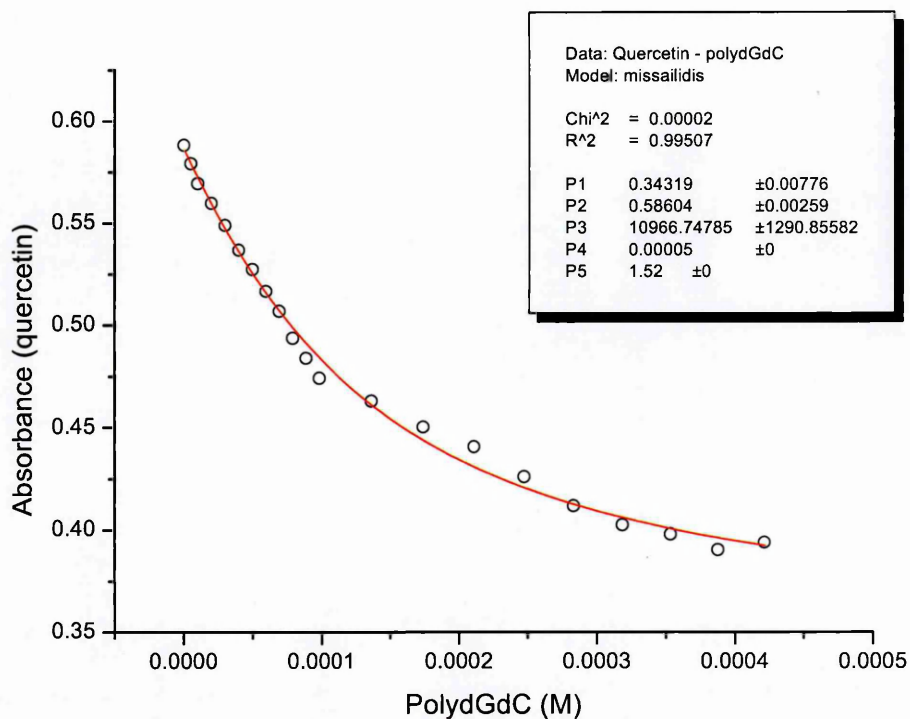


Figure 57: Quercetin – PolydGdC

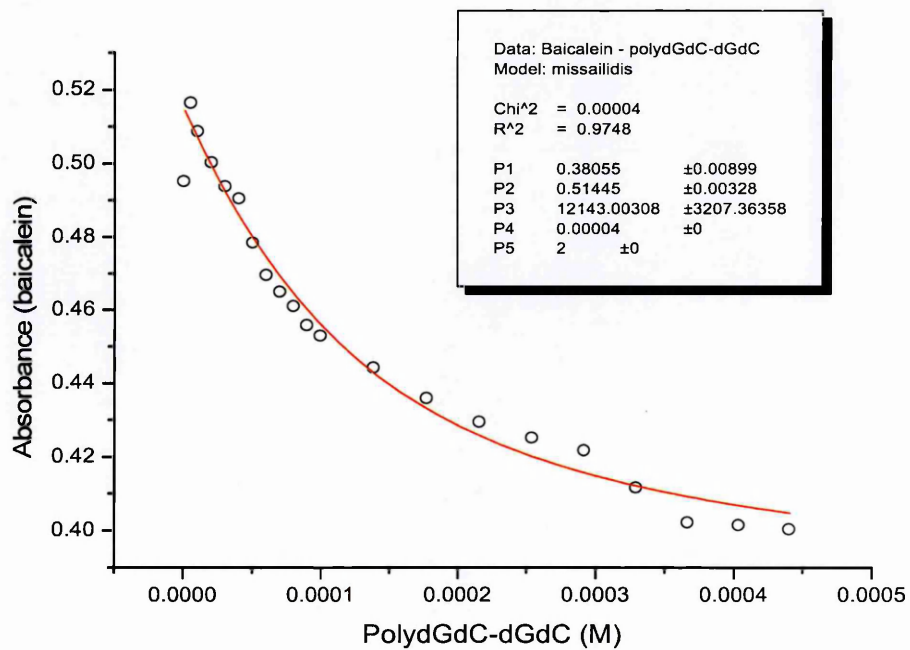


Figure 58: Baicalein – PolydGdC-dGdC

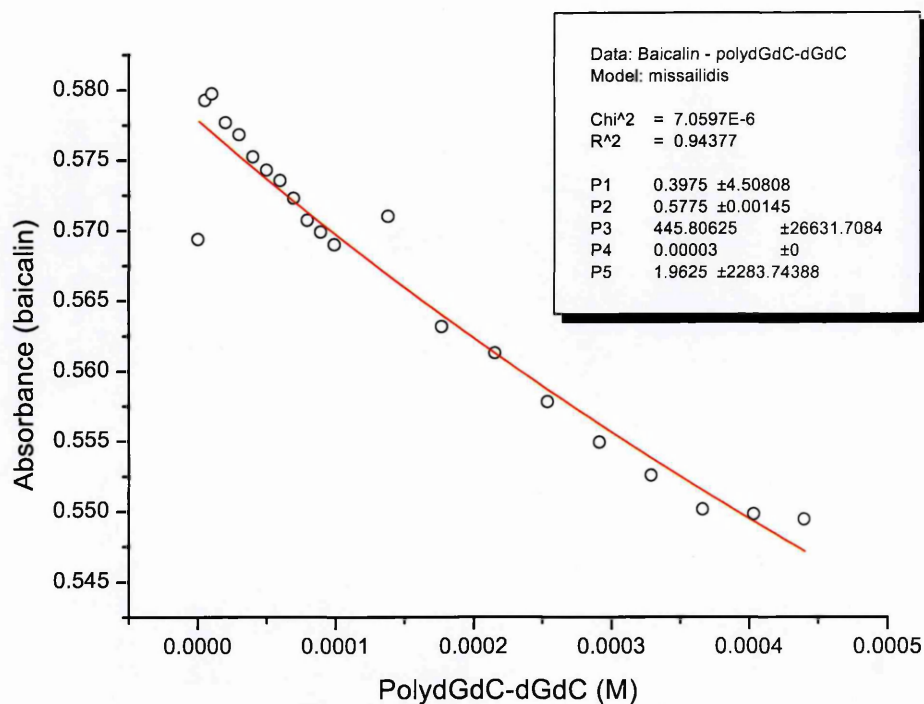


Figure 59: Baicalin – PolydGdC-dGdC

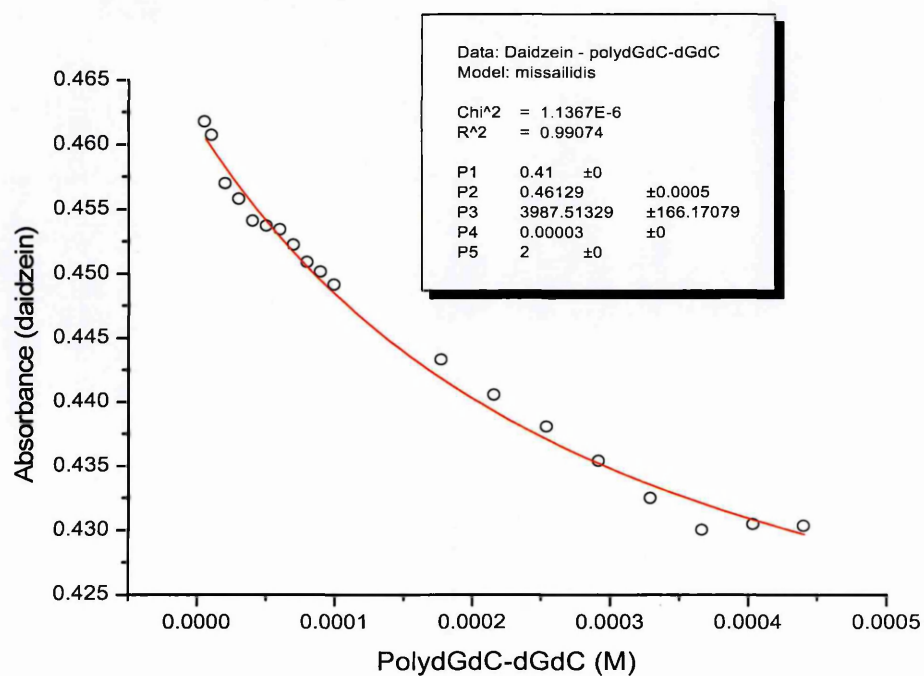


Figure 60: Daidzein – PolydGdC-dGdC

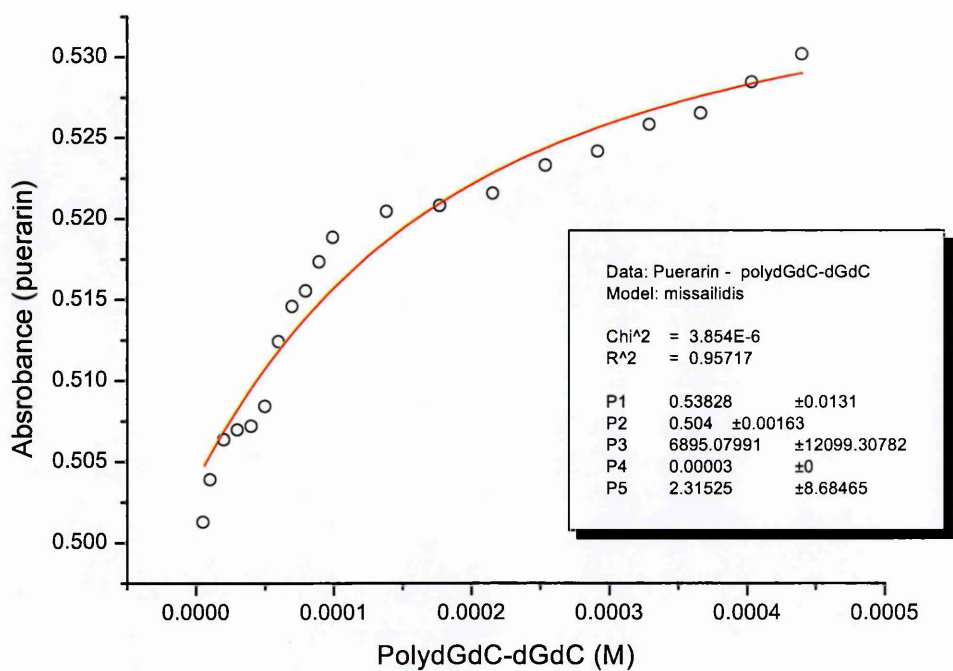


Figure 61: Puerarin – PolydGdC-dGdC

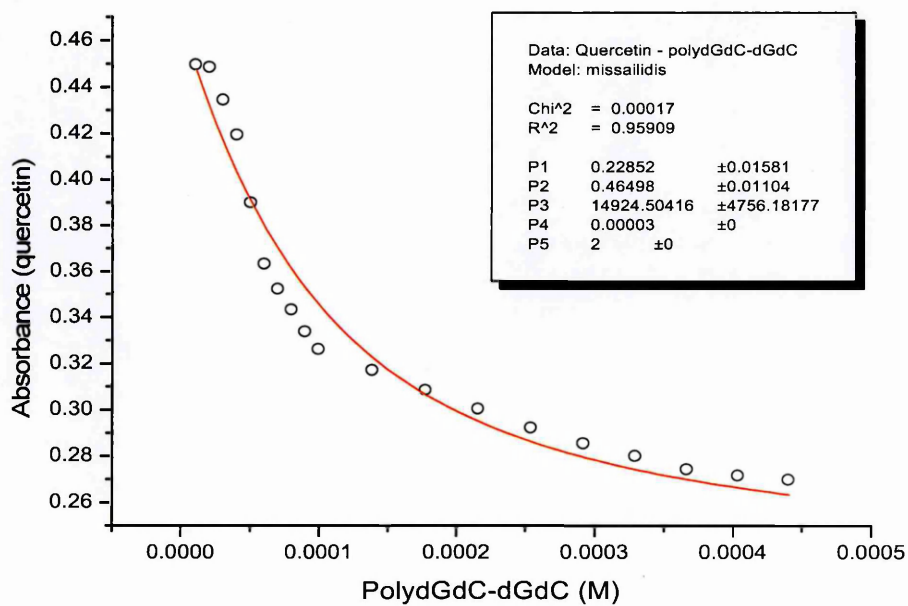


Figure 62: Quercetin – PolydGdC-dGdC

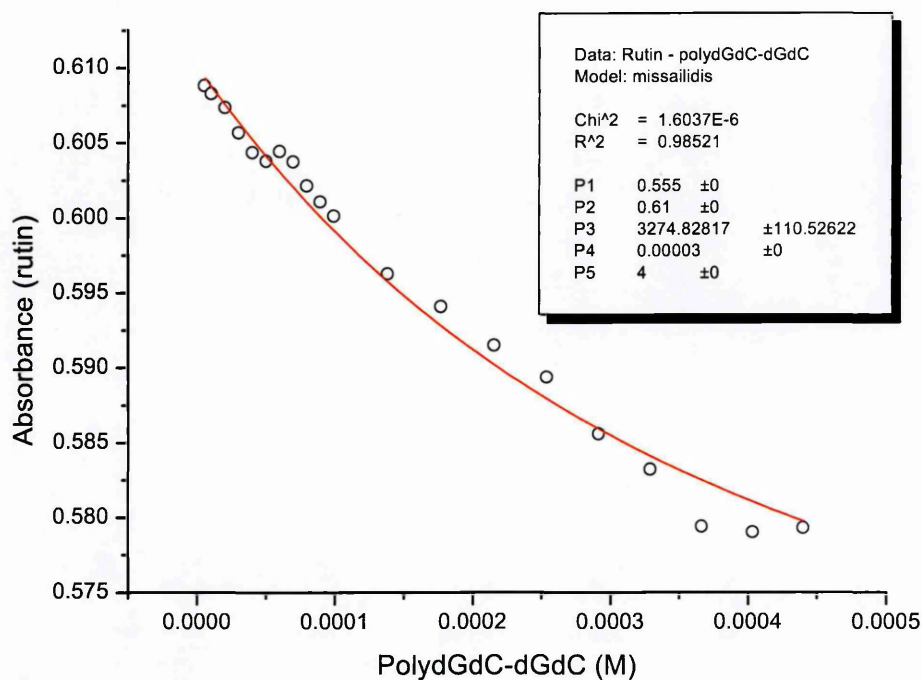


Figure 63: Rutin – PolydGdC-dGdC

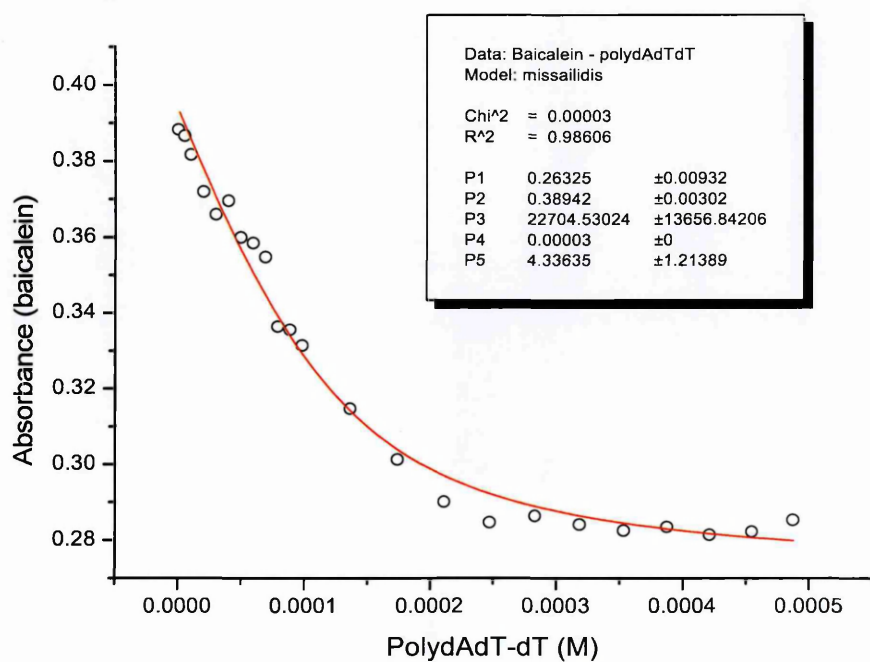


Figure 64: Baicalein – PolydAdT-dT

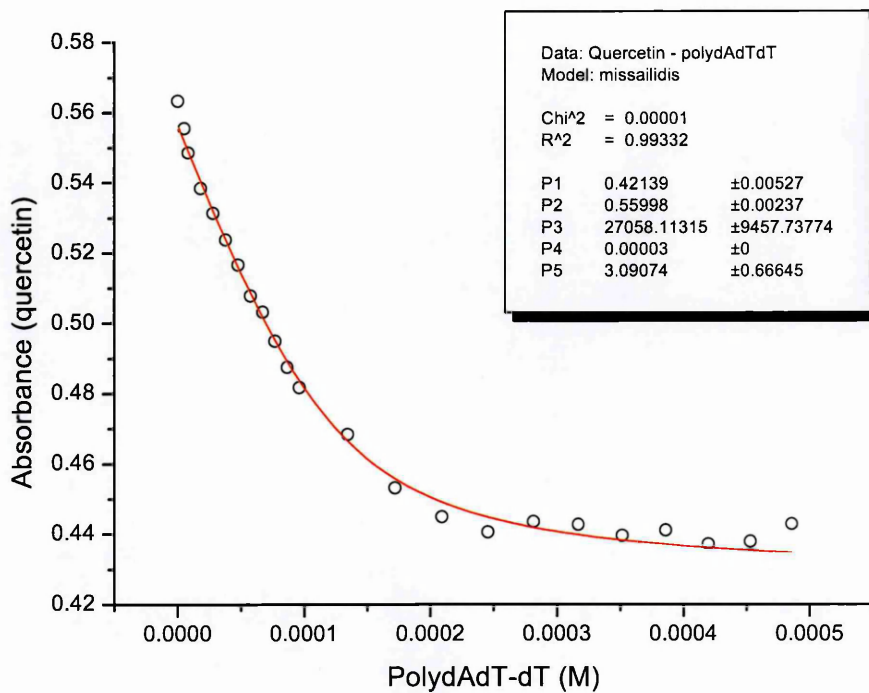


Figure 65: Quercetin – PolydAdT-dT

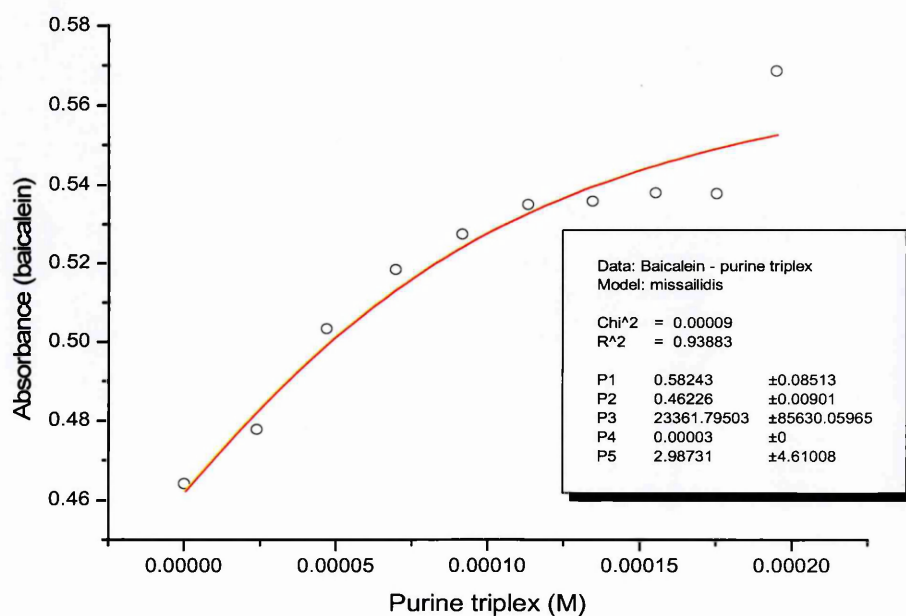


Figure 66: Baicalein – Purine triplex

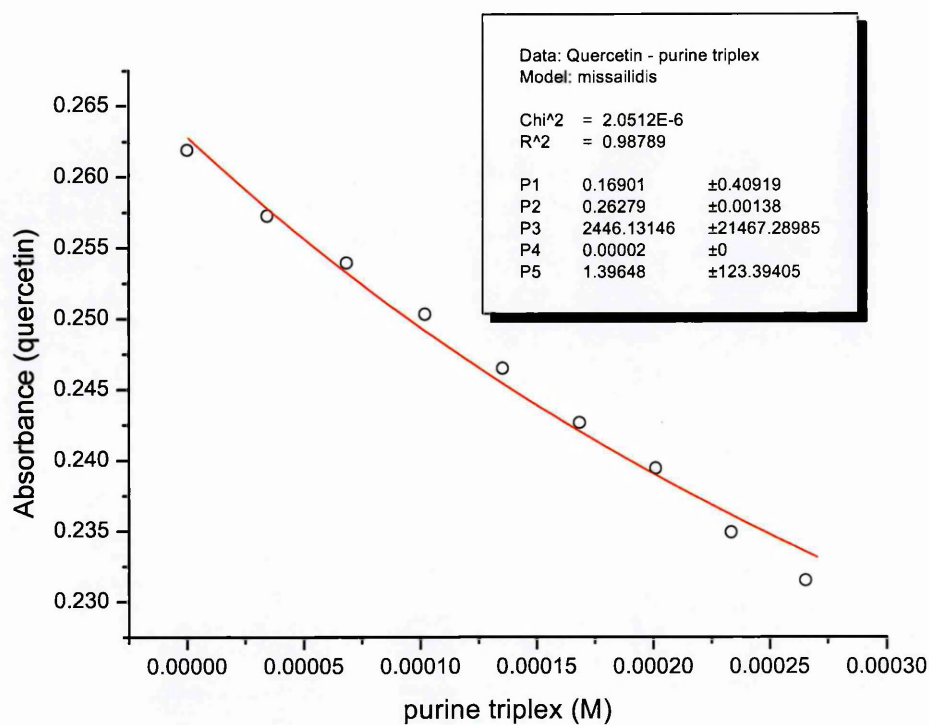


Figure 67: Quercetin – Purine triplex

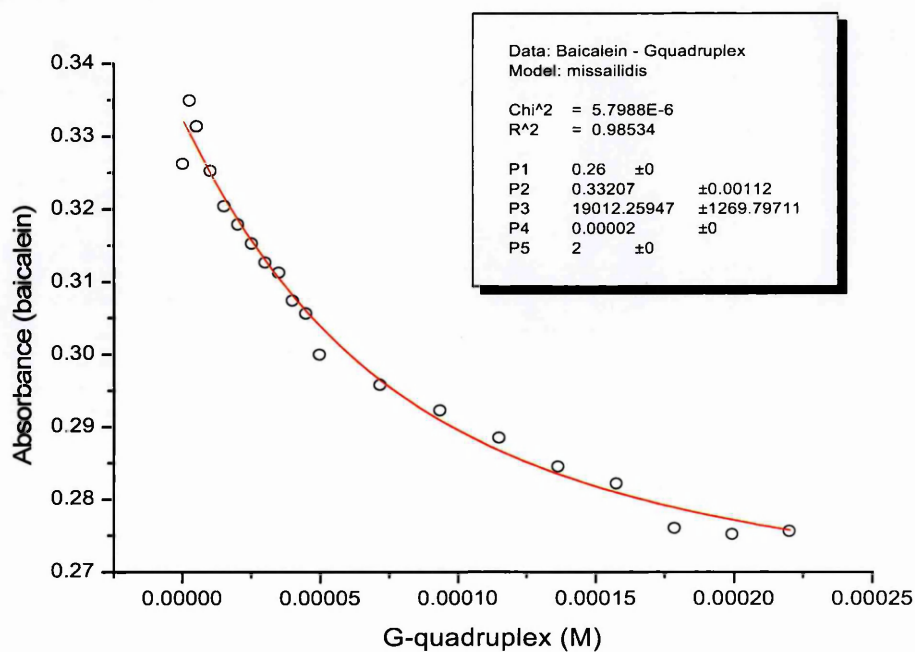


Figure 68: Baicalein – G-quadruplex

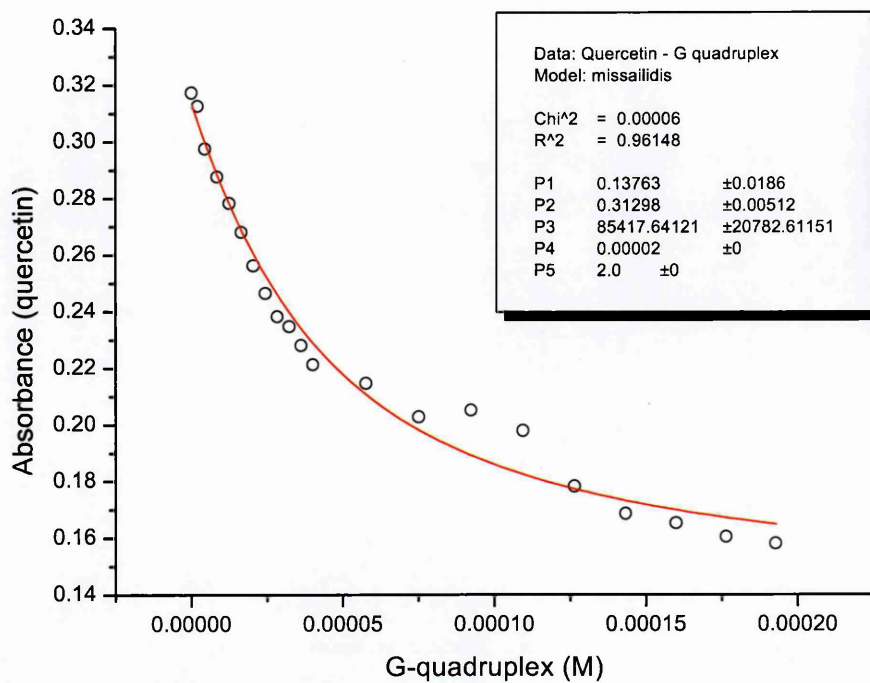


Figure 69: Quercetin – G-quadruplex

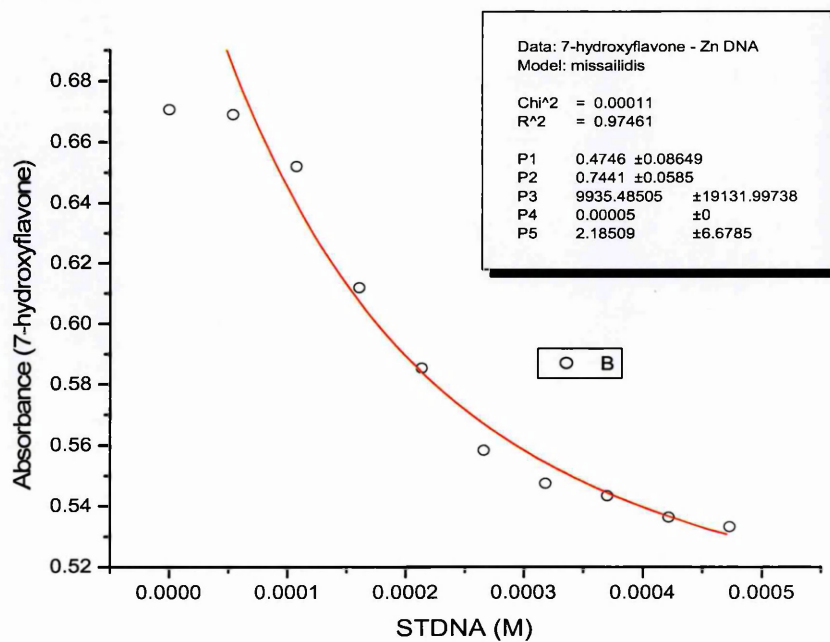


Figure 70: 7-Hydroxyflavone – STDNA –Zn

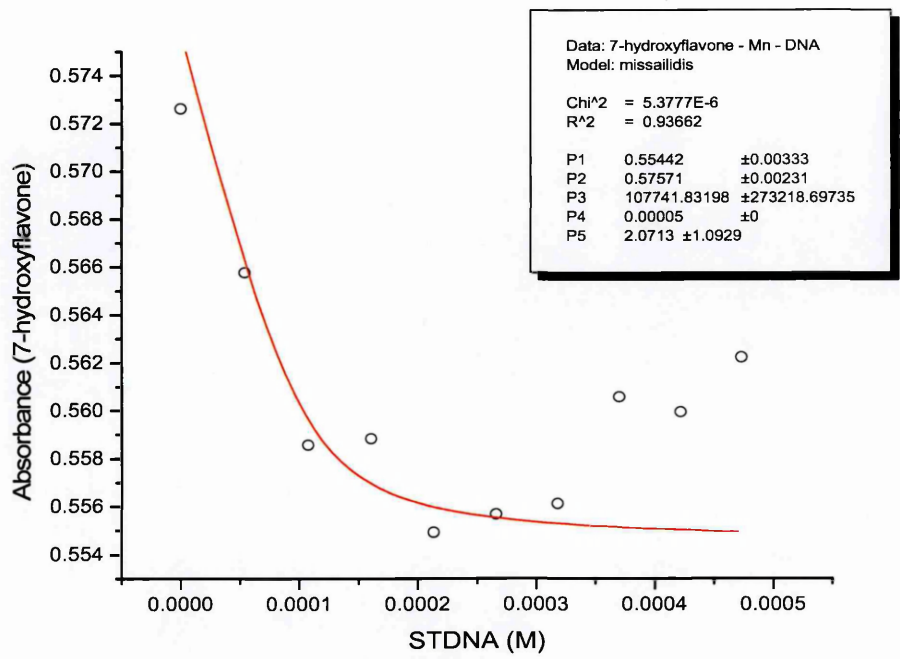


Figure 71: 7-Hydroxyflavone – STDNA – Mn

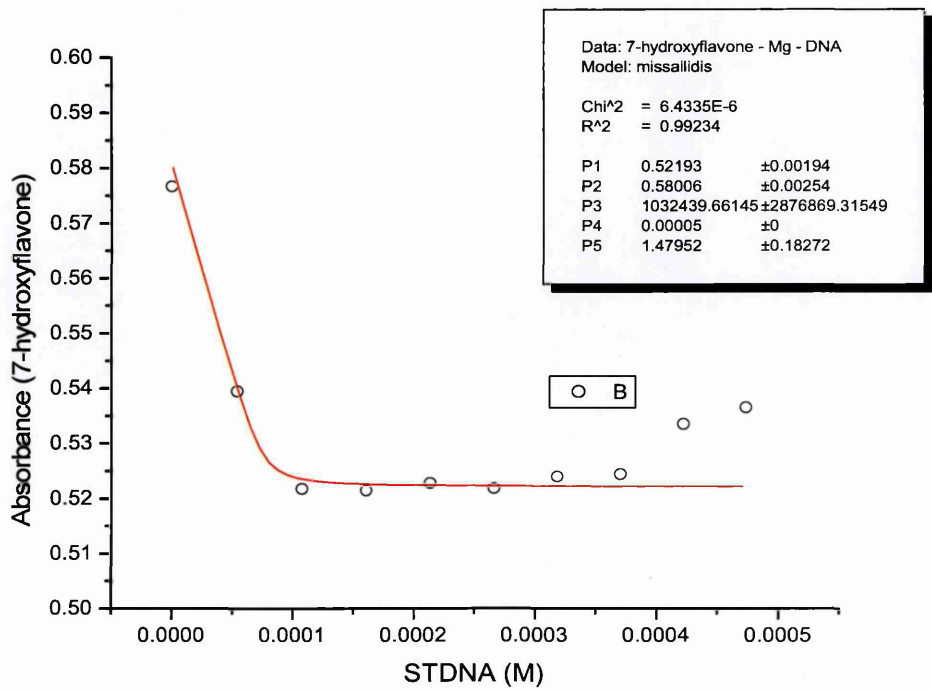


Figure 72: 7-Hydroxyflavone – STDNA – Mg

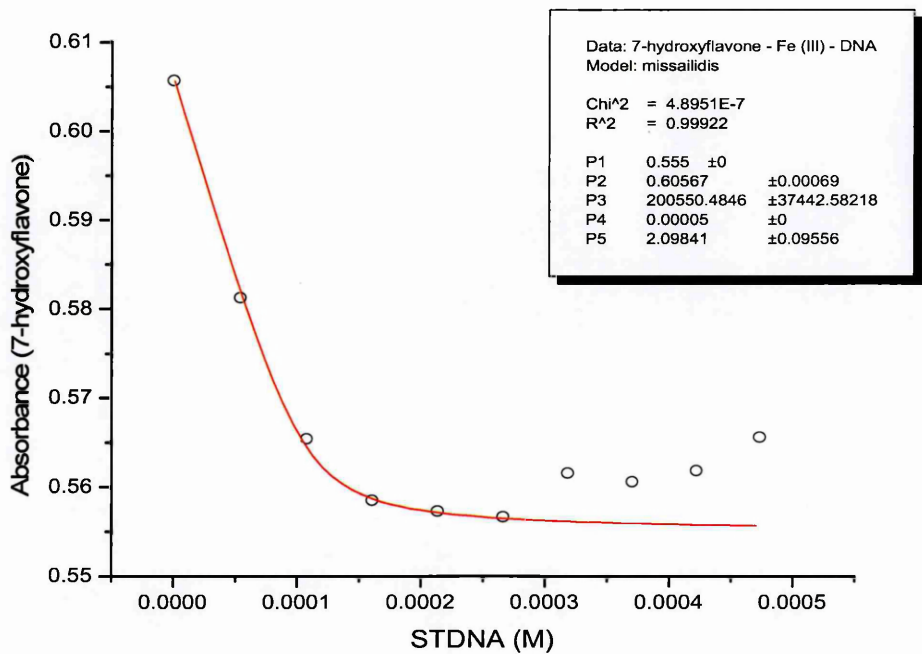


Figure 73: 7-Hydroxyflavone – STDNA – Fe(II)

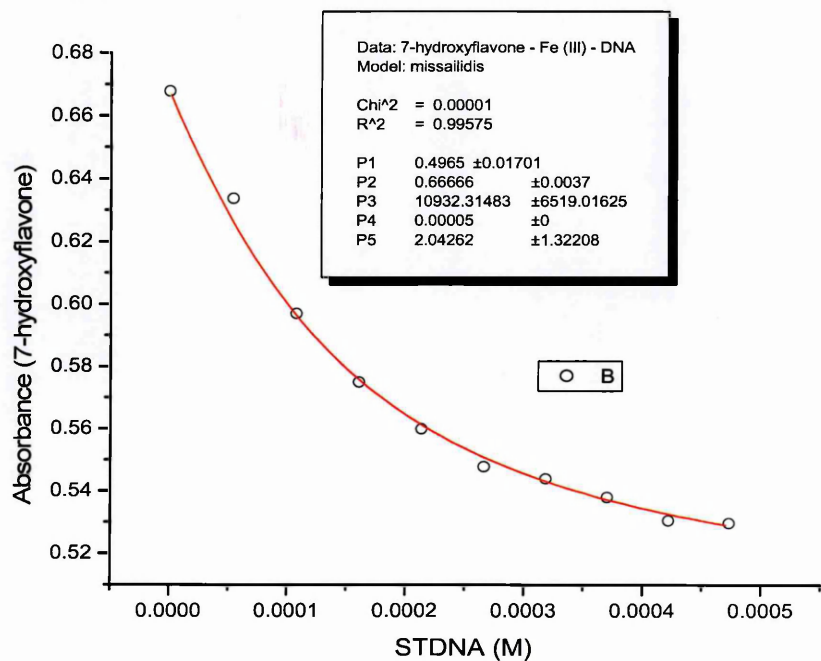


Figure 74: 7-Hydroxyflavone – STDNA – Fe(III)

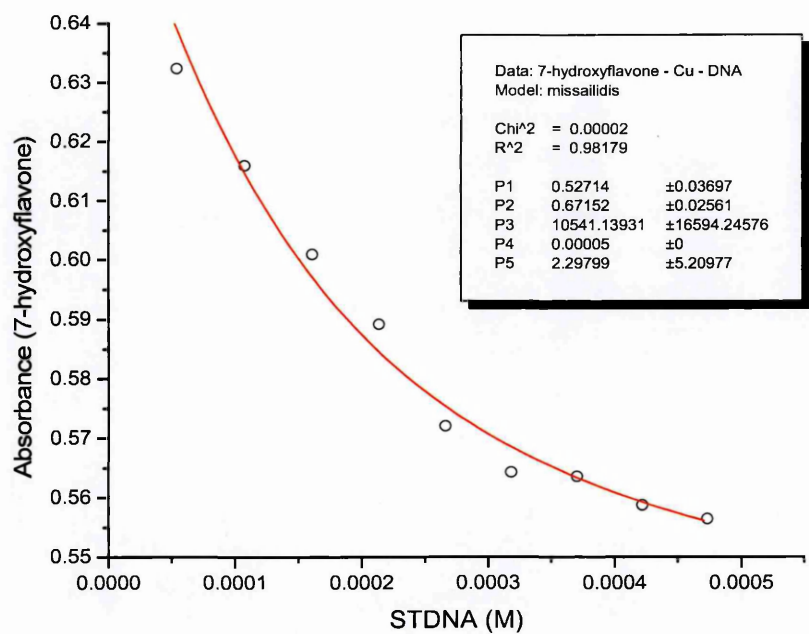


Figure 75: 7-Hydroxyflavone – STDNA – Cu

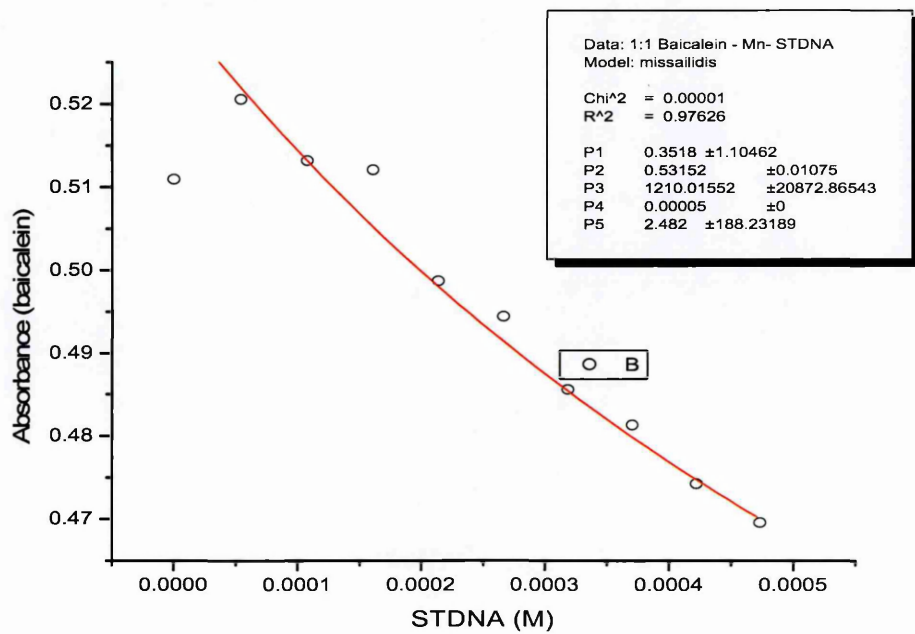


Figure 76: Baicalein – STDNA- Mn

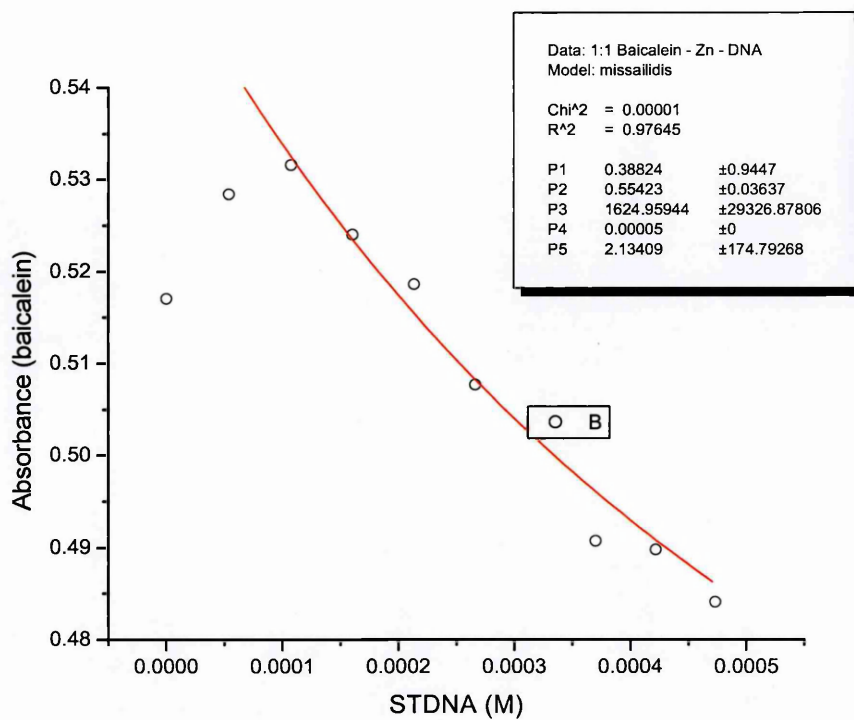


Figure 77: Baicalein – STDNA – Zn

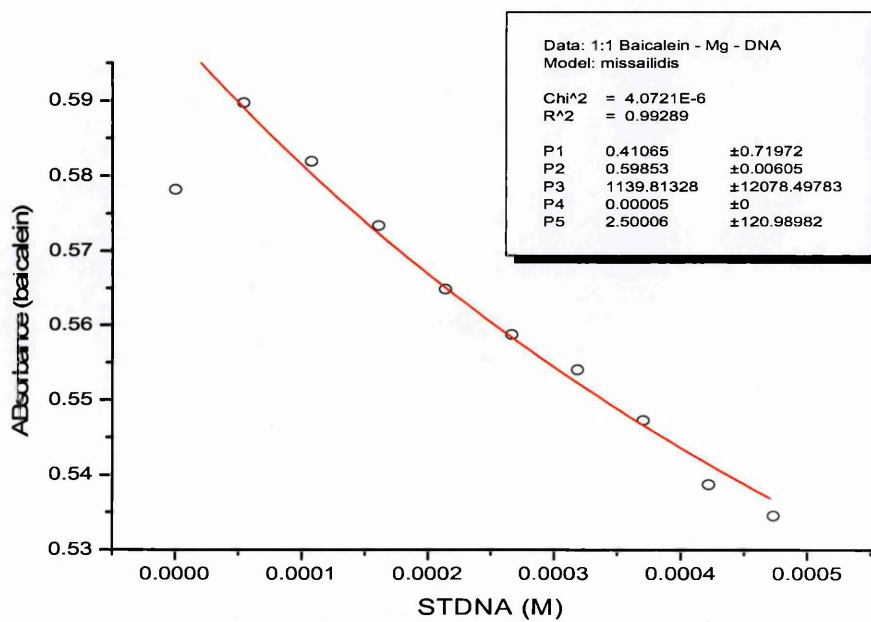


Figure 78: Baicalein – STDNA – Mg

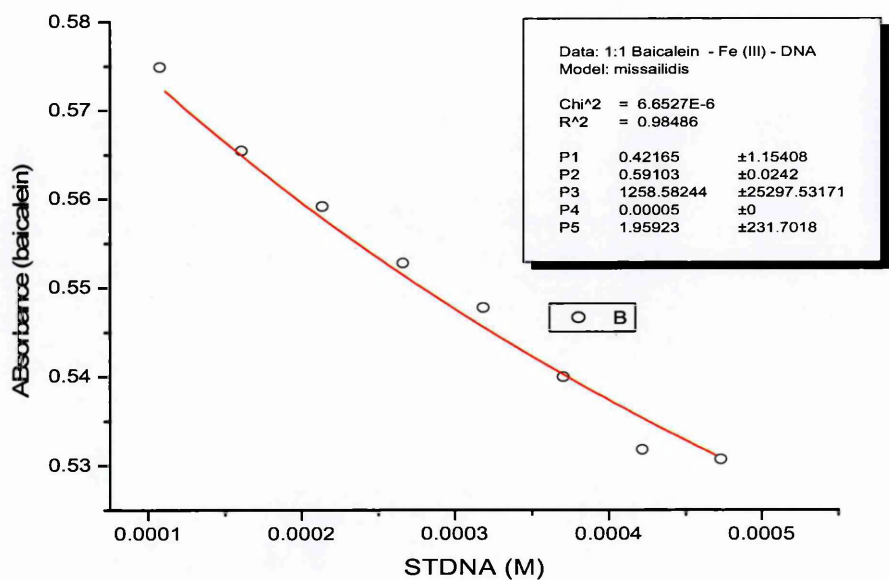


Figure 79: Baicalein – STDNA – Fe(III)

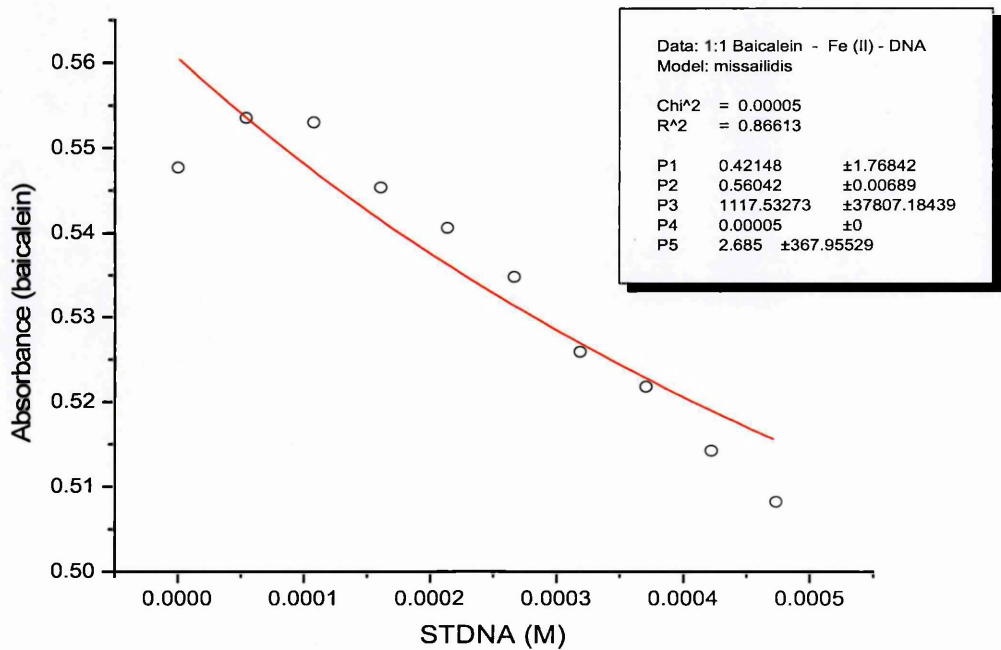


Figure 80: Baicalein – STDNA – Fe(II)

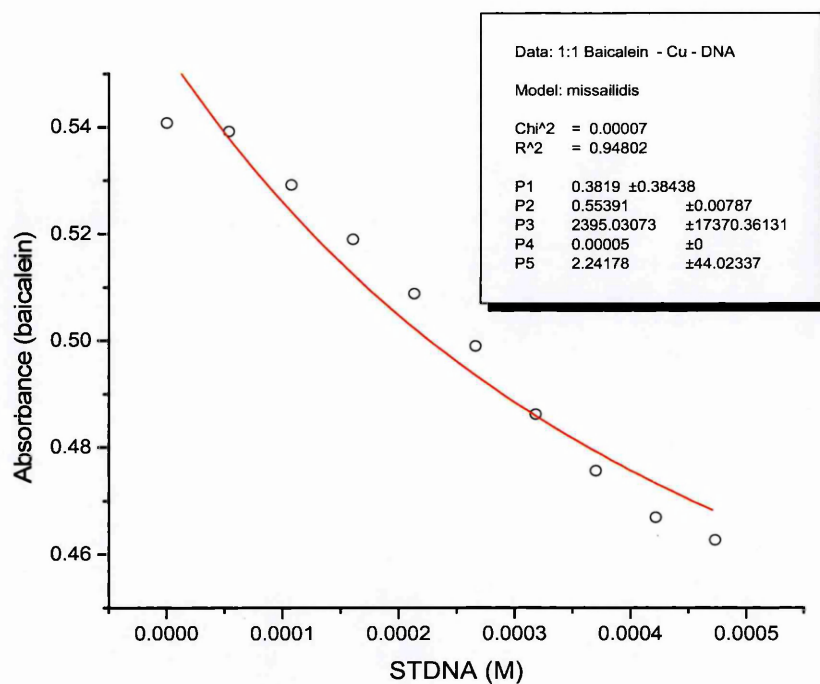


Figure 81: Baicalein – STDNA – Cu

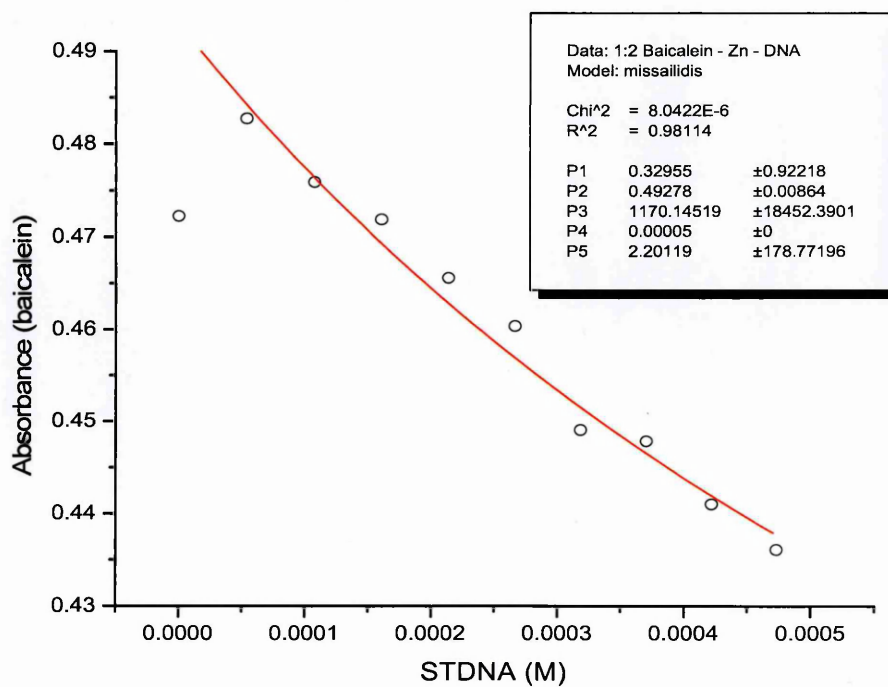


Figure 82: Baicalein – STDNA - Zn

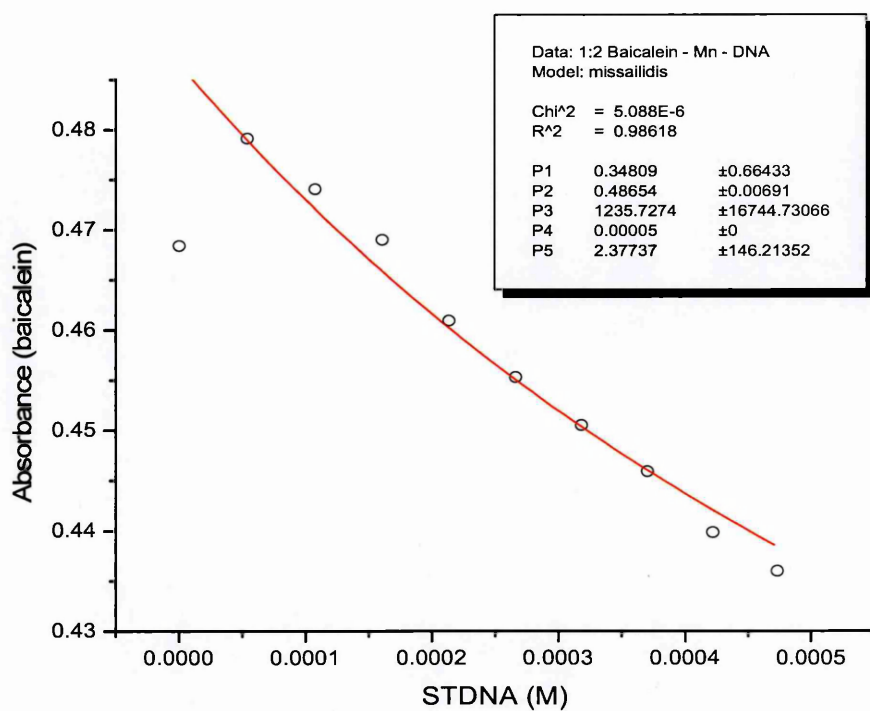


Figure 83: Baicalein - STDNA – Mn

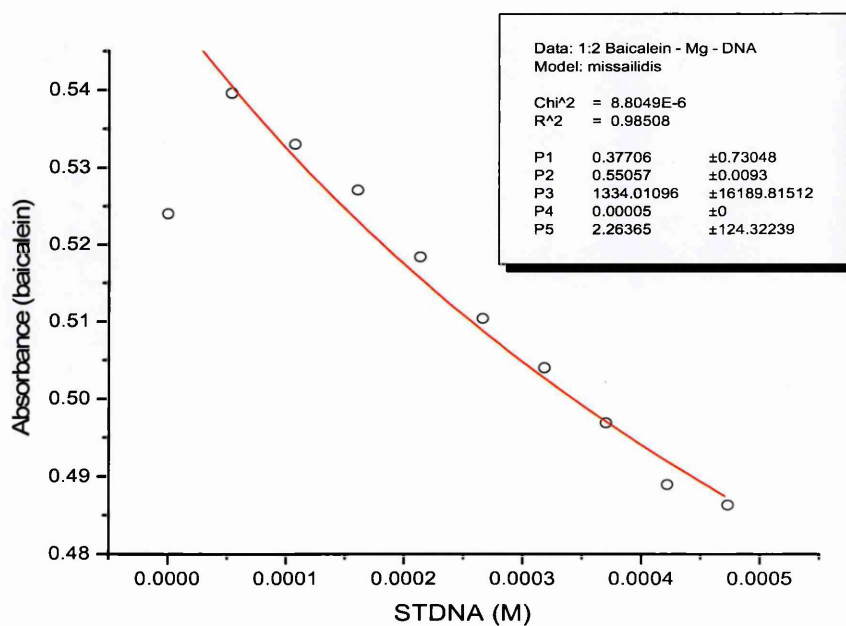


Figure 84: Baicalein – STDNA – Mg

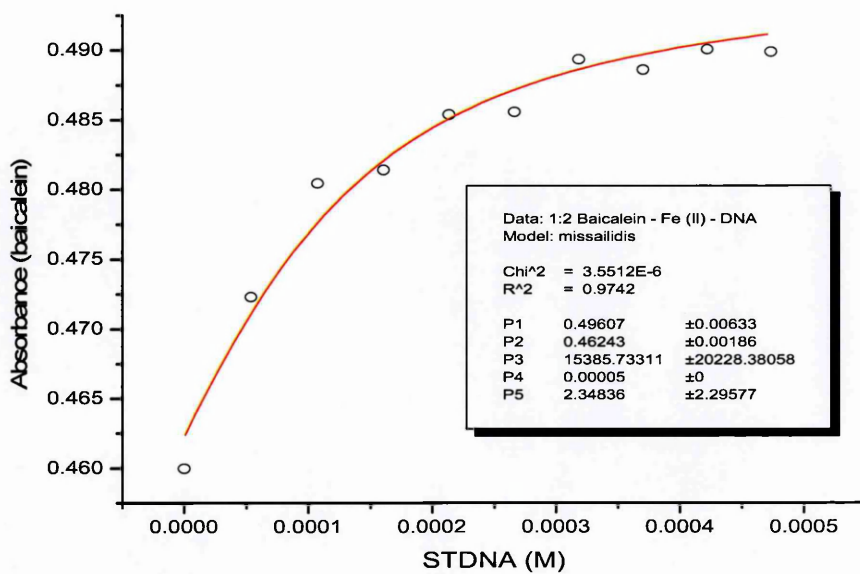


Figure 85: Baicalein - STDNA – Fe(II)

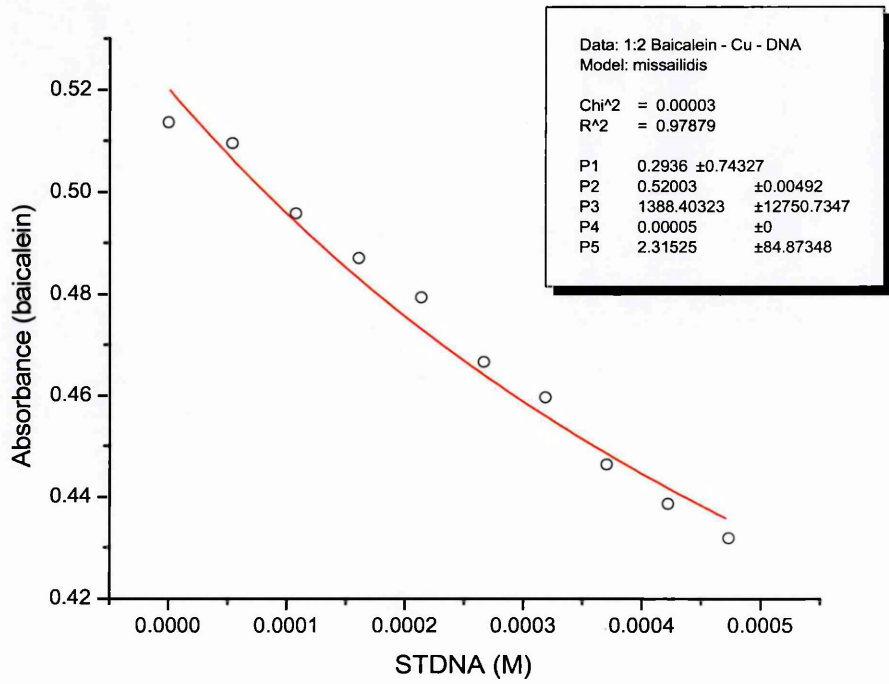


Figure 86: Baicalein – STDNA – Cu

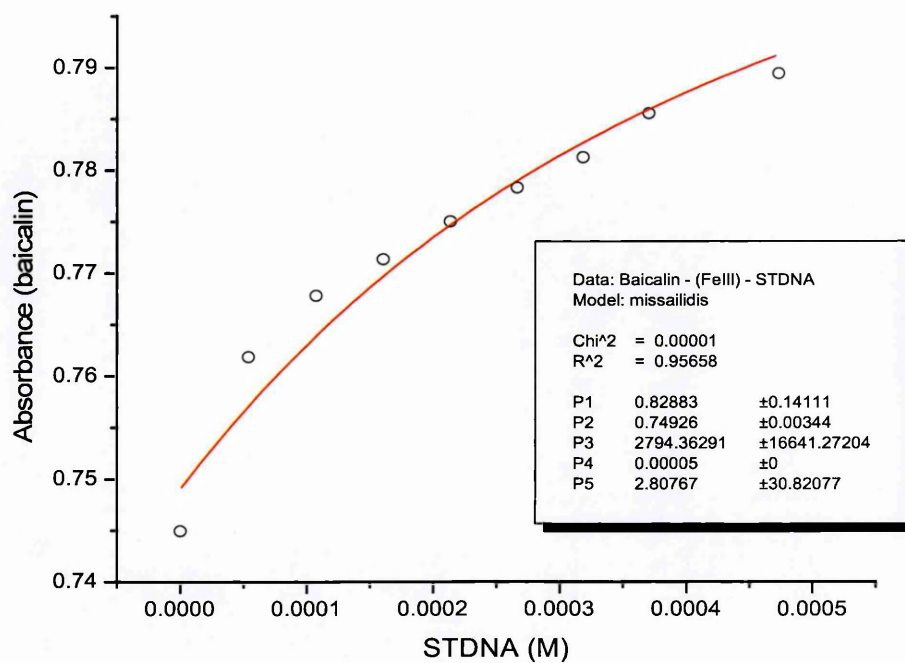


Figure 87: Baicalin – STDNA – Fe(II)

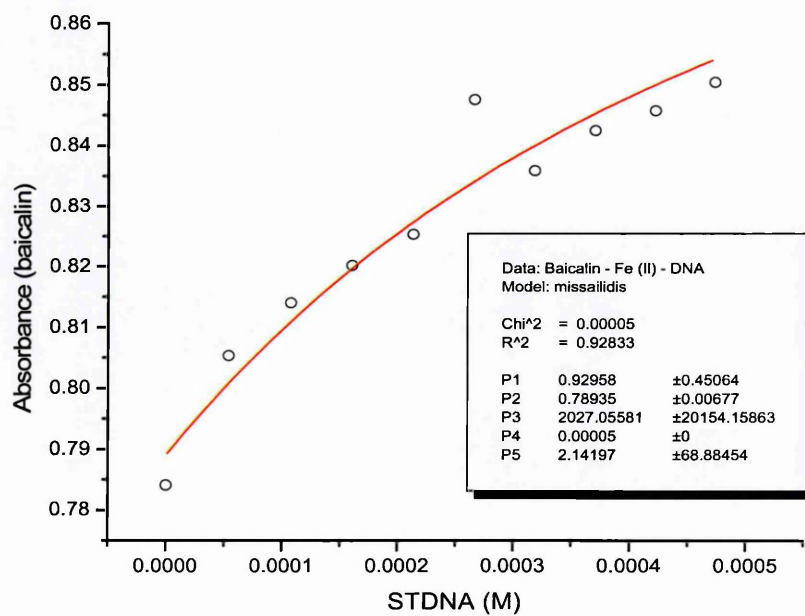


Figure 88: Baicalin – STDNA – Fe(III)

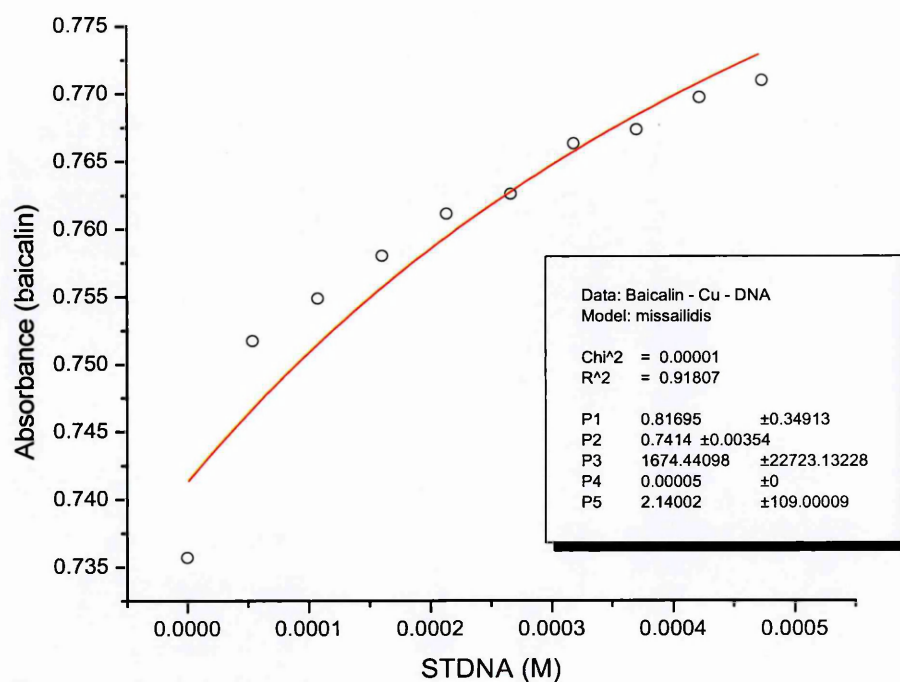


Figure 89: Baicalin – STDNA – Cu

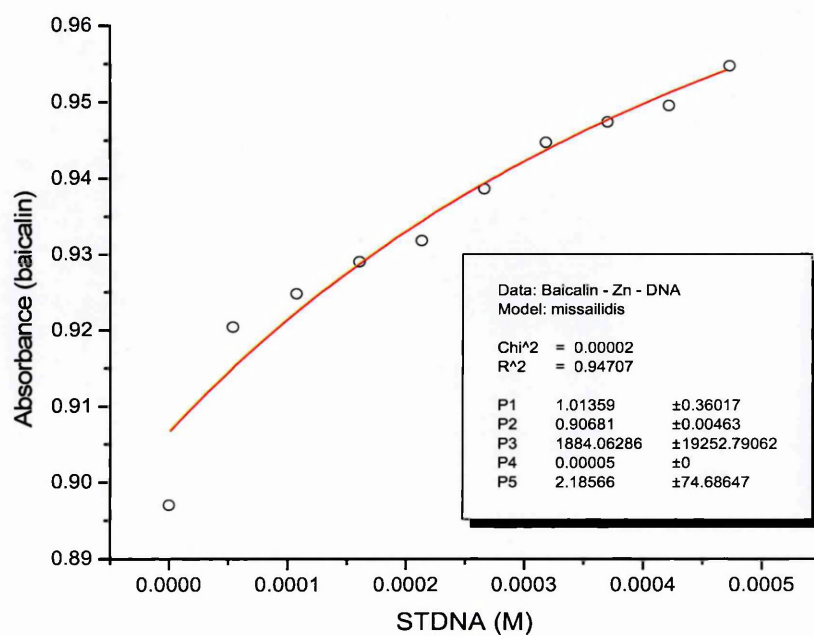


Figure 90: Baicalin – STDNA – Zn

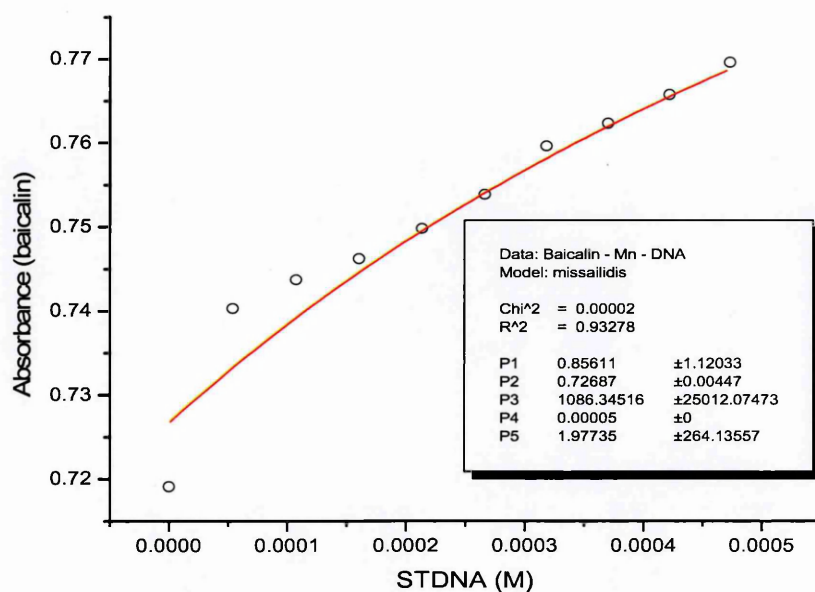


Figure 91: Baicalin – STDNA – Mn

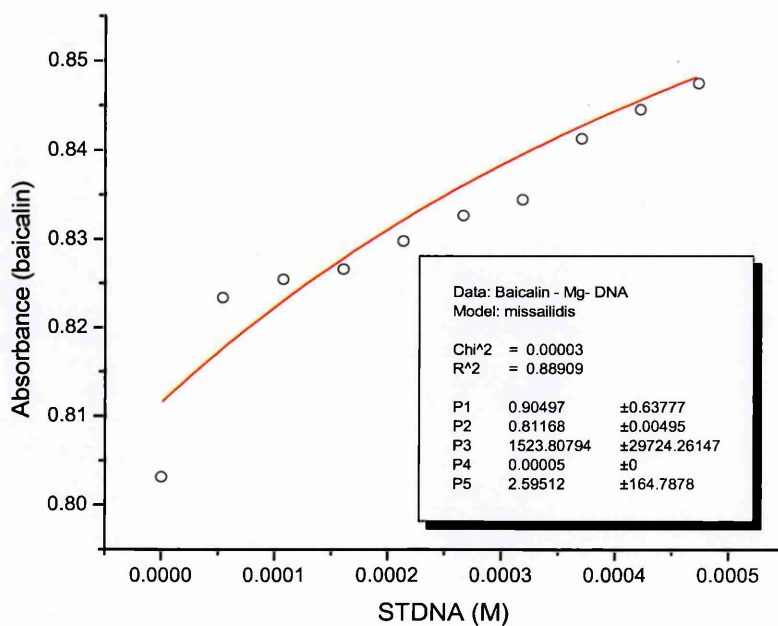


Figure 92: Baicalin – STDNA –Mg

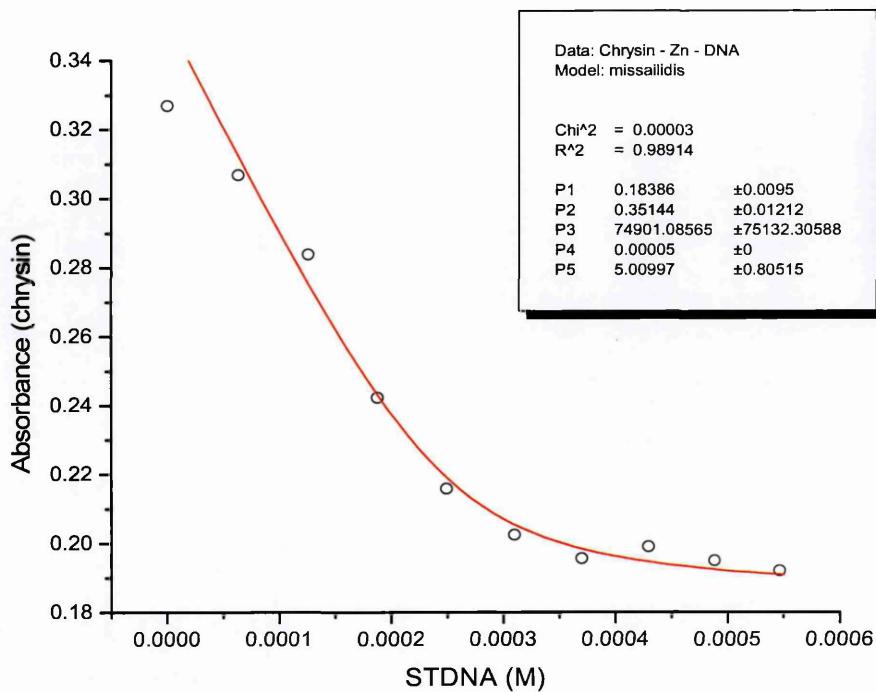


Figure 93: Chrysin – STDNA- Zn

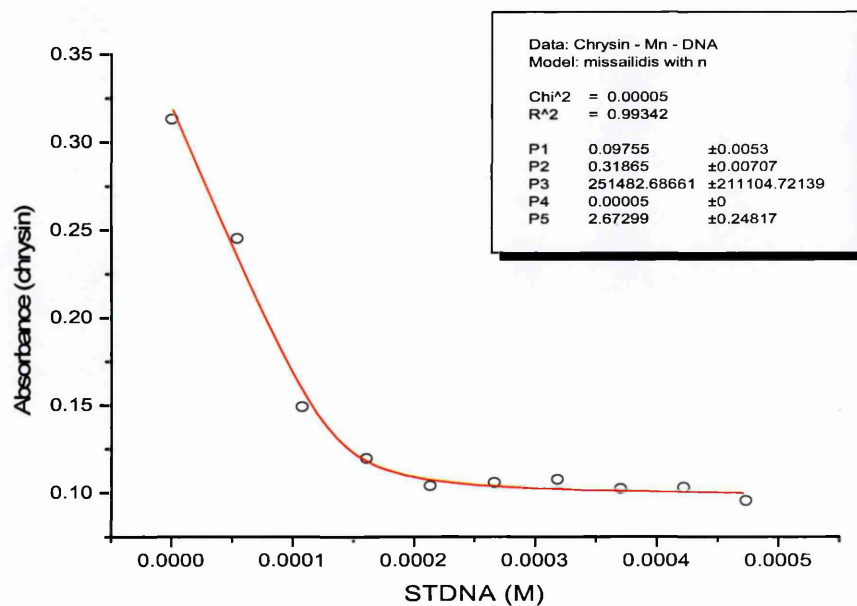


Figure 94: Chrysin – STDNA – Mn

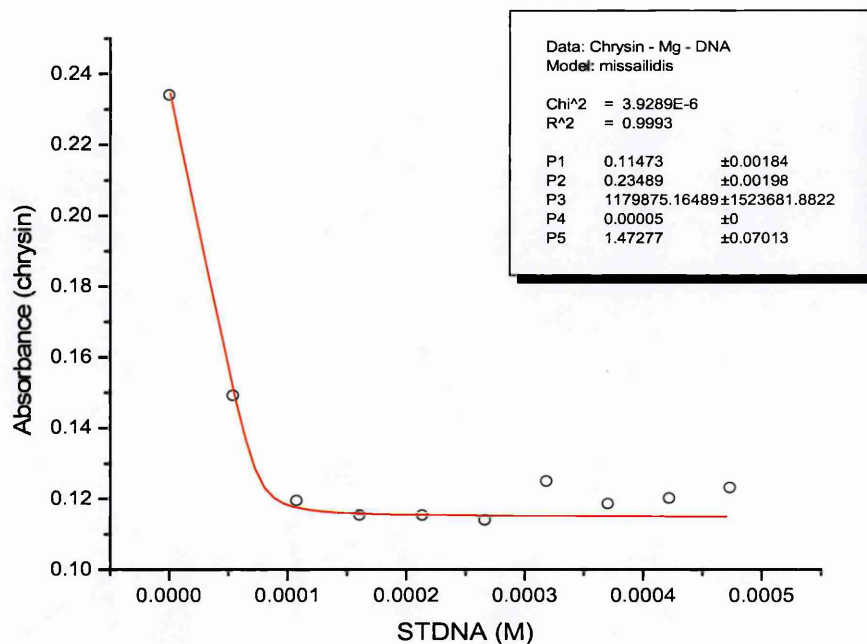


Figure 95: Chrysin – STDNA – Mg

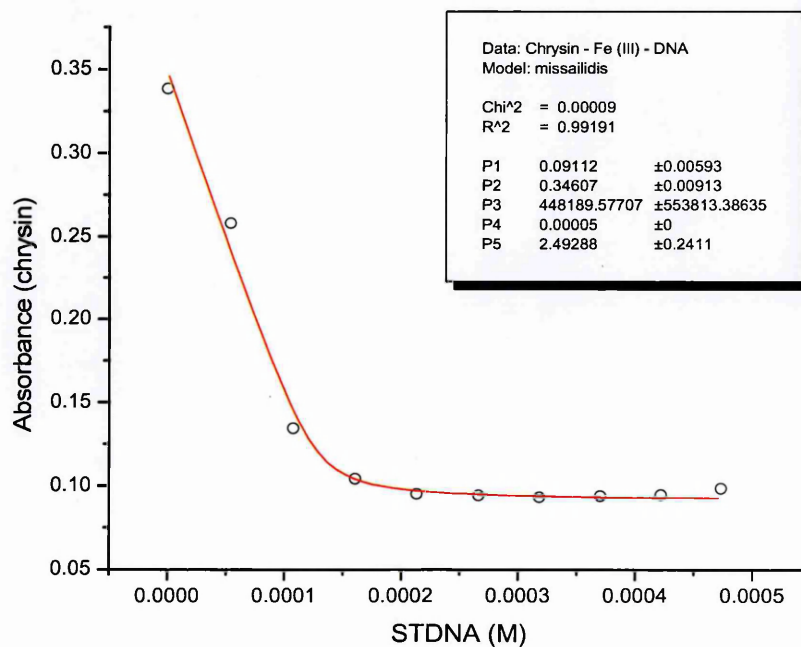


Figure 96: Chrysin – STDNA- Fe(III)

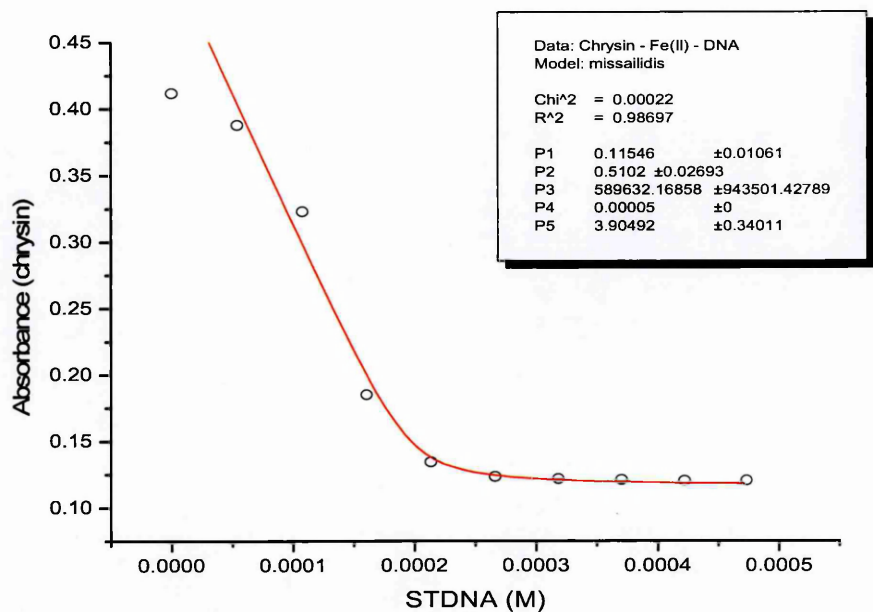


Figure 97: Chrysin – STDNA – Fe(II)

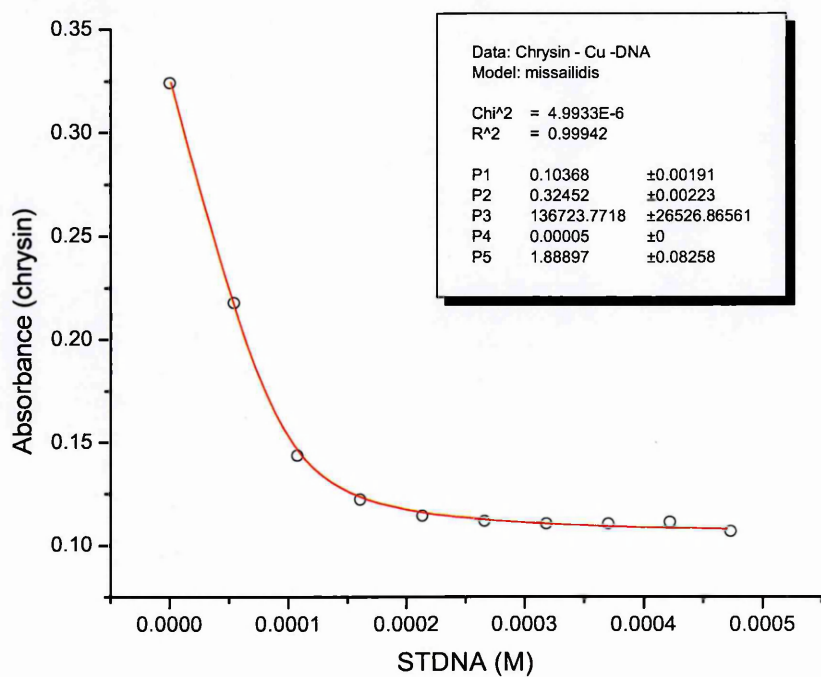


Figure 98: Chrysin – STDNA – Cu

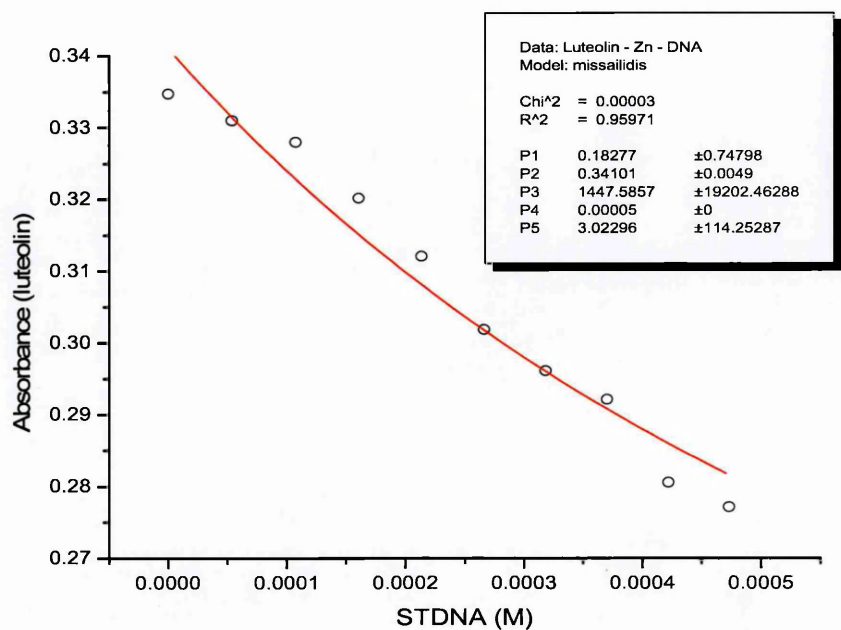


Figure 99: Luteolin – STDNA – Zn

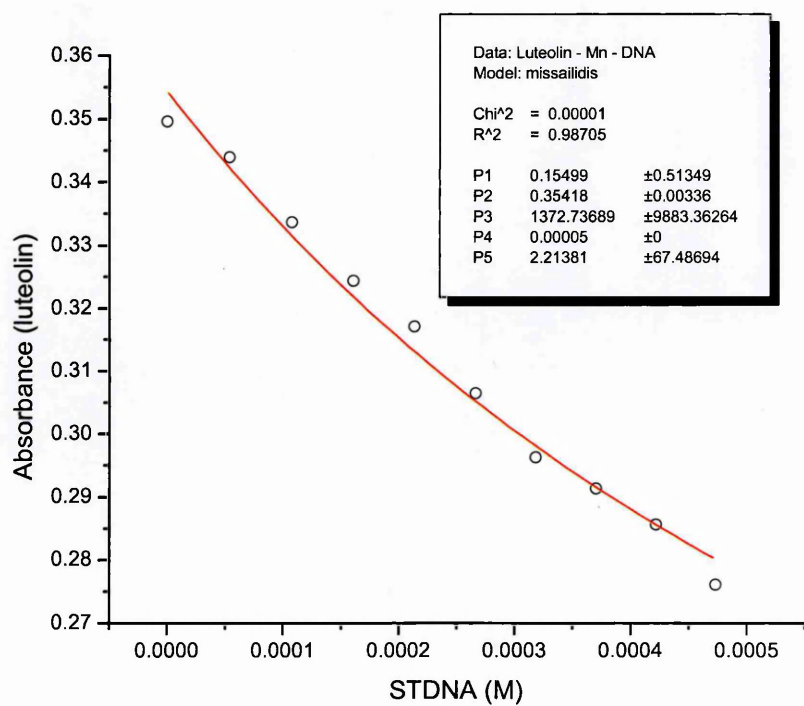


Figure 100: Luteolin – STDNA- Mn

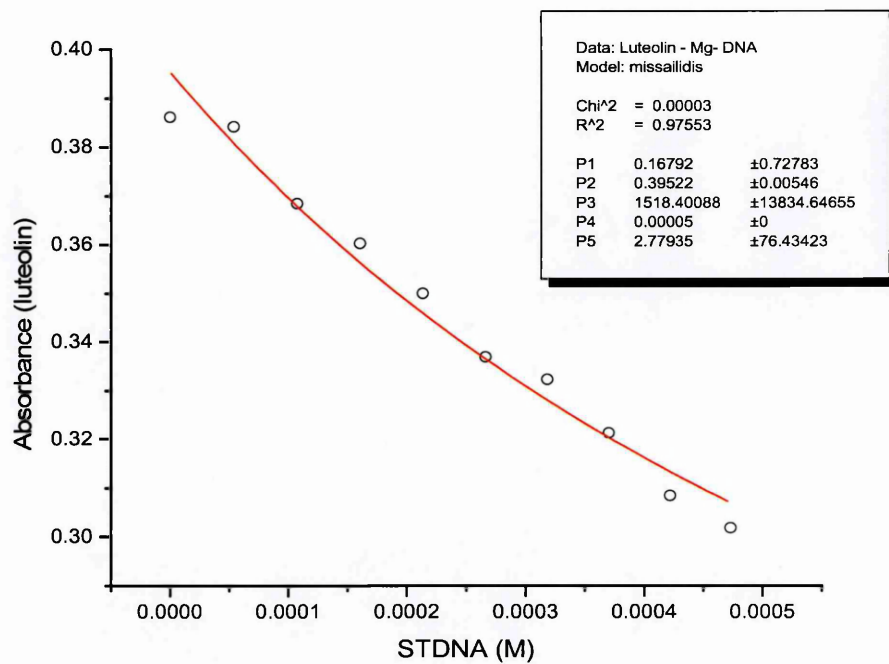


Figure 101: Luteolin – STDNA – Mg

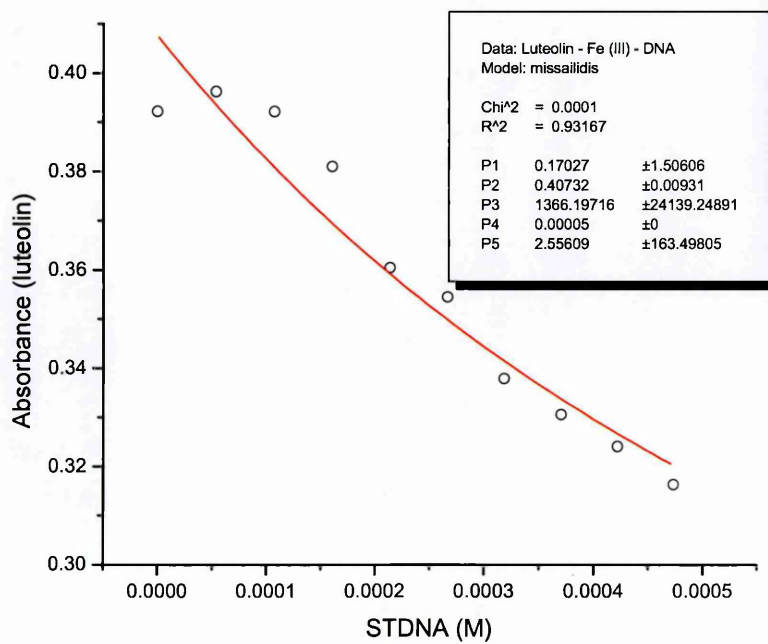


Figure 102: Luteolin – STDNA – Fe(III)

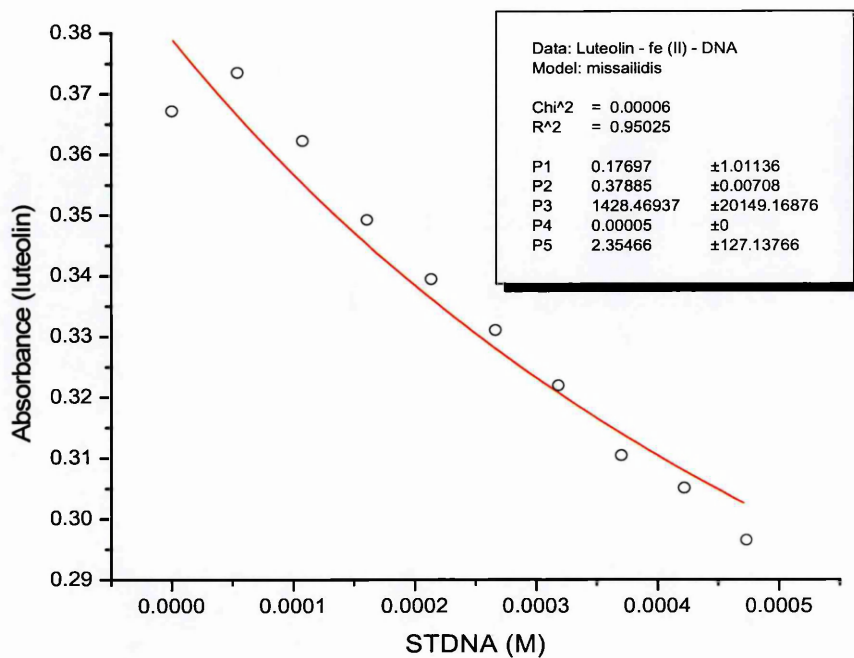


Figure 103: Luteolin – STDNA – Fe(II)

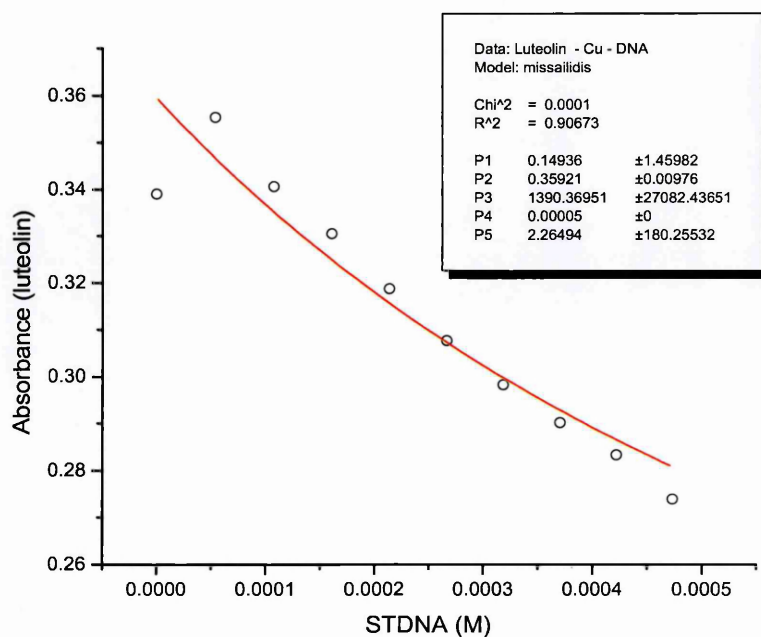


Figure 104: Luteolin – STDNA – Cu

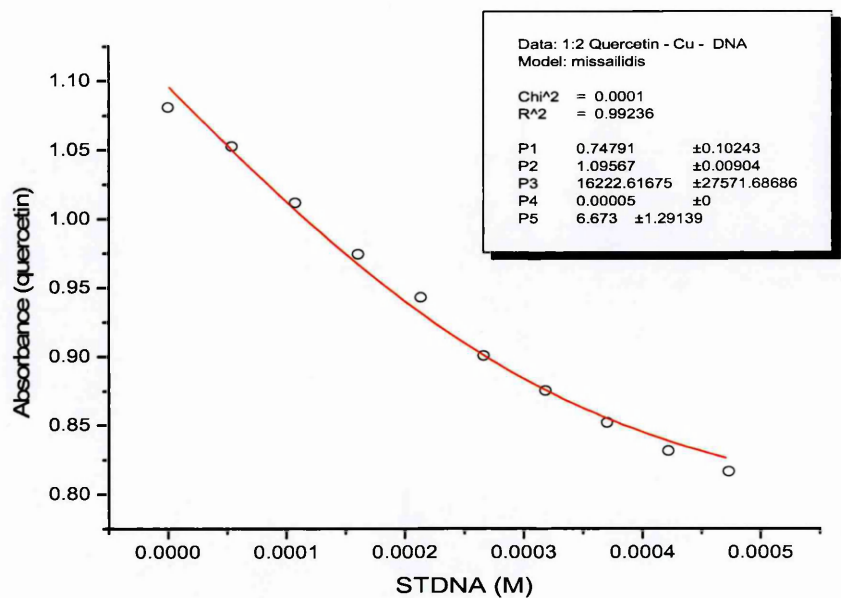


Figure 105: Quercetin – STDNA – Cu

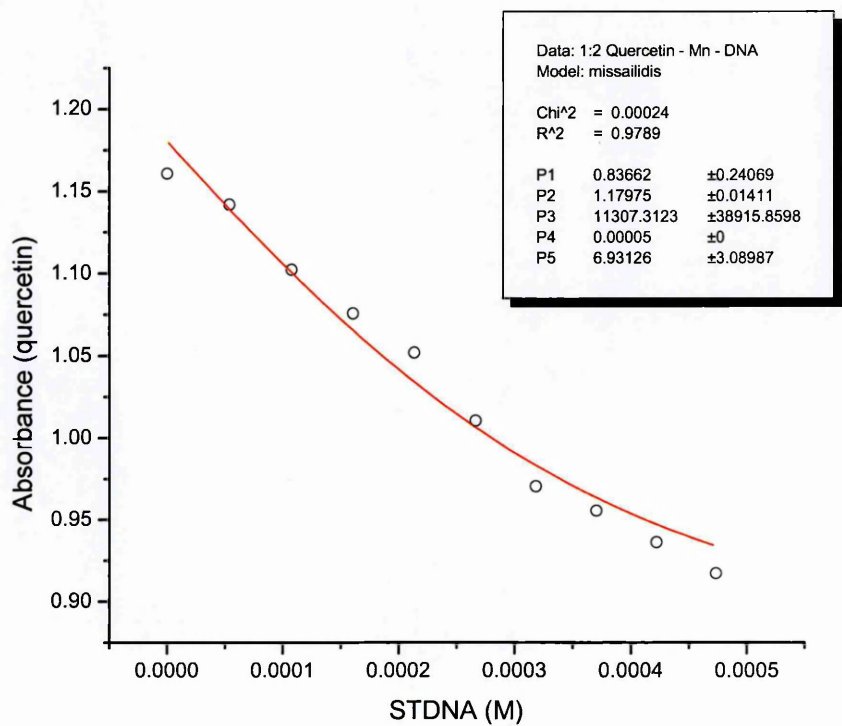


Figure 106: Quercetin – STDNA- Mn

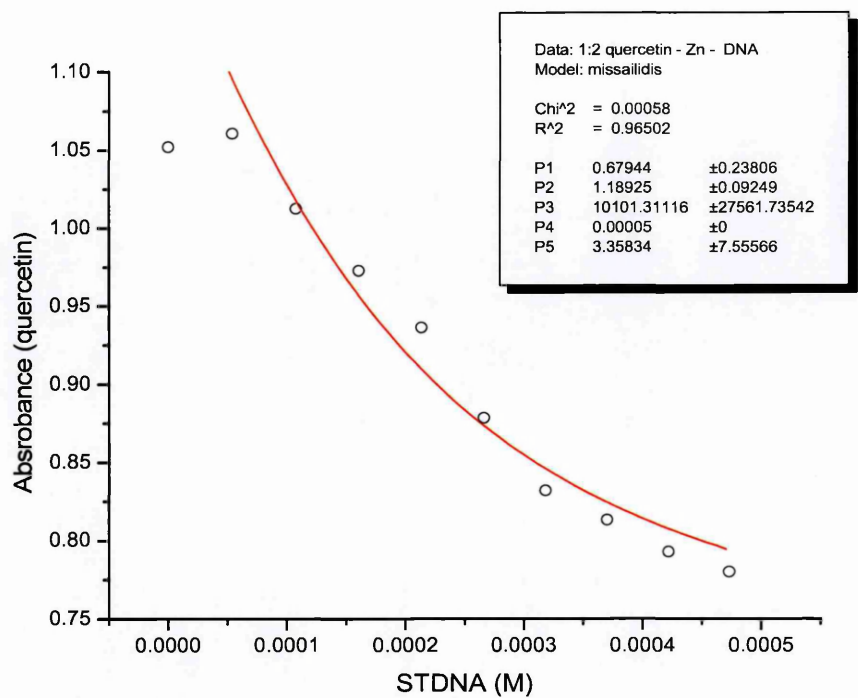


Figure 107: Quercetin – STDNA – Zn

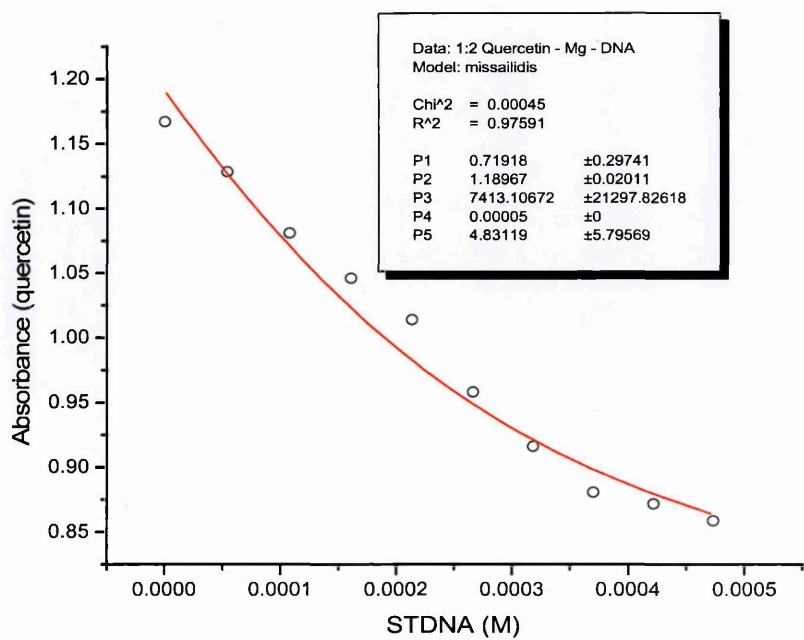


Figure 108: Quercetin –STDNA – Mg

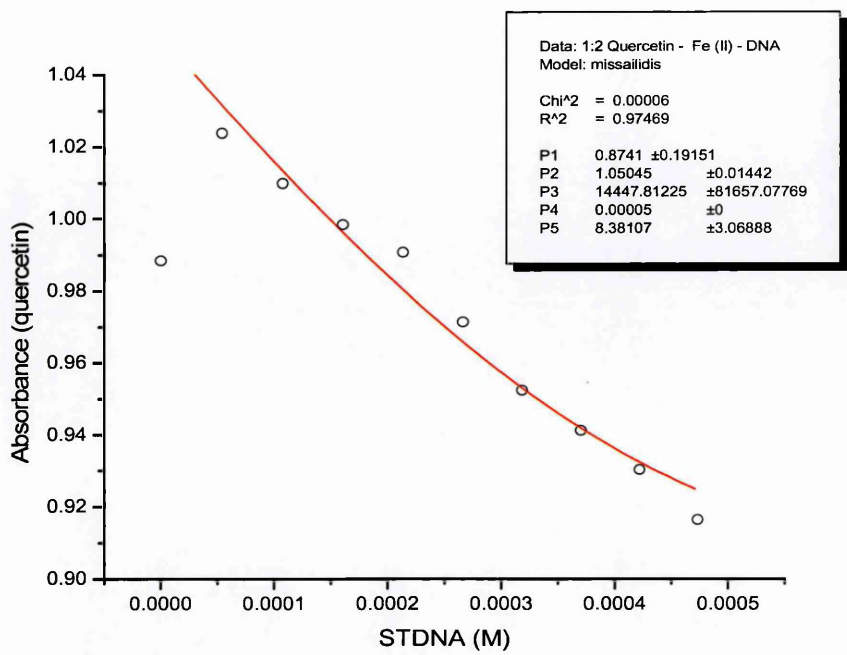


Figure 109: Quercetin – STDNA – Fe(II)

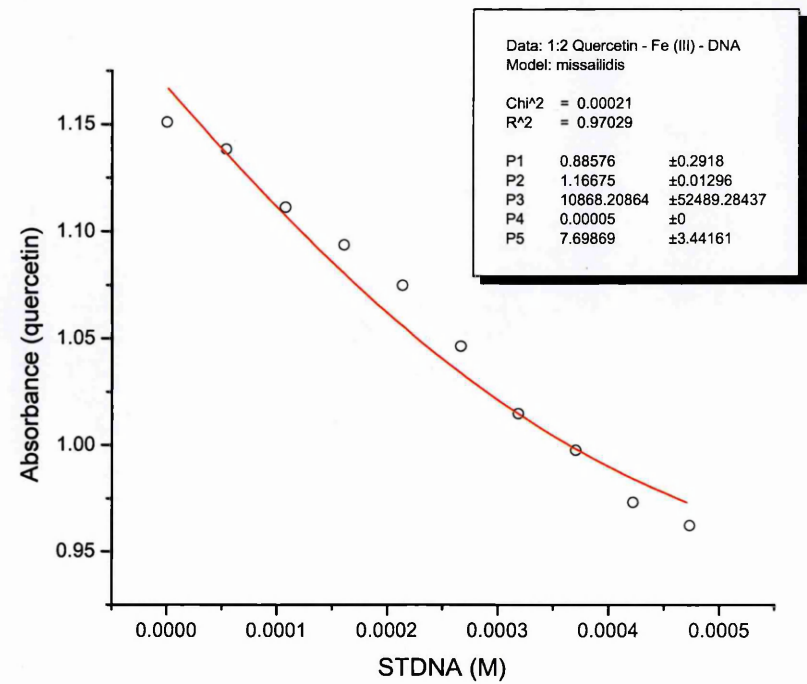


Figure 110: Quercetin – STDNA – Fe(III)

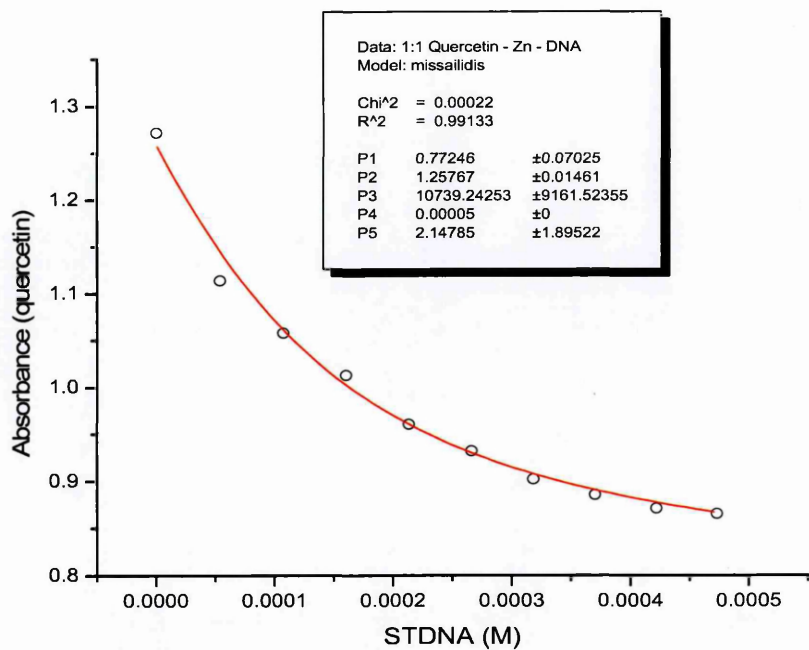


Figure 111: Quercetin - STDNA – Zn

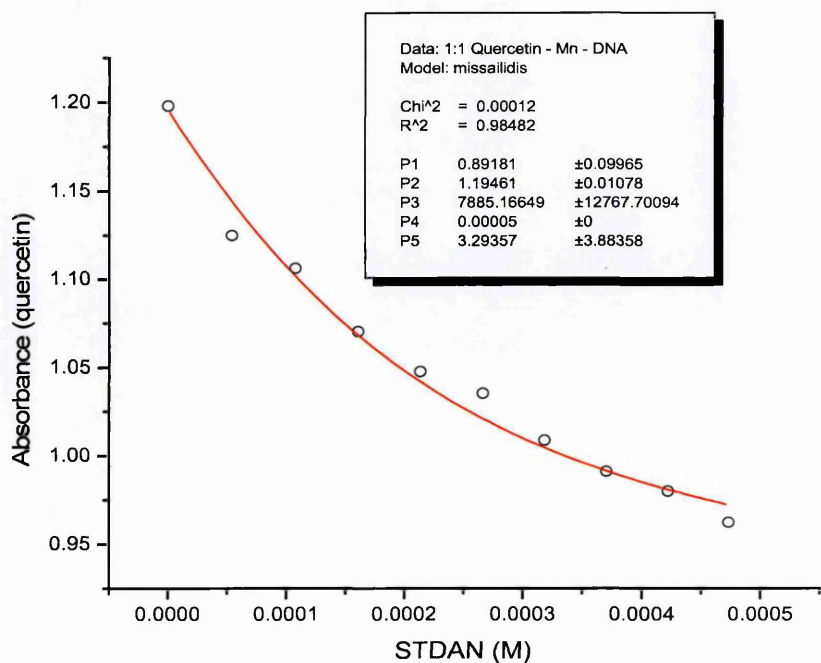


Figure 112: Quercetin – STDNA – Mn

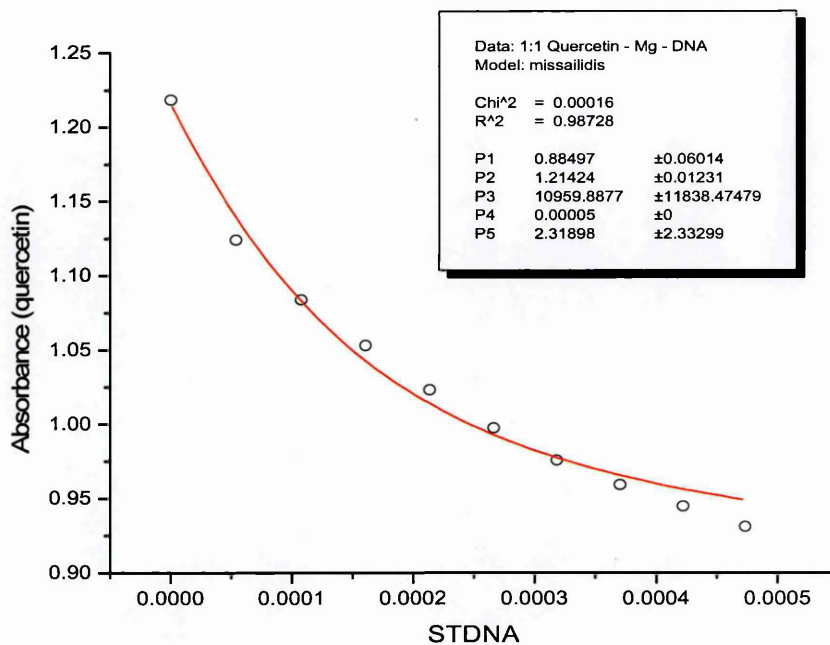


Figure 113: Quercetin – STDNA – Mg

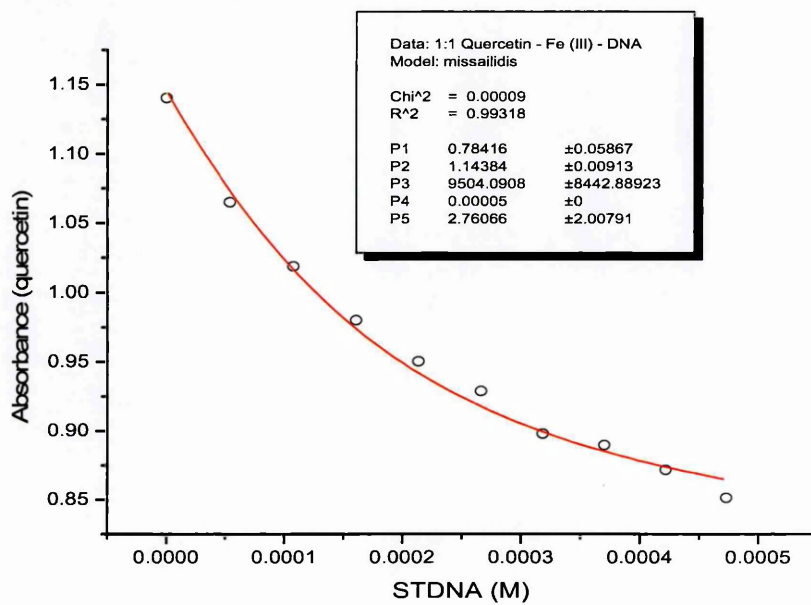


Figure 114: Quercetin - STDNA – Fe(III)

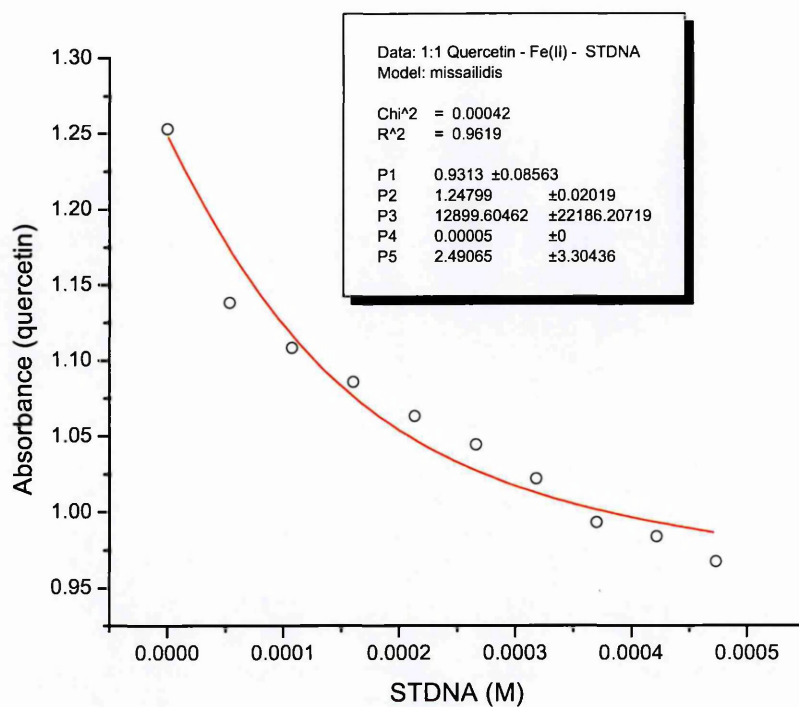


Figure 115: Quercetin - STDNA – Fe(II)

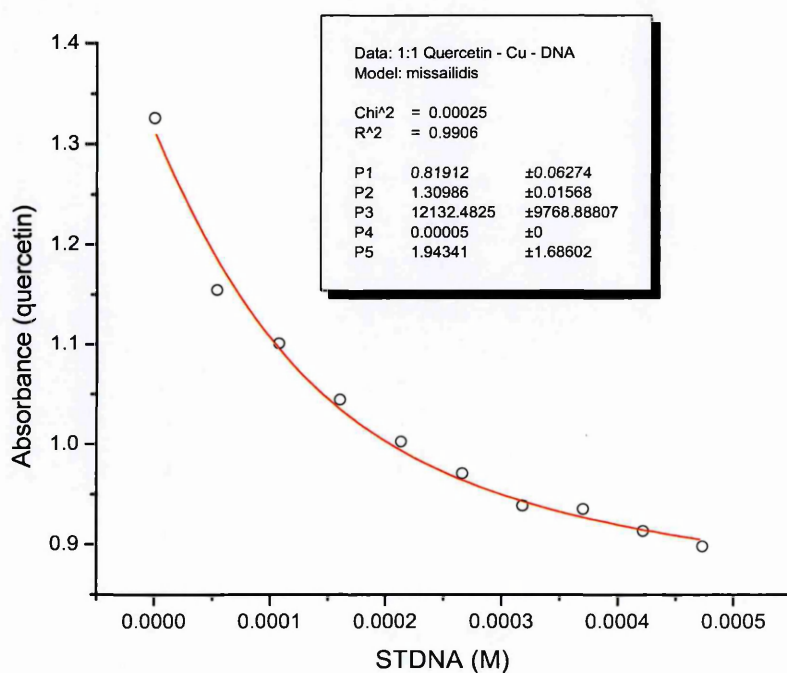


Figure 116: Quercetin – STDNA – Cu

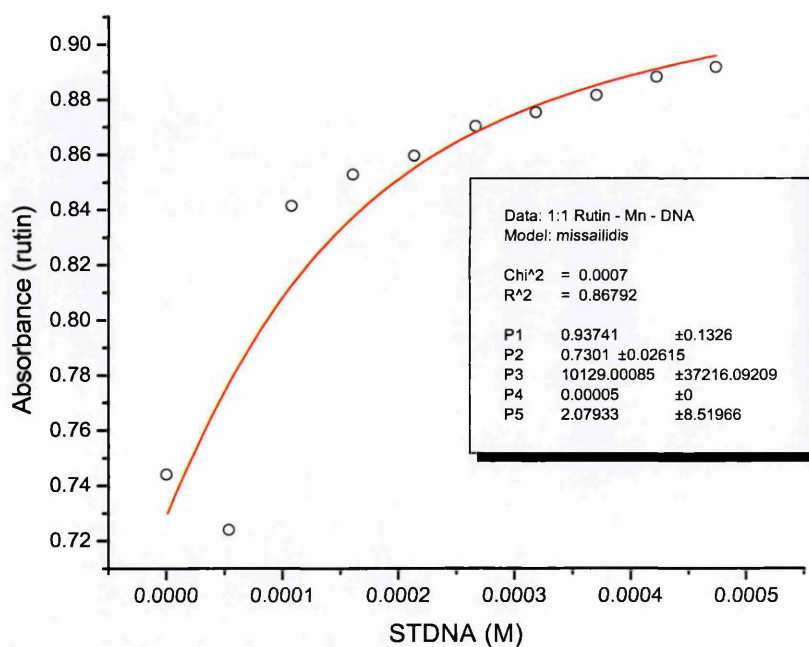


Figure 117: Rutin – STDNA – Mn

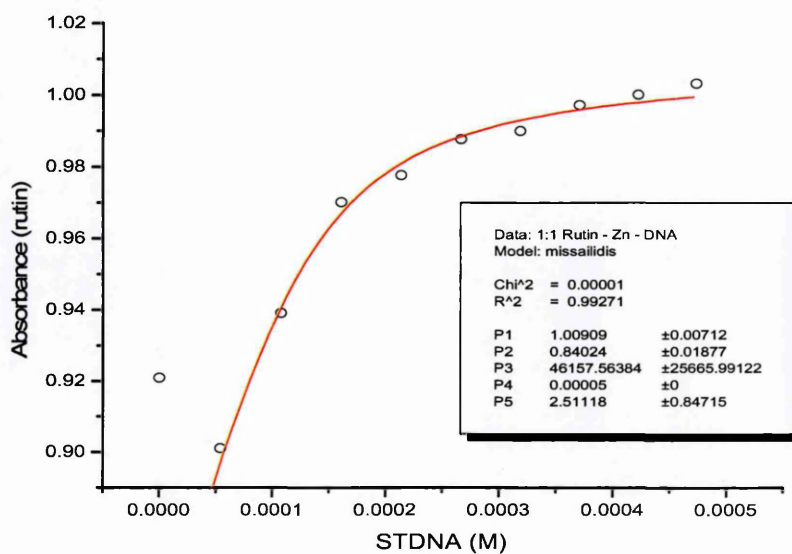


Figure 118: Rutin – STDNA- Zn

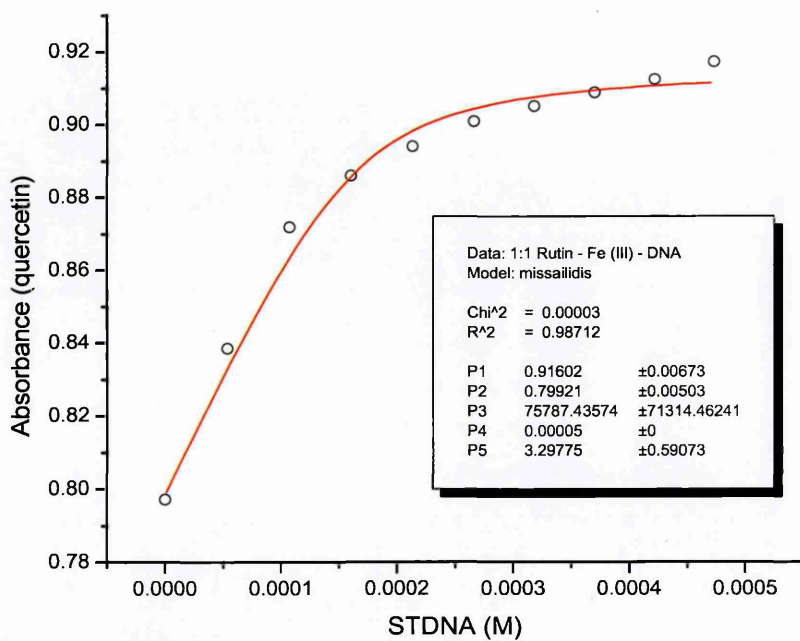


Figure 119: Rutin – STDNA – Fe(II)

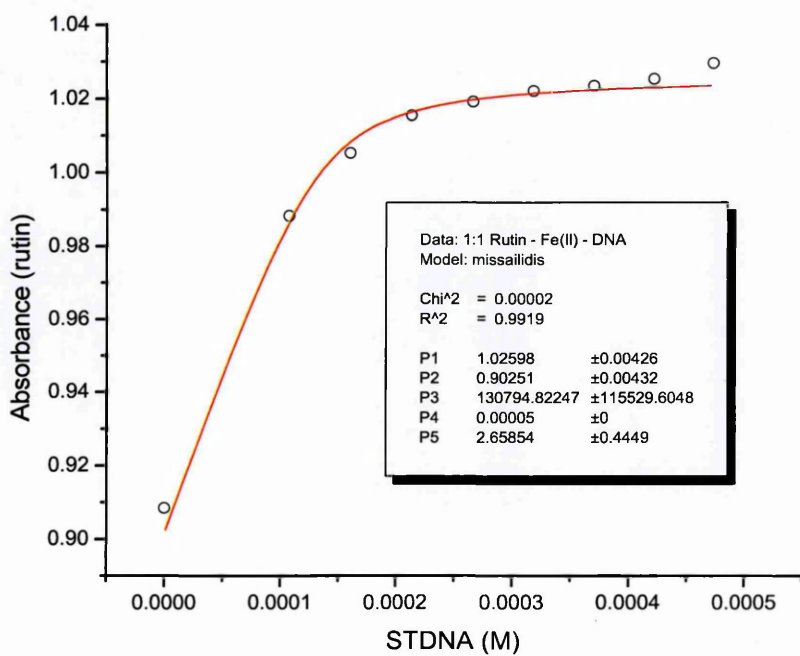


Figure 120: Rutin – STDNA – Fe(III)

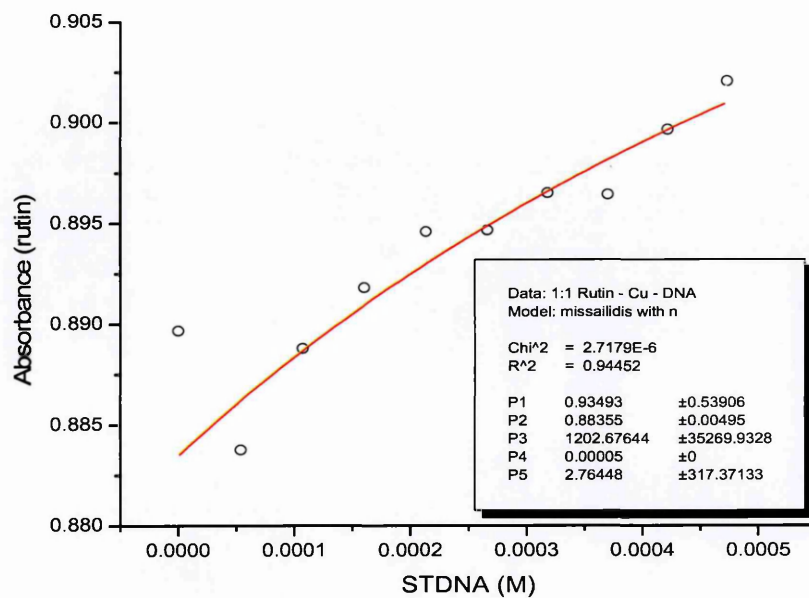


Figure 121: Rutin – STDNA – Cu

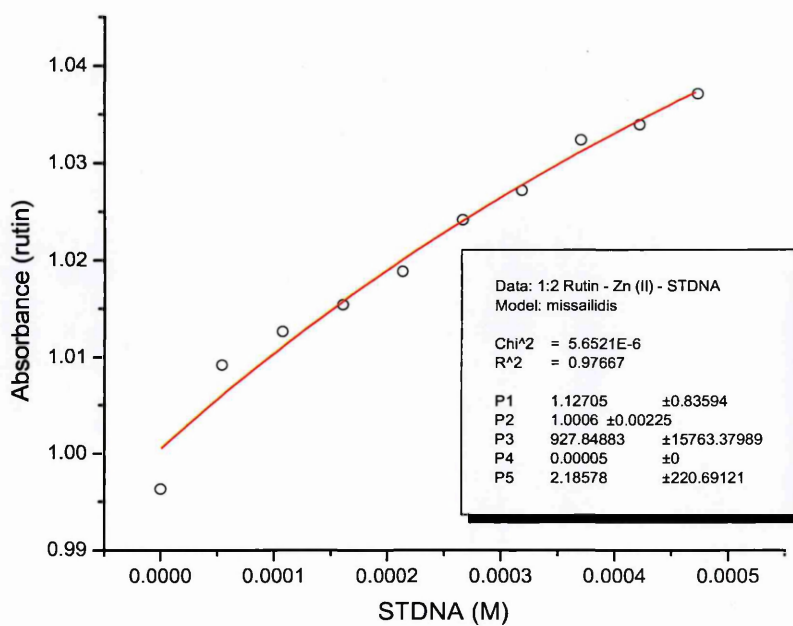


Figure 122: Rutin – Zn – STDNA

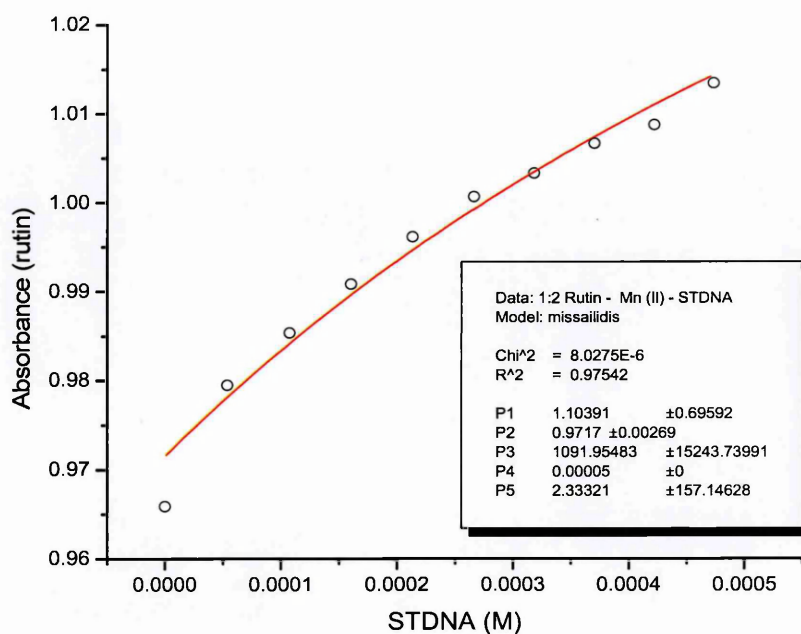


Figure 123: Rutin – STDNA – Mn

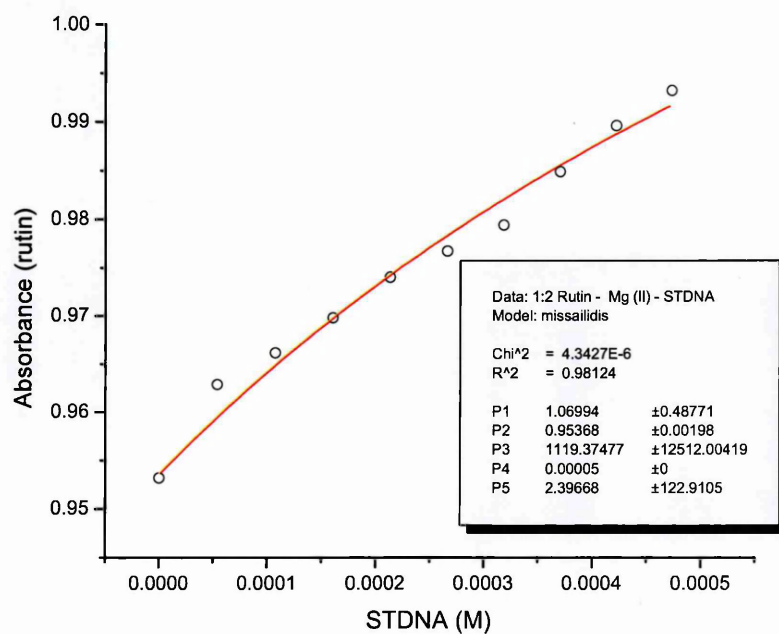


Figure 124: Rutin – STDNA – Mg

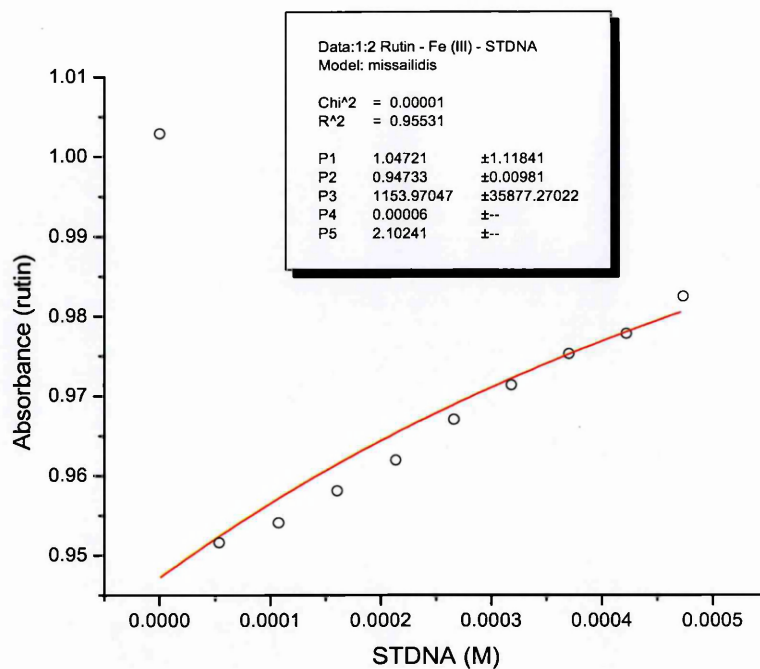


Figure 125: Rutin – STDNA – Fe(III)

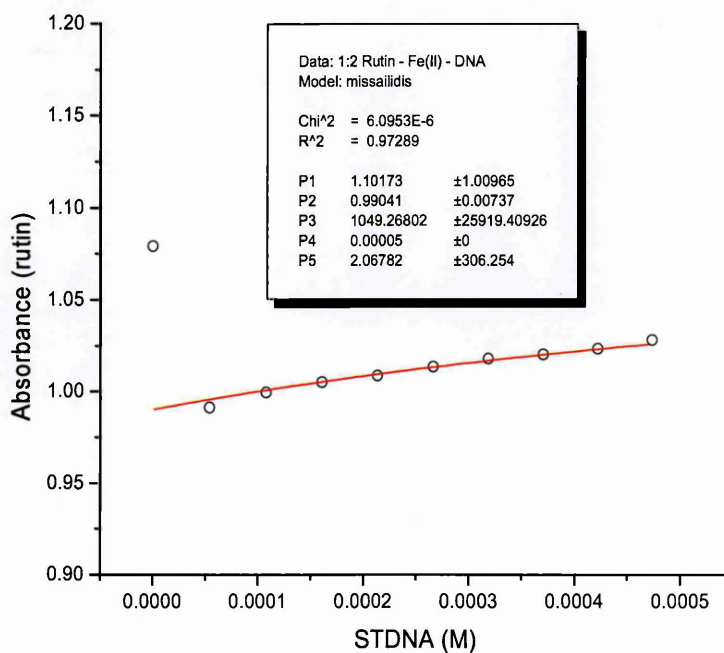


Figure 126: Rutin – STDNA – Fe(II)

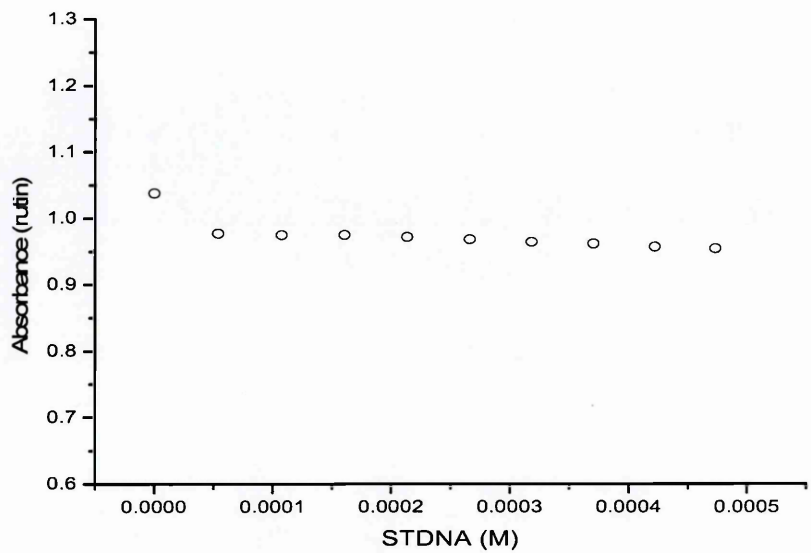


Figure 127: Rutin – STDNA – Cu

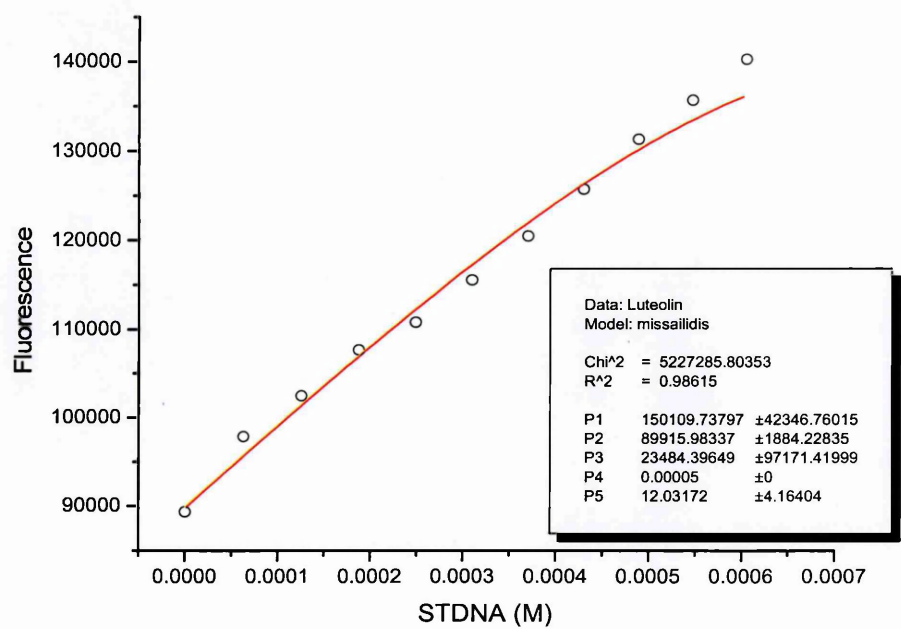


Figure 128: Luteolin – STDNA

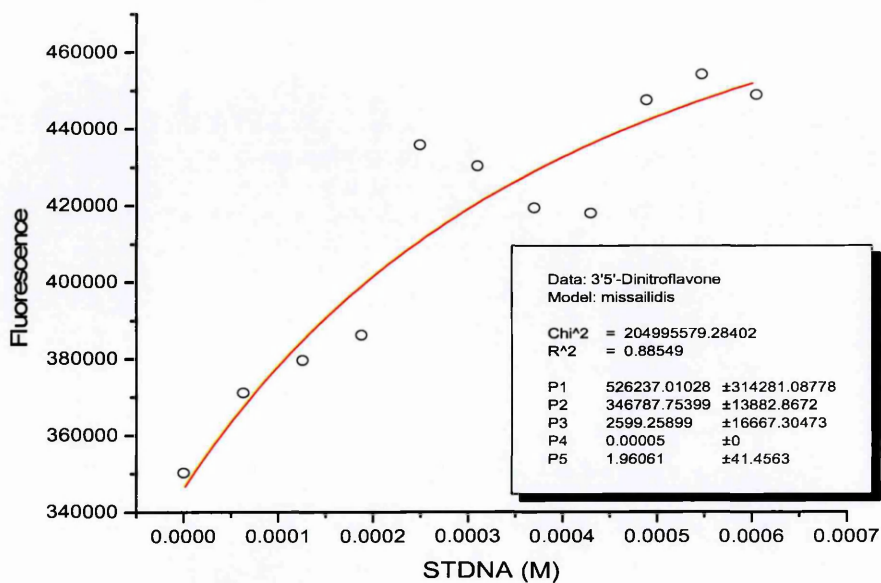


Figure 129: 3'5'- dinitroflavone - STDNA

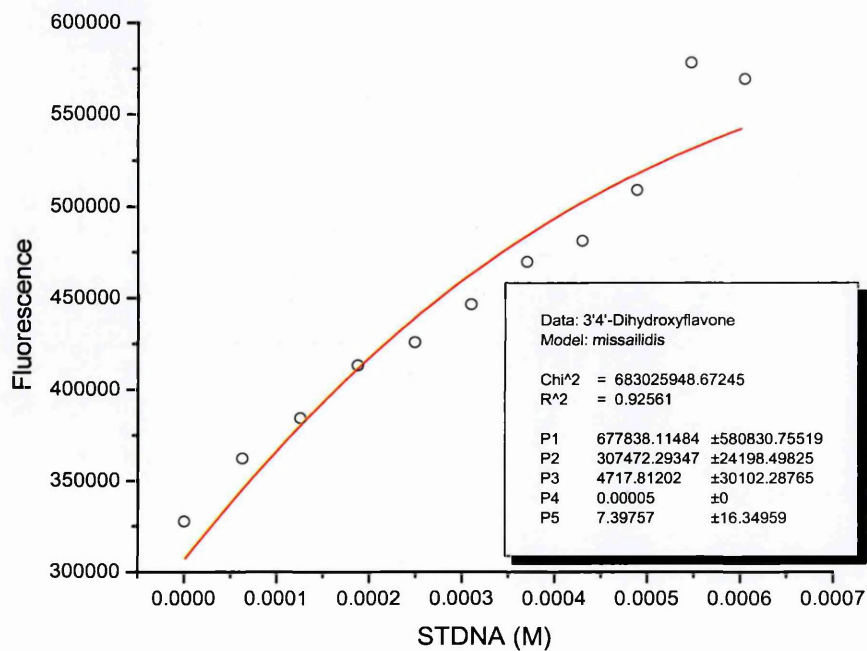


Figure 130: 3'4'-dihydroxyflavone – STDNA

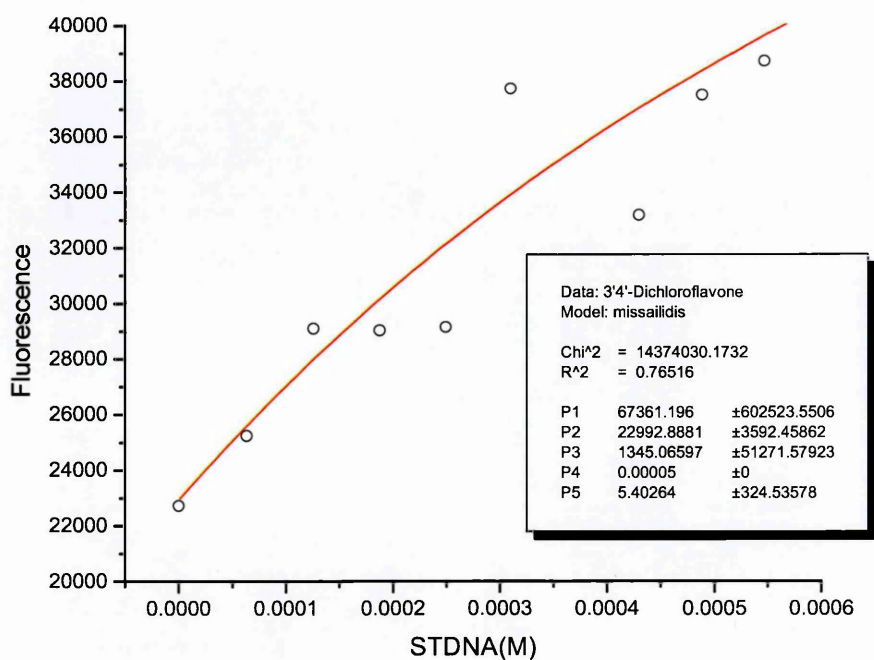


Figure 131: 3',4'-dichloroflavone – STDNA

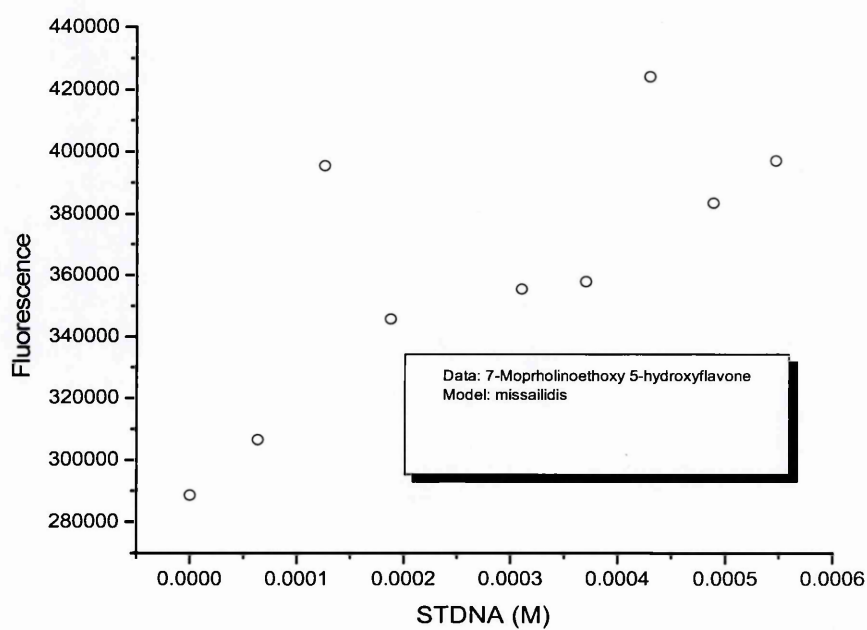


Figure 132: 7-morpholino, 5-hydroxyflavone – STDNA

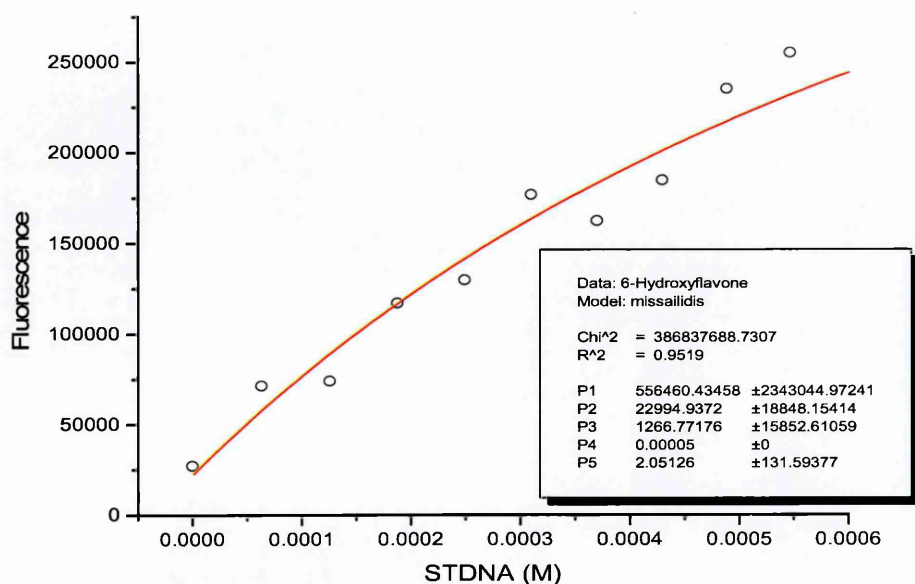


Figure 133: 5-hydroxyflavone – STDNA

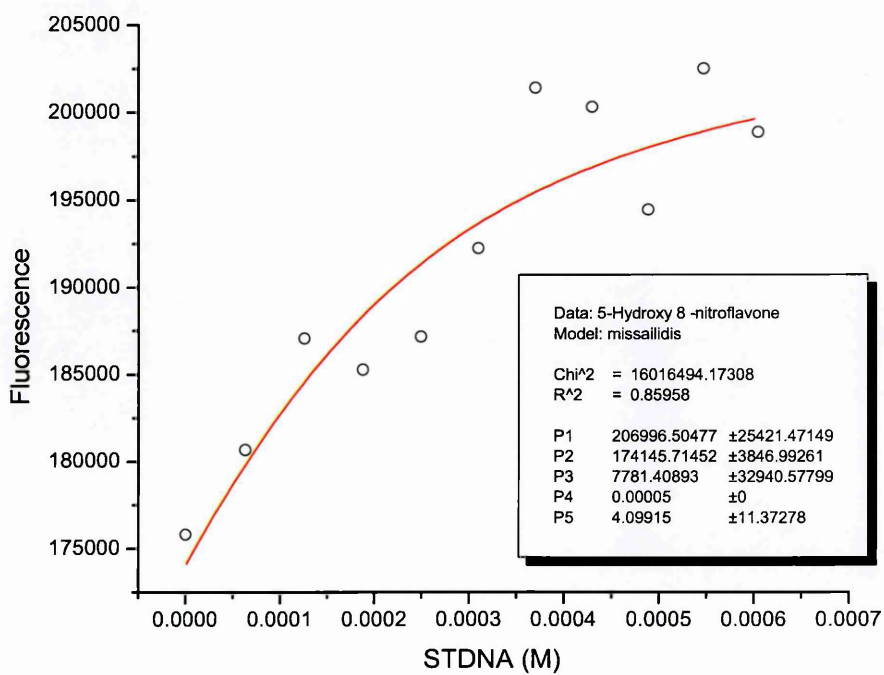


Figure 134: 5-hydroxy,8-nitroflavone - STDNA

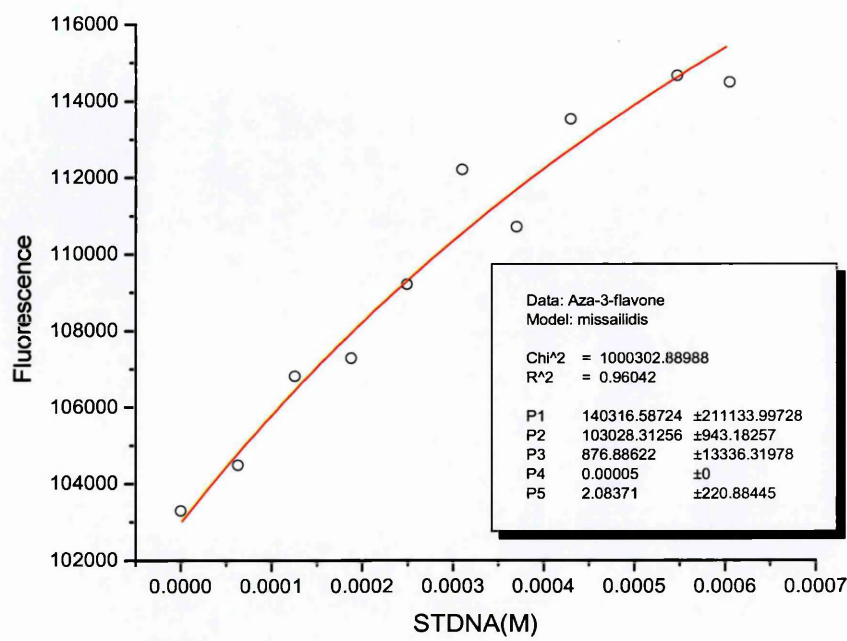


Figure 135: Aza-3-flavone - STDNA

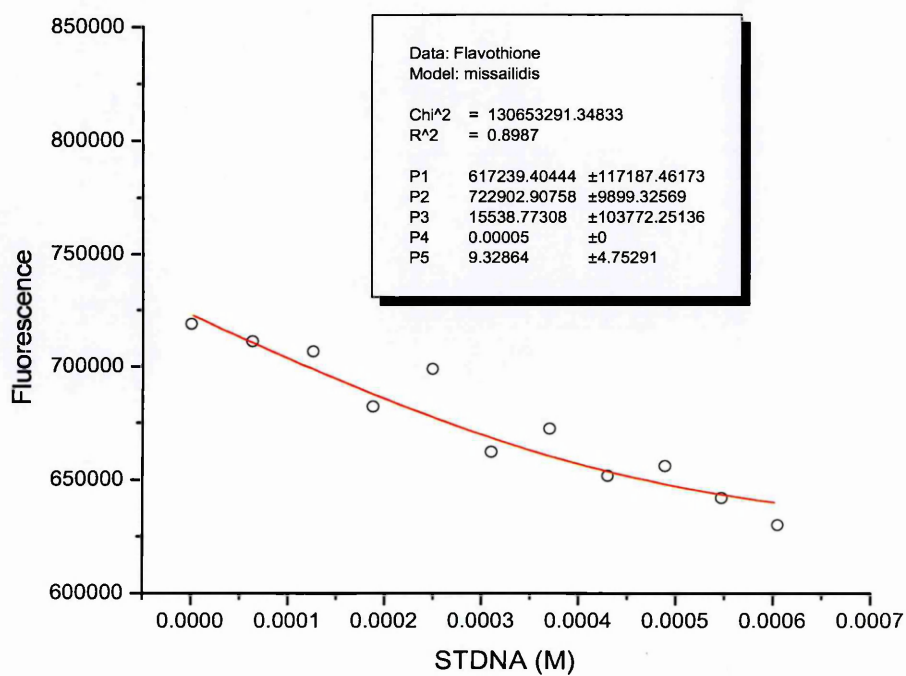


Figure 136: Flavothione - STDNA

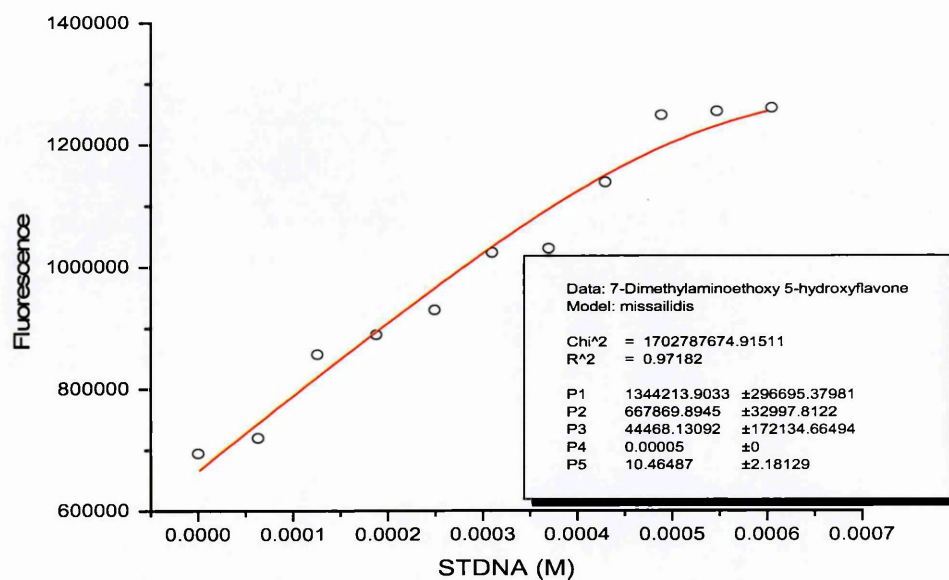


Figure 137: 7-dimethylaminoethoxy,5-hydroxyflavone – STDNA

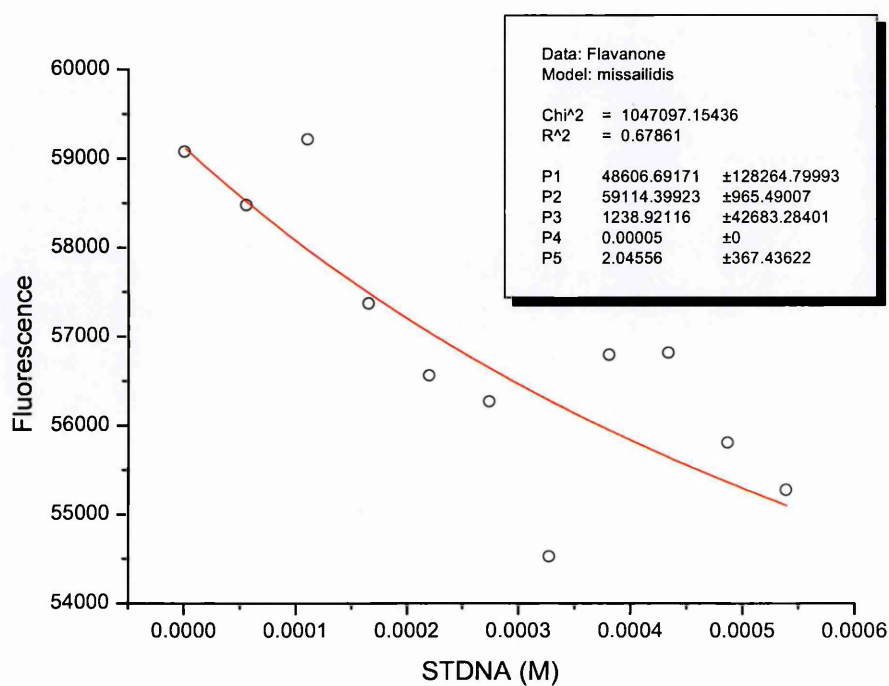


Figure 138: Flavanone - STDNA

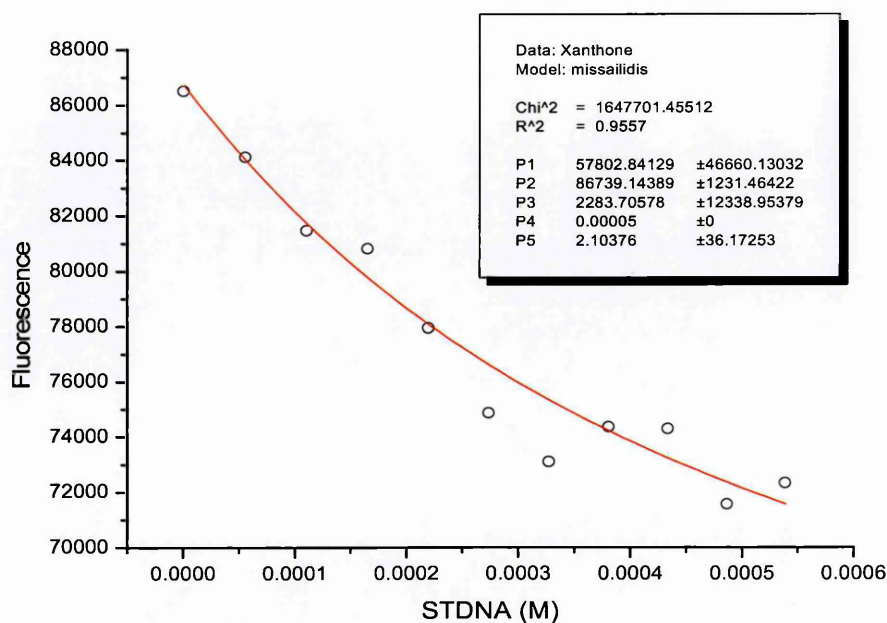


Figure 139: Xanthone – STDNA

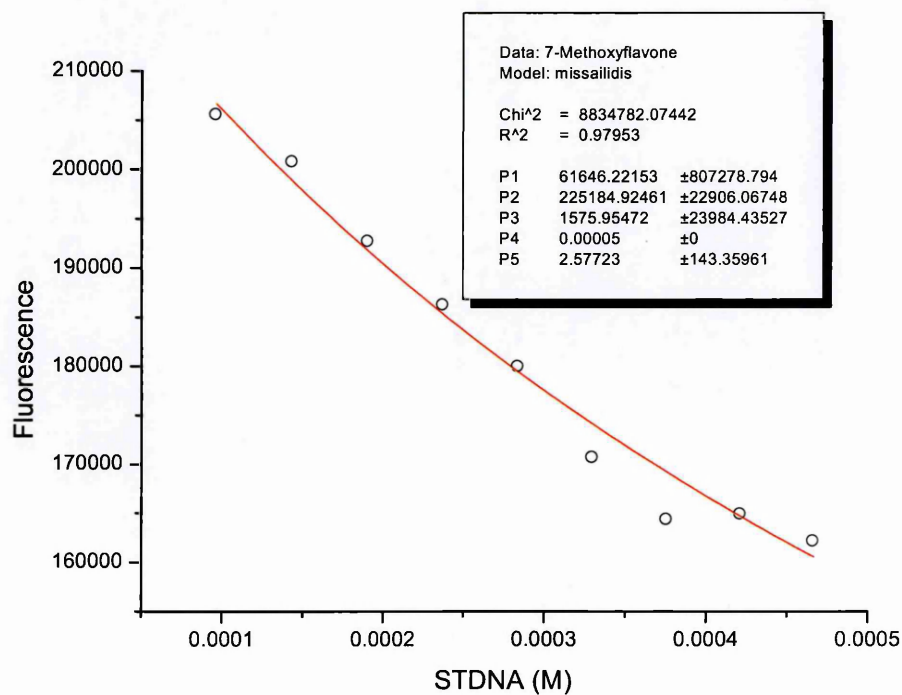


Figure 140: 7-methoxyflavone - STDNA

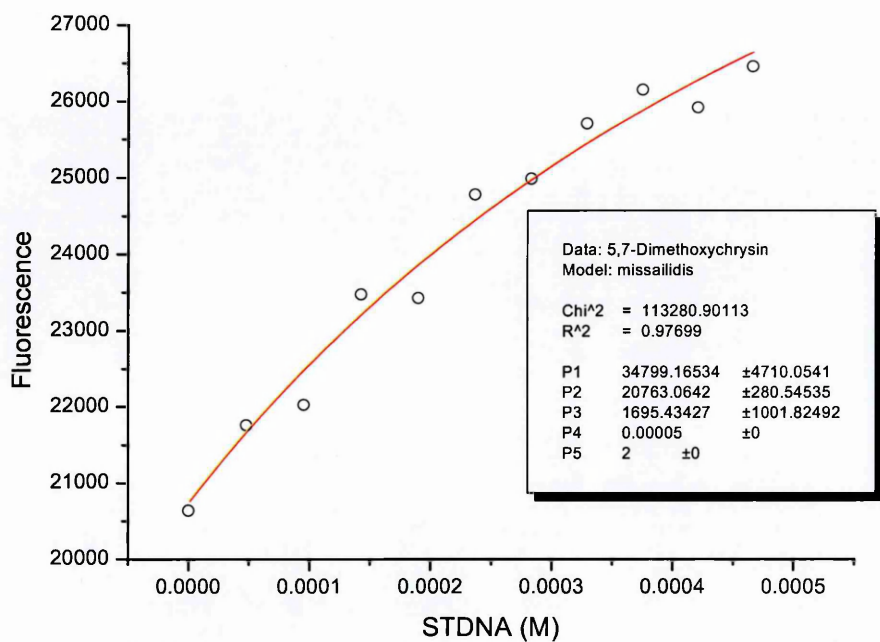


Figure 141: 5,7-dimethoxyflavone - STDNA

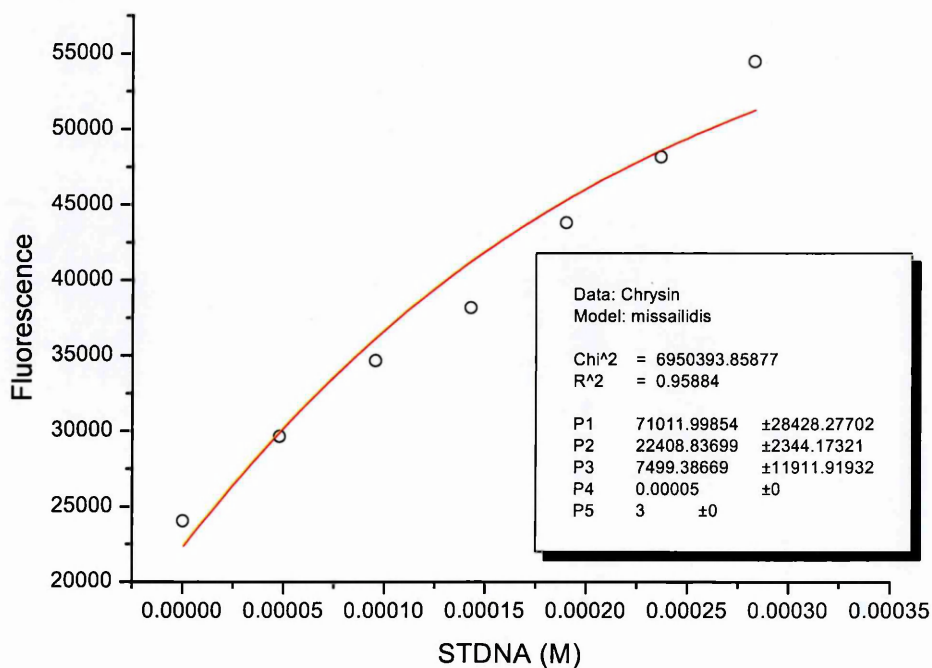


Figure 142: Chrysin – STDNA

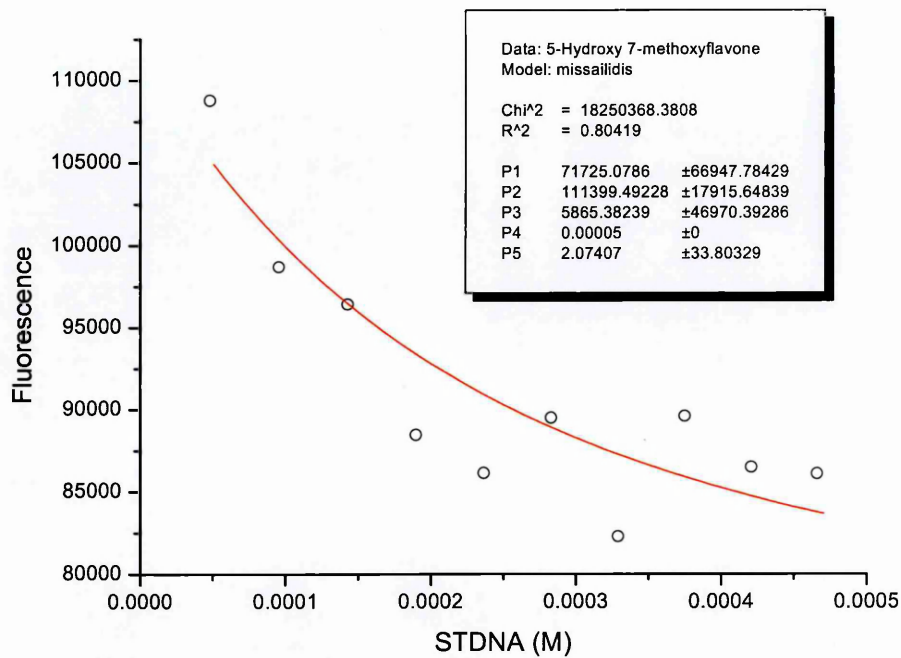


Figure 143: 5-hydroxy,7-methoxyflavone – STDNA

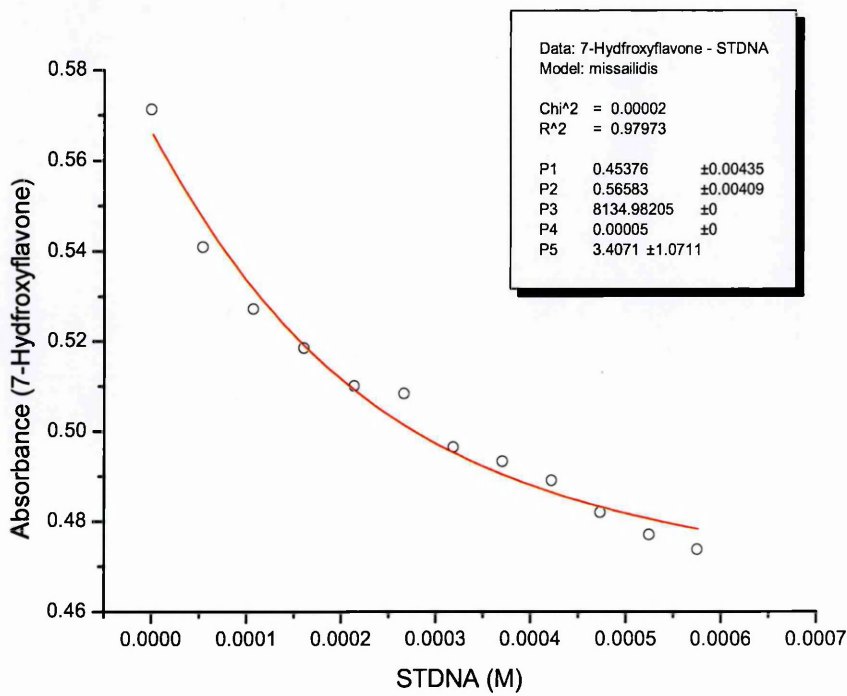


Figure 144: 5-hydroxyflavone – STDNA

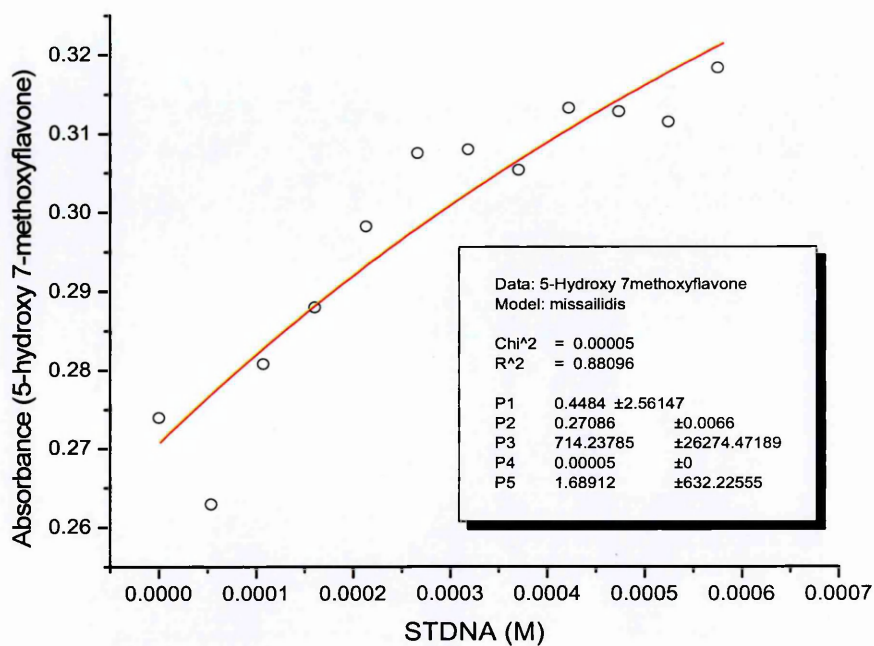


Figure 145: 5-hydroxy,7-methoxyflavone – STDNA

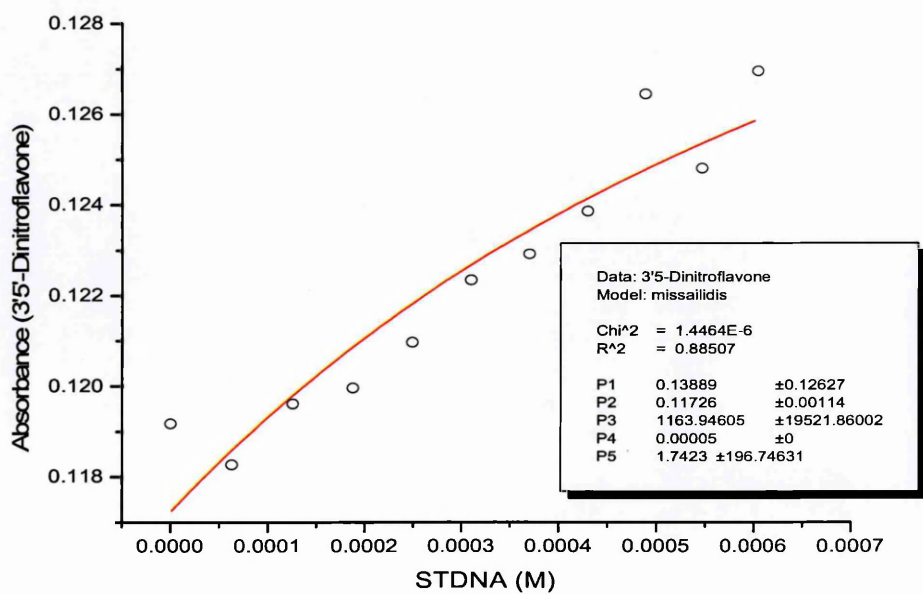


Figure 146: 3',5'-dinitroflavone – STDNA

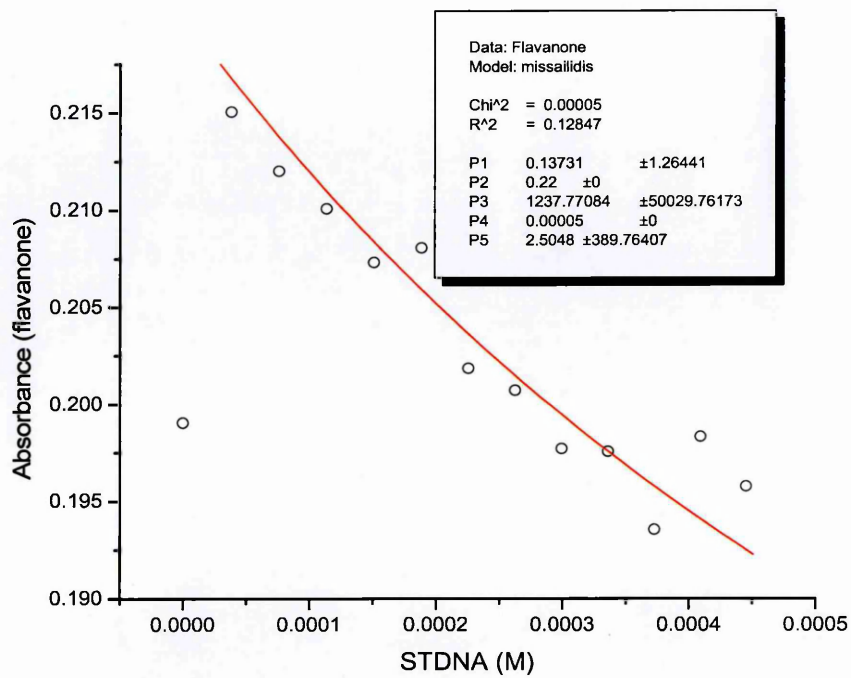


Figure 147: Flavanone – STDNA

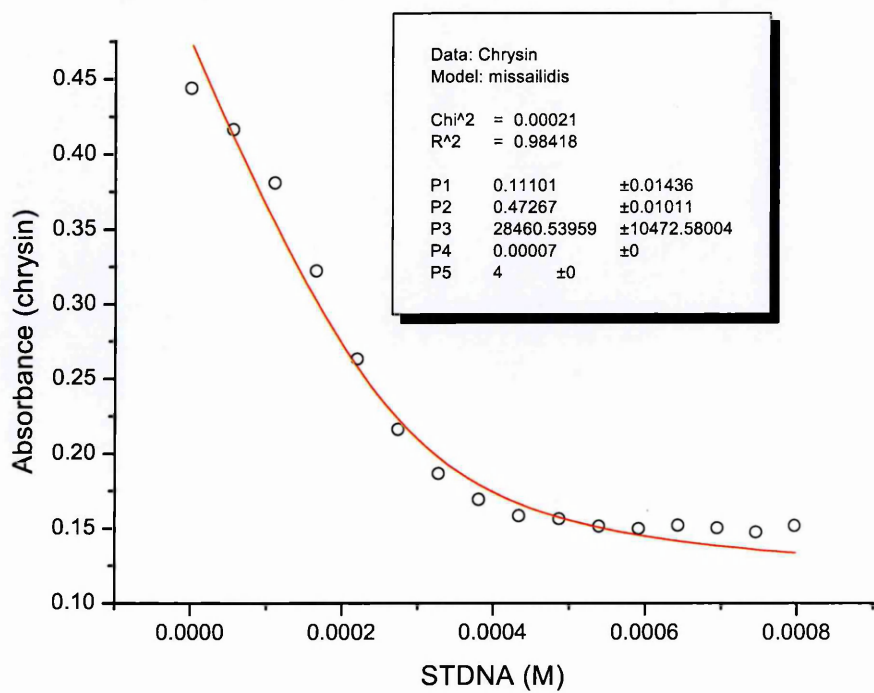


Figure 148: Chrysin - STDNA

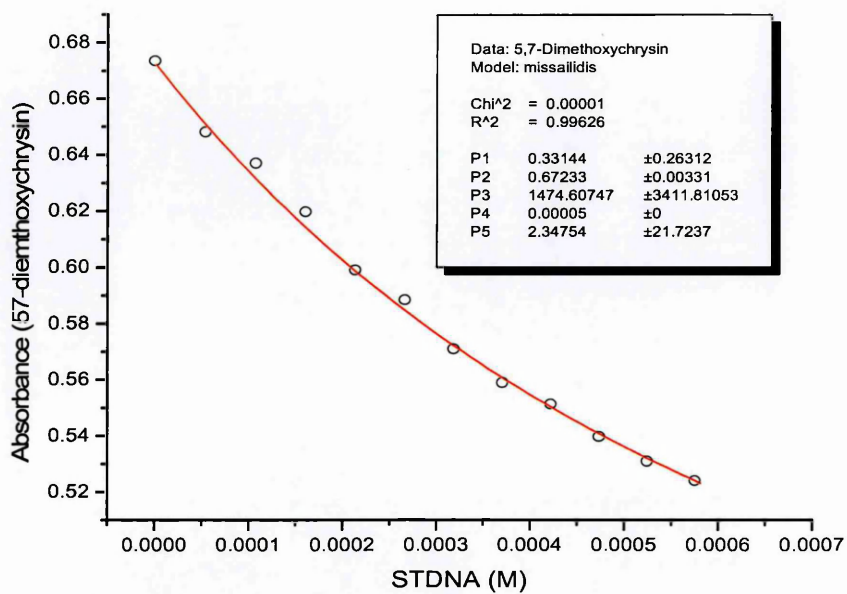


Figure 149: 5,7-dimethoxychrysin – STDNA

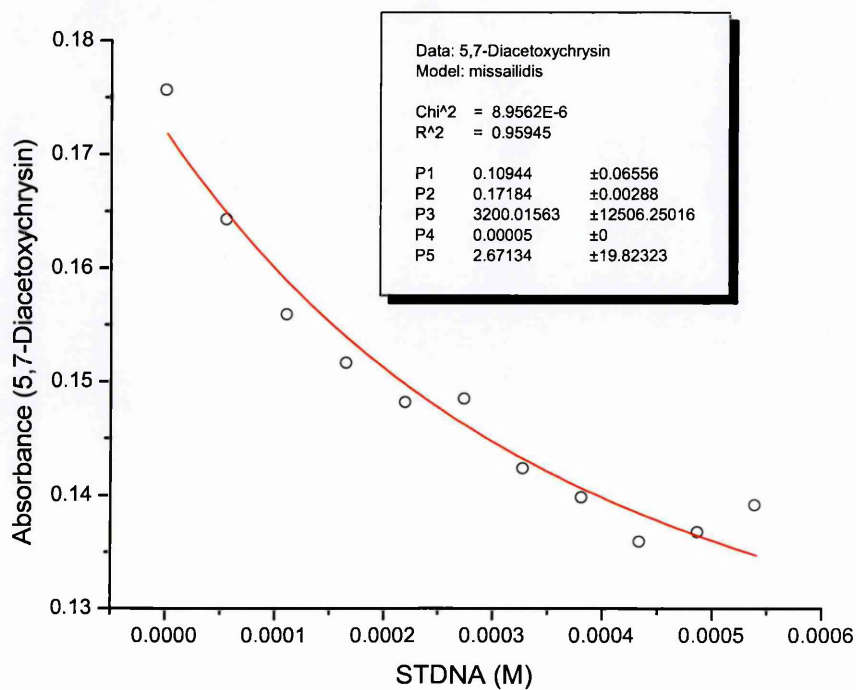


Figure 150: 5,7-diacetoxychrysin – STDNA

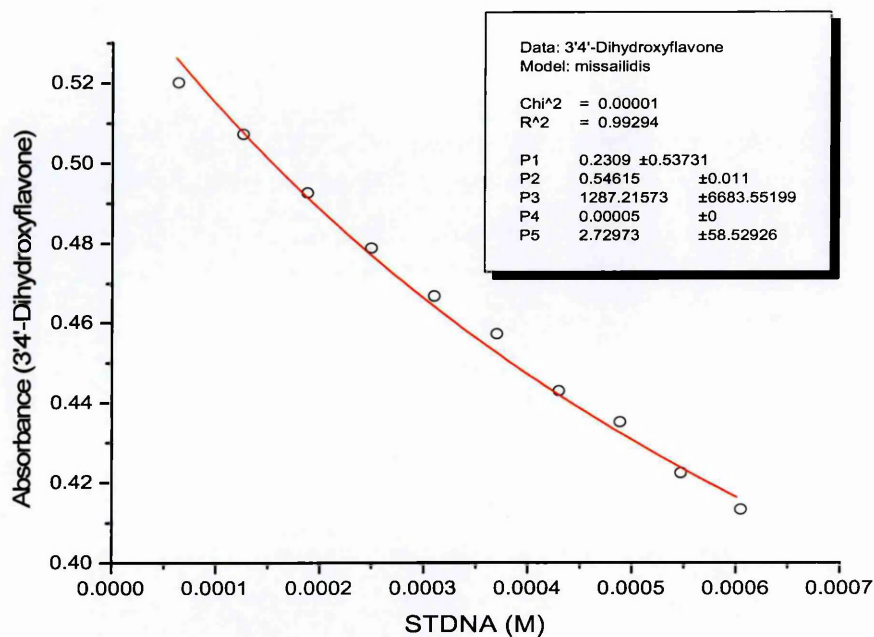


Figure 151: 3',4'-dihydroxyflavone – STDNA

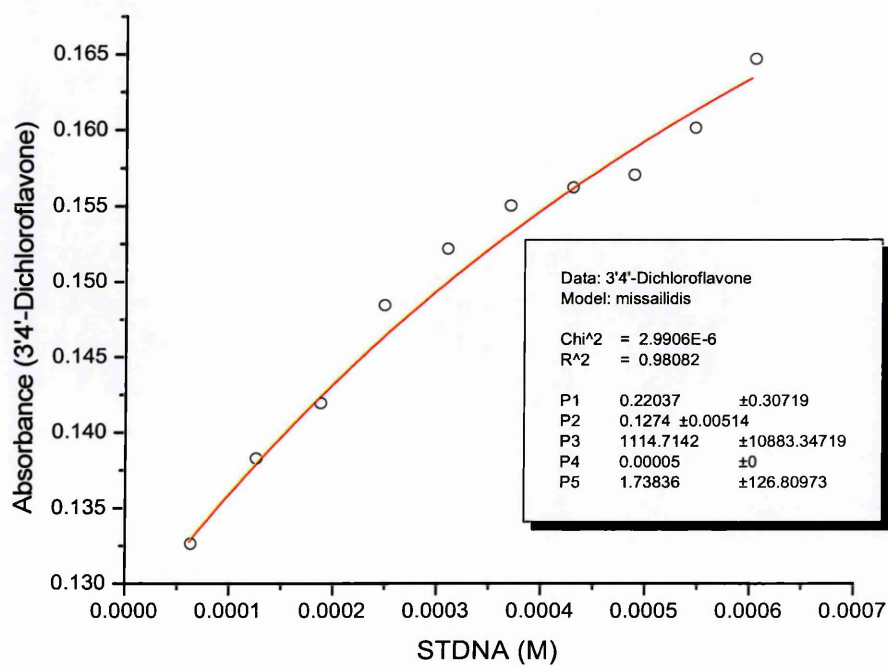


Figure 152: 3',4'-dichloroflavone – STDNA

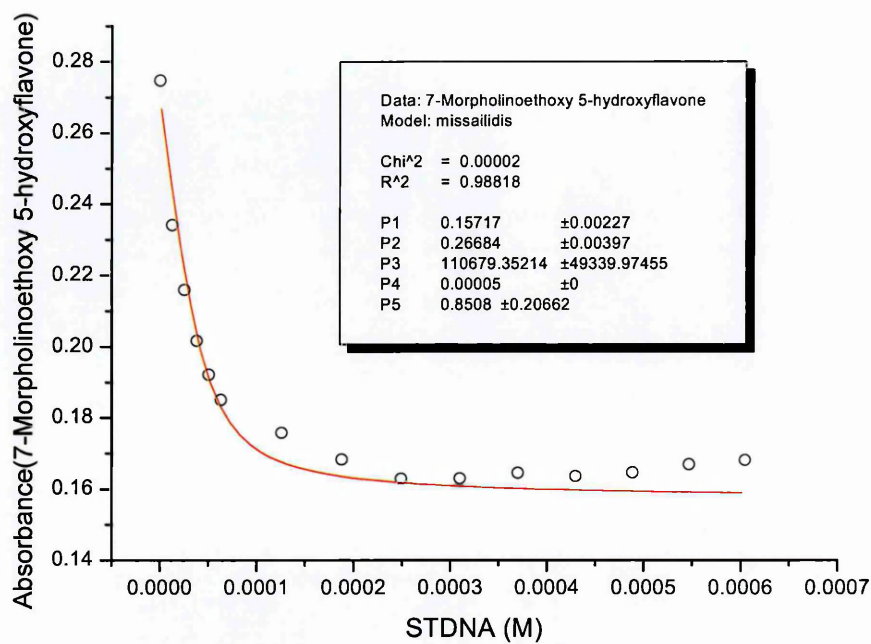


Figure 153: 7-morpholinoethoxy,5-hydroxyflavone - STDNA

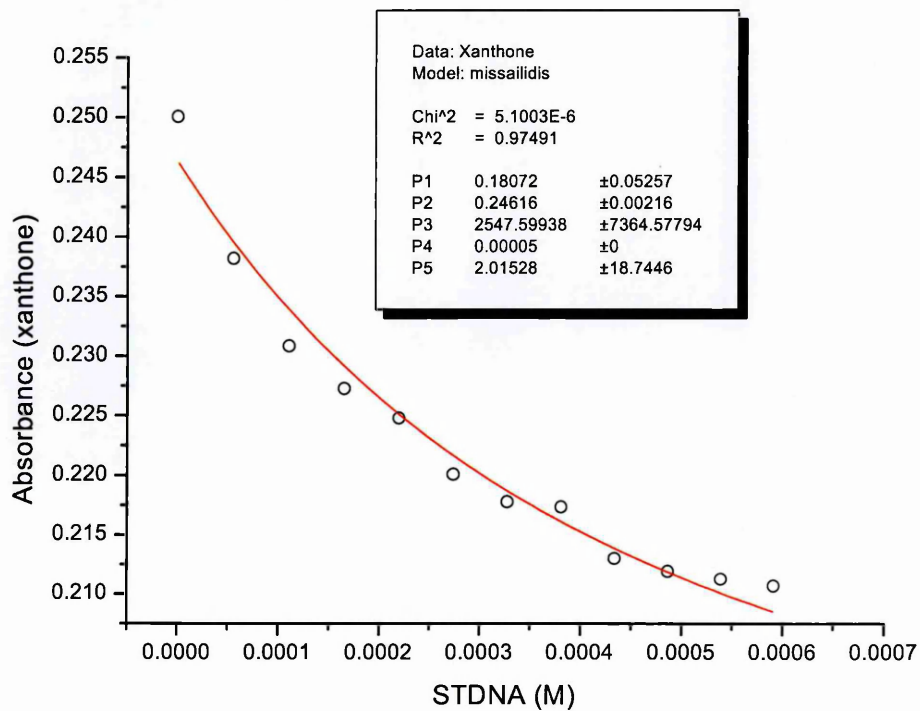


Figure 154: Xanthone – STDNA

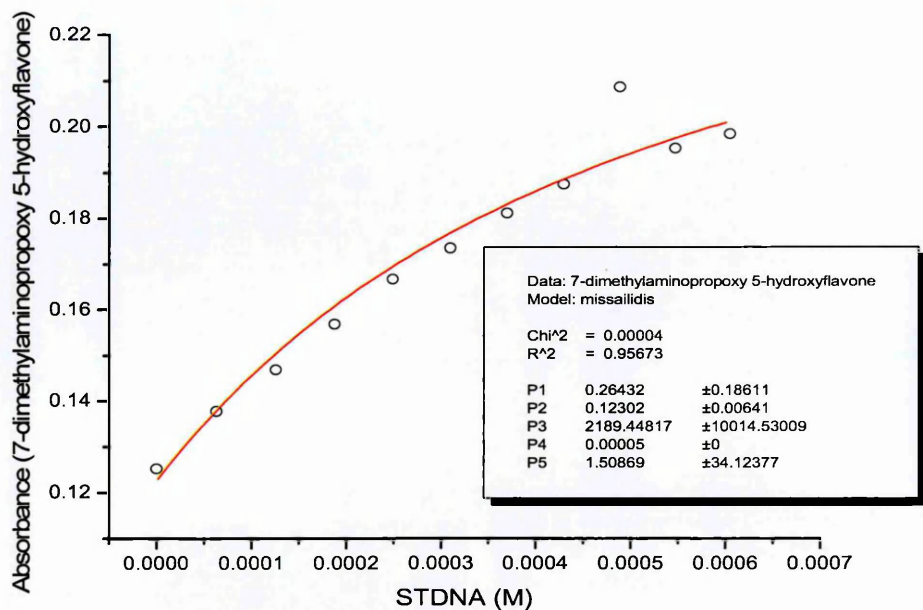


Figure 155: 7-dimethylaminopropoxy,5-hydroxyflavone – STDNA

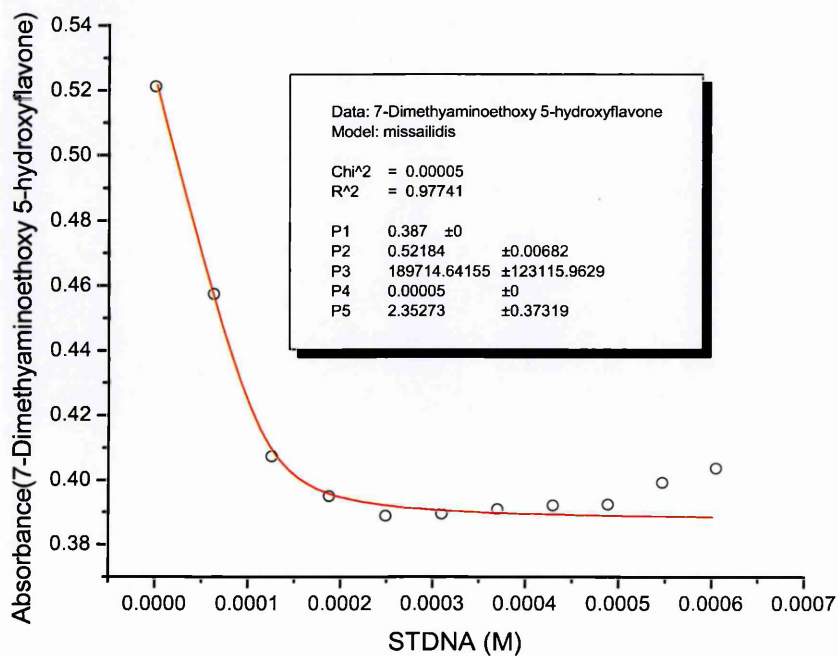


Figure 156: 7-dimethylaminoethoxy,5-hydroxyflavone – STDNA

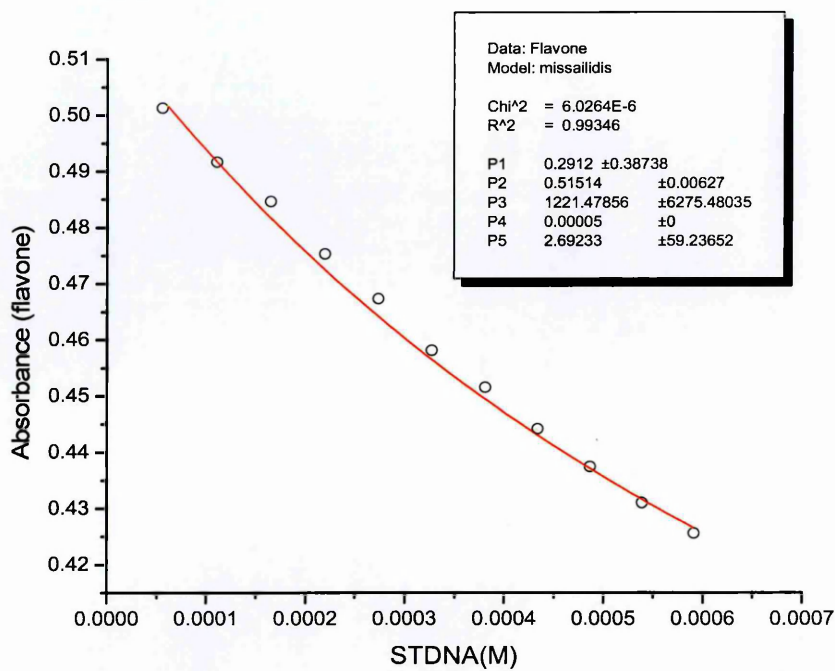


Figure 157: Flavone – STDNA

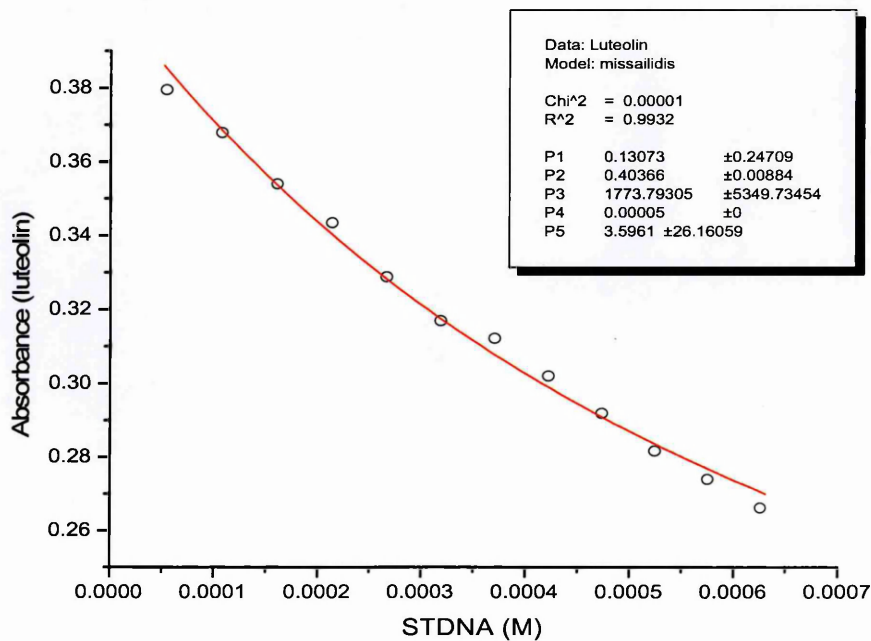


Figure 158: Luteolin – STDNA

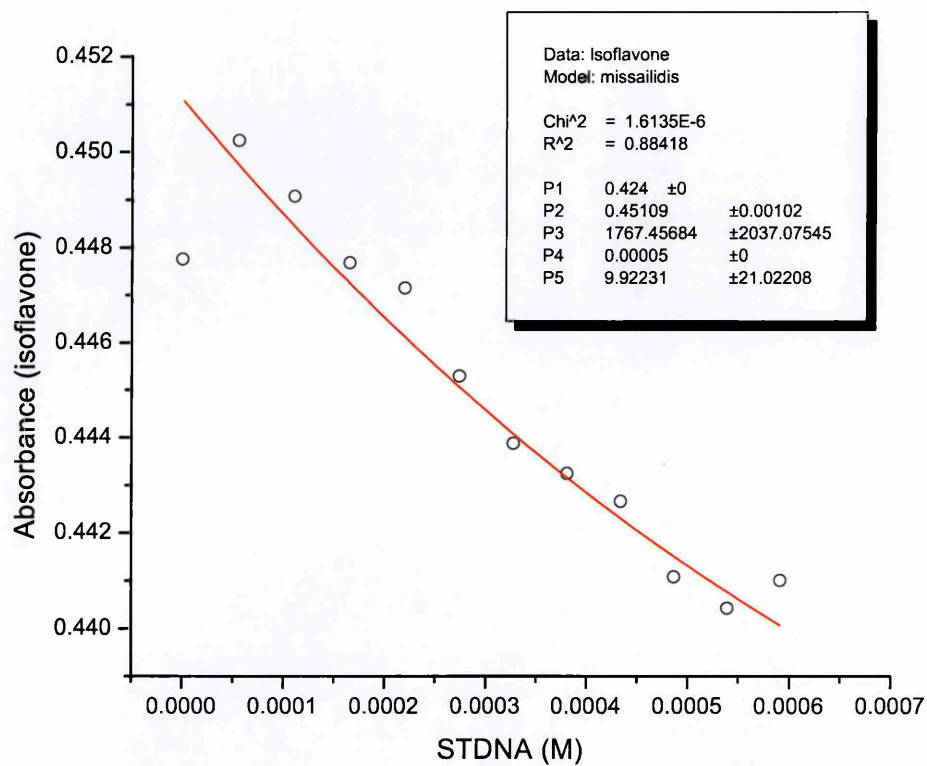


Figure 159: Isoflavone – STDNA

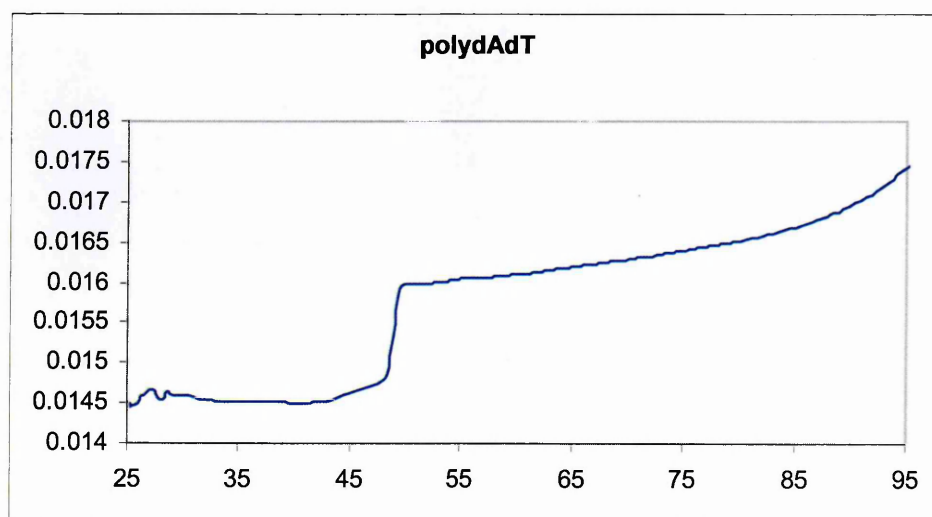


Figure 160: Melting denaturation curve of polydAdT alone

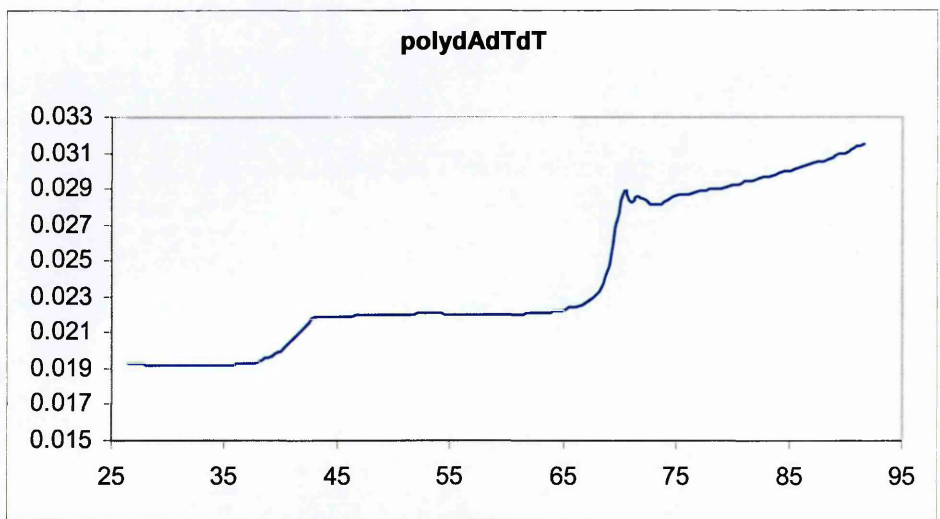


Figure 161: Melting denaturation curve of polydAdTdT

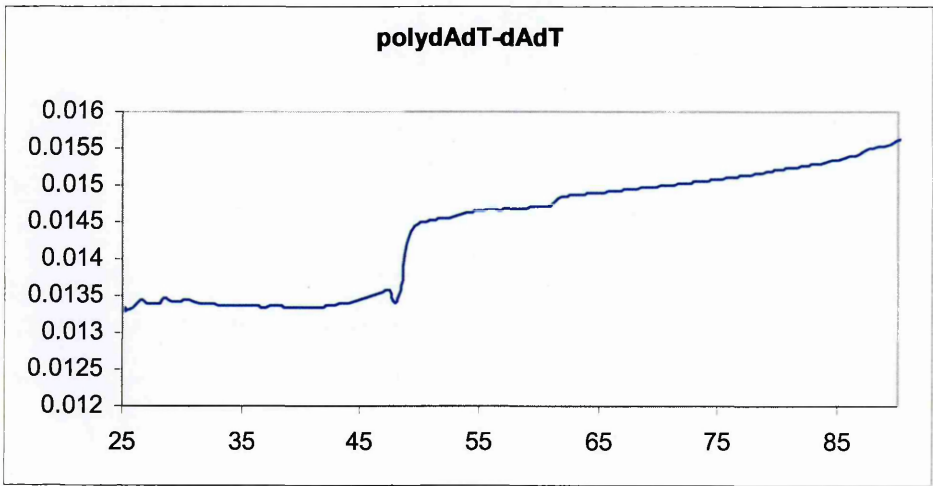


Figure 162: Melting denaturation curve of polydAdT-dAdT

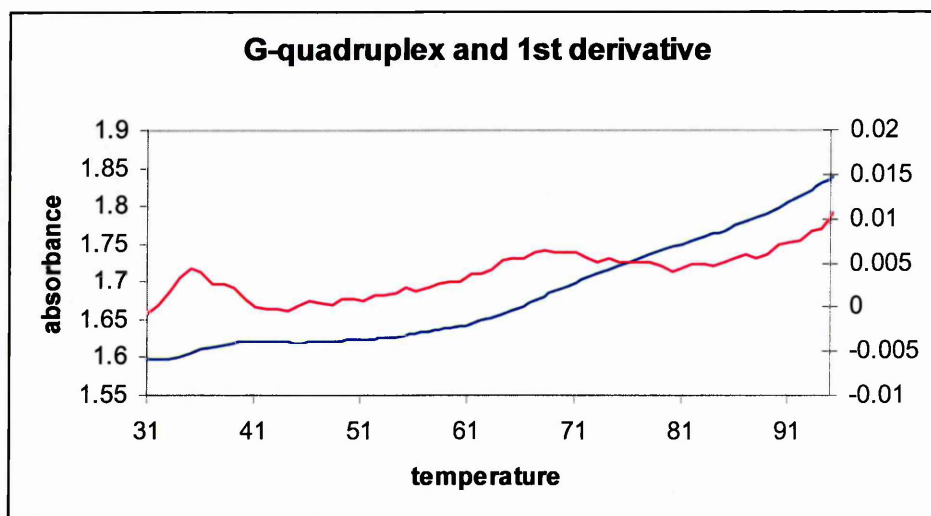


Figure 163: melting denaturation curve of G-quadruplex with the 1st derivative

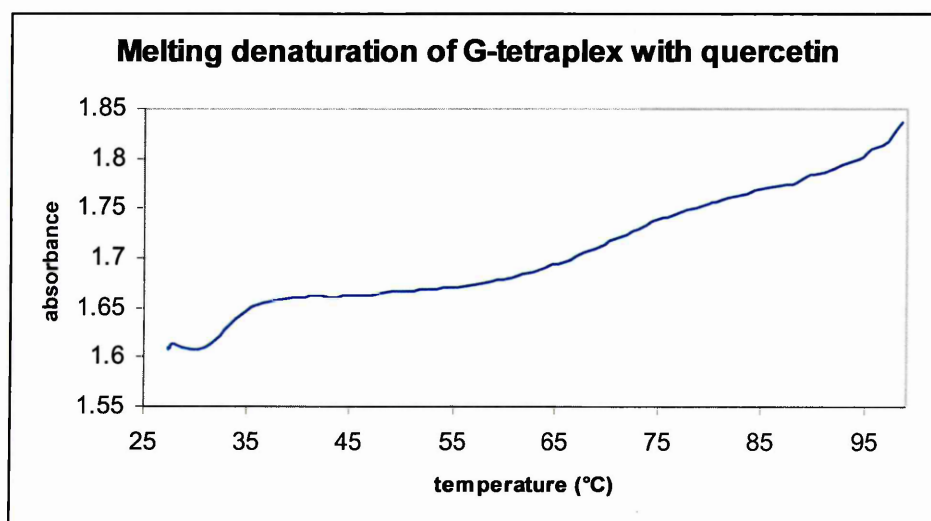


Figure 164: melting denaturation curve of G-quadruplex in the presence of quercetin